Climate Responsive Façade Optimization Strategy

by

Rudai Shan

A dissertation submitted in partial fulfillment
of the requirements for the degree of
Doctor of Philosophy
(Architecture)
in The University of Michigan
2016

Doctoral Committee:

Assistant Professor Lars Junghans, Chair
Assistant Professor Carol C. Menassa
Associate Professor Geoffrey Thun
Professor Peter D. von Buelow

© Rudai Shan 2016
All Rights Reserved

This dissertation is dedicated to my parents, Dachuan Shan and Yanli Ding.

ACKNOWLEDGEMENTS

I would like to take this opportunity to express my thanks to everyone who contributed directly and indirectly to my dissertation. First and foremost, I would like to thank my committee members, especially Professor Lars Junghans for his support, patience, and tremendous counsel as my academic advisor and for sharing his knowledge of the field with me; Professor Geoffrey Thün for his constant guidance and critical encouragement; Professor Peter von Bülow for his theoretical insight and constructive advice on my research and Professor Carol Menassa for her steadfast support and infinite wisdom throughout my graduate studies.

There are several individuals I wish to thank for helping me complete my doctoral training: Professor Mojtaba Navvab for his powerful words of encouragement and advice about research methodology; Professor Harry Giles, for his precious help when I was giving my first steps in the field; Nuri Bae, Niloufar Emami, Omid Oliyan Torghabehi, Anahita Khodadadi, Azadeh Omidfar, Alaa Algargoosh and Deokoh Woo of the Building Technology program for their support during my PhD study in Tabuman College.

I am thankful to the architecture department at the University of Michigan to provide me continuous financial support and teaching opportunity. I would also like to thank the faculty, staff, and my colleagues at the architecture department for their advice, assistance, and encouragement.

Finally, I would like to express my heartfelt gratitude to my parents, who have supported me while I worked to accomplish my goal, who have tolerated my absence

and distraction for many years and who have given me love when it was needed. Without you, I would not be here. Thank you.

TABLE OF CONTENTS

LIST OF FIGURES

Figure

LIST OF TABLES

Table

LIST OF APPENDICES

Appendix

ABSTRACT

Climate Responsive Façade Optimization Strategy

by

Rudai Shan

Chair: Lars Junghans

The building façade plays a key role in the entire building's energy performance. In commercial buildings, energy demand is dominated by space heating, cooling, and artificial lighting. Façade design variables for these three factors have always been interacting and sometimes even in conflict with each other. For different climates, adaptive façade design solutions should be implemented to achieve optimal design objectives, such as energy performance, human comfort, and life cycle cost. While the optimal solution is traditionally identified through "trial-and-error", for complex optimization problems that contain a great number of design variables, it might require extensive hours of computation at early design stage, a condition that is increasingly infeasible in practice due to cost or time constraints.

Since 2008, there has been a significant trend in building performance optimization techniques (that used to emphasize solely on simulation) being implemented, instead of building simulation techniques, to obtain design solutions for building performance optimization problems. Among widely implemented optimization algorithms, the genetic algorithm (GAs) have proven effective with its robustness in dealing with discontinuous variables. However, for complex optimization problems with a great

number of variables, such as façade performance optimization (FPO) problems, GAs are still too time-consuming to be implemented at the early design stage, thus efficiency becomes the main area for its augmentation.

The main objective of this study is to develop a new evolutionary algorithm method, adaptive radiation (AR), based on simple GAs to solve complex optimization problems relative to the design approach of the climate-responsive façades. AR is derived from the biological process of adaptation where specific species are evolutionarily adapted to their immediate ecological niches. This process can obtain optimal solutions of façade design variables (infiltration, window-to-wall ratio, shading geometry, glazing types, wall insulation, etc.) in significantly less computation time than GA. In this study, AR is implemented in three different climates in the United States to demonstrate its robustness and efficiency. The results validated the potential of AR through façade design scenarios. The procedure can also be extended towards a broad field of complex simulation-based architectural optimization problems.

CHAPTER I

Introduction

1.1 Background

The building industry is the largest energy sector in the United States. It has a substantial impact on the environment. Building energy consumption accounts for up to 40 percent of total U.S. energy consumption, including 19% for commercial buildings and 21% for residential buildings (*DOE*, 2011). Almost half of the building energy consumption is implemented for the following three main sectors: space heating (27% for residential, 14% for commercial), space cooling (16% for residential, 19% for commercial), and artificial lighting (10% for residential, 17% for commercial) (*DOE*, 2011). The residential and commercial sectors also contribute to almost 40 percent of carbon dioxide (CO2) emissions in the U.S. (*DOE*, 2011). It is imperative to develop the techniques to improve building energy efficiency and sustainability. Building façade is the main interface between the indoor and outdoor environment. Improving building façade performance with appropriate design strategies are essential to reduce building energy consumption and carbon emissions (*Fernandes et al.*, 2013).

However, the design of appropriate building façade is not straightforward. All buildings are unique due to the local climate. Façade design variables include such as Window-to-Wall Ratio (WWR), Glazing Type, Shading Shape and Insulation have

to be appropriately designed to adapt to the local climate. A conventional approach known as "parametric simulation", or sensitivity analysis (SA) is usually used to identify the uncertainties in input and output of a system and provide decision support (*Wang et al.*, 2007). According to this approach, the input of each variable is varied to see the effect on the design objectives while all other variables stay unchanged. This procedure is then repeated iteratively with all variables. There are two main disadvantages of this method. First, this method does not provide clear solutions for designers. Second, it only leads to partial improvement while fails to focus on the interrelationship between underlying variables. In addition, for a complex façade, the design space of possible solutions is very large, which usually makes this methodology time-consuming.

To achieve an optimal solution (or a solution near the optimum) to a façade design problem, iterative methods which are known as 'simulation-based optimization' automated by computer program are usually implemented. Simulation-based optimization techniques can significantly improve the efficiency and robustness of optimization procedure based on great advances of computational science and mathematical optimization methods. Genetic algorithm (GA) is one of the most widely used algorithms in building performance optimization field for its feasibility in solving non-linear simulation-based optimization problems. However, GAs are still extremely time-consuming for solving complex façade performance optimization problems (FPOs). There is a significant need to improve the existing GAs to reduce the computation time and labor.

1.2 Research Objectives

The primary objectives of this research are to improve the existing GA, and develop a new evolutionary algorithm based on it to find the optimal solutions of FPOs in different climates. This new algorithm is named adaptive radiation (AR), which

is known as a principle in evolution of ecological diversity. AR describes the process how a single ancestor diverges into an array of species that are adapted to a variety of environments. Feasibility and robustness of this approach are demonstrated and validated through a series of case studies for different climates in the United States.

Therefore, this study specifically addresses the following research approaches:

1) To develop a new optimization algorithm – Adaptive Radiation, based on simple GAs in solving FPOs;

2) To validate the feasibility of the application of AR through different design scenarios;

3) To provide climate responsive façade design strategies for different climates in the United States based on the optimization results of design scenarios.

1.3 Dissertation Outline

This chapter made a brief introduction of the background, research objectives and structure of this dissertation. The main theme of this dissertation is presented: improving existing GA and extending a hierarchical optimization methodology, Adaptive Radiation, to façade optimization problems.

Chapter 2 reviews the methodological foundations of this dissertation. The first section reviews the research trends in high-performance building optimization problems. It then narrows down the research area to façade performance optimization problems (FPOs). The third section introduces design optimization algorithms that are most widely implemented in FPOs. The fourth section reviews the development of GAs and points out the imperative of improving the efficiency of existing GAs. The fifth section presents the frequently implemented optimization tools. The last section summarizes this chapter.

Chapter 3 explains the optimization methodology of AR and its integration of FPOs. The first section explains the design variables and objectives, as well as the

complexity of the FPOs. The second section introduces the integrated thermal and lighting simulation methodology. The third section presents the model of AR and the process involved in its implementation. Chapter 4 extends the AR methodology to the FPOs context through one design scenario. GA optimization runs are executed to validate the efficiency and robustness of AR. Chapter 5 implements AR in two other climates in the U.S. to validate its applicability and stability. Chapter 6 summarizes this work, enumerates the main contributions, and points out further research areas.

CHAPTER II

Literature Review

This chapter reviews the implementation of optimization in building optimization problems in view of current research and practice trends in numerical algorithms and solution techniques. Recent developments in numerical algorithms validates the availability and effectiveness of diverse optimization methods in solving simulation-based optimization problems.

2.1 Optimization Study in High-Performance Building

There is a growing trend in research and practice in the architectural, engineering and construction (AEC) industry, where optimization approaches have been more and more frequently implemented in high-performance building optimization problems. The optimization problem in building design is unique when compared with optimization problems in other manufacturing industries, such as the automotive or naval industry. The climatic and environmental situation for each building is unique, which makes large scale test model production before real construction infeasible. Therefore, unlike cars or ships, prototypes for buildings are usually not constructed and tested before manufacture. However, at the early design stage, it is essential to make a great deal of decisions which aim to achieve the building design objectives, such as energy performance, cost, environmental impact as well as thermal comfort

(*Negendahl and Nielsen*, 2015). Therefore, optimization studies are most commonly performed at the early-design stage, where the majority of design decisions have yet to be made.

The study of building optimization has been developed since the year 1980s, which is based on the advancing development in computational technique and mathematical optimization methods. A pioneering study was presented by Wright in 1986 which applied the 'direct search' method in HVAC system optimization (*Wright*, 1986). The optimization studies were then developed in a variety of building optimization categories, including shape/geometry (*Adamski*, 2007), HVAC system (*Palonen et al.*, 2009), envelope insulation (*Baglivo et al.*, 2014) and control strategies (*Coffey et al.*, 2010).

Even though the studies in building optimization problems were implemented much earlier, most studies were published in the late 2000s. Using keyword searches in ScienceDirect reflects an exponential evolution in the number of research papers that utilize building optimization algorithms in the past two decades (Figure 2.1). These type of optimization techniques have increased sharply since the year 2008. About 80% of the papers in this field have been published in the last 5 years, presenting great potential for future utilization of these techniques, and identifying this as an emerging field of research.

It is important to know the capability of the optimization method in achieving the design objectives with less simulation effort, which helps the designers choose an appropriate method among a number of approaches. It's worth pointing out that in optimization problems, efficiency and accuracy usually conflict with each other. In building optimization problems, it is not necessary to find the global optimal solution(s) of a problem precisely, since this effort may be infeasible due to the nature of the simulation-based optimization problems (*Baños et al.*, 2011). Using simulation-based optimization methodology to achieve sub-optimal solutions with relatively less

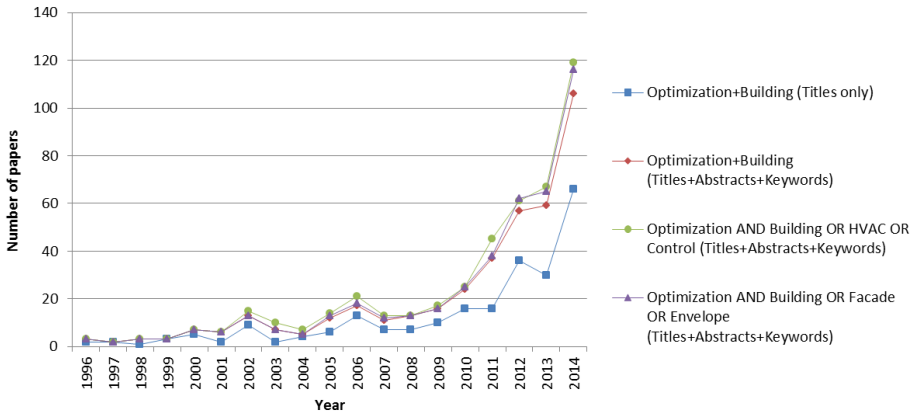

Figure 2.1: Number of papers for selected keyword searches in ScienceDirect for years 1996-2014.

time and simulation effort is one main purpose of researchers. This process is usually automated by the integration of building simulation engines and optimization algorithms. A flow chart for simulation-based optimization is shown in Figure 2.2.

While applications for optimization methodologies related to building optimization problems are vast and constantly evolving, many researchers focus their interest on the area of façade optimization (*Bichiou and Krarti*, 2011; *Gossard et al.*, 2013; *Baglivo et al.*, 2014; *Futrell et al.*, 2015). This section examines the state-of-the-art with respect to the most recent optimization algorithms study in FPOs. The aim of the content is to provide an overview of FPOs, as well as the most widely implemented algorithms and tools.

FPOs can be expressed as the solution process to achieve the optimal façade design variables that satisfy the design objectives, based on the integration of building simulation program(s) with appropriate optimization algorithm(s). The design objectives are a set of evaluation criteria, including energy performance, human comfort and/or life cycle cost (*Attia et al.*, 2013). When there is only one design objective, the problem is called single-objective optimization problem, whereas if when there are more than one design objective, it is called multi-objective optimization problem. This study only discusses the field of single-objective optimization problems to

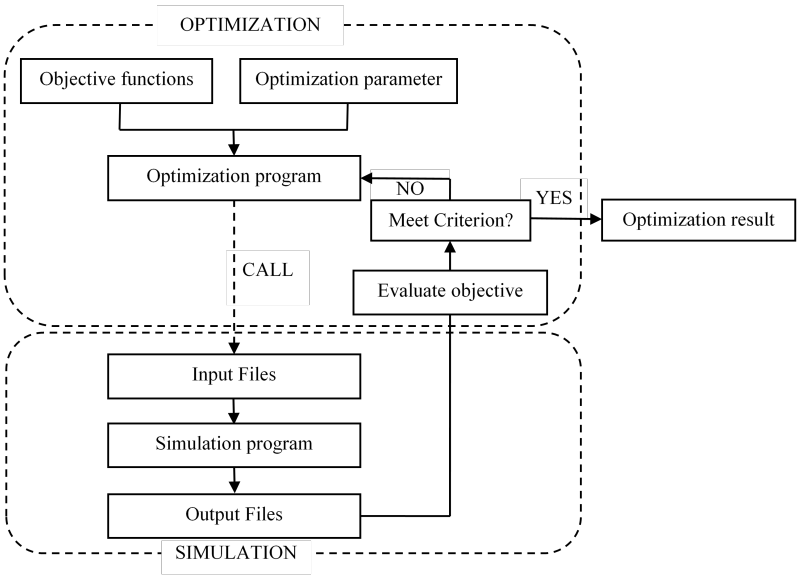

Figure 2.2: The coupling loop implemented to simulation-based optimization.

simplify the optimization model.

Today, simulation-based optimization has become an efficient technique to provide high-performance façade design solutions. There have been a great number of studies using optimization techniques in this process (*Wang et al.*, 2007, 2010; *Rapone and Saro*, 2012; *Stazi et al.*, 2012).

The term 'optimization' often refers to the procedure of finding the global minimum or maximum of a function by choosing a number of variables subject to a number of constraints. The general formulation for an optimization problem can be summarized as

$$\begin{aligned} &\min_{x \in X} f(x) \\ &\qquad s.t. \\ &x \subset R^n \end{aligned} \tag{2.1}$$

where $\min_{x \in X} f(x)$ is the objective (cost function or optimization criterion) to be optimized, $x \in X$ the vector of design variables, and $x \subset R^n$ is the constraint set.

Design variables of optimization problems are gathered in vector x, and reflect

the total set of alternative solutions that is available to improve design objective. The optimum of $f(x)$ can be achieved by gradually changing the vector x. The value of design variables can be continuous (real numbers), integer or discrete (integer numbers), or combinatorial (e.g., permutation on a set of numbers of finite size) (*Collette Y*, 2013). The set of decision variables constraints can be either linear or non-linear (or both). The solution set can be reduced through the identification of feasible solutions subject to the constraints.

In FPO problems, façade design variables can have either integer or discrete values (e.g. SHGC, U-Value, shading dimension) due to the nature of the simulation-based algorithms, which lead to a series of disordered and discontinuous simulation outputs (*Wetter*, 2004). These discontinuities make the optimization result to be trapped in the local optimum and stray away from the global optimum. The traditional 'gradient methods' thus are infeasible for FPOs. Figure 2.3 represents an example of how these discontinuous outputs are misled in the Hooke–Jeeves algorithm in a facade optimization problem. Therefore, 'non-gradient methods' are more applicable in solving façade optimization problems.

The general procedure of non-gradient methods is to sample the design space for good points, and then use the evaluation result to decide where to sample for the next loop. There is a great variety of possible approaches. The general categories include direct search methods, heuristic methods and black-box methods. These terms are also interchangeable since modern method variants blur classification distinctions. Genetic Algorithm (GA) is one of the heuristic methods that inspired by natural processes. GAs are widely implemented in FPOs since they are simple to implement and make no assumptions about the mathematical form of the functions.

Figure 2.4 shows an estimation of the utilization trend of optimization algorithms by using the data from the literature related to building optimization algorithms (*Nguyen et al.*, 2014). It can be seen that the heuristic algorithms such as GA, PSO,

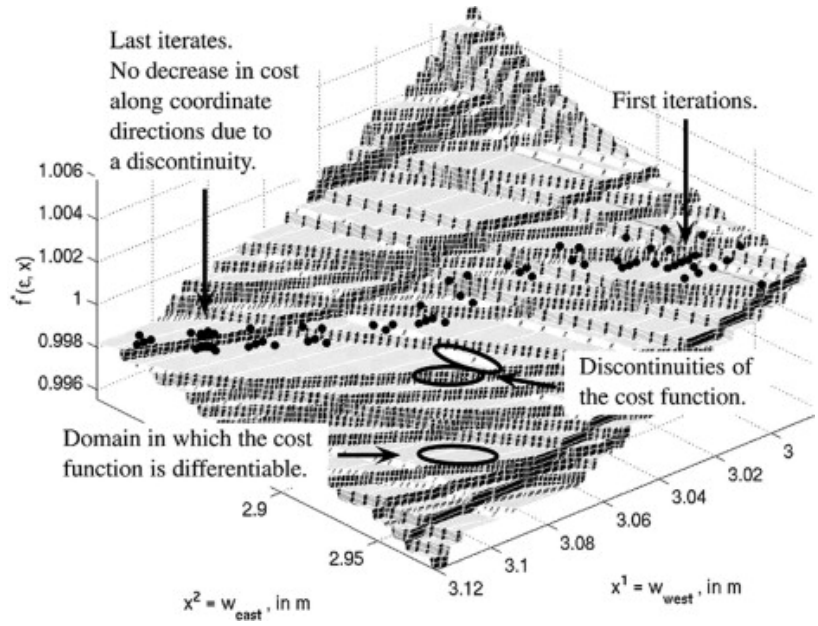

Figure 2.3: Discontinuity in energy consumption as a function of east and west window configurations. The dots show the optimization process of the Hooke–Jeeves algorithm (*Wetter and Polak*, 2004).

SA, Hooke-Jeeves, hybrid algorithms or other evolutionary algorithms, are the most frequently implemented algorithms in building optimization problems. Even though these stochastic algorithms cannot guarantee the global optimal solution(s), they can provide valuable solution(s) which are close to the global optimum without requiring a prohibitively long time. Brief introductions of heuristic methods are given below.

Heuristic algorithms are optimization techniques used in solving optimization problems when classic 'direct search' methods are not feasible. Heuristic algorithms have great potential to find the optimal solutions with less simulation time, but carry the risk of sacrificing accuracy, precision, or completeness for speed. Heuristic algorithms are often implemented in those problems with unknown mathematical measures to find a solution quickly and accurately (*Cook*, 1983). Evolutionary algorithms (EAs) are a family of optimization algorithms under the umbrella of heuristic methods. EAs are based on the Darwin's 'Theory of Evolution', which explains the adaptive change of species by the principle of natural selection that those species best

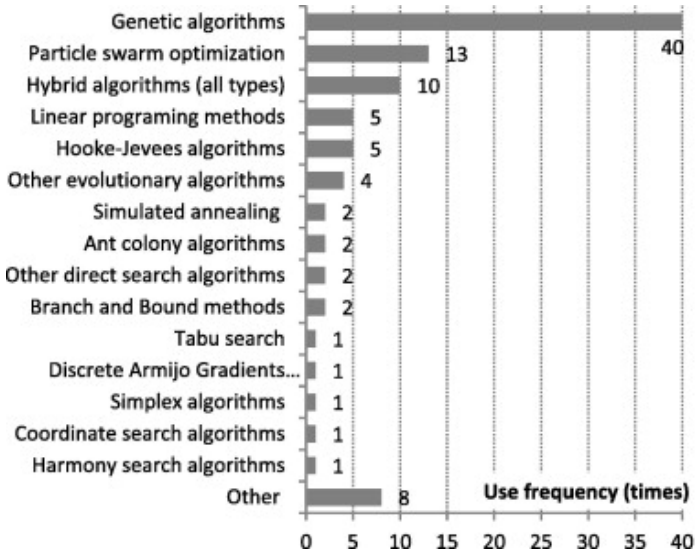

Figure 2.4: Use frequency of different optimization algorithms, derived from more than 200 building optimization studies given by SciVerse Scopus of Elsevier (*Nguyen et al.*, 2014).

adapted to the environmental conditions will survive for further evolution (*Darwin*, 1859). Darwinian Theory was then extended by microscopic findings concerning the mechanisms of heredity, which is called 'Synthetic Theory of Evolution'. EAs involve implementation of biological evolutionary processes which apply the Darwinian principle of survival of the fittest, by maintaining a population of solutions from which the elitisms are passed down to subsequent generations. Techniques inspired by mechanisms of organic evolution are implemented to generate new solutions by means of mutation, crossover, recombination, and natural selection to find an optimal configuration for a specific system within specific constraints. Types of evolutionary algorithms include:

- Genetic algorithm (GA) (*Holland*, 1975; *Goldberg*, 1989): the most popular type of EA which seeks the solution of a problem in the form of strings of numbers, by applying operators such as recombination and mutation. For example, non-dominated sorting genetic algorithm (NSGA) and NSGA-II are the GAs most widely implemented for multi-objective problems (*Brownlee and Wright*, 2015;

Carlucci et al., 2015). GA has a fixed, linear data structure.

- Genetic programming (*Sette and Boullart*, 2001): this method is implemented in the form of computer programs, and the fitness is determined by the ability to solve a computational problem. Genetic programming and Evolutionary programming both have tree-structures that allow hierarchical variables or representations of functions and programs.

- Evolutionary programming (EP) : this method was laid by Lawrence Fogel in San Diego, California (*Fogel*, 1966). Similar to genetic programming, its numerical variables are allowed to evolve while the structure of the program is fixed. Mutation is the main variation operator of EP.

- Evolution strategy (ES): this algorithm is developed by Rechenberg in the Technical University of Berlin in 1965 (*Rechenberg*, 1965). It works with vectors of real numbers as representations of solutions, and typically uses self-adaptive mutation rates. New variable values are sampled from probability distributions, in which the dependencies are represented by a covariance matrix, updated each generation, e.g. Covariance Matrix Adaptation Evolutionary Strategy (CMA-ES) (*Hansen et al.*, 2003).

- Differential Evolution (DE) (*Price and Storn*, 1997): the values of design variable are iteratively improved to find a candidate solution and perturbed by introducing components of other effective solutions.

There are also other heuristic algorithms that mimic natural processes including:

- Particle Swarm Optimization (PSO) (*Kennedy*, 1995): this method mimics the movement of a bird flock or fish school and simplifies it to perform optimization. The movement of solutions in a design space is based on their individual positions and that of the best positions within the swarm.

- Simulated Annealing (SA): this method is proposed by Kirkpatrick, Gelett and Vecchi (*Kirkpatrick et al.*, 1983) and Cerny (*Černỳ*, 1985). It works by emulating the heating and controlled cooling process of a solid material to increase the size of its crystals and reduce defects at a minimum energy configuration. It is often implemented in solving discrete optimization problems.

- Ant Colony Optimization (ACO) (*Dorigo et al.*, 1996): this method mimics the process by which ants deposit pheromones on paths to encourage other ants to follow, and the variable values are most often implemented will accumulate 'pheromones' biasing their selection in future choices.

- Harmony Search (HS) (*Geem and Kim*, 2001): this method is inspired by the improvisation process of musicians proposed by Zong Woo Geem in 2001. The values of each variable are recombined to find a best harmony (global optimum) all together, with some perturbation to neighboring values.

- Pattern Search (PS, also known as direct-search, derivative-free or black-box methods), e.g. Hooke-Jeeves (*Kolda et al.*, 2003): this method executes a trial on one theoretical parameter at a time by steps in each dimension; step size is halved if there is no further improvement within this dimension. This process is repeated until steps are deemed sufficiently small. PS can be implemented in discontinuous or differentiable problems.

Many studies have been investigated to compare the performance of these heuristic algorithms in building optimization problems. Wetter and Wright compared the performance of direct search, Hooke-Jeeves, coordinate search, GA and PSO in minimizing cost functions with different smoothness. The results indicated that GA can achieve the solutions with fewer simulations with a slight decrease in accuracy (*Wetter and Wright*, 2003). Another comparative study examined optimization algorithms including PSO, GA, Coordinate Search, Hooke–Jeeves, Nelder–Mead, Discrete Armijo

gradient and a hybrid version of PSO and Hooke–Jeeves (*Wetter and Wright*, 2004). The results found that Nelder–Mead and the Discrete Armijo gradient algorithms didn't perform well and shouldn't be implemented for problems solved by Energy-Plus. The hybrid PSO + Hooke–Jeeves can achieve the best optimal solution but require more simulation time. In addition, Tuhus-Dubrow and Krarti compared GA, PSO and the sequential search (SS) method in building envelope optimal design cases with more than ten parameters (*Tuhus-Dubrow and Krarti*, 2010). The results indicated that the GA was more efficient than both approaches of the PSO and the SS, with a difference in accuracy of 0.5% in locating the optimal solution, and demanding less than 50% of the iterations. Bichiou and Krarti compared the same three algorithms to evaluate the robustness and effectiveness (*Bichiou and Krarti*, 2011). They found that the computation time for SS is significantly higher than both PSO and GA. Also, GA can save as much as 70% computation time compared with SS. The results also indicated that even though the hybrid PSO and Hooke-Jeeves achieved the largest cost reduction, GA got close to a solution with fewer simulation runs. Wright and Alajmi then investigated the robustness of GA in solving unconstrained optimization problems with a restricted number of simulation runs (*Wright*, 2005). It indicated that the probabilistic nature of GA lacks robustness in finding solutions and insensitive to the selection of GA control parameters. It also indicated that the better solutions were obtained by using a small population size with high probabilities of crossover and mutation.

There are also several doctoral dissertations which implemented GAs to optimize a specific aspect of the façade design. For example, Caldas implemented GA to generate and optimize building layouts (*Caldas*, 2001; *Sung*, 2014). Comparative studies using simulated annealing and Tabu Search are presented to validate the efficiency and accuracy of GA. Results indicated the feasibility of GA in generating entire building geometries.

These studies validate the application of GAs in solving building optimization problems. The main purpose of the next section is to introduce the methodology of GA, its advantages and disadvantages, as well as the development of its efficiency for façade optimization problems.

2.2 Development of Genetic Algorithm

Genetic algorithms are heuristic methods originally motivated by Darwin's principle of evolution. It was first proposed by John Holland at the University of Michigan in the early 1970s, particularly in his book Adaptation in Natural and Artificial Systems (*Holland*, 1975). Holland's genetic algorithm is usually called simple genetic algorithm (sGA). In his description, the basic techniques of the GAs are designed to simulate the natural processes of evolution, which follow the principles first defined by Charles Darwin of "survival of the fittest", the competition among individuals for insufficient resources results in the fittest individuals dominating over the fragile ones. The main process/functions of GAs consist of a series, beginning with initial population, selection mechanism, coupling mechanism, and coalescence algorithm and mutation. Figure 2.5 shows an entire loop of GA, which is presented in following steps:

1. Initial population: to randomly generate the initial population of genes (bit strings) depending on the nature of the optimization problem.

2. Selection Mechanism: to extract a subset of genes from the generated genomes, according to a definition of fitness function. Therefore a set of parents is selected from the current population to create the next generation. There are three types of general selection mechanisms. The first is Isotropic Selection, which means that every genome simply gets the chance to mate. The second is Exclusive Selection, where only the top N% of genomes can mate. The third is Elitist

Selection, where the chance of mating increases as fitness increases. Elitist selection is the most widely implemented in the process of genetic algorithm. It is a very successful variant of the general process of constructing a new genome since it allows the better genomes from the current generation to be carried over to the next generation.

3. Coupling Algorithm: to randomly mate the genomes generated by the active Selection Mechanism.

4. Coalescence Algorithm: the algorithm that decides which gene of the genomes can be assigned to the offspring when two genomes are mated. The most widely implemented mechanisms for Coalescence Algorithm are Crossover Coalescence and Blend Coalescence.

5. Mutation: to maintain genetic diversity by altering one or more gene values in a chromosome from its initial state, since all the other mechanisms (Selection, Coupling and Coalescence) have a tendency to reduce the bio-diversity in a population.

GAs are widely implemented in solving FPOs due to the following advantages. First, GAs can solve multi-dimensional, non-differential and non-continuous problems, which are very common in FPOs. Second, the evolutionary process of GA makes it effective in solving problems with great complexity. Third, it is easy to understand and does not require deep knowledge of mathematics. Last but not least, existing studies show that it can be easily integrated with building simulation programs.

Since genetic algorithms (GA) can efficiently handle non-linear problems with discontinuities very common in building optimization problems, they have been widely implemented in this field. Wright and Farmani implemented GA in a multi-objective optimization for building elements thermal design, HVAC system size, and the control strategy (*Wright et al.*, 2002). Best et al. implemented GA to minimize building

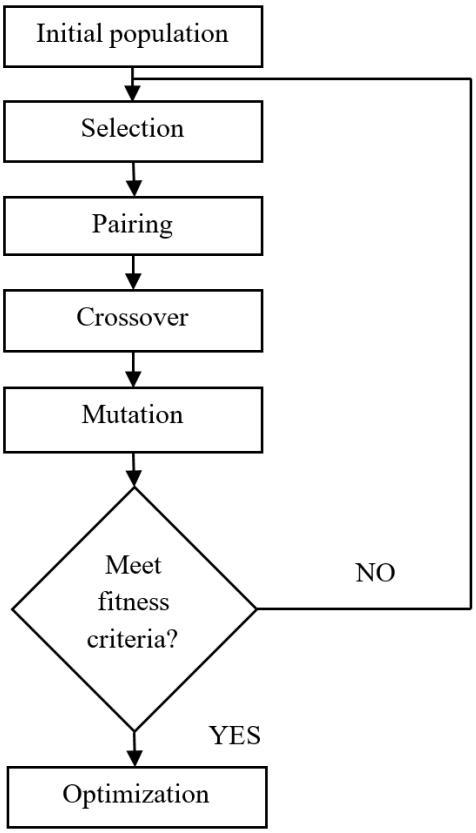

Figure 2.5: Schematic diagram of the genetic algorithm

mix and energy supply technology for urban districts (Best et al. 2015). Bichiou and Krarti used GA to optimize the envelope and HVAC system for residential buildings (*Bichiou and Krarti*, 2011). Oliveira Panão et al. implemented GA for the optimization of urban building forms in energy efficiency improvement (*Oliveira Panão et al.*, 2008). Asadi et al. implemented GA for multi-criteria optimization of building retrofit (*Asadi et al.*, 2012b). Adamski (*Adamski*, 2007), and Yi and Malkawi (*Yi and Malkawi*, 2009) used GA to optimize the form of the building. Wang et al. implemented GA in a multi-objective optimization model which assisted designers in green building design (*Wang et al.*, 2005).

There are also some disadvantages that limit the efficiency and applicability of GA. Most of these disadvantages are caused by the evolutionary mutation and selection

process. First, GAs sometimes cannot solve variant optimization problems, due to poor knowledge about fitness functions, which in turn generate bad chromosomes. Second, GAs cannot guarantee a global optimum, since the optimal solutions are very easily trapped in a local optimum rather than the global optimum. Third, GAs cannot guarantee that the best individual will always survive and be transformed to the next generation. Additionally, the 'crossover' process of the simple GAs may not be efficient when searching the parameter space as expected. Last but not least, the optimization process of GAs is still very time-consuming in practice, especially when it almost reaches and varies near the global optimum.

There have been many variations of GAs developed to solve specific problems. The development of simple GAs occurred in the 1980s. However, most of the improvements for GAs were developed after the 1990s, such as Non-dominated-and-crowding Sorting Genetic Algorithm II (NSGA-II), Hybrid Genetic Algorithm (HGA) and Pareto Genetic Algorithm (Pareto GA). NSGA-II is one of the most widely implemented algorithms in building optimization problems. NSGA-II developed by Deb in 2001, is one of the most popular multi-objective algorithms (Deb 2001). Brownlee and Wright applied NSGA-II to three examples of a typical building optimization problem and compared the results (*Brownlee and Wright*, 2015). Carlucci et al. implemented NSGA-II to minimize the thermal and visual discomfort of a nearly zero-energy building (*Carlucci et al.*, 2015). Lu et al. presented a comparison study for renewable energy systems optimization using a single-objective GA and a multi-objective NSGA-II (*Lu et al.*, 2015). These studies show great potential to improve GAs to solve single-objective or multi-objective problems in different building optimization areas.

Another trend is to integrate GA with other forms of optimization algorithms to improve their efficiency. For example, Palonen et al. integrated NSGA-II with Hooke–Jeeves pattern search method for building envelope and HVAC system opti-

mization (*Palonen et al.*, 2009). Magnier and Haghighat integrated NSGA-II with Artificial Neural Network (ANN) for optimization of building design (*Magnier and Haghighat*, 2010) while Gossard et al. implemented the same method in building envelope optimization for thermal performance (*Gossard et al.*, 2013). Michalek et al. used GA and SA to search for global solutions of architectural layout design optimization problems (*Michalek et al.*, 2002). Junghans and Darde presented an integration of GA and SA to solve building optimization problems (*Junghans and Darde*, 2015). Additionally, Hamdy et al. proposed a hybrid algorithm (PR-GA-RF), which involved running a deterministic algorithm before (PR_GA) or after (GA_RF) a multi-objective genetic algorithm (*Hamdy et al.*, 2011). This approach presented an effort to use the advantages of both methods of PR_GA and GA_RF. The PR_GA algorithm can prepare the initial population in order to reduce the random behavior of GA, therefore obtaining effective solutions with a lower number of simulations. The GA_RF can refine the GA results when high quality results are required, offering a well-defined criterion for terminating the process. Caldas and Norford implemented a micro-GA procedure to build a design optimization tool (*Caldas and Norford*, 2002). Caldas then developed a micro-GA and Pareto GA based generative design system (GENE-ARCH) (*Caldas*, 2008). These studies presented great potential in the improvement of GAs by using their advantages and complementing their disadvantages through integration with other optimization algorithms.

Rather than arbitrarily framing a problem and applying an optimization algorithm to it, some researchers divided the entire optimization problem into different levels and solve this multi-level problem through hierarchical optimizations. For instance, Lee developed a single-objective optimization methodology for an optimal design tool using a genetic algorithm (GA) and computational fluid dynamics (CFD) (*Lee*, 2007). The design variables include random variables (fluctuating outdoor conditions), passive design elements (model variables) and active design elements (HVAC

system). The optimization process is divided into two steps: a simple analysis using a coarse mesh to lower the calculation load; and a detailed CFD analysis using a fine mesh based on the cases in the first step. A reduction of the calculation time was achieved through this two-step procedure. Evins et al. developed a three-step framework using the design-of-experiments approach (*Evins et al.*, 2012). In the first step all variables are selected based on contribution to all outputs. This allowed the variables to be reduced to a more manageable number by eliminating those with less impact on the objectives. In the second step an initial optimization was performed using all significant variables. The variables that remained constant for all optimum solutions are eliminated. In the third step a detailed optimization was performed for the remaining variables and the design rules are inferred. This method shows great potential to improve the efficiency of optimization and maximize the benefit gained from optimization.

2.3 Building Performance Optimization Tools

The integration of optimization tools with building simulation program(s) to solve building optimization problems is one of the most popular trends in recent years. These optimization tools implemented can be classified into two categories: stand-alone optimization tools and simulation-based optimization tools (*Attia et al.*, 2013). The 19 tools that can be integrated building optimization are shown in Table 2.1. This section mainly introduces the stand-alone optimization tools which have been more and more frequently implemented in building optimization research, such as GenOpt®, MATLAB®, modeFRONTIER®, Topgui® and BuildOpt®.

GenOpt® developed at the Lawrence Berkeley National Laboratory (LBNL), is one of the most widely used building optimization programs. It was originally developed as an optimization program for a single-objective function which can be coupled with an external building performance simulation program such as EnergyPlus, TRN-

Table 2.1: Classification of BPO tools (*Attia et al.*, 2013)

	Simulation based optimization	Optimization packages		Tailor made-programming
Public	TRNOPT (2004) BeOpt (2005) OptiMaison (2005) OptiPlus (2006)			
Commercial	ARDOT (2002) Polysun (2006) GENE_ARCH (2008) Lightsolve (2008) ParaGen (2011) ZEBO (2012)	MATLAB optimization toolbox (1990) Phoenix integration (1995) GAlib (1995) modeFrontier (1999) Homer (2000) DER-CAM (2000)	Topgui (1990) GenOpt (2001) Paradiso EO (2003) ThermalOpt (2011)	C++ Cygwin Java R Visual Studio

SYS, DOE-2, SPARK, BLAST, IDA-ICE, Radiance, or any user-written code that has input and output as text files (*Wetter*, 2001). The original algorithm library of Genopt® does not include multi-objective algorithms. Some multi-objective algorithms such as NSGA-II are developed and recently added to the algorithm library by the users (*Gossard et al.*, 2013; *Carlucci et al.*, 2015).

Genopt® has been widely implemented in building optimization problems in plenty of studies (*Asadi et al.*, 2012a; *Bigot et al.*, 2013; *Carlucci et al.*, 2015; *Futrell et al.*, 2015). It's worth illustrating that Wetter and Wright implemented GenOpt to achieve the office building design solutions for energy efficiency in three different climates in the U. S. (*Wetter and Wright*, 2003).

The cost functions of GenOpt can cover any BPO objective functions (energy,

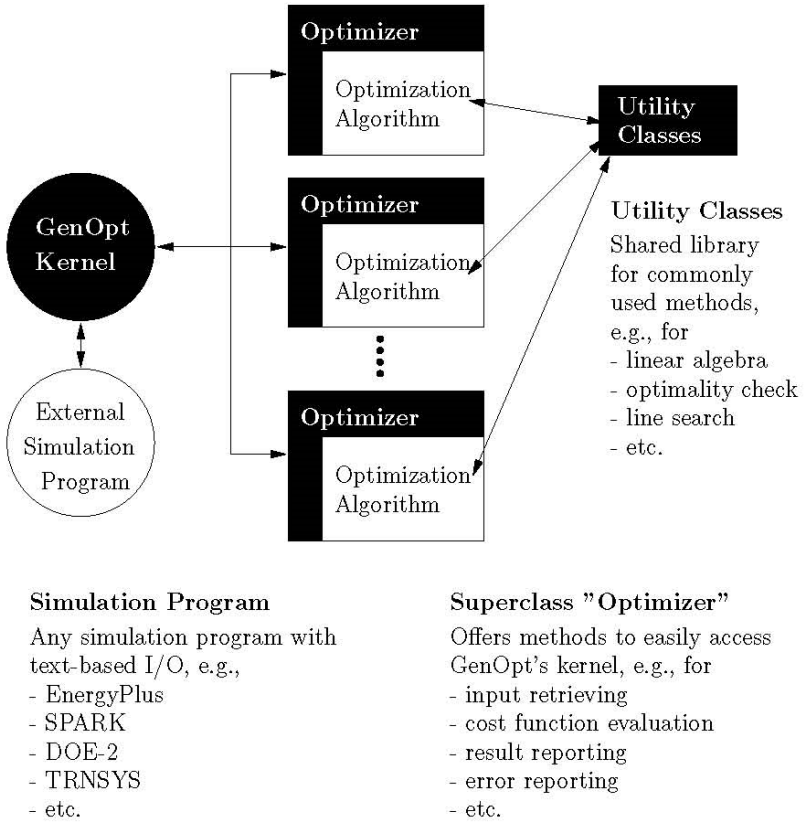

Figure 2.6: Implementation of optimization algorithms into GenOpt (*Wetter*, 2001)

indoor air quality, thermal comfort, etc.) from minimization to maximization. The GenOpt library provides local and global multi-dimensional and one-dimensional optimization algorithms (*Wetter and Wright*, 2004). The multi-dimensional optimization algorithms include:

- Generalized pattern search algorithms (the Hooke-Jeeves algorithm and the coordinate search algorithms) for continuous independent variables, which can be run by using multiple starting points.
- Discrete Armjio gradient for continuous independent variables.
- Particle swarm optimization (PSO) for continuous and/or discrete independent variables, with inertia weight or constriction coefficient and velocity clamping, and with a modification that constricts the continuous independent variables to

a mesh to reduce computation time.

- Hybrid generalized pattern search algorithm with particle swarm optimization for continuous and/or discrete independent variables.
- Nelder-Mead simplex algorithm for continuous independent variables.
- NSGA-II for continuous and/or discrete independent variables.

The one-dimensional optimization algorithms include:

- The golden section interval division.
- The Fibonacci division.

Another widely implemented optimization tool is MATLAB® Optimization ToolboxTM, which provides a variety of algorithms for optimization problems. MATLAB has been implemented in building optimization problems by several researchers (*Dounis and Caraiscos*, 2009; *Asadi et al.*, 2012b; *Baglivo et al.*, 2014; *Hu and Karava*, 2014; *Ascione et al.*, 2015). The algorithms in MATLAB® Optimization Toolbox™ can solve both constrained or unconstrained and, continuous or discrete problems. MATLAB® includes functions for linear programming, quadratic programming, binary integer programming, nonlinear optimization, nonlinear least squares, systems of nonlinear equations, and multi-objective optimization. This allows finding optimal solutions, performing trade-off analyses, balancing multiple building design alternatives, and incorporating optimization methods into algorithms and models. The functions and toolbox in MATLAB provide opportunities to make use of their additional functions or the integration of these functions by the users, including data analysis, plotting functions, curve fitting functions, and graphical user interface (*Hamdy et al.*, 2011).

Topgui® is a toolbox that provides a number of optimization methods similar to Genopt®. In addition, it provides algorithms for multi-objective optimization

problems. It consists of a Java graphical user interface (Gui). The batch commands (that can be controlled by the Gui) can be inserted to start the optimization algorithm such as number of evaluations and design variables. Extra strategy variables can be provided for some algorithms, e.g., for the evolution strategy by editing the population size variables. There are multiple algorithms available in Topgui® and the list can be easily extended through inserting new algorithms. Topgui has been implemented in some studies in building optimization problems (*Emmerich et al.*, 2003, 2008). It provides several single-objective and multi-objective optimization techniques such as:

- Hooke-Jeeves algorithm
- Generalized pattern search methods (GPS)
- Particle swarm optimization algorithms (PSO)
- Evolution Strategy (ES)
- Non-dominated Sorting Genetic Algorithm II (NSGA-II)
- S-metric selection evolutionary multi-objective optimization algorithm (SMS-EMOA).

BuildOpt® is an automated multivariate optimization tool which is an energy simulation program that is built on models that are defined by differential algebraic equations (DAE) (*Wetter*, 2004). It is implemented by Ellis et al. through an optimization model which employs multiple modules, including a graphical user interface, a database, a preprocessor, the EnergyPlus simulation engine, an optimization engine, and a simulation run manager.

Besides the aforementioned optimization tools, there are other optimization tools that can be implemented in building optimization problems, such as modeFRONTIER® (*Shi*, 2011; *Baglivo et al.*, 2014; *Padovan and Manzan*, 2014; *Baglivo and Congedo*,

2015)(Shi 2011, Baglivo et al. 2014, Padovan and Manzan 2014, Baglivo and Congedo 2015), BEoptTM (*Parker*, 2009; *Fazli et al.*, 2015; *Rhodes et al.*, 2015; *Robertson et al.*, 2015).

2.4 Summary

This chapter gave an overview of the entire research context. The background and trends of building optimization problems are introduced first. The research content is then narrowed down to the field of FPO problems. The background of a simple genetic algorithm is specifically described. The improvement and implementation of design optimization algorithms in this field are introduced. Conclusions are reached show that there is a significant need and great potential to improve the efficiency of existing GAs to solve FPO problems. The existing optimization tools in the FPO field are also introduced. The following chapter will explain the objectives and structure of this study.

CHAPTER III

Methodology

As discussed in Chapter 2, even though GAs have been proven to be one of the most efficient optimization methodologies, they remain time-consuming when solving complex FPO problems with a great number of design variables. It is essential to improve the efficiency of the existing GA, while not affecting its robustness.

The goal of this chapter is to introduce a new evolutionary optimization methodology that is based on improvement of the simple GA. The definition of this algorithm is derived from 'adaptive radiation (AR)' - a phenomenon which was observed by Darwin, that describes the evolutionary process of species become adapted to ecological niches (*Schluter*, 2000).

The first section explains the characteristics of FPO problems, the design variables, the optimization objectives and the simulation methodology implemented in this study. The second section presents an overview of the design optimization algorithms. The distinguishing characteristics of these algorithms are highlighted, which can help to categorize the optimization problems. The third section focuses on the simple GA and its implementation in architectural design contexts. The fourth section defines AR, an explicit approach proposed to improve the simple GA with a hierarchical optimization structure and interpolation methodology. The methodology of AR is introduced, the optimization process is explained and its feasibility regardless

of FPOs is validated.

3.1 FPO Problems

A thorough understanding of the problem is a prerequisite for optimization. The modeler has to understand how the design variables will impact the solution process as well as optimal results. The mathematical model of optimization problems can describe the relationships between design variables and optimization objective(s). This requires a comprehensive understanding of the implemented formulations and the nature of the problem(s). The designed optimization model will have a significant impact on the optimization algorithm to be implemented, the setting of the optimization process, and the optimization results. Thus, this section focuses on the design variables and objective functions of FPO problems, which help to better clarify the FPO problems of this study.

3.1.1 FPO Design Variables

The design variables for FPO problems include parameters such as glazing types, infiltration, insulation and shading shapes. These design variables can be classified into different categories by their impacts on optimization objectives, such as the heating energy demand, daylighting, environmental impact and initial investment. Studies have investigated the relationship between these design variables and objective functions. For example, Yang et al. investigated the impact of U-values of the exterior wall, roof and windows on the retrofitted building envelopes in the hot summer and warm winter climate of southern China and the cold climate of northern China (*Yang et al.*, 2012). The results showed that by identifying appropriate façade design variables, the annual heating energy demand can be reduced by about 66% in cold climate of northern China, and the annual cooling energy demand can be reduced by about 33% in hot summer and warm winter climate of southern China. In

another study, the air tightness performance and its impact on residential buildings in northern China was investigated (*Chen et al.*, 2012). The results indicated that the district heating energy use can be reduced by 12.6% by reducing the average natural air infiltration from 1.0 h^{-1} to 0.5 h^{-1}.

Researchers have placed a particular focus on the impact ratio of building design variables on different design approaches. One traditional methodology is to perform a sensitivity analysis. For example, Heiselberg et al. made a comprehensive sensitivity analysis of design parameters of an office building design in Denmark (*Heiselberg et al.*, 2009). Since the heating demand was dominant in this climate with less ventilation and a lower lighting demand and no cooling demand, the result of sensitivity analysis shows lighting control and the amount of ventilation during winter are the two most important parameters to change in order to reduce energy demand. Yu et al. also conducted a sensitivity analysis of energy performance for the envelope of high-rise residential buildings (*Yu et al.*, 2013). The results indicated that the most important factors are the shading coefficient and window-to-wall ratio (WWR) in the cooling season, while the heat transfer coefficient of walls and the shape coefficient have crucial effects in the heating season. They concluded that the heat transfer coefficient of the walls and WWR play the most important role for annual energy use. Moreover, for small and large WWRs, the effects of solar absorption of the walls and the roof and the roof heat transfer coefficient are very small.

The aforementioned studies present the façade design variables that have the most significant impact on total building energy demand. The following list represents the most widely studied variables of the FPOs:

- Building shape and orientation
- Window-to-wall ratio (WWR)
- Glazing types

- Shading shapes
- Insulation
- Infiltration
- Natural ventilation
- Blind/shading control

Natural ventilation and blind/shading control systems are not within the scope of the passive façade design strategies that are discussed in this study. Also, due to the aesthetic expectations of conventional office façade design, there are also uniform requirements for window openings. Therefore, different WWRs are also not included in this study. The main design variables included in this study are glazing types, insulation, infiltration, and different parameters that affect the shapes of shading elements, which are based on the orientation and local environment of the optimization models.

Studies using conventional methodologies such as sensitivity analysis can help the designers to get an overview of how design variables affect the objectives. This can be supportive in the decision-making process by providing comprehensive design options, which leads to better guidance at the early design stage. However, as the number and complexity of design variables increase, the complexity of the FPO problems will also significantly increase. As such, it is very time-consuming to evaluate all the design variables by these conventional methodologies. In addition, the values of FPO design variables usually conflict with each other on different objective function(s) (i.e., energy demand vs. lighting comfort), which will also reduce the feasibility of conventional methodologies in achieving comprehensive solutions. Thus, a methodology of optimization is more efficient for solving FPO problems in a systematic way by providing a set of solutions based on predefined optimization objectives.

In general, the design variables of FPOs can be characterized as continuous or discrete, based on the mathematical properties of the values. Design variables that can use any values over a particular range of real numbers are continuous. For instance, the WWRs can be represented as continuous values within specified bounds, such as 20% ¡ WWR ¡ 90%. In contrast, design variables that only use certain values over a particular range of real numbers are discrete. Examples of discrete variables include sizes of standardized insulation thickness or building elements, glazing types and material selection. Most FPO problems have both continuous and discrete design variables. Sometimes mixed-discrete problems can be represented as entirely discrete problems. For instance, shading depth, which is seen as a continuous variable in some problems, can also be represented as a continuous range or incremented over discrete depths (for example, in 100 millimeter intervals). Also, the dimensions of building elements must always fit in some specific building module, which makes continuous variables almost impossible. Therefore, only discrete design variables are implemented in the optimization scenarios in this study.

The particular problem described in this chapter is the façade design of a typical office building, in order to optimize its total energy demand of heating, cooling, and artificial lighting. The façade design variables, which have a significant effect on the environmental performance of a building, are typically determined at the early design stage. The optimal values of design variables depend on the local climate, the orientation the façade is facing, the shading elements from the surrounding environment, and the function of the building (office, commercial, residential, etc.).

3.1.1.1 Glazing

Glazing is the translucent or transparent surface (like windows or skylights) which covers the opening on the building envelope. The fenestration system is a critical interface between the indoor and outdoor environment, and impacts indoor comfort,

lighting and thermal performance of perimeter spaces for commercial buildings. The key properties of glazing include thermal conductance (U-Value), solar radiation coefficient (SHGC), and visible transmittance (Tvis). Appropriate selection of the values of these glazing properties depends on factors such as the local climate, façade orientation and window-to-wall ratio (WWR). However, it is not easy to predict the impact of different glazing types on the heating, cooling, and artificial lighting energy demand.

Table 3.1: Total energy demand for different glazing system

Glazing		1	2	3	4	5	6
U-value	[W/m^2K]	6.0	2.7	1.8	1.5	1.1	0.7
SHGC	[-]	0.70	0.62	0.60	0.34	0.31	0.24
Tvis	[-]	0.88	0.80	0.65	0.65	0.47	0.30
H	[kWh]	282.5	114.8	61.5	83.7	56.6	40.3
C	[kWh]	843.5	637.8	697.7	282.8	331.6	352.5
L	[kWh]	119.8	135.7	184.7	184.7	273.0	459.0
Total	[kWh]	1245.8	888.3	944.0	551.2	661.1	851.8

Table 3.1 represents the total energy demand of the typical office room in San Francisco with different glazing systems on the southern orientation façade. It can be seen in Figure 3.1 that with southern façade, the various types of glazing have different impacts on the heating, cooling, and artificial lighting energy demand. The heating and cooling energy demands are influenced by the change of U-value and SHGC. The artificial lighting energy demand is mainly impacted by the values of SHGC and visible transmittance. On the southern façade, glazing type 1 has the lowest, a difference of 55.8%. It can be seen that changing the glazing types, especially the SHGC value, has a larger impact on the cooling energy demand on the southern façade, thus influencing the total energy demand. The results represent that the variation of glazing types, especially the SHGC values, have a significant impact on the total energy demand.

To achieve the goal of energy efficiency, different kinds of glazing may be imple-

mented in different places on the same building façade. However, the same type of glazing is usually implemented on the entire façade for aesthetic purposes.

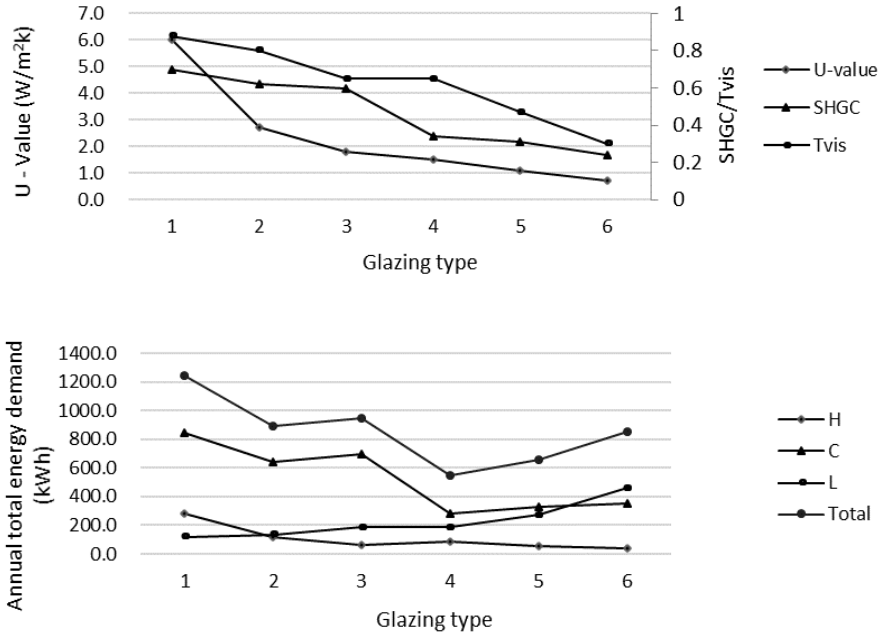

Figure 3.1: Total energy demand for different glazing system.

3.1.1.2 Insulation

The thermal insulation of the façade has an essential impact on the heating and cooling energy demands. Table 3.2 represents the energy demands on the southern façade with different insulation U-values in the climate of San Francisco. It can be seen in Figure 3.2 that both heating and cooling energy demands decrease with the increase U-value of insulation. Therefore, the total energy demand decreases as the U-value of insulation increases in this case. However, the impact of insulation is not significant. The total energy demand (when insulation is 0.19 W/m^2K) is the smallest in this case, which is only 4.5% smaller than the highest (when insulation is 0.7 W/m^2K). In this case, the results represent that improving the insulation of exterior walls does not have a significant impact on the total energy demand of south

facade.

Table 3.2: Total energy demand for different insulation

	1	2	3	4	5	6
$[W/m^2K]$	0.70	0.46	0.37	0.32	0.26	0.19
H	282.4	266.8	260.5	256.9	252.4	247.1
C	843.5	837.1	834.6	833.3	831.7	829.8
L	120.0	120.0	120.0	120.0	120.0	120.0
Total	1245.9	1223.8	1215.1	1210.1	1204.0	1196.8

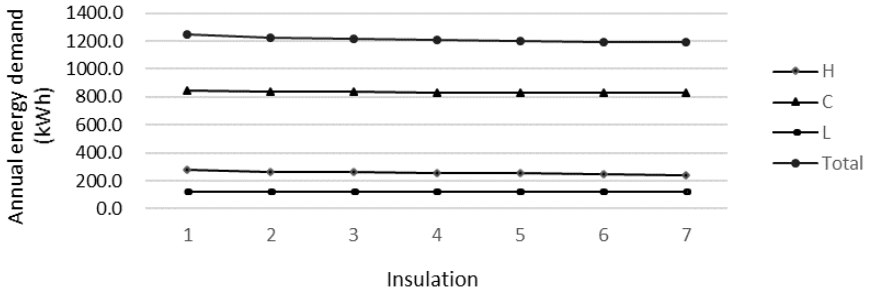

Figure 3.2: Total energy demand for different insulation.

3.1.1.3 Infiltration

Similar to thermal insulation, the infiltration value of a building façade also has a significant impact on the heating and cooling energy demands. Table 3.3 represents the impacts of different insulation values on the total annual energy demand. At first, the heating energy demand increases with the decreasing of infiltration, and then decreases. In contrast, the cooling energy demand decreases with decreasing of infiltration at first and then increases. At first, the total energy demand increases and then decreases with the improvement of infiltration. The results show that in this climate, the improvement of infiltration has a more significant impact on the heating energy demand than the cooling energy demand on the south orientation. However, the impact of infiltration is not as significant as the glazing type. When the infiltration is 0.15, the total energy demand is the smallest, which is only 4.6%

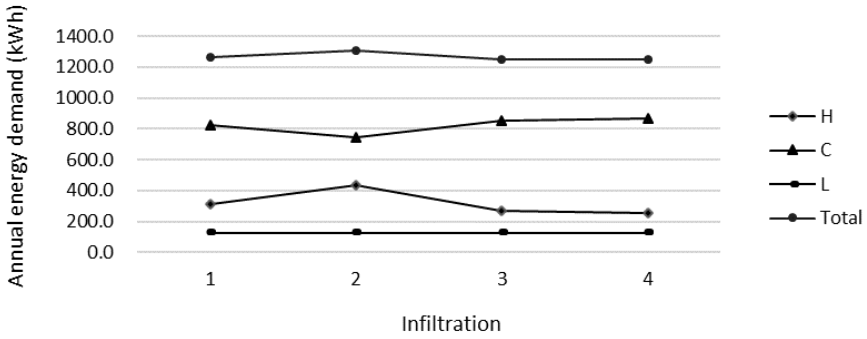

Figure 3.3: Total energy demand for different infiltration values.

smaller than the highest when infiltration is 0.18.

Table 3.3: Total energy demand for different infiltration values

	1	2	3	4
[-]	0.25	0.18	0.15	0.12
H	314.4	436.2	266.9	252.8
C	820.5	744.5	855.9	867.1
L	127.4	127.4	127.4	127.4
Total	1262.2	1308.0	1250.1	1247.3

3.1.1.4 Overhang depth

Table 3.4: Overhang depth

	1	2	3	4	5	6	7	8	9	10
[mm]	100	200	300	400	500	600	700	800	900	1000
H	282.4	281.2	284.3	290.2	289.7	294.2	297.7	297.7	303.8	302.2
C	843.6	716.9	605.8	507	428.5	364.9	311.5	311.5	240.3	207.4
L	120.0	130.4	139.6	142.8	149.4	159.7	158.9	158.9	180.3	182.9
Total	1246.0	1128.5	1029.6	939.9	867.7	818.8	768.1	768.1	724.4	692.5

Overhang shading has an essential impact on the daylight and solar radiation received by the façade, thus influences heating, cooling, and artificial lighting energy demands. In this case, the cooling energy demand decreases, while the heating and artificial lighting energy demands increase, with the increase overhang depth. The reason is that there is less solar radiation and daylight by the variation of overhang

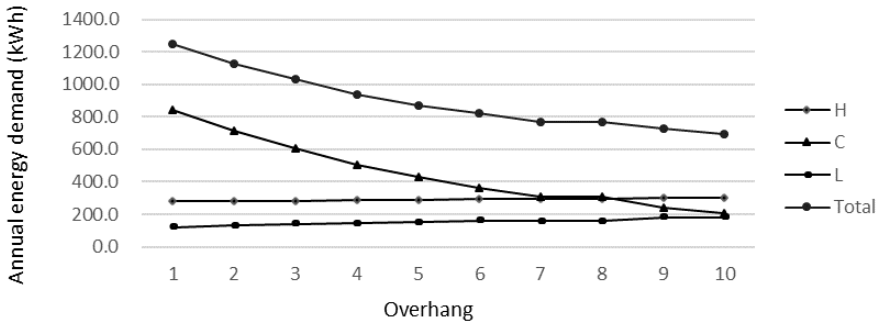

Figure 3.4: Total energy demand for different overhang depth.

depth. The total energy demand is the smallest when overhang depth is 1000 mm in this case, which is 44% smaller than the highest when overhang depth is 100 mm. The results represent that improving overhang depth has a significant impact on the total energy demand.

3.1.1.5 Vertical fin

Table 3.5: Total energy demand for different fin depth

	1	2	3	4	5	6	7	8	9	10
[mm]	100	200	300	400	500	600	700	800	900	1000
H	281.7	297.1	312.0	329.8	349.5	363.6	381.6	392.6	402.3	409.9
C	842.2	690.1	574.1	490.4	433.5	393.4	363.3	346.0	330.5	327.6
L	119.1	126.2	142.0	141.9	144.4	148.4	147.4	154.5	155.6	165.5
Total	1243.0	1113.4	1028.1	962.1	927.4	905.4	892.4	893.0	888.4	903.0

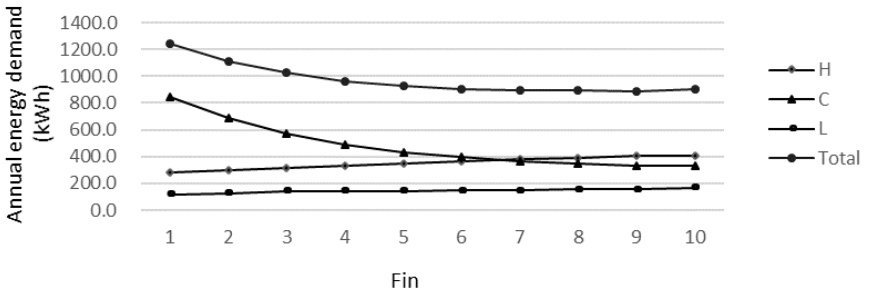

Figure 3.5: Total energy demand for different fin depth.

The fin shading system also has a significant impact on the heating, cooling, and

artificial lighting energy demands. In this case, the cooling energy demand decreases, while the heating and artificial lighting energy demands increase, with the increase of overhang depth. The reason is that there is less solar radiation and daylight by the increasing of the fin's depth. The total energy demand is the smallest when the fin depth is 1000 mm in this case, which is 27.3% smaller than the highest when the fin depth is 100 mm. The results represent that fin depth has a significant impact on the total energy demand, but not as significant as the overhang depth.

3.1.1.6 Fin angles

Table 3.6: Total energy demand for different fin angle

	1 30	2 45	3 60	4 75	5 90	6 105	7 120	8 135	9 150
H	275.3	277.4	291.5	285.0	281.7	276.5	284.4	272.0	268.4
C	893.4	893.9	784.4	861.7	842.2	836.0	778.5	851.2	849.3
L	128.3	129.1	129.9	110.7	119.1	132.1	124.5	142.2	142.8
Total	1296.9	1300.4	1205.8	1257.4	1243	1244.6	1187.4	1265.4	1260.5

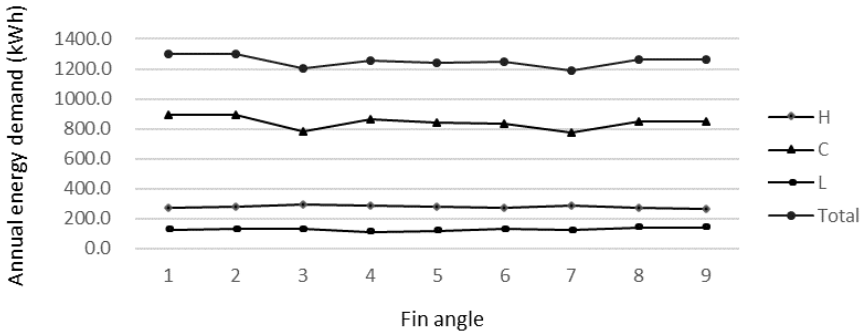

Figure 3.6: Total energy demand for different fin angles.

The angles of fins have significant impacts on how much solar radiation and daylight will get in through the window. In this case, the heating, cooling, and artificial energy demands all vary with the change of fin angle. The total energy demand is the smallest when the fin angle is 120° in this case, which is 8.7% smaller than the

highest demand when the fin angle is 45°. The results represent that fin angle has an impact on the total energy demand, but not as significant as the shading depth.

It can be seen from the results that all the façade design variables listed above will impact the total energy demand. Furthermore, the glazing type, overhang depth, fin depth have more significant impact than the insulation, infiltration and fin angle on the total energy demand. This is because cooling is domain in the climate of San Francisco. The next section discusses the combinations of these design variables and the impacts on different orientations.

3.1.2 FPO Objectives

The objective of FPOs is the function $f(x)$ that is to be optimized. Objective function can be either linear or non-linear with respect to the design variables. The goal of optimization is either to find the global minimum $\min_{x \in X} f(x)$ or maximum $max_{x \in X} f(x)$ solutions of the objectives. However, the mathematical optimization problems are usually defined as minimizations of the quantity. When the goal of an optimization problem is to achieve the maximization $max_{x \in X} f(x)$, it generally converts to minimize the objective's opposite $min_{x \in X} - f(x)$.

According to the existing research, the objectives for FPOs include but are not limited to:

- Energy demand: i.e., the heating, cooling, and artificial lighting energy demands (*Seo et al.*, 2011; *Gossard et al.*, 2013).
- Human comfort: i.e., thermal comfort (*Gossard et al.*, 2013) and lighting comfort (PVM, PPD values, discomfort hours, daylight) (*Carlucci et al.*, 2015; *Futrell et al.*, 2015).
- Cost: i.e., life cycle cost (LCC) that includes investment cost, operation cost and maintenance cost, etc. (*Keoleian et al.*, 2000; *Hasan et al.*, 2008).

- Carbon emissions: i.e., life cycle assessment (*Baños et al.*, 2011; *Weber et al.*, 2006; *Stazi et al.*, 2012; *Keoleian et al.*, 2000).

Generally, FPO problems can be either single-objective or multi-objective problems. A conventional single-objective optimization problem involves a single objective function, while a multi-objective optimization problem involves multiple contradictory objective functions. However, FPO problems usually have to achieve more than one optimization objectives. The optimization objectives usually conflict. Thus they can be considered through strategies that preserve trade-offs between two or more of them (*Coello*, 2006). There are two widely applied approaches for multi-objective optimization problems. One is the utilization of the weight function that each of the objectives is normalized with one associated weight factor, thus an entire cost function is achieved through an equation consisted of different objectives and associated weight factors. This method is efficient and simple to be implemented. However, this method requires prior knowledge of the optimization problem and does not provide information on the compromise between different objectives. Another approach is Pareto optimal or non-dominated solution. The definition of a Pareto optimal is that there is no other feasible solution that improves one objective without deteriorating another one. A set of all these non-dominated solutions is called a Pareto frontier, which can be represented as a curve. The solutions provided by the Pareto optimal method can have a great diversity. The disadvantage of this method is that it represents inadequate efficiency and effectiveness in the optimization process (*Machairas et al.*, 2014) (Figure 3.7).

The main objective of this study is to improve the existing GA rather than to achieve solutions for different FPOs. Therefore, it is mainly focusing on single-objective optimization problem to simplify the FPO model. The configuration of the FPOs can affect three terms of the annual energy demand: the heating energy demand ($Q_{heating}$), the cooling, and dehumidification energy demand ($Q_{cooling}$), and

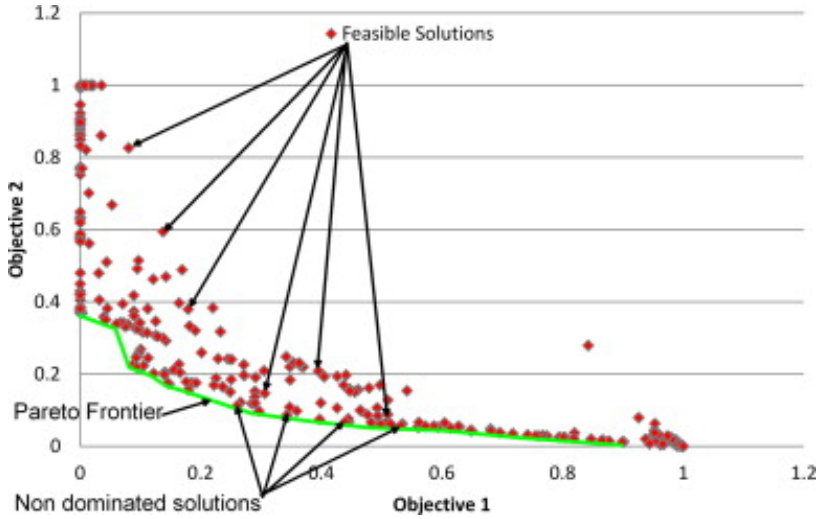

Figure 3.7: Pareto frontier of a double-objective problem(*Machairas et al.*, 2014)

the artificial lighting energy demand ($Q_{lighting}$). The other terms of building energy demands such as energy demands for ventilation, humidification and hot water are not discussed in this study. The objective function is then the minimum of total energy demand of heating, cooling, and artificial lighting.

$$\begin{aligned} \min f\{Q_{total}(\mathrm{v}_1, v_2, v_3, \ldots, v_n)\} \\ Q_{total} = Q_{heating} + Q_{cooling} + Q_{lighting} \end{aligned} \tag{3.1}$$

where $v_1, v_2, v_3, \ldots, v_n$ are the design variables according to this problem.

Climate and site environment conditions play important roles in the design of a façade system. The orientation, dimension and properties of the façade have a significant impact on both daylight and thermal performance of the perimeter zones of an office building. The hourly change of sun position, cloudiness, shading and reflection from the surrounding environment have a comprehensive effect on daylight availability and solar radiation gains on the same façade. The complexity and number of façade design variables also increase the difficulty to examine the impact of design variables on optimization objectives. Simplified modeling methods for FPO problems that were implemented in conventional studies, have been proven to be inaccurate in the pre-

diction of thermal and daylight impact. The most effective means of establishing a high-performance façade that is adapted to local climate should be through detailed, dynamic, hourly computer simulations for the specific building design, environment situation and local climate.

In FPO problems, it is essential to achieve the appropriate combination of façade design variables to keep a good balance between the heating, cooling, and artificial lighting energy demands. However, some traditional studies to configure the optimal façade design solution only include running thermal simulation, while the impact on the artificial lighting energy demand is often neglected.

In addition, the process of thermal (to obtain the heating and cooling energy demands) and lighting (to obtain the SHGC value of shading elements and lighting control schedule) simulation is interactive. For instance, small depth shading elements can lead more daylight into an internal space that may reduce artificial lighting energy demands as well as cooling energy demands. It will also bring in excessive solar gains, which may increase glare problems, thus have a significant impact on internal heating and cooling energy demands, especially for rooms on south and west orientations. Even though some studies included lighting simulations in the entire simulation process, the traditional method generally uses static simulation programs to obtain lighting and thermal energy demands in a separate simulation process, and then simply adds up the simulation results. This method neglects the hourly interactive relationship between the lighting and thermal simulations. The façade design variables should be selected based on the integrated performance indices obtained through the continuous interaction between transient hourly thermal and lighting simulations. Therefore, it is essential to integrate thermal and lighting simulations in a dynamic simulation process. This study makes a comprehensive approach of FPOs, which includes the heating, cooling, and artificial lighting energy demands.

Researchers have focused on integrated thermal and daylighting simulations in

recent years (*Franzetti et al.*, 2004). Pioneering research by Janak that provided a new method of direct run – time coupling between building energy simulation and global illuminance (*Janak*, 1997). By direct coupling at the time step level between ESP-r and RADIANCE, the building energy simulation is able to get access to an internal illuminance calculation engine, thus enabling modelling of the complex interactions between artificial lighting control and the rest of the building energy domain in a fully integrated way. Tzempelikos then implemented a systematic methodology which performed a detailed and dynamic simulation for automatic control of motorized shading in conjunction with controllable electric lighting systems (Tzempelikos and Athienitis 2007). Jakubiec and Reinhart developed a simulation program that can integrate the thermal and lighting simulation by coupling Daysim and EnergyPlus on a Rhinoceros 3D platform (Jakubiec and Reinhart, 2011). This methodology is then coupled with GA to perform a dynamic and interactive optimization process to achieve more accurate design solutions in an effective way.

In this case study, the 3D model is generated on a 3D/CAD modeling platform. The thermal simulation-based on EnergyPlus and the lighting simulation-based on Radiance are dynamically integrated to achieve the annual total energy demand Q_total. The Rhinoceros/Grasshopper platform can prepare 3D/CAD models for complex façades, which is not executable in EnergyPlus platform. At present, there are limited user interfaces specifically designed for the implementation of optimization algorithms in architectural design. This workflow represents a visualization platform between 3D/CAD modeling, building simulation and optimization process, and provides quick feedback of architectural design variables, which helps architects to make design decisions at the early design stage and scrutinize the results clearly.

An optimization program is implemented to run AR optimizations and make a call to the EnergyPlus and Radiance simulation runs on the Rhinoceros/Grasshopper platform. The optimization process is initiated by executing the optimization pro-

gram, which accept the design variables to be optimized from the input file. Then, the optimization engines execute Radiance and EnergyPlus scene files by replacing these design variables in template files with the values of variables for the initial run. Thirdly, the optimization engines execute a script that coordinated the execution of Radiance and EnergyPlus. Radiance is executed first to achieve annual hourly illuminance values, which are implemented to calculate the annual lighting schedules. EnergyPlus is then executed to achieve the total energy demand of heating, cooling, and artificial lighting. After all the simulations are complete, the optimization engines evaluate the achieved objective function Q_{Total} and produce the design variables for the next generations. This process will continue until AR meets its convergence criterion.

Since EnergyPlus calculates illuminance based on the daylight factor method (*Tregenza*, 1980), which is not dynamic. The ray-tracing software Radiance is utilized in conjunction with EnergyPlus to achieve hourly illuminance values since it uses the daylight coefficient method (*Tregenza*, 1983). The sky model is divided in to 578 patches for the daylight coefficient method in Radiance. Additionally, these scripts calculate the annual hourly lighting schedules that account for the electric lighting control for the EnergyPlus simulations. For each hour in the office room, a scalar between 0.1 and 1 is produced to bind the lighting power density to a level that complement the amount of illuminance value on the work plane. The reduction in electricity consumption by daylight is accounted for thus, together with the associated reduction in artificial lighting heat gains. Hourly lighting schedule is obtained through Radiance, which is based on a target illuminance of 500 lux on the work plane.

$$L = \begin{cases} 0, \text{ if E} \geq 500 \\ 1, \text{ if E} < 500 \end{cases} \tag{3.2}$$

where

L = lighting power scalar value for current hour

E = average zone illuminance for current hour

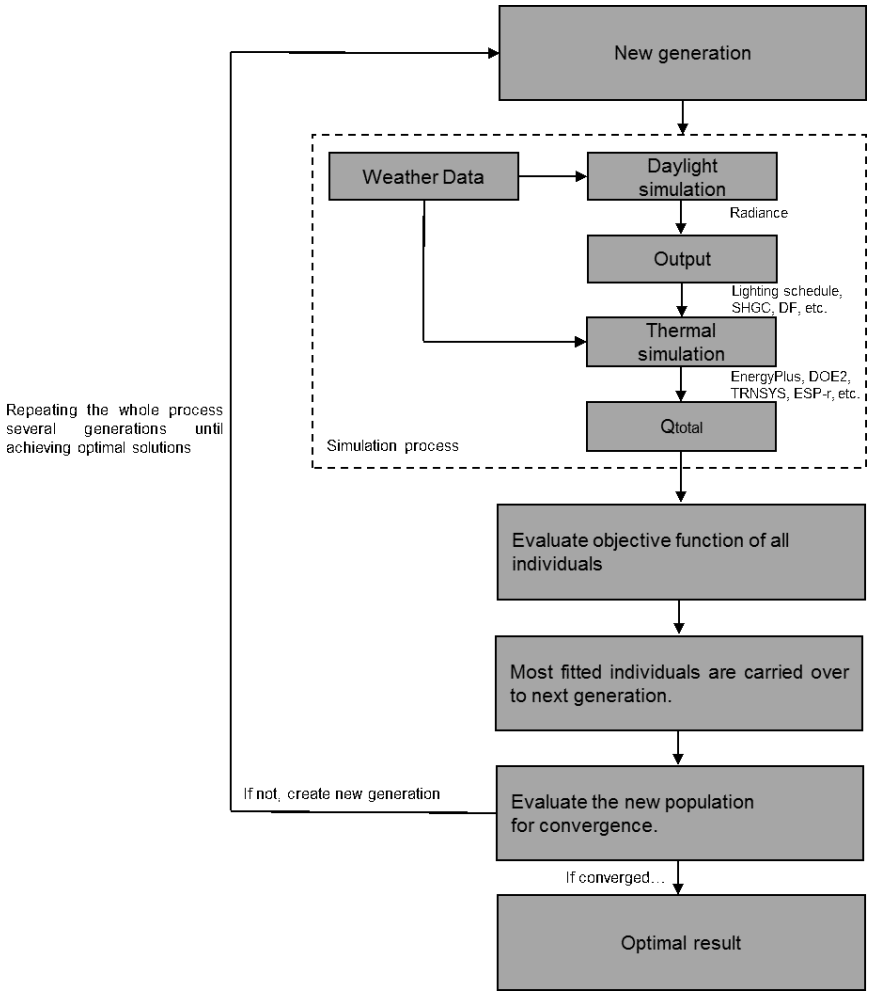

Figure 3.8: The integrated GA and whole building energy simulation.

The objective function of optimization is thus the result of running EnergyPlus thermal simulation of the office room under study, which in the simplest case is the annual energy demand of heating, cooling, and artificial lighting, based on the lighting schedule obtained thru lighting simulations. The energy model is simulated based on the same EPW weather file of the U.S. cities implemented to obtain the hourly illuminance results. The simulation module performs the evaluation of the design variables, and returns its fitness function value to the optimization engine.

This value is sent to the AR algorithms to guide the generation progression. When the AR reaches the last population, the corresponding solutions can be fed back to the 3D/CAD modeling module to perform visualization models for the architects. Figure 3.8 shows the workflow of integration of GA and whole building energy simulation programs.

3.1.3 Solution Space of Variable Combinations

The solution space for combinations of two selected of the façade design variables are examined in this section.

Figure 3.9 shows the solution space for the combinations of insulation and fin angle of the four orientations. Seven exterior wall insulations and nine fin angles are considered at discrete steps, creating a solutions space of 70 for each orientation. In general, the solutions spaces have several local minima and a global minimum for all orientations. The existence of local minima and its similarity with the global minimum makes derivative-based search method inappropriate in solving FPO problems. Therefore, GA is a reasonable approach.

Figure 3.9 (a) shows the solution space for the south-orientation façade. It can be seen that there is a relatively flat surface of configurations corresponding to low energy demand. Within that flat surface there are however several local minima and a global minimum. Being trapped in a local minima would not be too serious in this case since the objective function difference in relation to the global minimum is small. The global minimum of 1129.9 kWh is located at point (7, 7), corresponding to fin angle 120° and insulation 0.12 W/m^2K. There are a couple of local minima when the fin angle is 120° or 60°, which shows the effect of accounting for fin angle in the space.

For the east orientation the global minimum is sharper than the south orientation (Figure 3.9 (b)). The global minimum of 851.1 kWh is located at point (1, 7),

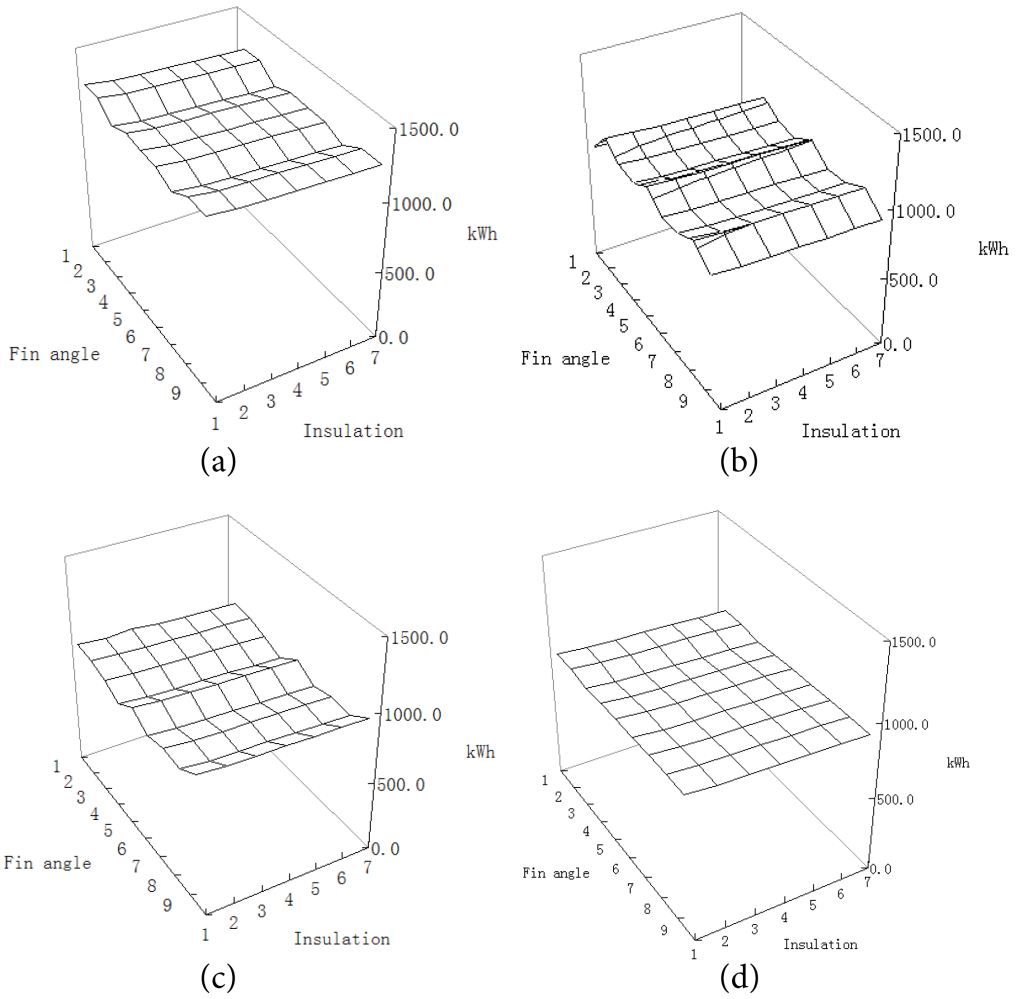

Figure 3.9: Annual energy demand [kWh] on different orientations for the design variables of fin angle and insulation.

corresponding to fin angle 30° and insulation 0.12 W/m^2K.

For the west orientation the global minimum is consistent with the south orientation (Figure 3.9 (c)). The global minimum of 790.2 kWh is located at point (4, 7), corresponding to fin angle 75° and insulation 0.12 W/m^2K.

For the north orientation the global minimum is flatter than the other orientations (Figure 3.9 (d)). The global minimum of 841.3 kWh is located at point (3, 7), corresponding to fin angle 60° and insulation 0.12 W/m^2K.

It could be seen that all the local minima on the four orientations happened when the insulation is 0.12 W/m^2K. However, there is a tiny difference in energy demands

for different insulation values when the fin angles are the same. Therefore, there is great potential that the optimization result will be trapped in the local minima which is close to the global minimum.

Figure 3.10 shows the solution space for the combinations of glazing types and overhang dimension of the four orientations. Six glazing types and ten overhang depths are considered at discrete steps, creating a solution space of 60 for each orientation. Similar to the insulation vs. fin-angle problem, the solutions spaces have several local minima and a global minimum for all orientations.

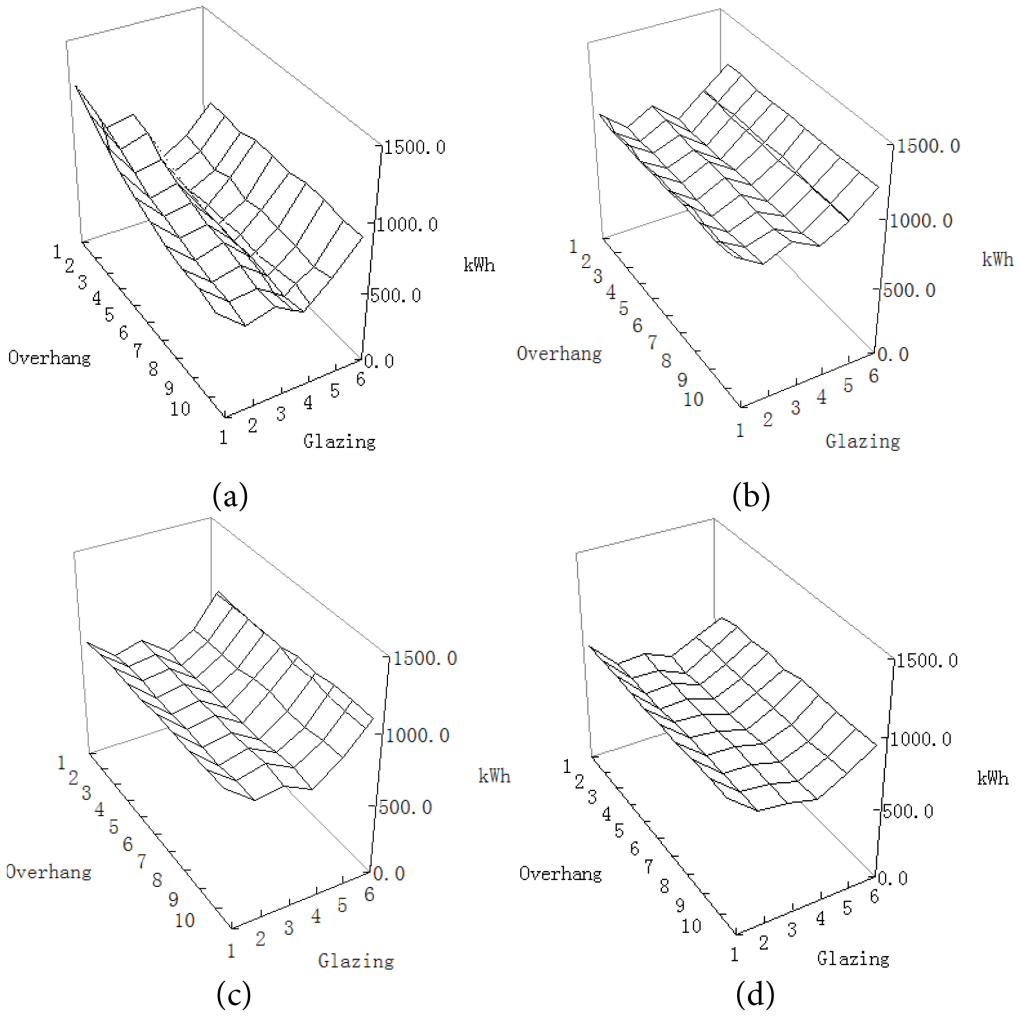

Figure 3.10: Annual energy demand [kWh] on different orientations for the design variables of glazing type and overhang depth.

Figure 3.10 (a) shows the solution space for the south-orientation façade. It can

be seen that there is a relative flat surface of configurations corresponding to low energy demand. Within that flat surface there are however several local minima and a global minimum. The global minimum of 443.2 kWh is located at point (9, 4), corresponding to a 900 mm overhang depth and glazing type 4. There are a couple of local minima when the glazing is type 4, which shows the effect of accounting for SHGC value in the space.

For the east orientation the global minimum is sharper than the south orientation (Figure 3.10 (b)). The global minimum of 828.6 kWh is located at point (2, 4), corresponding to a 200 mm overhang depth and glazing type 4. There are a couple of local minima when the glazing is type 4, which also shows the effect of accounting for SHGC value on this orientation.

For the west orientation the global minimum is similar to the south orientation (Figure 3.10 (c)). The global minimum of 674.2 kWh is located at point (1, 4), corresponding to 100 mm overhang depth and glazing type 4.

For the north orientation the global minimum is flatter than the other orientations (Figure 3.10 (d)). The global minimum of 641.6 kWh is located at point (2, 4), corresponding to 200 mm overhang depth and glazing type 4.

It could be seen that all of the local minima on the four orientations were seen when the glazing is type 4. However, there is a tiny difference in the energy demand for different overhang depths when the glazing types are the same. Therefore, the optimization will be easily trapped in the local minima next to the global minimum.

These solution spaces in Figure 3.9 and Figure 3.10 show that there are several local minima and a global minimum for all orientations. The presence of local minima makes the 'trial and error' or derivative-based search methods infeasible for façade optimization problem.

3.2 Adaptive Radiation

3.2.1 Overview

Adaptive radiation is an evolutionary phenomenon in biology wherein a group of animal or plant species develops into a wide variety of types to be adapted to specialized modes of different living environments. This phenomenon was first observed by Charles Darwin on the Galapagos Islands, where he observed native birds from the same family, in which different finches evolved to adapt to their different living environments (Figure 3.11). Darwin then named this phenomenon Adaptive Radiation. There are four features that are identified by Schluter of adaptive radiation (*Schluter*, 2000): (1) a common ancestry for subsequent species, (2) a phenotype-environment association, (3) trait utility, and (4) rapid speciation.

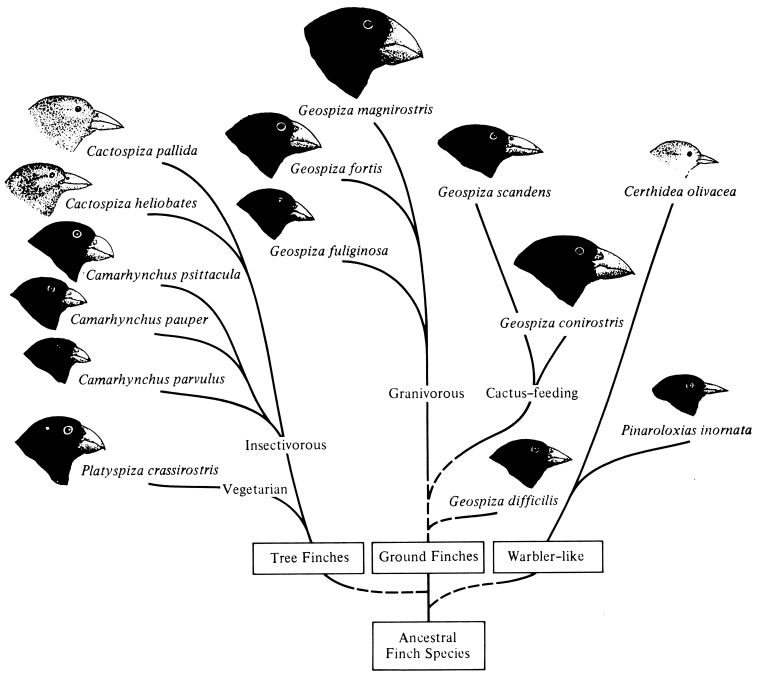

Figure 3.11: Phylogeny of the Galapagos finches. [Phylogenetic tree after Lack (1947); head sketches from Grant (1986) after Swarth and Bowman.]

Similar to the Galapagos finches, design variables of building façades also have to develop their own features to adapt to the local climate. A climate adaptive façade

should be a building shell with climate adaptive characteristics, which have excellent energy performance while maintaining a comprehensive series of objectives such as energy conservation, thermal comfort, cost efficiency and environmental friendness.

Also, with the development of industrial manufacturing technology, modern architectural design tends toward complex façades. Since the building also has to adapt to its site environment, the shapes of windows or shading elements can also be different on varied positions of a façade, which means architects and engineers nowadays have to solve FPO problems with great complexity.

Take for example, a typical square-plan mid-rise office building located in an urban area surrounded by several existing mid-rise or high-rise constructions that may block the annual illuminance and solar irradiation on the office building façade. The constrcutions on the south or east orientation may cast shadows on the neighboring south and east windows, while the reflection from the ground and the surrounding façades will also reflect daylight on the neighboring windows, therefore increasing the solar radiation for these windows. To achieve the optimal façade design solutions, each window should have a specific solution. For a typical 5-floor office building with 5 windows on each orientation, there are 100 different windows in total. In the GA process, it is very common to spend several hours running simulations for one window (depending on the number and complexity of design variables), so the simulation time for the entire façade optimization will be multiplied by 100 times, which means several hundred hours, or half a month. This is not feasible in architecture firm, especially at the early design stage.

For a flexible organic shape high-rise office building located in a more complicated environment, the simulation time will be significantly increased since each window has a unique orientation, which greatly increases the complexity of the FPO problem. As contemporary architectural design tends toward organic, geometric and parametric shapes, it is imperative to improve the existing GA optimization, to reduce the

simulation time at the early design stage.

3.2.2 Formulation and Coordination

The Adaptive Radiation algorithm in this study is an improvement of simple GA to solve FPOs with great complexity. The main methodology of the AR is to divide the entire optimization process into different niches and then solve them step by step. Instead of treating all the design variables equally, AR places the variables with the same characteristics in the same niche of the optimization process. Additionally, AR won't execute optimization for all of the design variables. Instead, AR will achieve the optimization solutions by making interpolations based on the optimization results achieved in the former optimization steps. AR can find the common features of the design variables and prevent optimization tasks for unessential design variables, therefore largely reduce the simulation times compared to a simple GA.

A nonlinear minimization problem is an optimization problem of the form:

$$\begin{aligned} & \min f(x) \\ s.t. \quad & g(x) \geq 0 \\ & h(x) = 0 \\ & x \in R^n \end{aligned} \tag{3.3}$$

For nonlinear problems, solutions are difficult to find when n is large and $f(x)$, $g(x)$ or $h(x)$ are very nonlinear, have many components, or are expensive for simulation.

For a hierarchical nonlinear problem,

$$
\begin{aligned}
& \min f_0(x_0) + \sum_{j=1}^{p} f_i(x_0, x_j) \\
& x \in R^n \\
s.t. \quad & g_0(x_0) \leq 0 \\
& h_0(x_0) = 0 \\
& g_j(x_0, x_j) \leq 0 \\
& h_j(x_0, x_j) = 0 \\
& j = 1, \ldots, p
\end{aligned}
\tag{3.4}
$$

where n and p are positive integers. Let f, g_i, and h_j be real-valued functions on x for each j in $1, \ldots, p$.

Linking variables: a vector of variables x_0 common to all groups of functions.

Sub-problems: A group of functions which depends only on the vector of linking variables and upon a single sub-vector x_j. Often written as a small nonlinear problem

$$
\begin{aligned}
& \min f_j(x_0, x_j) \\
& x_j \in R^{n_j} \\
s.t. \quad & g_j(x_0, x_j) \leq 0 \\
& h_j(x_0, x_j) = 0
\end{aligned}
\tag{3.5}
$$

There are several main advantages of hierarchical optimization: (1) it can transform a large FPO problem into smaller manageable pieces; (2) each sub-problem is autonomous; (3) it allows for parallel implementation; and (4) smaller problems are easier to solve.

The main process of AR is to decompose the optimization problem hierarchically. Different decomposition strategies can be implemented in the AR process based on the characteristics of the FPO problem. The problem can be decomposed into sub-problems by the physical components (for example, zones and components), by sim-

ulation performance (for example, lighting and thermal simulation), or by design variable characteristics (for example, variables that stay unchanged and parameters that keep changing during the entire optimization process). Once the FPO problem has been decomposed appropriately, different optimization algorithms can be implemented based on the characteristics of each sub-problem. There are horizontal and vertical links between these sub-problems. Each sub-problem will take the variables and parameter settings as input from the sub-problem of its upper level, and generate new variables and parameter settings as the output.

Figure 3.12 shows an example of one optimization system which is decomposed into five sub-problems (1, 2, 3, 4 and 5) with four design variables (A, B, C and D). The AR optimization is executed through four stages from Level 1 to Level 4. On Level 1, the problem is decomposed into five sub-problems (1, 2, 3, 4 and 5) based on their individual locations. On Level 2, the values for design variables A_x, B_x, C_n and D_n are achieved for all the sub-problems. The values of linking variables A_x and B_x are treated as parameters, those for all sub-problems are the same and stay unchanged during the entire optimization process. The values of the design variables C_n and D_n are different for each sub-problem. On Level 3, the unchanged design variables A_x and B_x are passed down from the upper level (Level 2), while each sub-problem achieves its own design variable $C_1, C_3, C_5, D_1, D_3, D_5$. On Level 4, the sub-problem 2 and 4 achieve the value of their design variables C_2, C_4, D_2, D_4, by the method of gradient interpolation, based on the values of $C_1, C_3, C_5, D_1, D_3, D_5$ that achieved on Level 3.

The plan of office buildings can be either square-plan or free-form plan. The traditional square-plan has four orientations, such as south, north, east and west. Since windows on different orientations achieve varied solar radiation and daylight, individual solutions should be considered for each window. For a free-form facade, there is no clear boundary between the orientations. But the optimization process can also begin with achieving solutions on several typical sub-problems on different

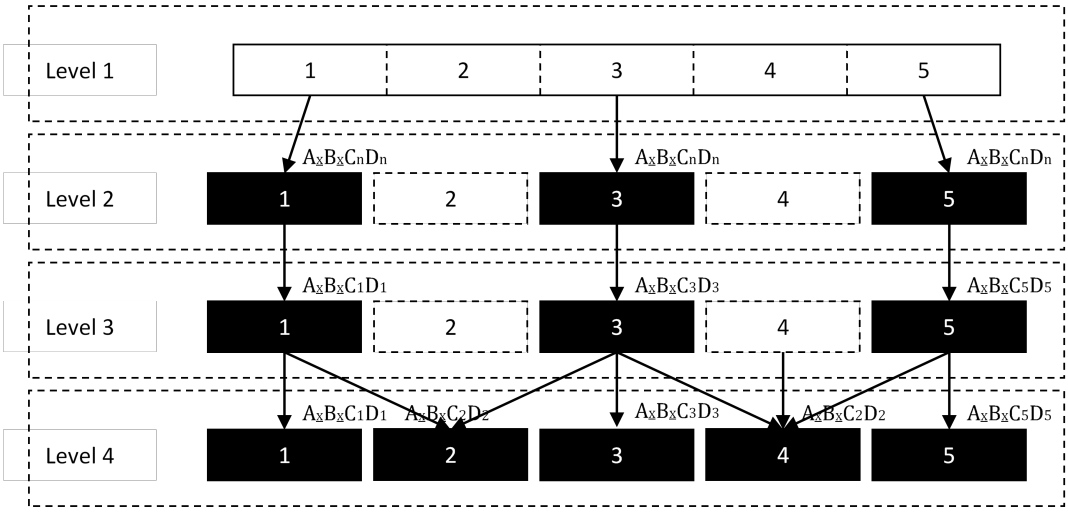

Figure 3.12: Workflow of Adaptive Radiation: a three-level process with four design variables (A, B, C and D) and five façade decompositions (1, 2, 3, 4 and 5).

orientations first, and then make interpolations between the achieved optimal results, to accomplish solutions for the remaining the sub-problems. Take for example, a typical 5-floor office building that has five windows on each orientation for each floor; an Adaptive Radiation optimization procedure in solving this FPO problem is as follows:

$$\begin{aligned} & \min_{x \in X} f(x) \\ s.t. \quad & a, b, c, d \subset R^n \end{aligned} \tag{3.6}$$

where $\min f(x)$ is the objective function (cost function or optimization criterion) to be optimized, $a \in A, b \in B, c \in C, d \in D$ are the vectors of design variables, $x \subset R^n$ is the constraint set.

x is a constant value for all design variables, which will be stay unchanged on the next levels;

n can be any number within the range of the design variables, which will be changed on the next levels.

Level 1: The first level of setting up an AR process is to decompose the entire

façade model into different sub-problems (based on individual orientations and floors in this case study). Then several specific sub-problems are selected to execute GA optimization on Level 2. As shown in Figure 3.13, each floor of the south façade is decomposed into 5 individual sub-problems ($S_{n-1}, S_{n-2}, S_{n-3}, S_{n-4}, S_{n-5}$) by the positions of windows. Sub-problems 1, 3, and 5 ($S_{n-1}, S_{n-3}, S_{n-5}$) are then selected for the next level of AR optimization.

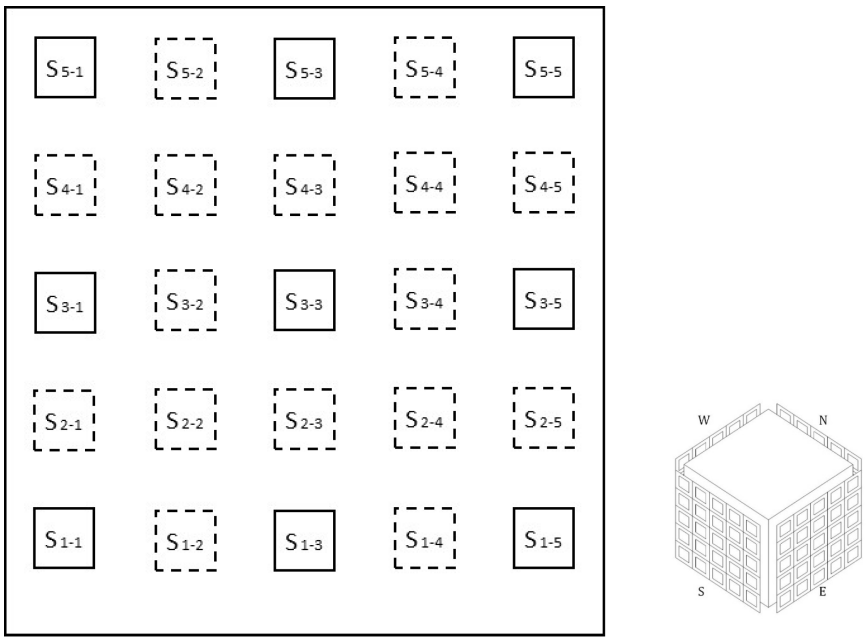

Figure 3.13: Level 1 Decomposition

Level 2: Execute optimization for all the design variables that will stay unchanged for the sub-problems, such as the glazing types or the wall insulation. Even though different windows on the same façade will receive varied amounts of annual solar radiation and daylight due to their diverse orientations and positions, which will lead to different material selections to achieve the minimum annual energy demand, these variables should be kept at the same value for the entire façade due to the aesthetic requirement and construction feasibility. On this level, the optimal solutions for glazing types and wall insulation can be achieved.

As show in Figure 3.14, the goal of Level 2 is to achieve the optimal value $minf(x)$

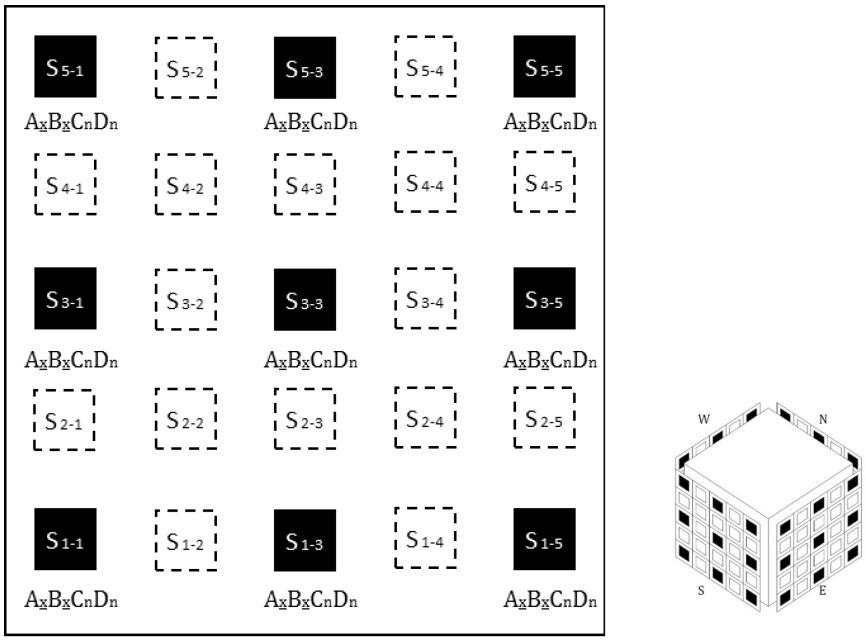

Figure 3.14: Level 2 Optimization for the unchanged design variables A and B

for the unchanged design variables such as glazing type and wall insulation (design variables A and B on this level) for the different window positions ($S_{n-1}, S_{n-3}, S_{n-5}$) and different floor heights (S_1, S_3, S_5). There are thus 9 (3 positions $\times$ 3 heights) subproblems ($S_{1-1}, S_{1-3}, S_{1-5}, S_{3-1}, S_{3-3}, S_{3-5}, S_{5-1}, S_{5-3}, S_{5-5}$) in total on this level. Just as the windows on different orientations receive varied solar radiation, the windows on the top floors ($S_{5-1}, S_{5-3}, S_{5-5}$) can receive more solar radiation and daylight, while the windows on the ground floors ($S_{1-1}, S_{1-3}, S_{1-5}$) are more affected by shadow casted by surrounding buildings. Also, the windows on the ground floors ($S_{1-1}, S_{1-3}, S_{1-5}$) also have the potential to receive more daylight compared with the upper floors ($S_{2-1}, S_{2-3}, S_{2-5}$) because they can receive more daylight from the ground reflection.

Level 3: Execute optimization for the sub-problems to achieve values for the changing design variables C and D. Keep the value of A_x and B_x achieved from the upper level unchanged, and run optimization for daylight-related design variables such as window-to-wall ratio, window shape, shading depth and shading angle (the

design variables are C and D in this case study). The design optimization solutions for each sub-problem can be achieved for each selected window at this step ($C_{1-1}D_{1-1}, C_{1-3}D_{1-3}, C_{1-5}D_{1-5}, C_{3-1}D_{3-1}, C_{3-3}D_{3-3}, C_{3-5}D_{3-5}, C_{5-1}D_{5-1}$, $C_{5-3}D_{5-3}, C_{5-5}D_{5-5}$) (Figure 3.15).

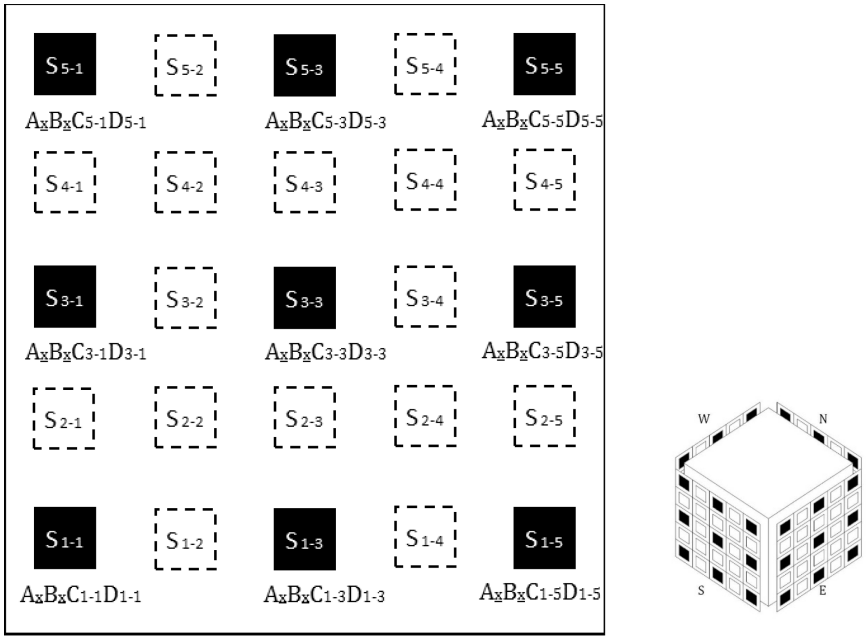

Figure 3.15: Level 3 Optimization for changing design variables

Level 4: Based on the optimization result achieved from Level 3, make interpolation to get the optimal or near-optimal solutions for the remaining the sub-problems on the same floor, since the change for design variables such as WWR, shading depth and shading angle is due to gradient impact from daylight or solar radiation. Computation time can be remarkably reduced by this interpolation methodology (Figure 3.16).

Level 5: Make interpolation and achieve the optimal or near-optimal solutions for sub-problems between different floors (Figure 3.17). Repeat the process until all sub-problems achieve their individual optimal solutions (Figure 3.18).

The main advantage of AR is that the computation time can be substantially reduced by the methods of hierarchical optimization and interpolation, which can

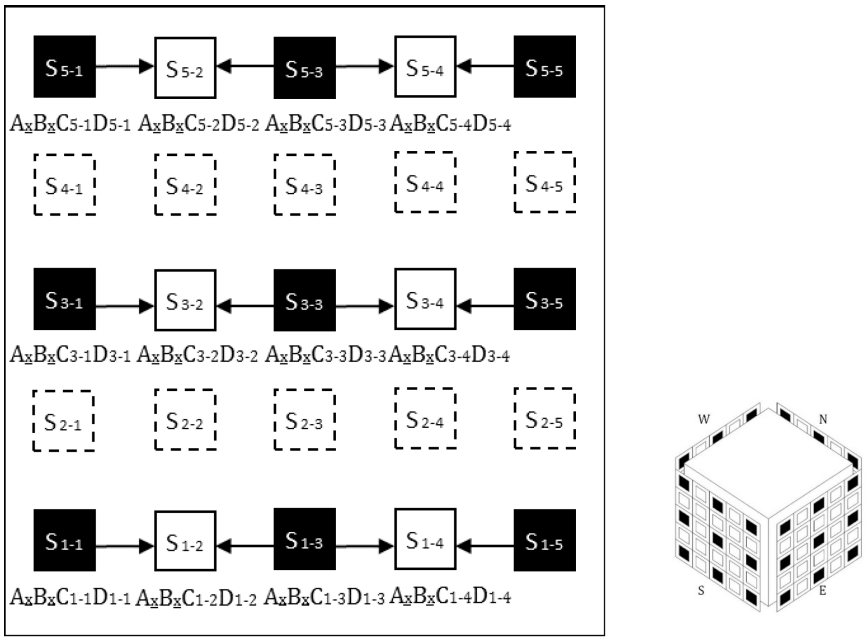

Figure 3.16: Level 4 Horizontal gradient interpolation

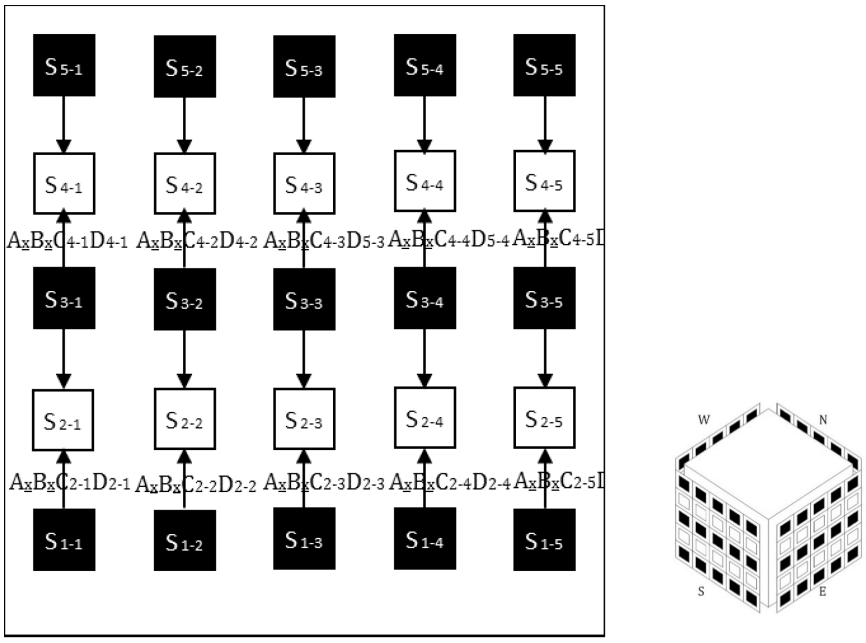

Figure 3.17: Level 5 Vertical gradient interpolation

prevent processing unessential simulation runs. Figure 3.19 represents a hierarchical workflow of the entire optimization process (Shan 2015) (https://www.researchgate.net/publication/299497585_Hierarchical_optimization_workflow_of_Adaptive_Radiation). The detail of the optimization process is described in the case studies in the next

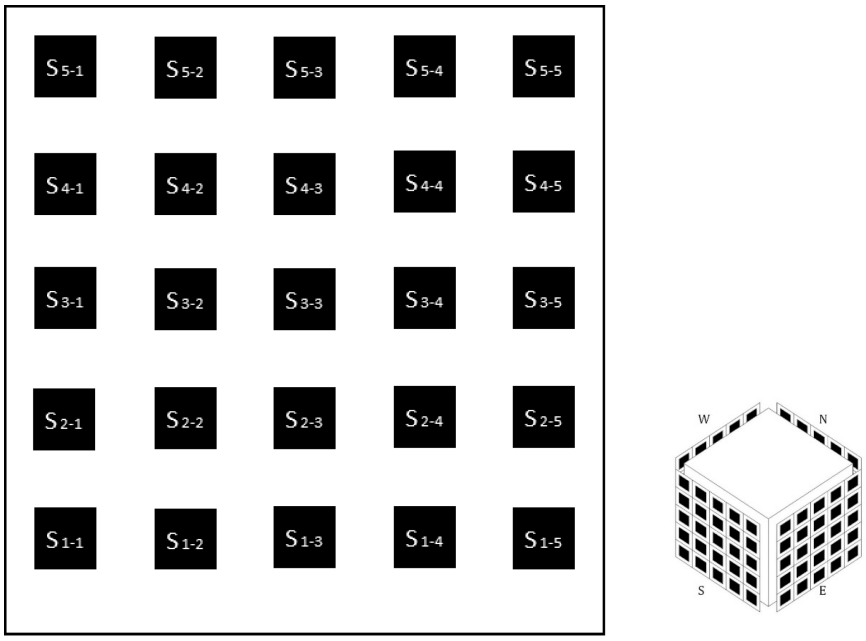

Figure 3.18: End of Adaptive Radiation

chapters.

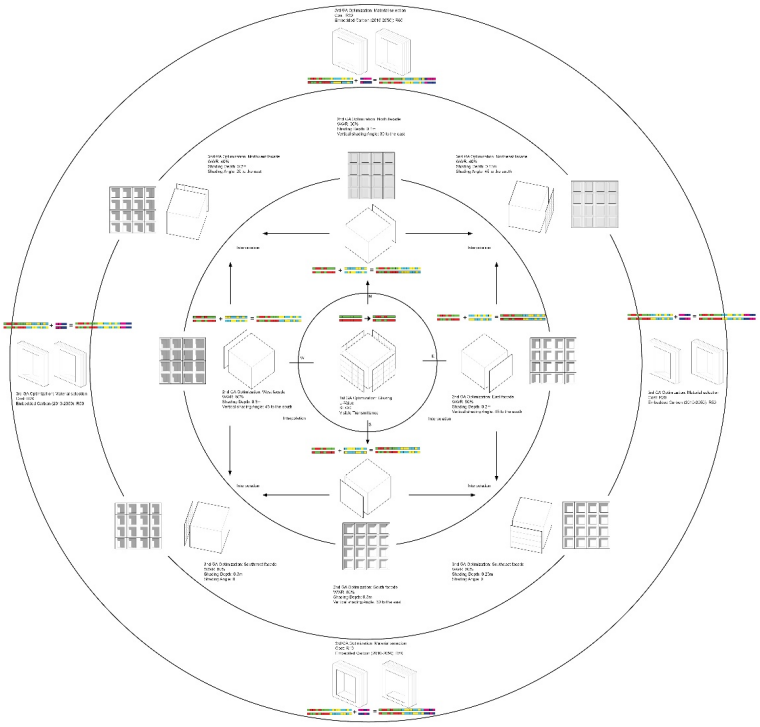

Figure 3.19: Hierarchical optimization workflow of Adaptive Radiation

3.3 Summary

Following an overview of the design optimization algorithms and simple GA, this chapter presents a simulation-based hierarchical optimization methodology, which is based on improvement of the simple GA. The following chapters extend and validate this methodology through a couple of façade design scenarios in different climates.

CHAPTER IV

Case Study

This chapter describes the first implementation test of the AR in an FPO problem in a design scenario. The objective of the test is to gain validation in AR's performance before implementing it in more different climates. A prototype of a typical mid-rise office building is shown. Simple GA is also used in this prototype to validate the efficiency and robustness of AR by comparing the simulation time and optimization results. The optimization results validate the feasibility of AR in FPOs.

4.1 Case Study Definition

An FPO problem for a typical mid-rise office building is shown below. The model is located in a proposed site that is surrounded by several high-rise or mid-rise constructions, which create shadows and reflections, affecting the annual total energy demand of each office room (Figure 4.1). The design scenario in this chapter is tested for the climate of San Francisco, California, a cooling-dominated situation. The next chapter will represent the implementations of AR for two other locations: Miami, Florida, a cooling-dominated climate; and Chicago, Illinois, a heating-dominated climate. The aim is to provide some insight on how the optimal values of façade design variables vary with different climatic conditions.

The climate of San Francisco is characterized by cool summers and temperate

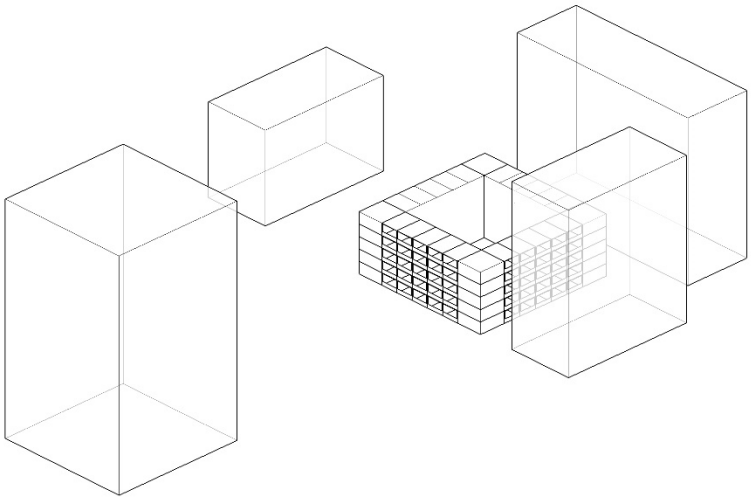

Figure 4.1: Building environment

winters with extremely rare snow. The summer has average maximum temperatures between 15°C and 21°C (60°F and 70°F), and minima between 10°C and 13°C (50 °F and 55 °F). Winter has high temperatures between 13°C and 15°C (55 °F and 60 °F) and low temperatures in the 7°C and 10°C (45 °F to 50 °F) range. The psychrometric chart shows that cooling is dominant in this climate (Figure 4.2).

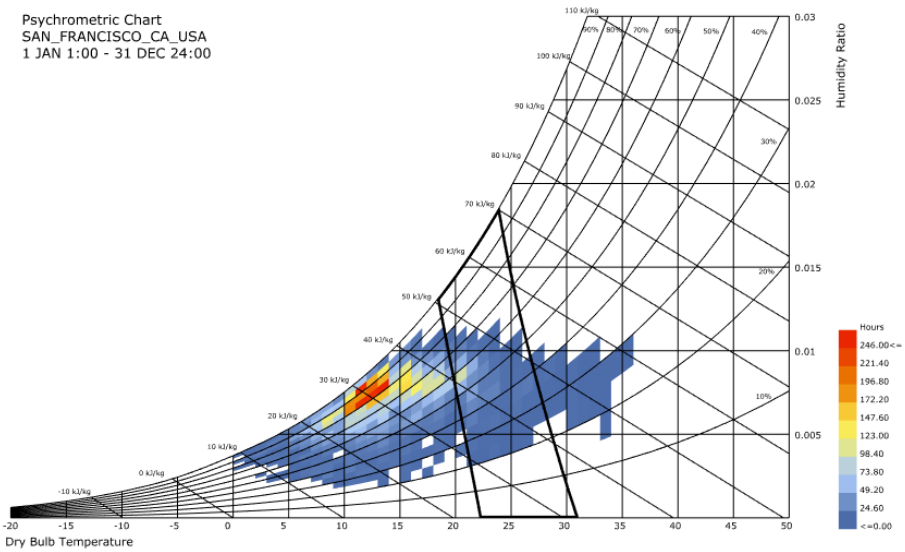

Figure 4.2: Psychrometric chart of San Francisco, CA, United States

The shade from the surrounding buildings and the reflections from the environment both have a significant impact on the solar irradiation and daylight on the façade of each office room. Figure 4.3 shows the variation of shading and radiation on the building façade on different dates and times throughout the year.

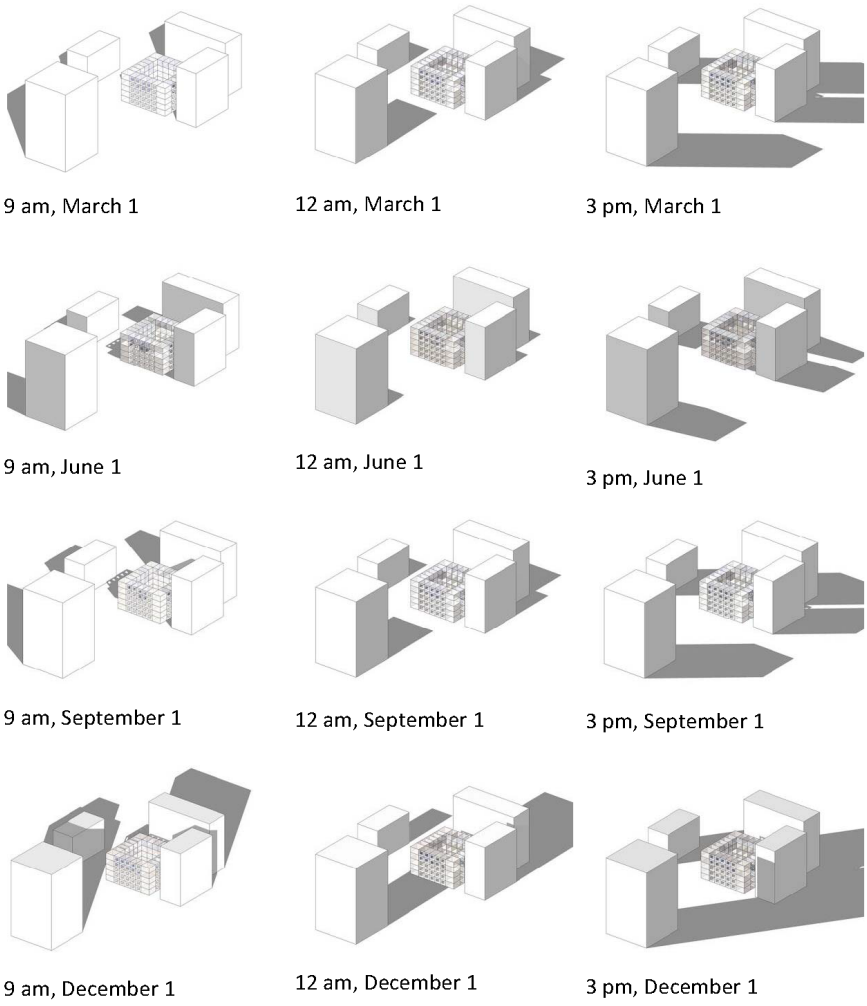

Figure 4.3: Annually variation of shading on the façade – San Francisco

The office building model has five floors. On each floor, there are five typical office rooms on each orientation. Therefore, there are 100 rooms total (4 orientations $\times$ 5 windows on each orientation $\times$ 5 floors) in this design scenario. For each window, different combinations of design variables should be considered to achieve the optimal solution, which means there are total 100 ($5 \times 5 \times 4$) sub-problems to be solved in

this umbrella FPO problem (Figure 4.4).

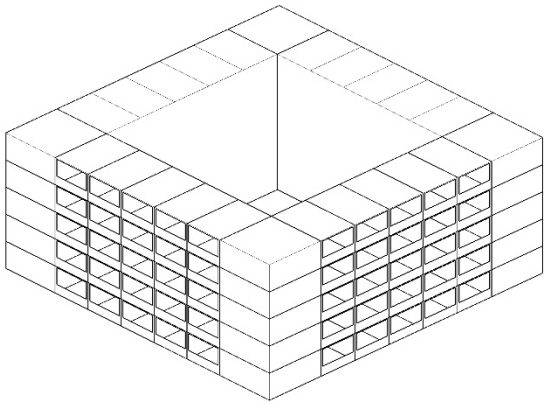

Figure 4.4: Case study: office building model

Figure 4.5 shows a 3D model of each typical office room. Each single-occupant office room has an area of 24 m^2, a volume of 57.6 m^3 (4m $\times$ 6m $\times$ 2.4m) and a window area of 3.2 m^2. For internal heat gains, the office room is assumed to have equipment heat gain of 9 W/m^2, artificial lighting heat gain of 13 W/m^2 (2 desktop computers, 2 monitors and 1 printer), and an occupancy of 0.1 $person/m^2$. The entire office building is assumed to be fully occupied on weekdays between 8 AM and 5 PM with a 1 hour break at noon. A daylight sensor is placed at a 1-meter high work plane, while the minimum illuminance set for the photo sensor is 500 lux. The lighting power density is 11.74 W/m^2.

Table 4.1: Model setup

Parameter	Value
Lighting power density	11.74 W/m^2
Equipment power density	9 W/m^2
Occupancy density	0.1 $person/m^2$
Floor	adiabatic
Ceiling	adiabatic
Inner walls	adiabatic

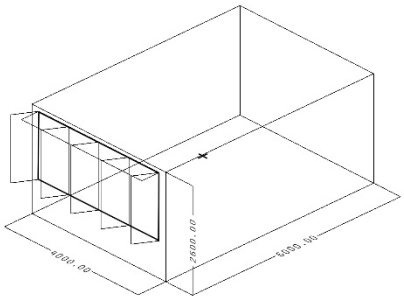

Figure 4.5: Building environment

4.2 Optimization Setup

Table 4.2: Variable Settings

Variable		Variable settings									
Glazing	(v_1)	1	2	3	4	5	6				
U-value	$[W/m^2K]$	6	2.7	1.8	1.5	1.1	0.7				
SHGC	[-]	0.7	0.62	0.6	0.34	0.31	0.24				
Tvis.	[-]	0.88	0.8	0.65	0.65	0.47	0.3				
Insu.	(v_2)	1	2	3	4	5	6	7			
U-value	$[W/m^2K]$	0.7	0.46	0.37	0.32	0.26	0.19	0.12			
R-Value		8.1	12.3	15.4	17.7	21.8	29.9	47.3			
Infil.	(v_3)	1	2	3	4						
ACH	[-]	0.25	0.18	0.15	0.12						
Fin	(v_4)	1	2	3	4	5	6	7	8	9	10
	[mm]	100	200	300	400	500	600	700	800	900	1000
Overhang	(v_5)	1	2	3	4	5	6	7	8	9	10
	[mm]	100	200	300	400	500	600	700	800	900	1000
Fin angle	(v_6)	1	2	3	4	5	6	7	8	9	
	[°]	30	45	60	75	90	105	120	135	150	

The proposed method is evaluated on a façade optimization problem with six design variables (Table 4.2). The total combinations of different design variables values is 151,200. These combinations in this case study can represent most of the varieties of the building façade design. The façade design variables of this FPO problem include: (a) the type of glazing (v_1); (b) wall insulation (v_2); (c) infiltration

(v_3); (d) the depth of vertical shading elements (window fins) (v_4); (e) the shading depth of window overhang (v_5); and (f) the rotation angle of vertical shading elements (window fins) (v_6).

Objective function

Generally the total energy demand for a typical office room is mainly consisted of space heating, space cooling, and artificial lighting. A climate-based calculation methodology is implemented here to estimate the total building energy demand, Q_{total}, which is the objective function of this study:

$$Q_{total} = Q_{heating} + Q_{cooling} + Q_{lighting} \tag{4.1}$$

where

$Q_{heating}$ – energy demand for space heating [kWh];

$Q_{cooling}$ – energy demand for space cooling [kWh];

$Q_{lighting}$ – energy demand for artificial lighting [kWh].

The population size is kept in a relatively small size in this study (n = 20). The optimization process will stop after repeating 10 generations without improvement for the objective function. If there improvement of the objective function happened, GA will run further optimizations and stops when there is no improvement in the next 10 generations. This logic is proved to be a valuable choice, since extending that number to 20 or 30 generations only lead to tiny improvement in the final solutions, but takes a much longer simulation time. The simulation time which is counted by the number of total simulation runs are implemented in this study to evaluate the performance of AR.

4.3 Results of AR - San Francisco

For the aesthetic requirement in façade design, the same insulation materials or glazing types should be implemented on the entire façade, despite the orientation. Therefore, the variable inputs of the glazing, insulation and infiltration are kept the same on all the sub-problems in this design scenario. In this case, the total number of possible solutions based on the combinations of different design variable inputs is:

$$6 \times 7 \times 4 \times (10 \times 10 \times 9)^{100} \tag{4.2}$$

For AR, in Step 1, only 36 rooms are considered to achieve the optimal solutions of the first three design variables. The optimal solutions for each room is then achieved in Step 2. Thus the total number of possible simulations of AR in this FPO is:

$$6 \times 7 \times 4 \times (10 \times 10 \times 9)^{36} + (10 \times 10 \times 9) \times 36 \tag{4.3}$$

Two AR optimization runs (AR I and AR II) are executed in this section to validate its feasibility and robustness.

4.3.1 AR Results I – San Francisco

Table 4.3 shows the optimization results achieved by Step 1 in AR optimization I, focusing on the values of the first three design variables that will stay constant in subsequent steps. In this step, the users can select the number of sub-problems to be optimized. However, it's worth pointing out that there is always a compromise between the efficiency and accuracy for the selection. Selecting more sub-problems improves the accuracy of the optimization result, but it takes more simulation effort, which reduces the efficiency. In this case study, to improve the efficiency, only one room located at the center of each façade is selected in Step 1. Therefore four runs $(S_{3-3}, N_{3-3}, E_{3-3}, W_{3-3})$ are executed in total.

Table 4.3: AR Results I - Step 1 – San Francisco

Unit	v_1	v_2	v_3	v_4	v_5v	v_6	Q_{Total} [kWh]	Gene. [-]	Simu. [-]
S_{3-3}	5	5	1	9	6	6	375.4	13	260
E_{3-3}	2	6	3	1	3	9	637.3	13	260
N_{3-3}	4	3	1	2	1	3	462.9	20	400
W_{3-3}	4	3	1	5	4	4	585.3	20	400
Avg.	4	4	2	-	-	-	515.2	16.5	330
Sum.								66	1320

Table 4.3 and Figure 4.6 show that the values of the first three design variables are achieved by averaging these optimization results, which are $v_1 = 4, v_2 = 4, v_3 = 2$. The glazing type 4, the insulation type 4 (0.32 W/m^2K), and infiltrate rate of 0.18 are selected by Step 1. San Francisco has cool summers and temperate winters. The southern façade receives extensive solar radiation in summertime, therefore, effective glazing and insulation are essential to block the solar heat and reduce the cooling energy demand. Compared with the south façade, the impact from the solar radiation is not that apparent on the east, north and west façades, thus lower insulation and SHGC values are selected on these façades. Additionally, the weather of San Francisco is not as severe as it is in Miami, which also explains why the design solutions don't select the highest insulation and SHGC values. Compromises are made between different façades, especially the south and east façades. These design variable values are then implemented for all the 36 sub-problems in Step 2 of AR optimization I.

It can also be seen in Figure 4.6 that the shading depth on the south façade is large, which is 600 mm for the overhang depth and 900 mm for the fin depth. In contrast, the shading depth on the north façade is small, which are 100 mm for the overhang depth and 200 mm for the fin depth. The shading depths on the east façade are also small, 300 mm for the overhang depth and 100 mm for the fin depth. The reason is that the high-rise building on the east orientation close to the east façade blocks most of the daylight and solar radiation over the year. The overhang depth

on the west façade is 400 mm, and the fin depth is 500 mm, which also reflects the need to block solar radiation on the western facades in the afternoon.

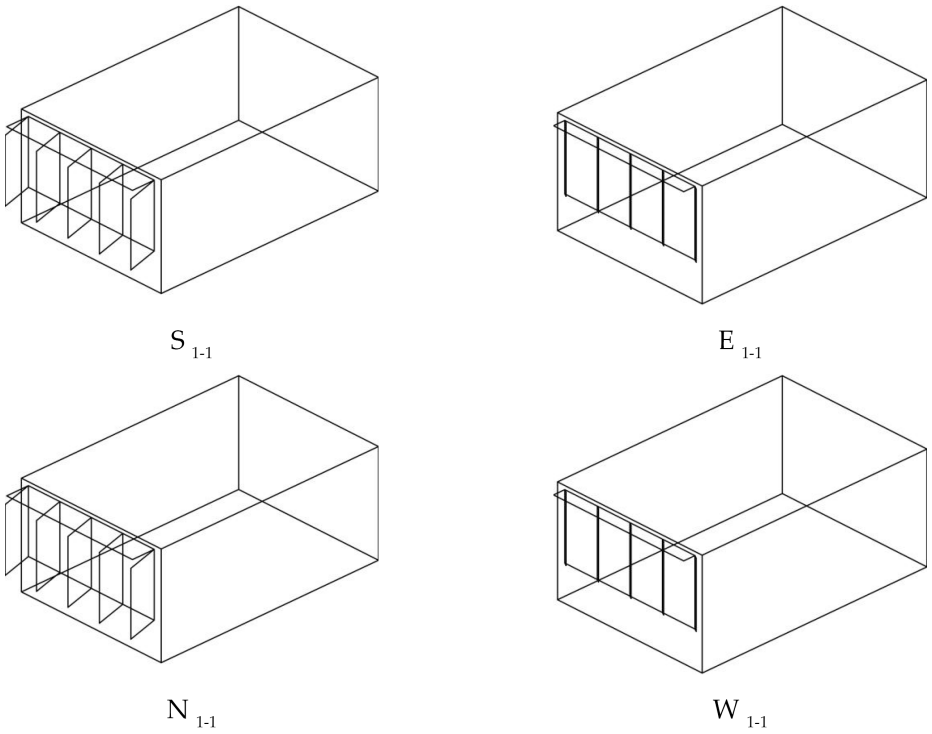

Figure 4.6: AR Results I – Step 1 – San Francisco

Step 2

Table 4.4 shows the optimization results for south façade achieved by Step 2 of the AR optimization I. The first three design variables ($v_1 = 4, v_2 = 4, v_3 = 2$) stay unchanged. The optimization runs are executed for 9 selected sub-problems ($S_{1-1}, S_{1-3}, S_{1-5}, S_{3-1}, S_{3-3}, S_{3-5}, S_{5-1}, S_{5-3}, S_{5-5}$) on the south orientation. The façade design solutions for these sub-problems are shown in Figure 4.7.

It can be seen in Table 4.4 and Figure 4.7 that the optimization solutions achieved by Step 2 show large fin and overhang shading depths on the south façade in this case study, which is consistent with the solutions achieved for S_{3-3} by Step 1. There is gradient for the change for the shading depth, especially for the overhang depth of

Table 4.4: AR Results I - Step 2 – South façade – San Francisco

Unit	v_1	v_2	v_3	v_4	v_5	v_6	Q_{Total} [kWh]	Gene. [-]	Simu. [-]
S_{1-1}	4	4	2	8	6	7	317.7	14	280
S_{1-3}	4	4	2	8	4	3	378.8	18	360
S_{1-5}	4	4	2	6	10	6	387.0	16	320
S_{3-1}	4	4	2	6	8	6	332.7	16	320
S_{3-3}	4	4	2	9	6	6	373.3	13	260
S_{3-5}	4	4	2	8	9	7	337.5	17	340
S_{5-1}	4	4	2	2	7	2	350.6	17	340
S_{5-3}	4	4	2	6	10	4	415.4	13	260
S_{5-5}	4	4	2	7	8	7	353.0	17	340
Avg.							360.7	15.7	313.3
Sum.								141	2820

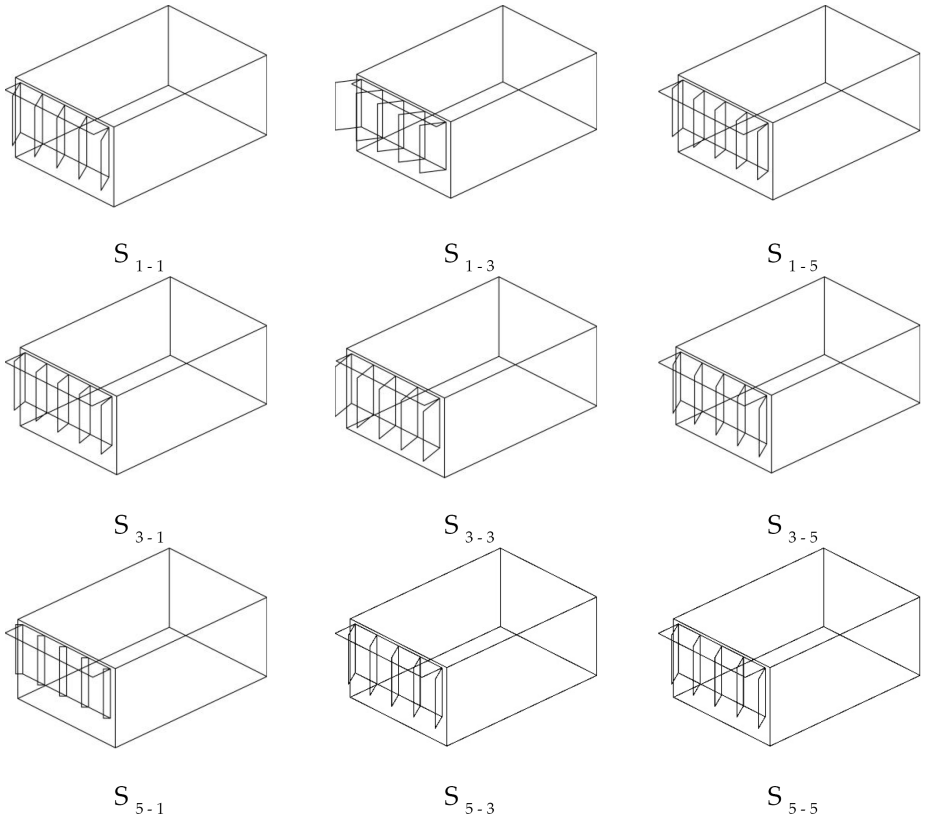

Figure 4.7: AR Results I – Step 2 – South façade – San Francisco

the solutions. For example, for the rooms in the middle of each floor (S_{1-3}, S_{3-3}), the overhang depths (400 mm for S_{1-3} and 600 mm for S_{3-3}) are smaller than those for the rooms on the edges (600 mm for S_{1-1}, 1000 mm for S_{1-5}, 800 mm for S_{3-1}, 900

mm for S_{3-5}). The reason is that the high-rise building on the south orientation casts shadows which mainly impact the rooms in the center of the façade. Additionally, the height and distance of the high-rise building determines that it has less impact on the rooms on the top floor. The average total energy demand for all the 9 sub-problems is 360.7 kWh. This result is 3.9% smaller than the 375.4 kWh achieved by Step 1. It's worth pointing out that since there are limited number of sub-problems in Step 2, the optimization solutions achieved by Step 2 can only show a trend but cannot guarantee the solutions are the global optimum for this FPO problem.

Table 4.5: AR Results I – Step 2 – East façade – San Francisco

Unit	v_1	v_2	v_3	v_4	v_5	v_6	Q_{Total} [kWh]	Gene. [-]	Simu. [-]
E_{1-1}	4	4	2	5	2	2	361.9	13	260
E_{1-3}	4	4	2	9	7	3	580.7	14	280
E_{1-5}	4	4	2	4	3	7	364.2	13	260
E_{3-1}	4	4	2	8	3	3	339.8	13	260
E_{3-3}	4	4	2	2	4	4	663.6	18	360
E_{3-5}	4	4	2	8	1	7	338.3	11	220
E_{5-1}	4	4	2	1	5	1	348.7	16	320
E_{5-3}	4	4	2	5	3	2	657.6	13	260
E_{5-5}	4	4	2	8	3	7	356.2	16	320
Avg.							445.7	14.1	282.2
Sum.								127	2540

Table 4.5 represents the optimization results for the east façade achieved by Step 2 of the AR optimization I. The optimization runs are executed for 9 selected sub-problems ($E_{1-1}, E_{1-3}, E_{1-5}, E_{3-1}, E_{3-3}, E_{3-5}, E_{5-1}, E_{5-3}, E_{5-5}$) on the east orientation. The façade design solutions for these sub-problems are shown in Figure 4.8.

It can be seen in Table 4.5 and Figure 4.8 that the optimization solutions achieved by Step 2 show deep fin shadings on the east façade in this case study, while deep overhang shadings are not as imperative, comparatively. This is because the eastern façade is mainly impacted by the sun on a relatively lower solar altitude, which means the overhang shadings are not as effective as the fin shadings. The average

total energy demand for all the 9 sub-problems is 445.7 kWh, which is 30.1% smaller than the 637.3 kWh achieved by Step 1. There is no apparent gradient for the shading depths on the east façade.

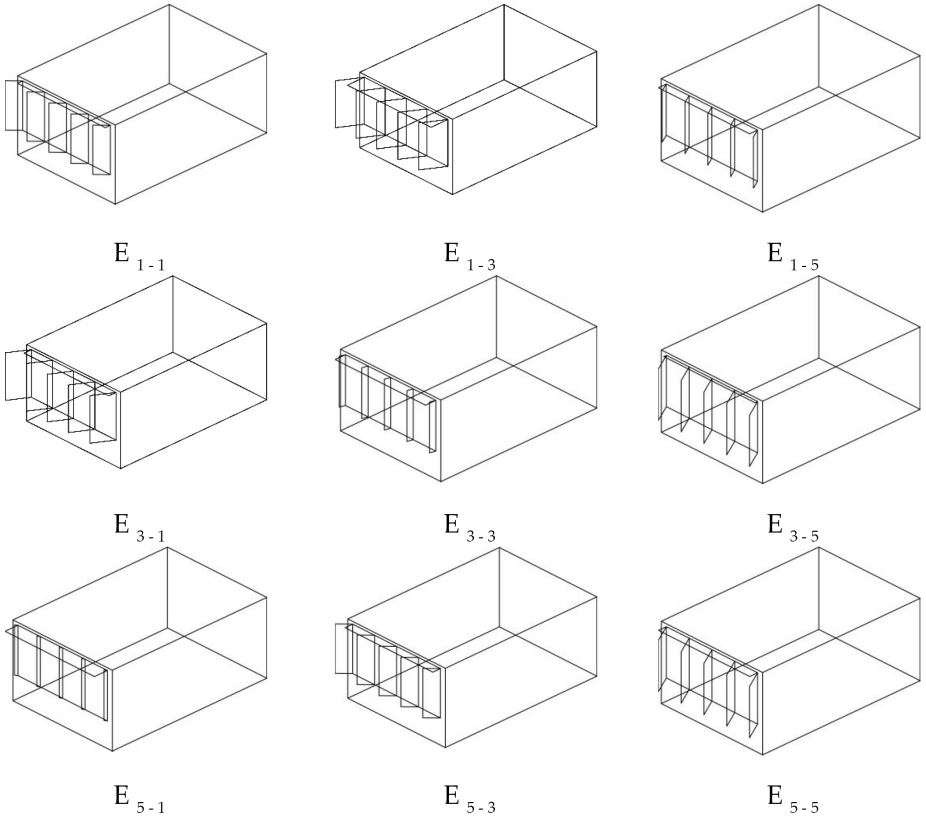

Figure 4.8: AR Results I – Step 2 – East façade – San Francisco

Figure 4.8 also shows that the fin angles for the third rooms ($E_{1-5}, E_{3-5}, E_{5-5}$) are relatively larger than that for the first two rooms on each floor ($E_{1-1}, E_{1-3}, E_{3-1}, E_{3-3}$, E_{5-1}, E_{5-3}). This is typical for fins to face the south orientation in order to receive more solar radiation, as well as reflect more daylight in to the room. In contrast, solutions for the third rooms on each floor ($E_{1-5}, E_{3-5}, E_{5-5}$) show a north-facing fin angle (120°). The reason is that the rooms on the northeast edge are blocked by the high-rise building on the east and north. The only available daylight and solar radiation is from the space between the east and north buildings. Therefore, the fin angles are facing this space to achieve as much daylight and solar radiation as possible.

Table 4.6: AR Results I – Step 2 – North façade – San Francisco

Unit	v_1	v_2	v_3	v_4	v_5	v_6	Q_{Total} [kWh]	Gene. [-]	Simu. [-]
N_{1-1}	4	4	2	2	2	4	639.8	20	400
N_{1-3}	4	4	2	8	1	3	579.1	14	280
N_{1-5}	4	4	2	1	3	6	385.8	13	260
N_{3-1}	4	4	2	4	1	3	541.1	14	280
N_{3-3}	4	4	2	1	1	6	593.5	13	260
N_{3-5}	4	4	2	2	4	7	292.7	11	220
N_{5-1}	4	4	2	4	1	4	528.3	14	280
N_{5-3}	4	4	2	2	1	3	418.3	12	240
N_{5-5}	4	4	2	10	4	6	364.0	20	400
Avg.							481.3	14.6	291.1
Sum.								131	2620

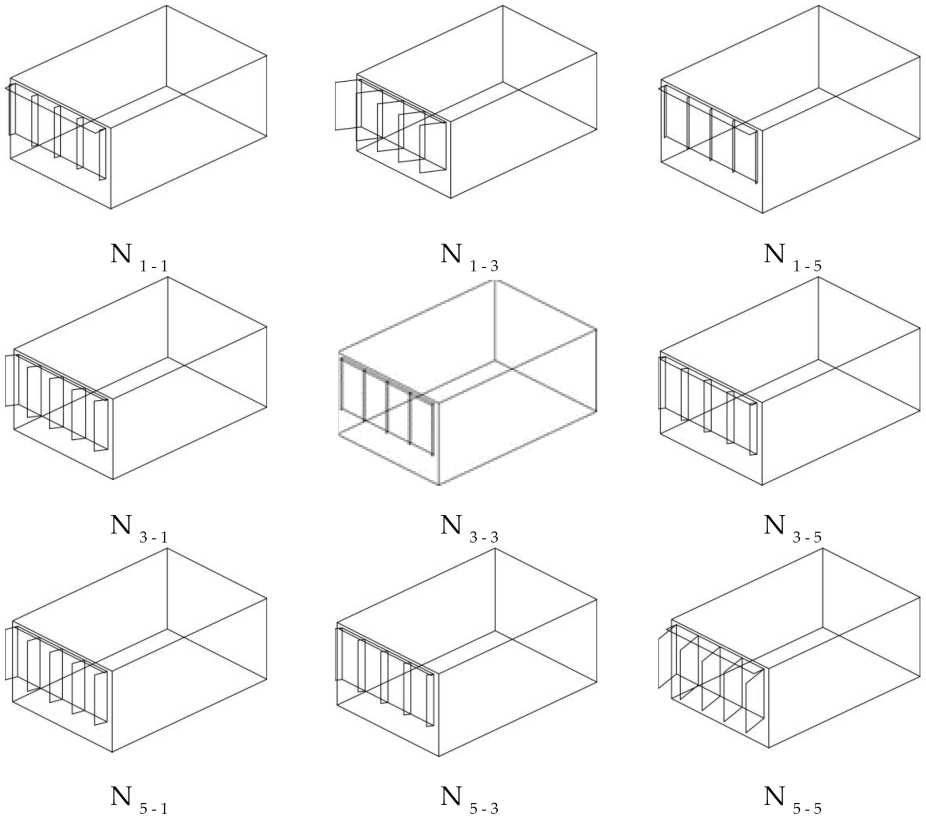

Figure 4.9: AR Results I – Step 2 – North façade – San Francisco

Table 4.6 represents the optimization results for north façade achieved by Step 2 of the AR optimization I. The optimization runs are executed for 9 selected sub-problems

($N_{1-1}, N_{1-3}, N_{1-5}, N_{3-1}, N_{3-3}, N_{3-5}, N_{5-1}, N_{5-3}, N_{5-5}$) on the north orientation. The façade design solutions for these sub-problems are shown in Figure 4.9.

It can be seen in Table 4.6 and Figure 4.9 that the optimization solutions achieved by Step 2 show small depths for fin and overhang shadings on the north façade in this case study. This is because the north façade does not receive as much daylight and solar radiation during the entire year. Thus overhang shading is not necessary on this orientation. The solutions achieved by this step show a consistent trend compared with the solutions achieved by Step 1. The average total energy demand for all the 9 sub-problems is 481.3 kWh, which is 4.0% greater than the 462.9 kWh achieved by Step 1.

It could also be found in Figure 4.9 that the fins are slightly facing east for the rooms on the east edge and facing west for the rooms on the west edge of north façade. This can help the rooms to receive as more as daylight and solar radiations through the reflections by the fin shadings.

Table 4.7 represents the optimization results for western façade achieved by Step 2 of the AR optimization I. The optimization runs are executed for 9 selected sub-problems ($W_{1-1}, W_{1-3}, W_{1-5}, W_{3-1}, W_{3-3}, W_{3-5}, W_{5-1}, W_{5-3}, W_{5-5}$) on the west orientation. The façade design solutions for these sub-problems are shown in Figure 4.10.

It can be seen that the optimization solutions achieved by Step 2 show small depths for fin and/or overhang shadings on the lower and middle floors on the west façade in this case study. Comparatively, the shading depths for sub-problems on the top floor is larger, especially the overhang depths. This is because the rooms on the top floor of western façade receive more solar radiation in the afternoons. Thus overhang shading is imperative to reduce exposure to solar radiation on this orientation. The average total energy demand for all the 9 sub-problems is 578.5 kWh, which is 1.2% smaller than the 585.3 kWh achieved by Step 1.

Table 4.7: AR Results I – Step 2 – West façade – San Francisco

Unit	v_1	v_2	v_3	v_4	v_5	v_6	Q_{Total} [kWh]	Gene. [-]	Simu. [-]
W_{1-1}	4	4	2	1	2	3	695.3	14	280
W_{1-3}	4	4	2	3	8	4	601.3	12	240
W_{1-5}	4	4	2	1	4	6	562.9	19	380
W_{3-1}	4	4	2	3	1	3	624.1	17	340
W_{3-3}	4	4	2	2	1	3	576.2	15	300
W_{3-5}	4	4	2	2	2	3	505.9	12	240
W_{5-1}	4	4	2	5	10	4	575.8	11	220
W_{5-3}	4	4	2	9	6	3	548.7	14	280
W_{5-5}	4	4	2	2	10	7	516.2	16	320
Avg.							578.5	14.4	288.9
Sum.								130	2600

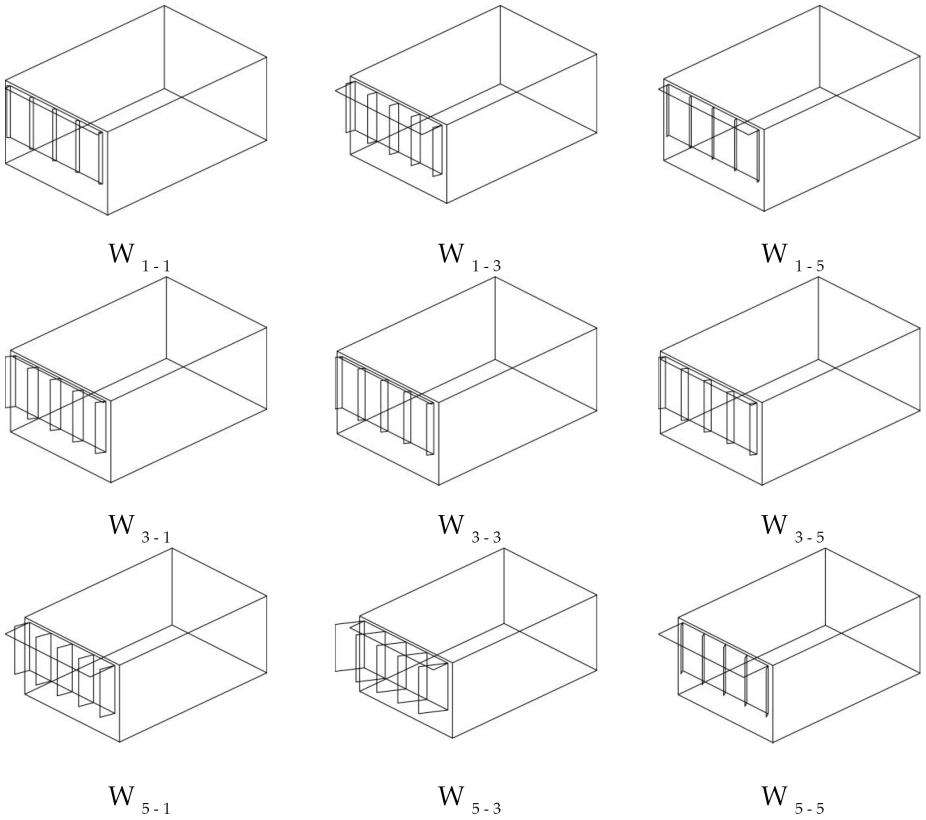

Figure 4.10: AR Results I – Step 2 – West façade – San Francisco

Figure 4.10 also shows a clear trend for the fin angles. The fins are slightly facing south for the rooms on the south edge ($W_{1-3}, W_{3-3}, W_{5-3}$), and facing north for the rooms on the north edge ($W_{1-1}, W_{3-1}, W_{5-1}$) of western façade. This can help the

rooms to receive daylight in the morning and block solar radiation in the afternoon as much as possible through the reflections by the fin shading elements.

Table 4.8: AR Results I – Step 3 – San Francisco

Unit	v_1	v_2	v_3	v_4	v_5	v_6	[kWh]	Unit	v_1	v_2	v_3	v_4	v_5	v_6	[kWh]
S_{1-1}	4	4	2	8	6	7	317.7	E_{1-1}	4	4	2	5	2	2	361.9
S_{1-2}	4	4	2	8	5	5	505.3	E_{1-2}	4	4	2	7	5	3	821.4
S_{1-3}	4	4	2	8	4	3	378.8	E_{1-3}	4	4	2	9	7	3	580.7
S_{1-4}	4	4	2	7	7	5	619.3	E_{1-4}	4	4	2	7	5	5	969.6
S_{1-5}	4	4	2	6	10	6	387.0	E_{1-5}	4	4	2	4	3	7	364.2
S_{3-1}	4	4	2	6	8	6	332.7	E_{3-1}	4	4	2	8	3	3	339.8
S_{3-2}	4	4	2	8	7	6	404.5	E_{3-2}	4	4	2	5	4	4	683.2
S_{3-3}	4	4	2	9	6	6	373.3	E_{3-3}	4	4	2	2	4	4	663.6
S_{3-4}	4	4	2	9	8	7	442.9	E_{3-4}	4	4	2	5	3	6	838.9
S_{3-5}	4	4	2	8	9	7	330.5	E_{3-5}	4	4	2	8	1	7	338.3
S_{5-1}	4	4	2	2	7	2	350.6	E_{5-1}	4	4	2	1	5	1	348.7
S_{5-2}	4	4	2	4	9	3	472.6	E_{5-2}	4	4	2	3	4	2	808.3
S_{5-3}	4	4	2	6	10	4	415.4	E_{5-3}	4	4	2	5	3	2	657.6
S_{5-4}	4	4	2	7	9	6	523.6	E_{5-4}	4	4	2	7	3	5	891.3
S_{5-5}	4	4	2	7	8	7	353.0	E_{5-5}	4	4	2	8	3	7	356.2
Avg.							413.8	Avg.							601.6
N_{1-1}	4	4	2	2	2	4	639.8	W_{1-1}	4	4	2	1	2	3	695.3
N_{1-2}	4	4	2	5	2	4	838.5	W_{1-2}	4	4	2	2	5	4	660.9
N_{1-3}	4	4	2	8	1	3	579.1	W_{1-3}	4	4	2	3	8	4	601.3
N_{1-4}	4	4	2	5	2	5	802.8	W_{1-4}	4	4	2	2	6	5	704.8
N_{1-5}	4	4	2	1	3	6	385.8	W_{1-5}	4	4	2	1	4	6	562.9
N_{3-1}	4	4	2	4	1	3	541.1	W_{3-1}	4	4	2	3	1	3	624.1
N_{3-2}	4	4	2	3	5	5	751.4	W_{3-2}	4	4	2	3	1	3	628.9
N_{3-3}	4	4	2	1	8	6	593.5	W_{3-3}	4	4	2	2	1	3	576.2
N_{3-4}	4	4	2	2	6	7	534.8	W_{3-4}	4	4	2	2	2	3	529.0
N_{3-5}	4	4	2	2	4	7	292.7	W_{3-5}	4	4	2	2	2	3	505.9
N_{5-1}	4	4	2	4	1	4	528.3	W_{5-1}	4	4	2	5	10	4	575.8
N_{5-2}	4	4	2	3	1	4	549.4	W_{5-2}	4	4	2	7	8	4	610.8
N_{5-3}	4	4	2	2	1	3	418.3	W_{5-3}	4	4	2	9	6	3	548.7
N_{5-4}	4	4	2	6	3	5	603.3	W_{5-4}	4	4	2	6	8	5	597.4
N_{5-5}	4	4	2	10	4	6	364.0	W_{5-5}	4	4	2	2	10	7	516.2
Avg.							556.9	Avg.							595.9

Table 4.8 represents the horizontal interpolation procedure in Step 3 of the AR optimization II. The design variables v_4, v_5, v_6 for each sub-problem are achieved, the total energy demand for each sub-problem are then achieved by simulation. The

average total energy demand for all the sub-problems is 413.8 kWh for the south façade, 601.6 kWh for the east façade, 556.9 kWh for the north façade, and 595.9 kWh for the west façade. The average total energy demand for all sub-problems achieved by this step is 542.1 kWh, which is 16.2% higher than the 466.5 kWh achieved by Step 3.

Step 4

Table 4.9 shows the vertical interpolation procedure in Step 4 of the AR optimization I. Interpolations are made for the vertical sub-problems based on the optimization solutions achieved by Step 4. The shading design variables v_4, v_5, v_6 for each sub-problem on the second and fourth floors are achieved by this step. The total energy demand for each sub-problem are then achieved through simulation. The average total energy demand for all the sub-problems is 422.0 kWh for the south façade, 601.6 kWh for the east façade, 581.4 kWh for the north façade, and 611.6 kWh for the west façade. The total energy demand achieved by Step 3 is higher than that achieved by Step 4.

Table 4.9: AR Results I – Step 4 – San Francisco

	v_1	v_2	v_3	v_4	v_5	v_6			v_1	v_2	v_3	v_4	v_5	v_6	
S_{1-1}	4	4	2	8	6	7	317.7	E_{1-1}	4	4	2	5	2	2	361.9
S_{1-2}	4	4	2	8	5	5	505.3	E_{1-2}	4	4	2	7	5	3	821.4
S_{1-3}	4	4	2	8	4	3	378.8	E_{1-3}	4	4	2	9	7	3	580.7
S_{1-4}	4	4	2	7	7	5	619.3	E_{1-4}	4	4	2	7	5	5	969.6
S_{1-5}	4	4	2	6	10	6	387.0	E_{1-5}	4	4	2	4	3	7	364.2
S_{2-1}	4	4	2	7	7	7	428.7	E_{2-1}	4	4	2	5	2	2	545.8
S_{2-2}	4	4	2	8	6	6	366.9	E_{2-2}	4	4	2	7	3	3	535.1
S_{2-3}	4	4	2	9	5	5	484.6	E_{2-3}	4	4	2	6	4	3	844.6
S_{2-4}	4	4	2	8	7	6	542.0	E_{2-4}	4	4	2	6	6	4	956.1
S_{2-5}	4	4	2	7	10	7	331.3	E_{2-5}	4	4	2	6	4	5	452.4
S_{3-1}	4	4	2	6	8	6	332.7	E_{3-1}	4	4	2	6	2	7	339.8
S_{3-2}	4	4	2	8	7	6	404.5	E_{3-2}	4	4	2	5	4	4	683.2
S_{3-3}	4	4	2	9	6	6	373.3	E_{3-3}	4	4	2	2	4	4	663.6
S_{3-4}	4	4	2	9	8	7	442.9	E_{3-4}	4	4	2	5	3	6	838.9
S_{3-5}	4	4	2	8	9	7	330.5	E_{3-5}	4	4	2	8	1	7	338.3
S_{4-1}	4	4	2	4	8	4	366.6	E_{4-1}	4	4	2	5	4	2	321.0

	v_1	v_2	v_3	v_4	v_5	v_6			v_1	v_2	v_3	v_4	v_5	v_6	
S_{4-2}	4	4	2	6	8	5	468.8	E_{4-2}	4	4	2	4	4	3	525.3
S_{4-3}	4	4	2	8	8	5	445.9	E_{4-3}	4	4	2	4	4	3	609.1
S_{4-4}	4	4	2	8	8	6	540.3	E_{4-4}	4	4	2	6	3	5	859.5
S_{4-5}	4	4	2	8	9	7	368.1	E_{4-5}	4	4	2	8	2	7	366.4
S_{5-1}	4	4	2	2	7	2	350.6	E_{5-1}	4	4	2	1	5	1	348.7
S_{5-2}	4	4	2	4	9	3	472.6	E_{5-2}	4	4	2	3	4	2	808.3
S_{5-3}	4	4	2	6	10	4	415.4	E_{5-3}	4	4	2	5	3	2	657.6
S_{5-4}	4	4	2	7	9	6	523.6	E_{5-4}	4	4	2	7	3	5	891.3
S_{5-5}	4	4	2	7	8	7	353.0	E_{5-5}	4	4	2	8	3	7	356.2
Avg.							422.0	Avg.							601.6
N_{1-1}	4	4	2	2	2	4	639.8	W_{1-1}	4	4	2	1	2	3	695.3
N_{1-2}	4	4	2	5	2	4	838.5	W_{1-2}	4	4	2	2	5	4	660.9
N_{1-3}	4	4	2	8	1	3	579.1	W_{1-3}	4	4	2	3	8	4	601.3
N_{1-4}	4	4	2	5	2	5	802.8	W_{1-4}	4	4	2	2	6	5	704.8
N_{1-5}	4	4	2	1	3	6	385.8	W_{1-5}	4	4	2	1	4	6	562.9
N_{2-1}	4	4	2	2	2	4	616.4	W_{2-1}	4	4	2	2	2	3	654.4
N_{2-2}	4	4	2	3	2	4	727.0	W_{2-2}	4	4	2	2	3	3	653.2
N_{2-3}	4	4	2	4	3	4	779.9	W_{2-3}	4	4	2	3	5	4	622.1
N_{2-4}	4	4	2	5	5	5	710.3	W_{2-4}	4	4	2	2	4	4	648.7
N_{2-5}	4	4	2	3	4	6	438.7	W_{2-5}	4	4	2	2	3	5	628.3
N_{3-1}	4	4	2	2	4	7	541.1	W_{3-1}	4	4	2	3	1	3	624.1
N_{3-2}	4	4	2	3	5	5	751.4	W_{3-2}	4	4	2	3	1	3	628.9
N_{3-3}	4	4	2	1	8	6	593.5	W_{3-3}	4	4	2	2	1	3	576.2
N_{3-4}	4	4	2	2	6	7	534.8	W_{3-4}	4	4	2	2	2	3	529.0
N_{3-5}	4	4	2	2	4	7	292.7	W_{3-5}	4	4	2	2	2	3	505.9
N_{4-1}	4	4	2	4	1	4	560.8	W_{4-1}	4	4	2	4	6	4	614.9
N_{4-2}	4	4	2	3	3	4	618.5	W_{4-2}	4	4	2	5	5	3	663.2
N_{4-3}	4	4	2	2	5	5	674.5	W_{4-3}	4	4	2	6	4	3	674.1
N_{4-4}	4	4	2	4	4	6	633.3	W_{4-4}	4	4	2	4	5	4	616.1
N_{4-5}	4	4	2	6	4	7	363.3	W_{4-5}	4	4	2	2	6	5	575.9
N_{5-1}	4	4	2	4	1	4	528.3	W_{5-1}	4	4	2	5	10	4	575.8
N_{5-2}	4	4	2	3	1	4	549.4	W_{5-2}	4	4	2	7	8	4	610.8
N_{5-3}	4	4	2	2	1	3	418.3	W_{5-3}	4	4	2	9	6	3	548.7
N_{5-4}	4	4	2	6	3	5	603.3	W_{5-4}	4	4	2	6	8	5	597.4
N_{5-5}	4	4	2	10	4	6	364.0	W_{5-5}	4	4	2	2	10	7	516.2
Avg.							581.4	Avg.							611.6

Figure 4.11 shows the optimization solutions for the entire south and east façades. Figure 4.12 shows the optimization solutions for the entire north and west façades. Detailed figures for the sub-problems in Step 4 are shown in Appendix A.

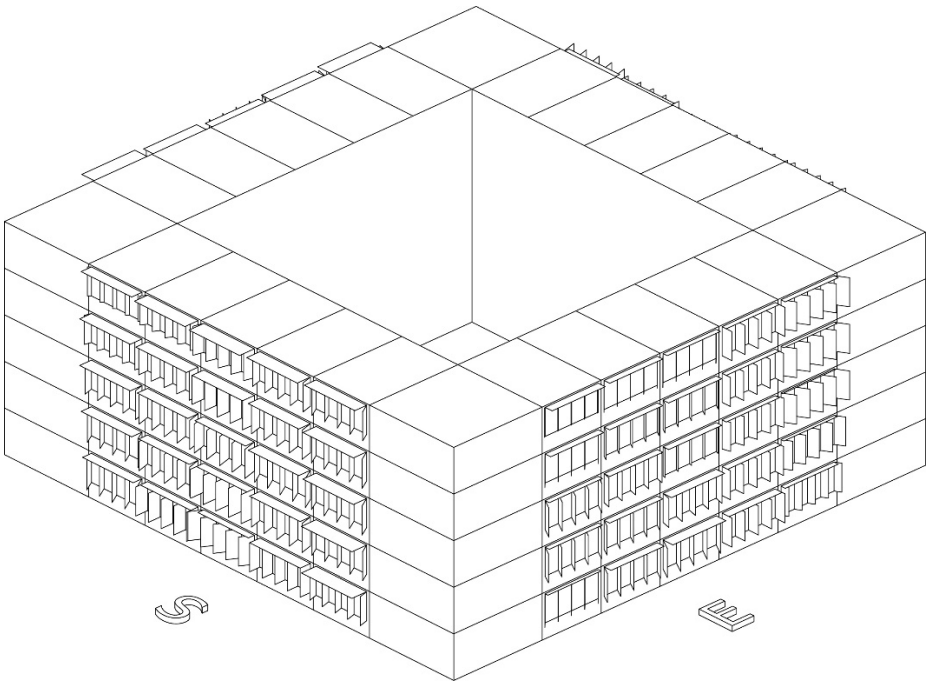

Figure 4.11: AR Results I – Step 4 – South and East façades – San Francisco

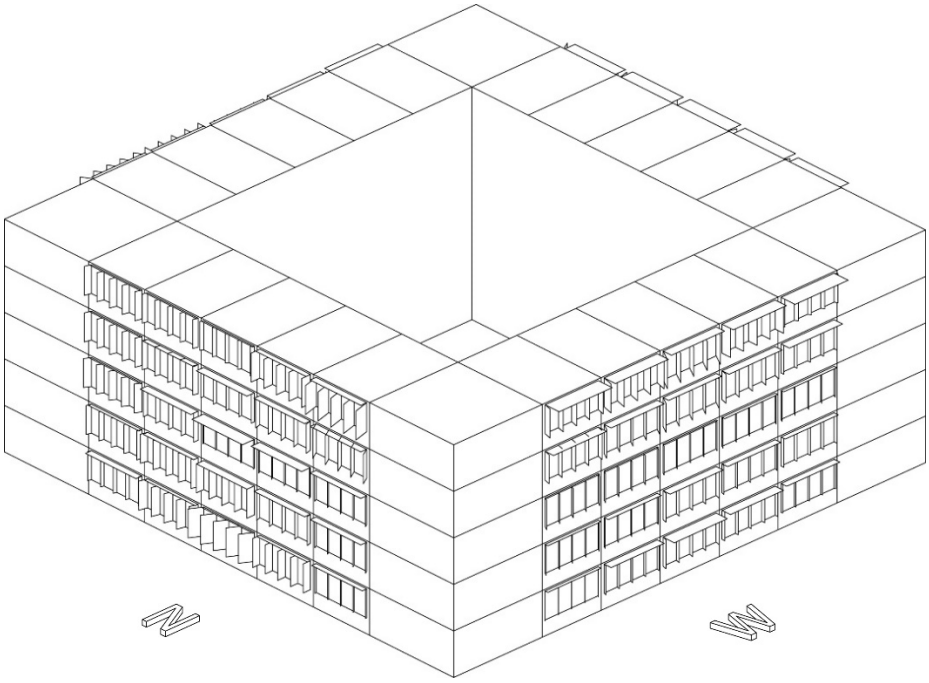

Figure 4.12: AR Results I – Step 4 – North and West façade – San Francisco

Table 4.10 represents the average total energy demand for all the rooms achieved by each Step in AR optimization I. It can be seen that the average total energy demand for all the sub-problems is 466.5 kWh in Step 2. After the interpolation

processes in Step 3 and Step 4, the average total energy demands increase, which are 542.1 kWh and 552.9 kWh, respectively. The reason the total energy demand increases is that the interpolation cannot guarantee the solutions achieved are the global optimum. In contrast, the design variables for each sub-problem have to be compromised with each other. The main objective of the interpolation processes in Step 3 and Step 4 is to reduce the optimization time and improve the efficiency of optimization process, while the accuracy is undermined sometimes. There are 1320 simulation runs executed in Step 1 and 10580 simulation runs in Step 2. Therefore, 11900 simulation runs are executed in total for AR optimization I.

Table 4.10: AR Results I - San Francisco

	S [kWh]	E [kWh]	N [kWh]	W [kWh]	Average [kWh]	Runs [-]
Step 1	375.4	637.3	462.9	585.3	515.2	1320
Step 2	360.7	445.7	481.3	578.5	466.5	10580
Step 3	413.8	601.6	559.6	595.9	542.1	
Step 4	422.0	601.6	576.5	611.6	552.9	
Total						11900

4.3.2 AR Results II – San Francisco

Table 4.11 shows the optimization results achieved by Step 1 in AR optimization II. The same as AR optimization I, only one room located at the center of each façade is selected in Step 1 and four runs $(S_{3-3}, N_{3-3}, E_{3-3}, W_{3-3})$ in total are executed in this step.

The values of the first design three variables are achieved by making an average of these optimization results, which are $v_1 = 4, v_2 = 3, v_3 = 1$. Therefore, for the entire façade, the glazing type 4 should be implemented, as well as the 0.37 W/m^2K exterior wall insulation and 0.25 infiltration. These design variable values are implemented for all the 36 sub-problems in Step 2 of AR optimization II.

Table 4.11: AR Results II - Step 1 – San Francisco

Unit	v_1	v_2	v_3	v_4	v_5v	v_6	Q_{Total} [kWh]	Gene. [-]	Simu. [-]
S_{3-3}	4	1	1	5	7	7	382.1	13	260
E_{3-3}	5	1	2	4	2	3	635.3	20	400
N_{3-3}	4	4	1	8	1	3	445.0	15	300
W_{3-3}	4	2	1	4	5	3	598.4	13	260
	4	3	1	-	-	-	-	-	-
Avg.							515.2	15.3	560
Sum.								61	1220

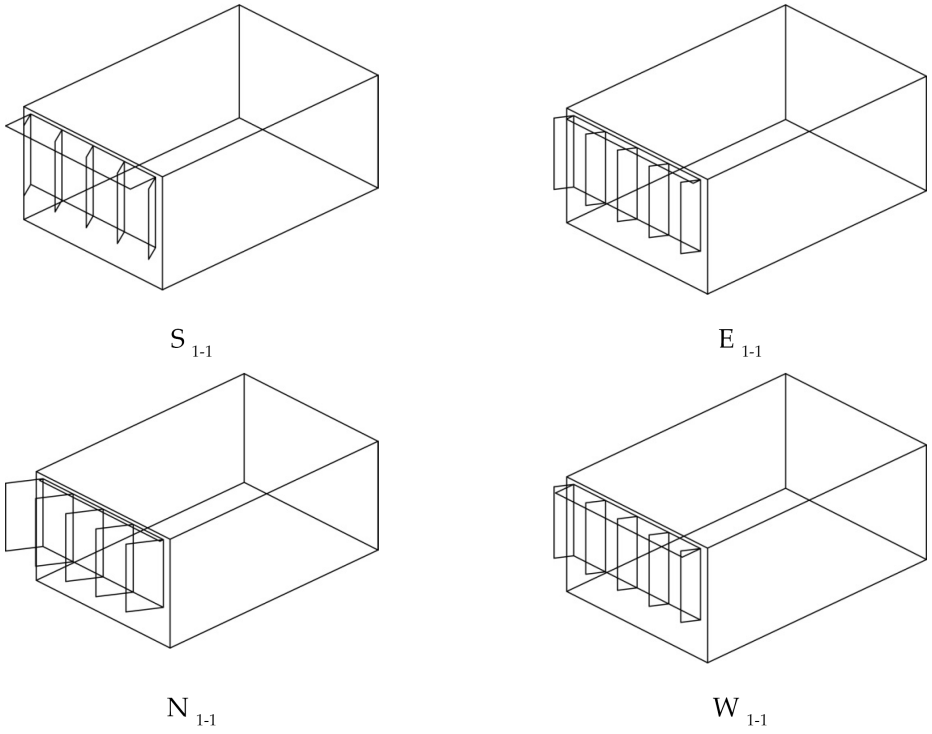

Figure 4.13: AR Results II – Step 1 – San Francisco

Step 2

It can be seen in Table 4.12 and Figure 4.14 that the optimization solutions achieved by Step 2 show large fin and overhang shading depths on the south façade in this case study, which is consistent with the solutions achieved for S_{3-3} by Step 1. The average total energy demand for all the 9 sub-problems is 328.6 kWh. This

result is 14.0% higher than the 382.1 kWh achieved by Step 1.

Table 4.12: AR Results II - Step 2 – South façade – San Francisco

Unit	v_1	v_2	v_3	v_4	v_5	v_6	Q_{Total} [kWh]	Gene. [-]	Simu. [-]
S_{1-1}	4	3	1	8	8	3	321.2	15	300
S_{1-3}	4	3	1	8	7	3	345.3	16	320
S_{1-5}	4	3	1	8	8	7	290.4	13	260
S_{3-1}	4	3	1	6	10	4	286.6	13	260
S_{3-3}	4	3	1	8	5	7	330.7	18	360
S_{3-5}	4	3	1	9	2	8	319.0	13	260
S_{5-1}	4	3	1	2	9	2	318.5	12	240
S_{5-3}	4	3	1	8	7	4	415.1	11	220
S_{5-5}	4	3	1	9	6	7	330.8	12	240
Avg.							328.6	13.7	273.3
Sum.								123	2460

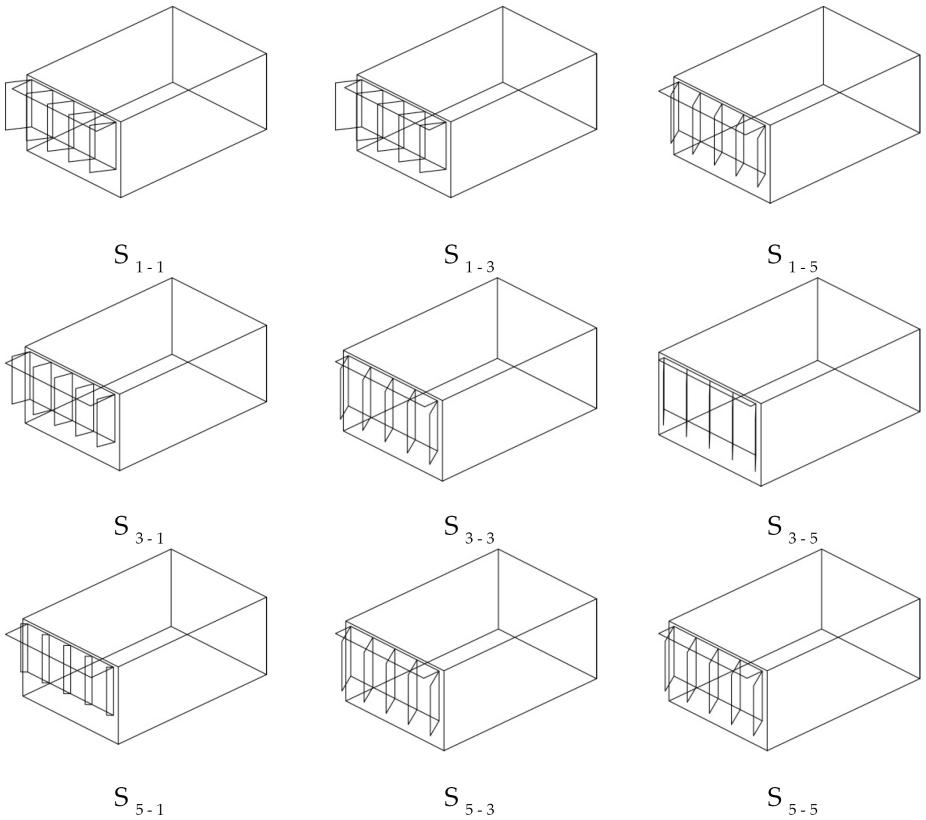

Figure 4.14: AR Results II – Step 2 – South façade – San Francisco

Table 4.13 represents the optimization results for east façade achieved by Step 2 of AR II. The optimization runs are executed for 9 selected sub-problems (E_{1-1}, E_{1-3},

$E_{1-5}, E_{3-1}, E_{3-3}, E_{3-5}, E_{5-1}, E_{5-3}, E_{5-5}$) on the east orientation. The façade design solutions for these sub-problems are shown in Figure 4.15.

Table 4.13: AR Results II - Step 2 – East façade – San Francisco

Unit	v_1	v_2	v_3	v_4	v_5	v_6	Q_{Total} [kWh]	Gene. [-]	Simu. [-]
E_{1-1}	4	3	1	5	2	2	349.0	13	260
E_{1-3}	4	3	1	2	8	4	735.9	18	360
E_{1-5}	4	3	1	3	2	9	394.2	16	320
E_{3-1}	4	3	1	8	6	3	312.9	11	220
E_{3-3}	4	3	1	9	1	3	541.1	12	240
E_{3-5}	4	3	1	1	1	9	334.3	18	360
E_{5-1}	4	3	1	9	7	3	407.3	12	240
E_{5-3}	4	3	1	1	1	1	635.7	14	280
E_{5-5}	4	3	1	8	4	7	338.6	12	240
Avg.							449.9	14	280
Sum.								126	2520

It can be seen in Table 4.13 and Figure 4.15 that the optimization solutions achieved by Step 2 show deep fin shadings on the east façade in this case study, while deep overhang shadings are not so necessary, comparatively. This is consistent with the solutions achieved by Step 1 of AR II, as well as Step 2 of AR I. The average total energy demand for all the 9 sub-problems is 449.9 kWh, which is 29.2% smaller than the 635.3 kWh achieved by Step 1 of AR II, and only 0.9% larger than the 445.7 kWh achieved by Step 2 of AR I.

It can also be found in Figure 4.15 that the solutions of some sub-problems ($E_{1-1}, E_{1-5}, E_{3-1}, E_{5-5}$) are quite similar with that achieved in AR I.

Table 4.14 represents the optimization results for north façade achieved by Step 2 of the AR optimization I. The optimization runs are executed for 9 selected sub-problems ($N_{1-1}, N_{1-3}, N_{1-5}, N_{3-1}, N_{3-3}, N_{3-5}, N_{5-1}, N_{5-3}, N_{5-5}$) on the north orientation. The façade design solutions for these sub-problems are shown in Figure 4.16.

It can also be seen in Table 4.14 and Figure 4.16 that the optimization solutions achieved by Step 2 show small depths for fin and overhang shadings for most of the

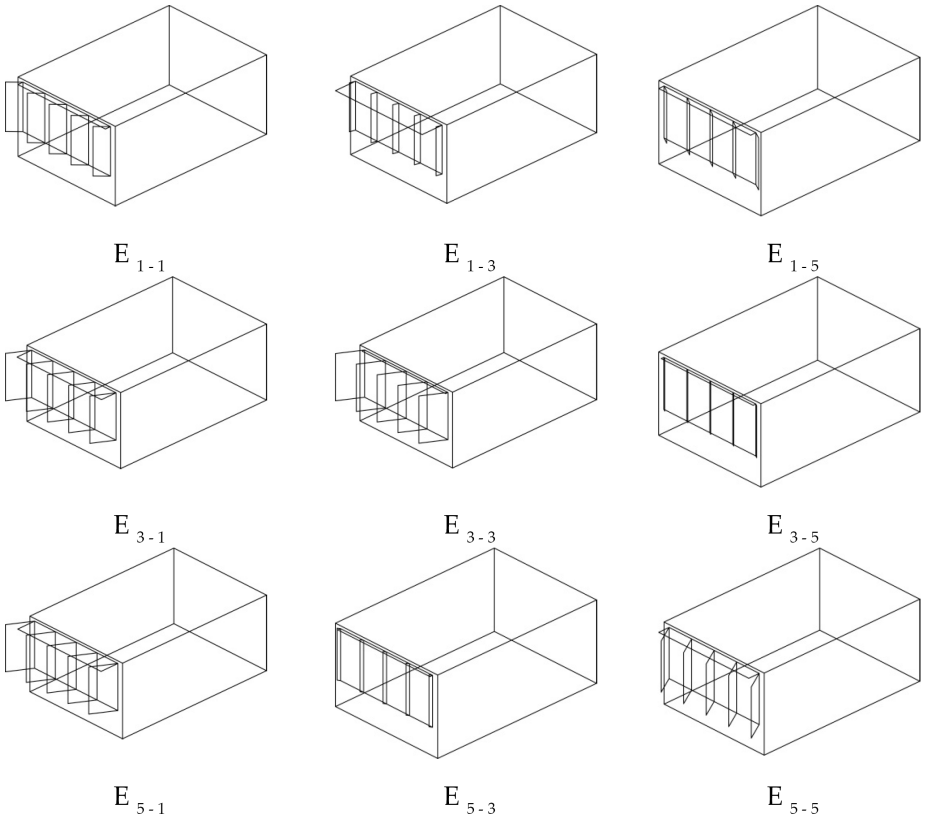

Figure 4.15: AR Results II – Step 2 – East façade – San Francisco

Table 4.14: AR Results II - Step 2 – North façade – San Francisco

Unit	v_1	v_2	v_3	v_4	v_5	v_6	Q_{Total} [kWh]	Gene. [-]	Simu. [-]
N_{1-1}	4	3	1	2	1	4	592.3	18	360
N_{1-3}	4	3	1	8	7	7	592.3	17	340
N_{1-5}	4	3	1	3	8	6	378.8	11	220
N_{3-1}	4	3	1	1	2	3	572.0	20	400
N_{3-3}	4	3	1	2	2	3	467.4	14	280
N_{3-5}	4	3	1	1	4	7	304.8	14	280
N_{5-1}	4	3	1	1	1	3	508.1	18	360
N_{5-3}	4	3	1	2	2	7	433.3	11	220
N_{5-5}	4	3	1	2	2	7	286.8	11	220
Avg.							459.5	14.9	297.8
Sum.								134	2680

sub-problems on the north façade, which is steady with that achieved in Step 1. The solutions achieved by this step also show a constant trend compared with the solutions achieved in AR I. The average total energy demand for all the 9 sub-problems is 459.5

kWh, which is 4.5% smaller than the 481.3 kWh achieved by AR I.

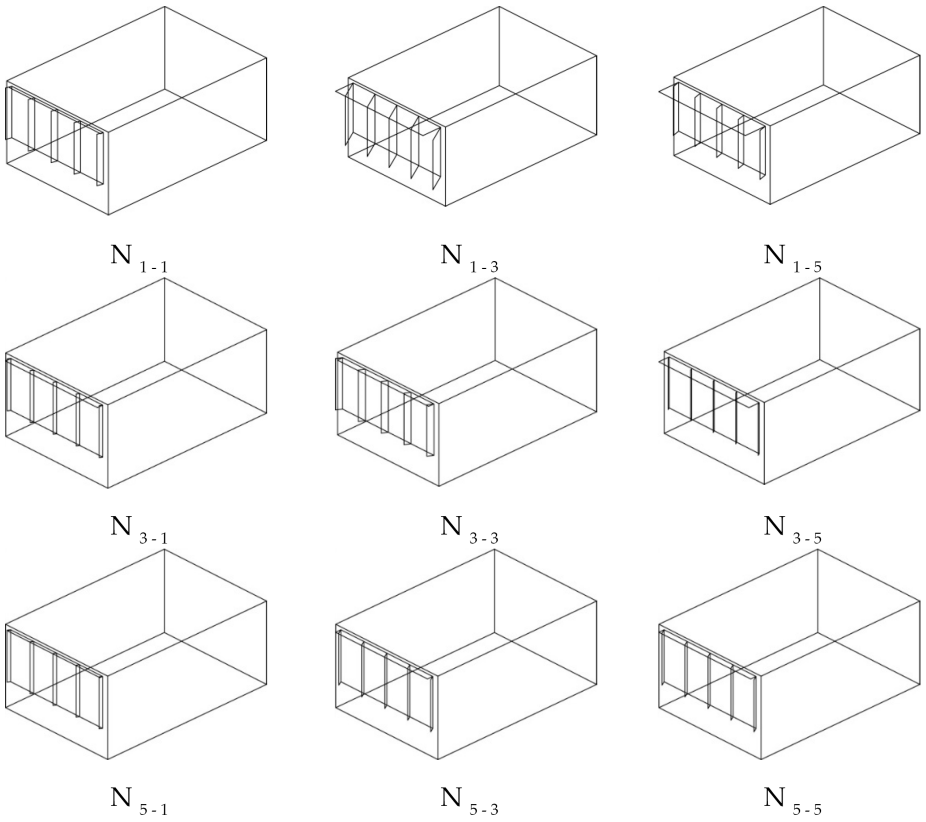

Figure 4.16: AR Results II – Step 2 – North façade – San Francisco

Table 4.15 represents the optimization results for western façade achieved by Step 2 of the AR optimization II. The optimization runs are executed for 9 selected sub-problems ($W_{1-1}, W_{1-3}, W_{1-5}, W_{3-1}, W_{3-3}, W_{3-5}, W_{5-1}, W_{5-3}, W_{5-5}$) on the west orientation. The façade design solutions for these sub-problems are shown in Figure 4.17.

It can be seen that the optimization solutions achieved by Step 2 show small depths for fin and overhang shadings for sub-problems on the west façade, which is consistent with AR I. The average total energy demand for all the 9 sub-problems is 561.1 kWh, which is 6.2% smaller than the 598.4 kWh achieved by Step 1.

It can also be found in Figure 4.17 that the solutions of some sub-problems ($W_{1-3}, W_{3-1}, W_{3-5}, W_{5-5}$) are consistent with that achieved in AR I.

Table 4.15: AR Results II - Step 2 – West façade – San Francisco

Unit	v_1	v_2	v_3	v_4	v_5	v_6	Q_{Total} [kWh]	Gene. [-]	Simu. [-]
W_{1-1}	4	3	1	2	3	6	603.0	15	300
W_{1-3}	4	3	1	2	1	4	576.8	16	320
W_{1-5}	4	3	1	6	1	5	612.2	11	220
W_{3-1}	4	3	1	1	1	6	567.7	15	300
W_{3-3}	4	3	1	2	9	3	586.0	13	260
W_{3-5}	4	3	1	2	3	7	479.2	18	360
W_{5-1}	4	3	1	9	1	8	546.0	16	320
W_{5-3}	4	3	1	3	10	4	566.2	12	240
W_{5-5}	4	3	1	2	4	7	512.3	18	360
Avg.							561.1	14.9	297.8
Sum.								134	2680

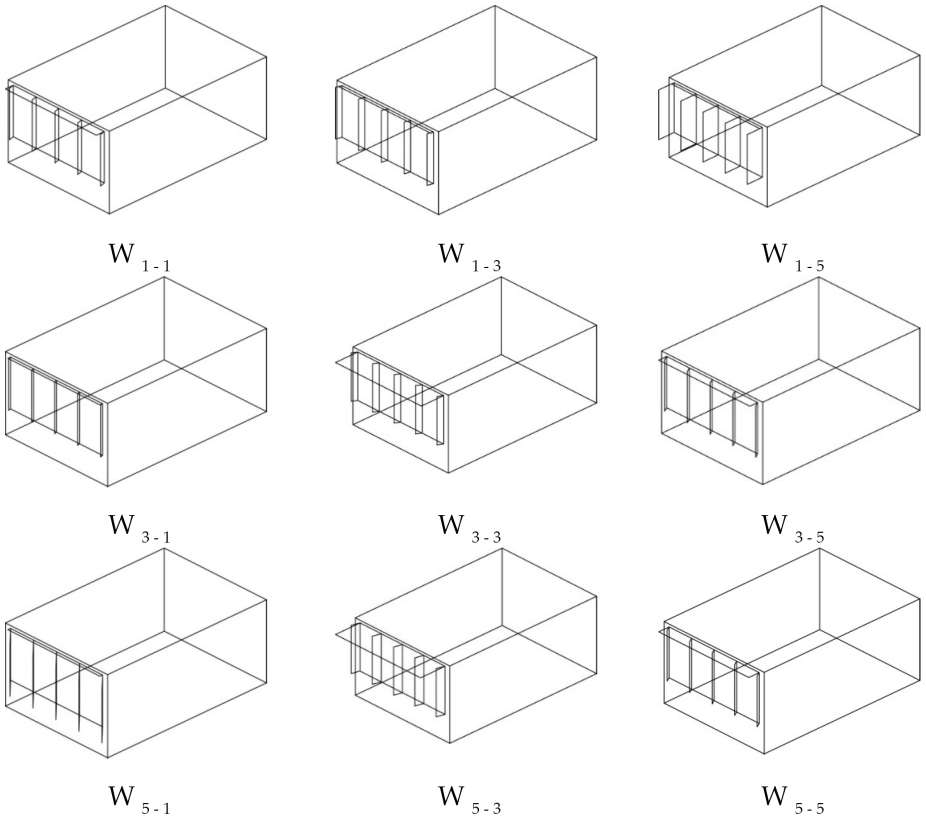

Figure 4.17: AR Results II – Step 2 – West façade – San Francisco

Step 3 and Step 4 of the second run of AR repeat the same optimization process as in AR optimization I. Tables and Figures are shown in Appendix B. The optimization solutions for the entire façade of AR II are shown in Figure 4.18 and Figure 4.19. The

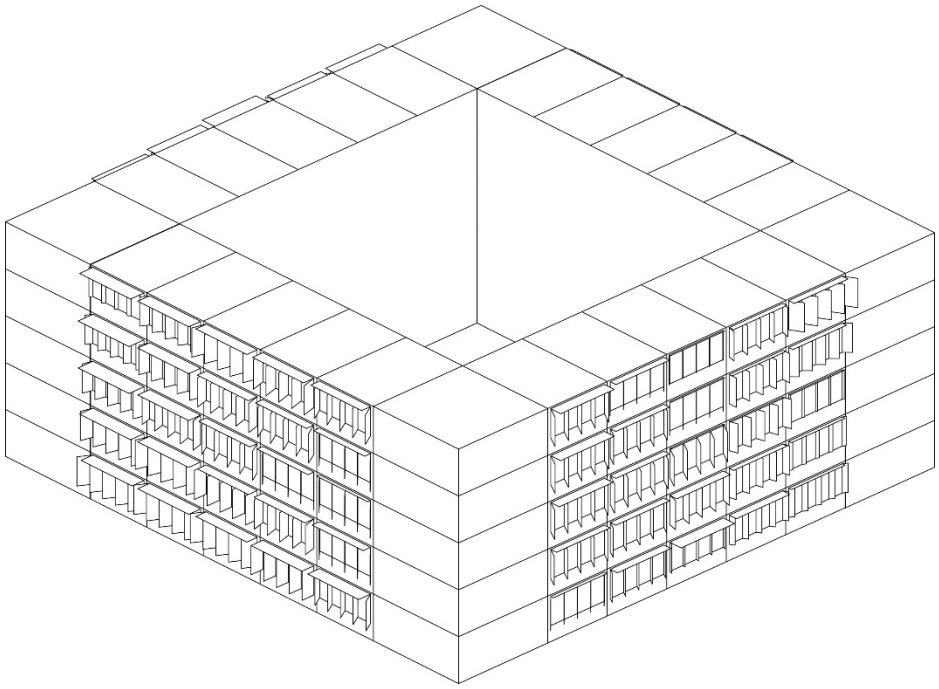

Figure 4.18: AR Results II – Step 4 – South and East façades – San Francisco

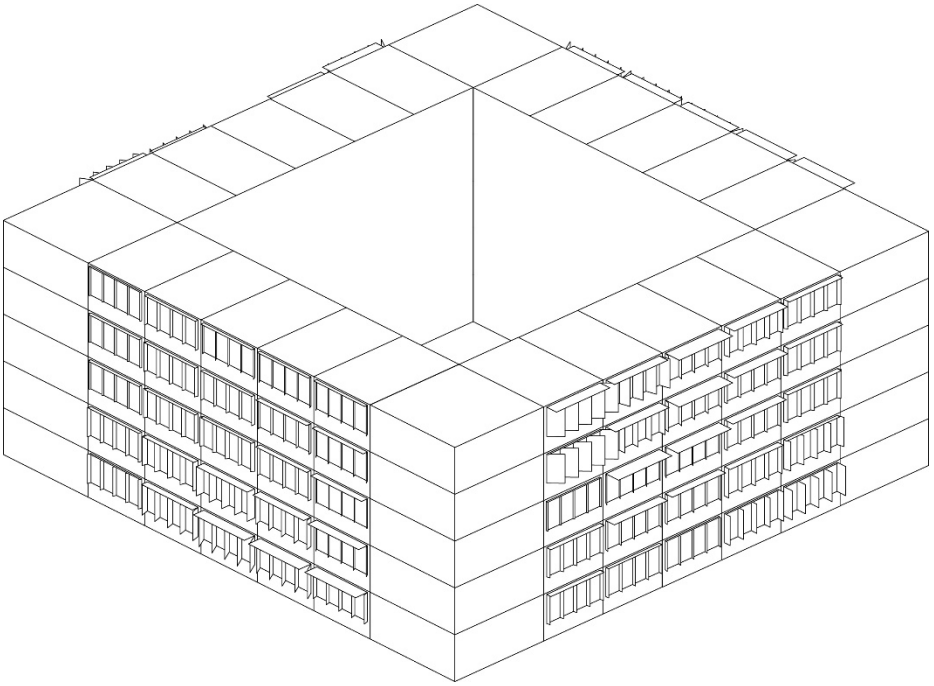

Figure 4.19: AR Results II – Step 4 – North and West façades – San Francisco

figures show a clear trend of large shading depths for the rooms receive more daylight and solar radiation, and small shading depths for the rooms receive less daylight and

solar radiation.

Table 4.16 represents the optimization result of AR optimization II on each step. It could be seen that the average total energy demand for all the rooms is 449.8 kWh in Step 2. After interpolation processes in step 3 and Step 4, the average total energy demand for each room is 506.3 kWh, which is 8.4% smaller than the 552.9 kWh achieved by AR I.

Table 4.16: AR Results II - San Francisco

	S [kWh]	E [kWh]	N [kWh]	W [kWh]	Average [kWh]	Runs [-]
Step 1	382.1	635.3	445.0	598.4	515.2	1220
Step 2	328.6	449.9	459.5	561.1	449.8	10340
Step 3	318.1	557.1	545.6	570.9	497.9	
Step 4	310.6	563.3	580.4	570.8	506.3	
Total						11560

4.3.3 Summary

Two AR optimization runs are executed in this section. The details of optimization results and optimal solutions for each step are presented. Table 4.17 and Table 4.18 represents a comparison of the design variables and optimization results of the two AR runs. It can be seen that, the values of the average total energy demand achieved by each step are steady in the two runs. The total number of simulation runs for each AR optimization are also consistent.

The glazing type 4 are shown by both AR I and AR II. Compared with the optimal solutions achieved by AR I, AR II shows lower insulation value (0.37 W/m^2K instead of 0.32 W/m^2K) and higher infiltration rate (0.25 instead of 0.18). The average total energy demand is 506.3 kWh, which is 8.4% smaller than the 552.9 kWh achieved in AR I.

Table 4.17: Comparison of Design Variables for AR I and AR II – San Francisco

	v_1	v_2	v_3	v_4	v_5	v_6		v_1	v_2	v_3	v_4	v_5	v_6
AR I							AR II						
S_{3-3}	5	5	1	9	6	6	S_{3-3}	4	1	1	5	7	7
E_{3-3}	2	6	3	1	3	9	E_{3-3}	5	1	2	4	2	3
N_{3-3}	4	3	1	2	1	3	E_{3-3}	4	4	1	8	3	1
W_{3-3}	4	3	1	5	4	4	E_{3-3}	4	2	1	4	5	3
	4	4	2	-	-	-	-	4	3	1	-	-	-

Table 4.18: Comparison of Results for AR and GA – San Francisco

		S	E	N	W	Average	Runs
AR							
AR I	Step 1	375.4	637.3	462.9	585.3	515.2	1320
	Step 2	360.7	445.7	481.3	578.5	466.5	10580
	Step 3	413.8	601.6	556.9	595.9	542.1	
	Step 4	422.0	601.6	576.5	611.6	552.9	
	Total						11900
AR II	Step 1	382.1	635.3	445.0	598.4	515.2	1220
	Step 2	328.6	449.9	459.5	561.1	449.8	10340
	Step 3	318.1	557.1	545.6	570.9	497.9	
	Step 4	310.6	563.3	580.4	570.8	506.3	
	Total						11560
Average							11070

4.4 Validation of AR Results against Simple GA

Two optimization runs of GA are executed in this section. Same design scenarios are used in these cases. The optimization results achieved by the two AR optimization runs are compared with that by these two GA runs. The purpose is to validate the accuracy and efficiency of AR.

For GA, the total number of possible solutions is:

$$6 \times 7 \times 4 \times (10 \times 10 \times 9) \times 100 \tag{4.4}$$

4.4.1 GA Results I

Table 4.19 represent the final results of all the sub-problems on the south orientation in the GA optimization I. The façade design solutions for each room are shown in Figure 4.20.

It can be seen in Table 4.19 that, the average inputs for south façade show by GA I are $v_1 = 4, v_2 = 4, v_3 = 1$. The average inputs for the shading elements are $v_4 = 6, v_5 = 6, v_6 = 5$. Relatively large overhang and fin depths are recommended for the south façade in GA I.

Table 4.19: GA Results I – South façade – San Francisco

Unit							[kWh]	[kWh]	[kWh]	[kWh]	Gene.	Simu.
S_{1-1}	6	1	1	7	5	4	13.1	204.8	96.4	314.3	19	380
S_{1-2}	4	4	1	8	7	3	31.8	149.7	140.2	321.7	26	520
S_{1-3}	4	1	1	8	4	7	44.5	129.4	176.7	350.6	17	340
S_{1-4}	4	4	1	8	6	7	30.9	131.2	194.6	356.8	31	620
S_{1-5}	4	6	1	8	5	7	27.6	126.3	130.3	284.2	32	640
S_{2-1}	4	4	1	3	10	1	20.8	204.2	146.8	371.9	21	420
S_{2-2}	4	3	1	9	5	6	42.1	141.2	158.8	342.1	27	540
S_{2-3}	4	3	1	5	5	6	26.1	204.7	152.2	382.9	24	480
S_{2-4}	4	2	1	1	9	4	20.7	201.3	137.5	359.4	29	580
S_{2-5}	4	7	1	7	5	7	24.6	133.6	129.2	287.4	50	1000
S_{3-1}	4	5	1	6	8	4	33.8	138.0	120.4	292.2	15	300
S_{3-2}	4	3	1	8	7	4	35.3	150.5	153.3	339.1	17	340
S_{3-3}	4	2	1	6	5	6	37.4	154.4	153.9	345.7	11	220
S_{3-4}	4	6	1	4	10	7	20.2	155.8	201.1	377.0	25	500
S_{3-5}	4	3	1	5	7	7	27.0	164.0	126.9	317.9	15	300
S_{4-1}	4	5	1	2	9	2	22.4	161.8	114.1	298.3	29	580
S_{4-2}	4	4	1	5	8	3	24.7	197.6	137.4	359.6	23	460
S_{4-3}	4	2	1	7	5	4	38.6	174.6	141.2	354.5	24	480
S_{4-4}	4	4	1	7	4	4	33.4	168.0	200.0	401.4	21	420
S_{4-5}	4	3	1	7	4	7	31.5	165.7	135.1	332.4	15	300
S_{5-1}	4	7	1	2	10	2	18.2	156.1	104.4	278.7	51	1020
S_{5-2}	4	3	1	4	7	2	24.3	206.1	146.0	376.4	22	440
S_{5-3}	4	5	1	8	5	4	33.0	218.5	154.5	406.1	37	740
S_{5-4}	4	2	1	9	5	7	36.8	200.5	190.4	427.7	9	180
S_{5-5}	4	3	1	9	5	7	34.3	164.7	128.8	327.9	45	900
Avg.	4	4	1	6	6	5	29.3	168.1	146.8	344.2	25.4	508
Sum.											635	12700

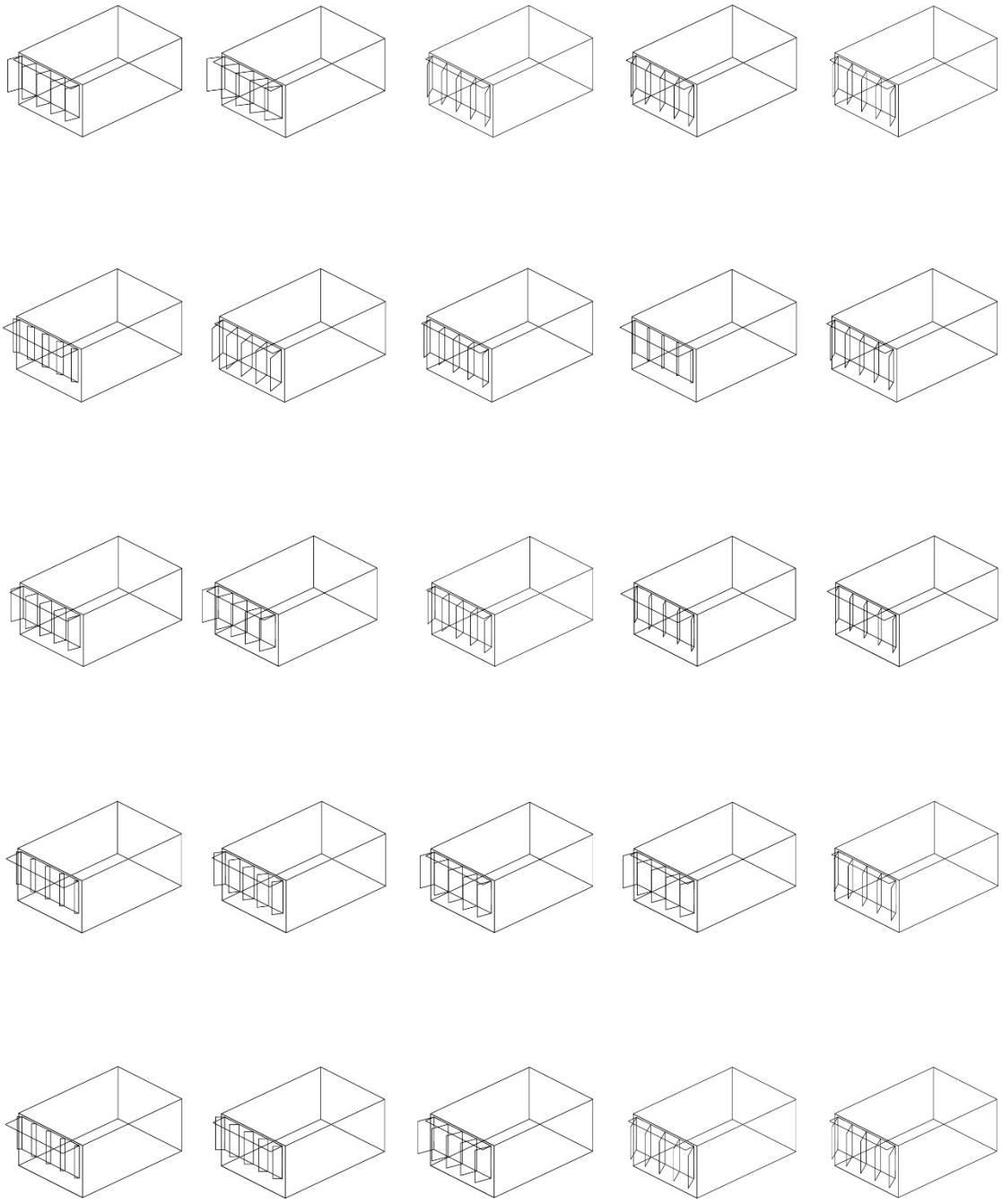

Figure 4.20: GA Results I – South façade – San Francisco

Table 4.20 represents the final results of all the sub-problems on the east orientation in the GA optimization I. The façade design solutions for each room are shown in Figure 4.21.

It can be seen in Table 4.20 that, the average inputs for east façade show by

Table 4.20: GA Results I – East façade – San Francisco

Unit							[kWh]	[kWh]	[kWh]	[kWh]	Gene.	Simu.
E_{1-1}	4	2	1	5	4	2	36.7	105.5	192.5	334.8	25	500
E_{1-2}	4	2	1	4	3	3	39.1	148.4	338.2	525.6	27	540
E_{1-3}	4	1	1	4	1	3	42.6	187.4	401.7	631.6	22	440
E_{1-4}	2	6	1	4	2	7	69.0	144.4	509.5	722.9	29	580
E_{1-5}	4	4	1	4	2	7	51.3	96.7	211.8	359.8	47	940
E_{2-1}	4	5	1	4	3	1	29.2	114.2	216.7	360.1	37	740
E_{2-2}	4	3	1	6	5	3	42.4	140.6	356.4	539.4	20	400
E_{2_3}	4	1	1	2	3	4	43.0	227.2	375.0	645.3	16	320
E_{2-4}	4	3	2	8	3	3	26.7	223.8	386.1	636.5	13	260
E_{2-5}	4	2	3	1	6	6	25.4	150.9	242.9	419.3	9	180
E_{3-1}	4	2	1	1	5	1	37.5	98.5	199.0	335.0	16	320
E_{3-2}	4	1	2	8	3	3	41.5	120.6	277.9	440.0	26	520
E_{3-3}	4	2	1	5	1	2	44.3	150.1	347.1	541.5	37	740
E_{3-4}	4	1	1	8	1	7	41.3	133.0	476.4	650.7	18	360
E_{3-5}	4	4	3	1	4	9	27.0	96.6	209.5	333.1	107	2140
E_{4-1}	4	7	1	1	5	1	26.3	106.5	193.7	326.5	51	1020
E_{4-2}	4	5	1	5	1	2	36.9	127.5	269.1	433.5	28	560
E_{4-3}	4	2	1	5	1	2	46.2	155.3	323.6	525.1	17	340
E_{4-4}	4	2	1	1	1	9	35.5	143.1	426.4	605.0	40	800
E_{4-5}	4	7	1	1	1	9	43.8	94.6	187.1	325.5	83	1660
E_{5-1}	4	7	1	5	3	2	27.3	118.7	158.9	304.9	75	1500
E_{5-2}	4	2	2	4	6	3	26.5	176.9	332.5	535.9	25	500
E_{5-3}	4	1	1	5	1	2	53.7	162.3	307.3	523.3	19	380
E_{5-4}	4	2	1	1	2	9	39.2	137.2	397.9	574.3	63	1260
E_{5-5}	4	3	2	8	4	7	38.8	116.2	202.1	357.1	20	400
Avg.	4	3	1	4	3	2	38.8	139.0	301.6	479.5	34.8	696
Sum.											870	17400

GA I are $v_1 = 4, v_2 = 3, v_3 = 1$. The average inputs for the shading elements are $v_4 = 4, v_5 = 3, v_6 = 2$. Relatively small overhang and fin depths are recommended for the east façade in GA I.

Table 4.21 represents the final results of all the sub-problems on the north orientation in the GA optimization I. The façade design solutions for each room are shown in Figure 4.22.

It can be seen in Table 4.21 that, the average inputs for north façade show by GA I are $v_1 = 4, v_2 = 3, v_3 = 1$. The average inputs for the shading elements are

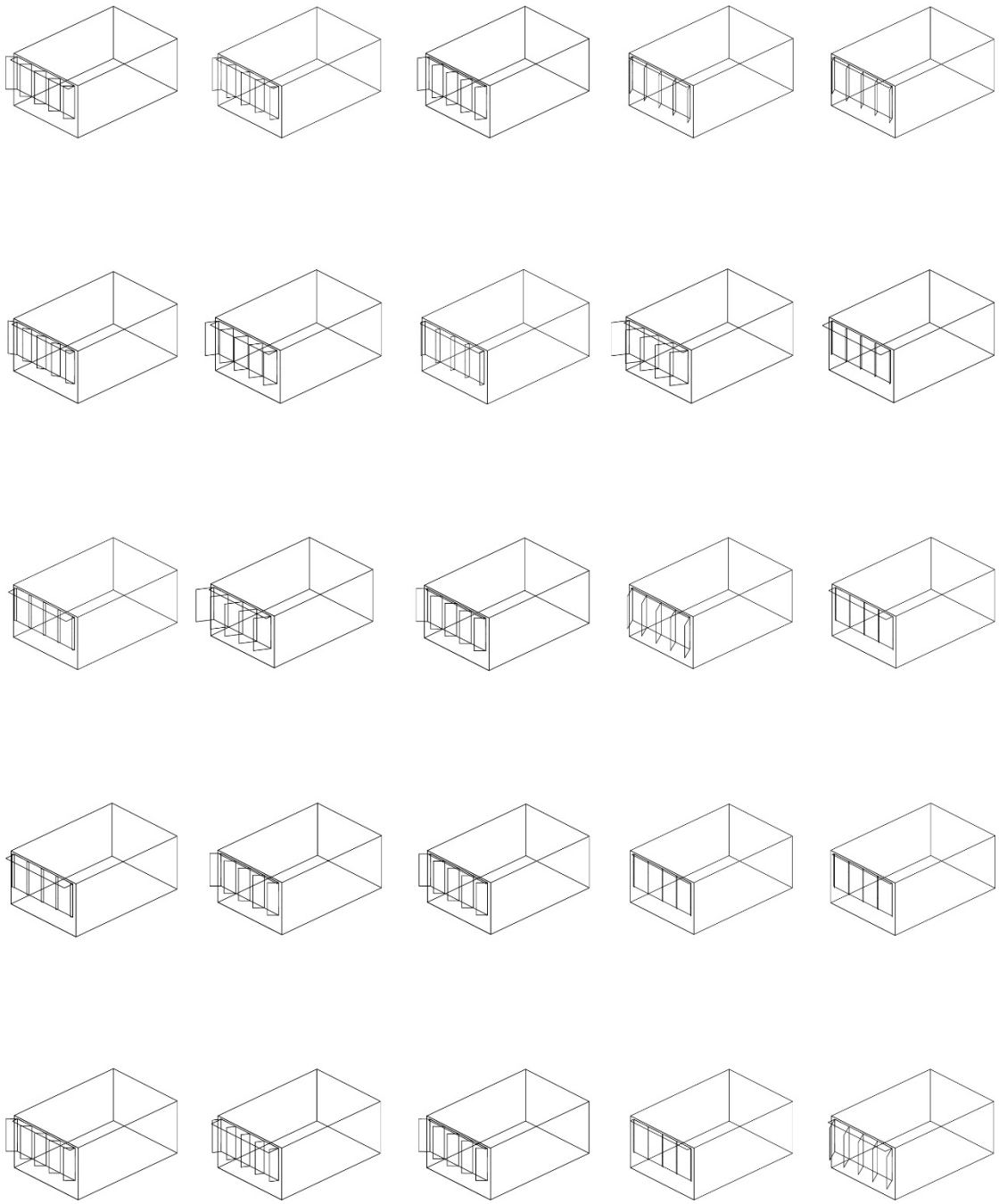

Figure 4.21: GA Results I – East façade – San Francisco

$v_4 = 3, v_5 = 2, v_6 = 4$. Small overhang and fin depths are recommended for the north façade in GA I.

Table 4.22 represents the final results of all the sub-problems on the north orientation in the GA optimization I. The façade design solutions for each room are shown

Table 4.21: GA Results I – North façade – San Francisco

Unit							[kWh]	[kWh]	[kWh]	[kWh]	Gene.	Simu.
N_{1-1}	4	1	1	2	1	4	36.9	180.4	375.1	592.4	13	260
N_{1-2}	4	1	1	2	2	4	43.8	170.2	374.3	588.3	35	700
N_{1-3}	4	1	1	2	1	4	42.1	175.0	375.1	592.2	19	380
N_{1-4}	4	4	1	5	1	2	35.6	114.8	379.2	529.6	43	860
N_{1-5}	6	1	1	1	2	6	31.6	164.6	158.3	354.6	50	1000
N_{2-1}	4	1	1	1	2	4	38.7	162.0	375.2	575.9	30	600
N_{2-2}	4	3	1	3	2	3	35.5	112.2	373.5	521.1	40	800
N_{2-3}	2	5	2	7	2	3	67.7	107.6	353.7	529.0	25	500
N_{2-4}	4	2	1	3	1	3	41.4	125.9	325.1	492.4	47	940
N_{2-5}	4	5	1	5	6	6	49.3	126.0	183.4	358.7	20	400
N_{3-1}	4	1	1	1	1	3	39.7	182.8	327.1	549.5	25	500
N_{3-2}	4	5	1	2	1	3	36.3	100.7	322.2	459.2	54	1080
N_{3-3}	4	4	1	2	3	7	40.6	112.5	341.9	495.0	25	500
N_{3-4}	4	4	1	2	1	3	47.6	113.8	293.8	455.2	16	320
N_{3-5}	4	3	2	2	2	7	49.7	94.4	126.2	270.3	29	580
N_{4-1}	4	2	1	8	1	3	38.0	113.0	325.5	476.5	26	520
N_{4-2}	4	3	1	4	1	3	45.6	91.2	277.7	414.4	29	580
N_{4-3}	4	1	2	4	2	3	38.7	101.1	308.3	448.2	36	720
N_{4-4}	4	3	1	2	2	3	54.0	102.9	269.1	426.1	22	440
N_{4-5}	4	7	2	2	2	7	39.2	101.0	122.4	262.6	32	640
N_{5-1}	4	2	1	1	1	7	37.7	140.2	323.4	501.3	18	360
N_{5-2}	4	4	1	2	1	3	43.7	97.4	283.9	425.1	26	520
N_{5-3}	4	4	1	2	6	3	46.0	105.9	323.5	475.5	13	260
N_{5-4}	4	5	1	2	1	3	47.0	113.5	232.8	393.3	24	480
N_{5-5}	6	1	1	2	2	7	37.7	112.2	123.5	273.4	34	680
Avg.	4	3	1	3	2	4	42.6	124.9	291	458.4	29.2	584.8
Sum.											731	14620

in Figure 4.23.

It can be seen in Table 4.22 that, the average inputs for west façade show by GA I are $v_1 = 4, v_2 = 2, v_3 = 1$. The average inputs for the shading elements are $v_4 = 2, v_5 = 3, v_6 = 5$, Small overhang and fin depths are recommended for the west façade in GA I.

Figure 4.24 and Figure 4.25 represent final design solutions of all the sub-problems on each orientation achieved by GA optimization I.

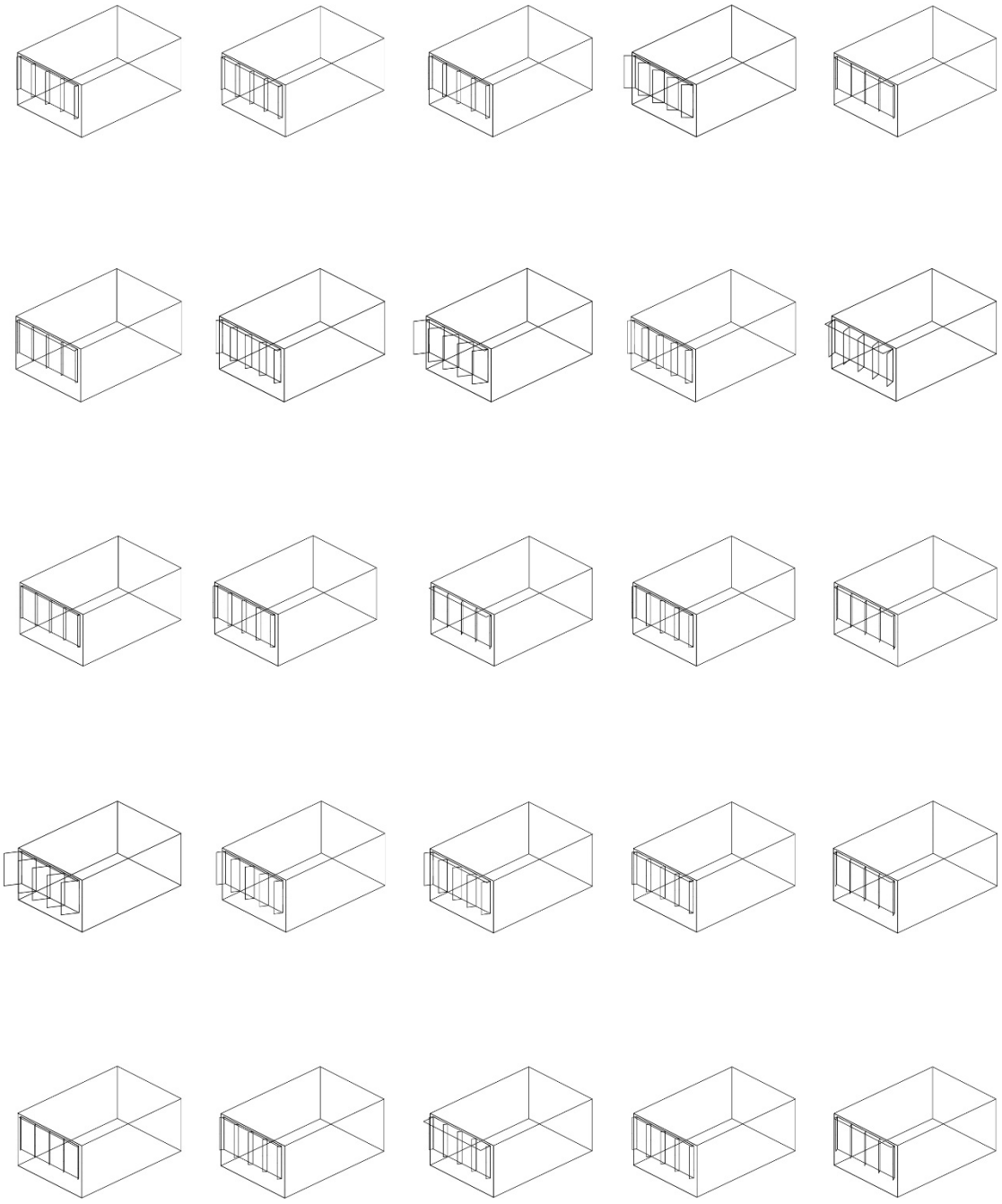

Figure 4.22: GA Results I – North façade – San Francisco

4.4.2 GA Results II

Figure 4.26 and Figure 4.27 represent the final design solutions of all the office rooms on each orientation for GA optimization II. Tables and Figures for details are shown in Appendix C.

Table 4.22: GA Results I – West façade – San Francisco

Unit							[kWh]	[kWh]	[kWh]	[kWh]	Gene.	Simu.
W_{1-1}	2	6	2	2	4	6	72.2	163.8	390.6	626.6	26	520
W_{1-2}	4	1	1	2	2	4	59.3	159.2	392.3	610.8	29	580
W_{1-3}	4	3	1	2	4	6	52.7	154.8	372.4	579.9	16	320
W_{1-4}	4	2	1	2	1	4	51.7	150.3	358	559.9	22	440
W_{1-5}	4	1	1	1	4	6	59.6	142.5	340.1	542.2	26	520
W_{2-1}	4	1	1	1	2	6	62.9	150.8	352.6	566.3	20	400
W_{2-2}	4	1	1	1	3	6	61.2	138.3	363.7	563.2	30	600
W_{2-3}	4	2	1	1	1	6	55.2	136.1	350.1	541.4	24	480
W_{2-4}	4	2	1	1	2	6	58.5	139.5	332.5	530.5	29	580
W_{2-5}	4	6	1	2	3	1	49.8	112.0	358.7	520.4	26	520
W_{3-1}	4	1	1	1	1	6	60.4	181.0	327.5	568.9	22	440
W_{3-2}	4	1	1	1	1	6	59.8	172.1	337.2	569.1	35	700
W_{3-3}	4	1	1	2	1	3	60.6	141.2	346.4	548.2	22	440
W_{3-4}	4	4	1	2	1	3	58.9	117.5	330.0	506.3	29	580
W_{3-5}	4	4	1	2	2	7	52.0	124.2	310.8	487.0	34	680
W_{4-1}	4	1	1	4	1	3	60.9	186.8	303.3	551.0	16	320
W_{4-2}	4	1	1	5	4	4	63.5	135.7	351.9	551.1	19	380
W_{4-3}	4	1	1	4	7	3	65.2	124.8	354.3	544.2	33	660
W_{4-4}	4	3	1	2	1	3	59.0	123.6	321.3	503.9	29	580
W_{4-5}	4	6	1	2	2	3	52.1	115.3	311.2	478.6	51	1020
W_{5-1}	4	2	1	5	10	4	56.0	141.4	350.0	547.4	23	460
W_{5-2}	6	1	1	9	1	3	27.5	199.3	292.9	519.7	35	700
W_{5-3}	4	2	1	2	7	3	55.7	167.4	327.0	550.1	18	360
W_{5-4}	4	5	1	2	7	7	53.2	137.9	304.3	495.4	36	720
W_{5-5}	6	1	1	2	1	3	29.2	201.7	263.9	494.8	35	700
Avg.	4	2	1	2	3	5	55.9	148.7	337.7	542.3	27.4	548
Sum.											685	13700

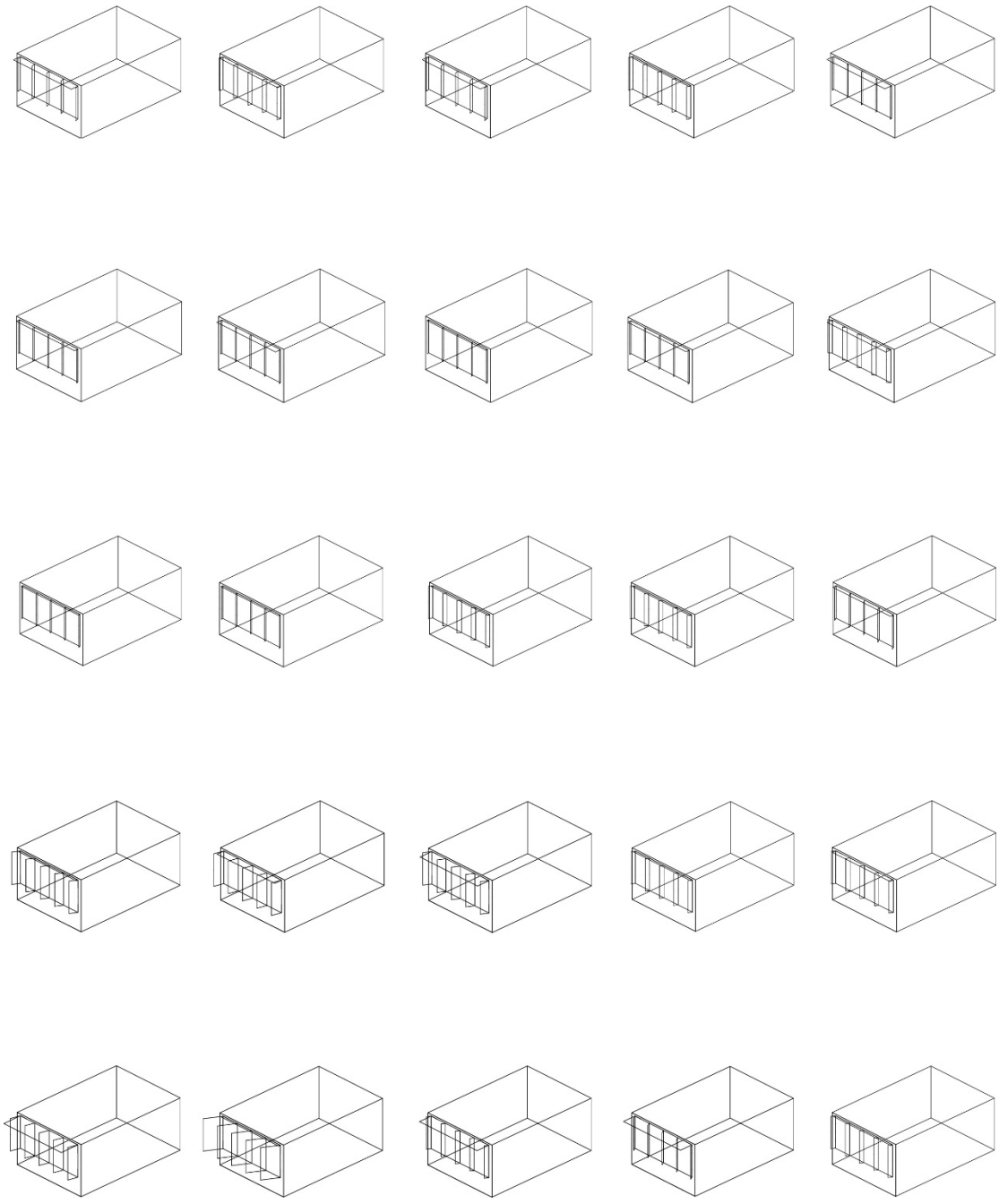

Figure 4.23: GA Results I – West façade – San Francisco

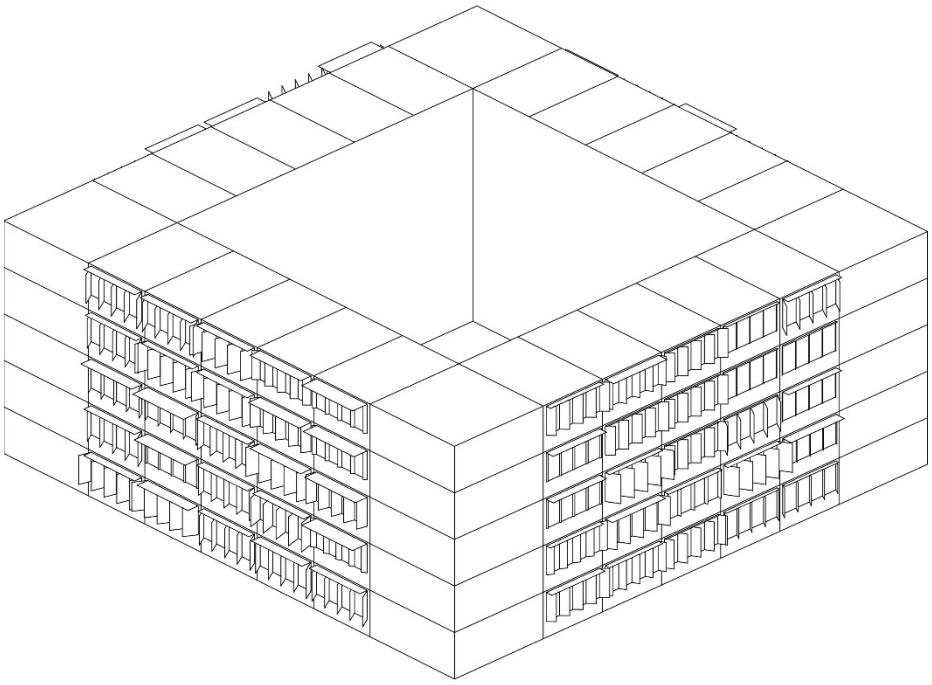

Figure 4.24: GA Results I – South and East façade – San Francisco

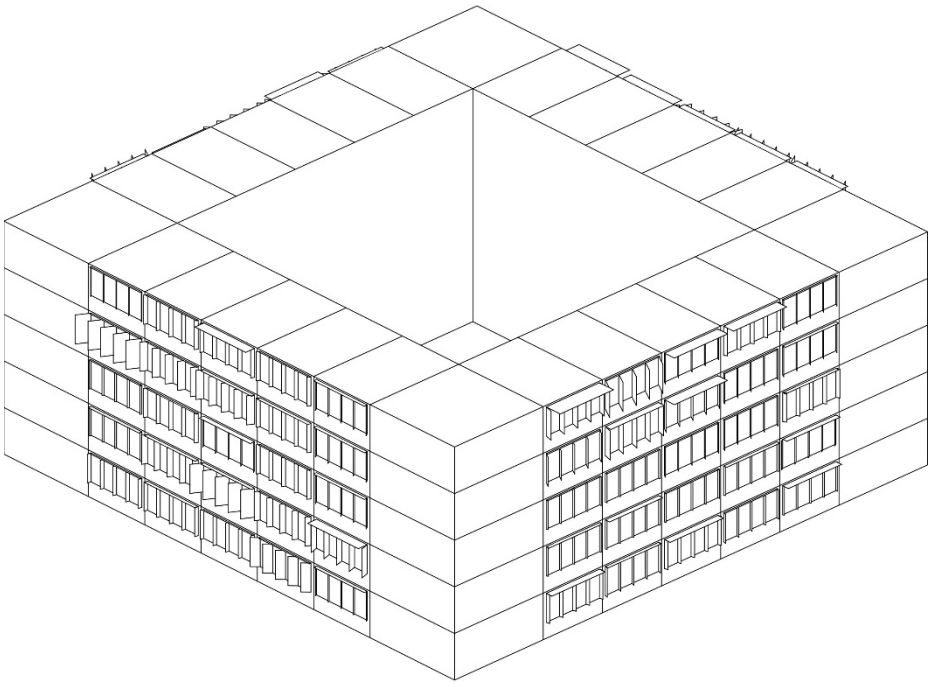

Figure 4.25: GA Results I – North and West façade – San Francisco

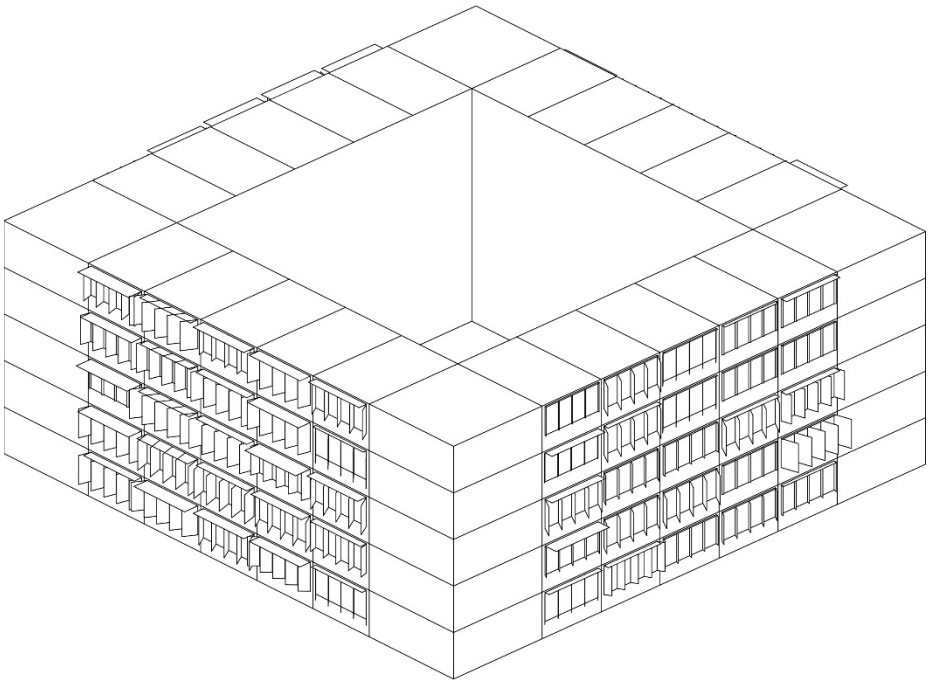

Figure 4.26: GA Results II – South and East façade – San Francisco

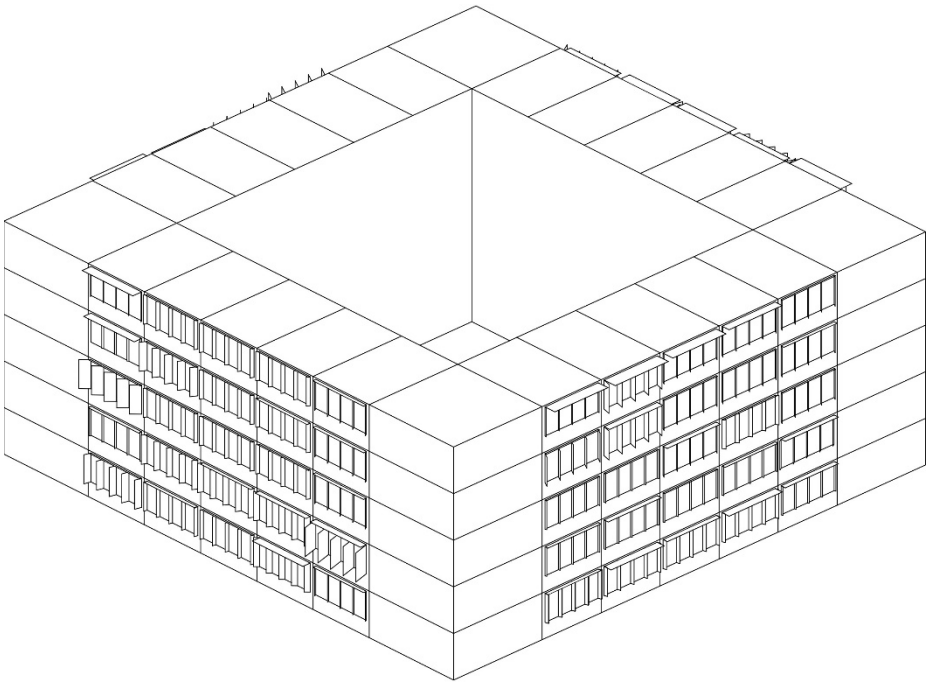

Figure 4.27: GA Results II – North and West façade – San Francisco

4.5 Summary

Table 4.23 shows the optimal design variables for the two AR and GA optimization runs. AR I achieves the optimal solutions for the glazing type, insulation and infiltration $v_1 = 4, v_2 = 4, v_3 = 2$. In the second run, AR II achieves the optimal solutions for the glazing type, insulation and infiltration $v_1 = 4, v_2 = 3, v_3 = 1$. Both GA I and GA II achieve the same optimal solutions $v_1 = 4, v_2 = 3, v_3 = 1$, which is the same as that achieved by AR II, and consistent with earlier solutions achieved by AR I.

Table 4.23: Comparison of Design Variables for AR and GA – San Francisco

	v_1	v_2	v_3	v_4	v_5	v_6		v_1	v_2	v_3	v_4	v_5	v_6
AR I							AR II						
S_{3-3}	5	5	1	9	6	6	S_{3-3}	4	1	1	5	7	7
E_{3-3}	2	6	3	1	3	9	E_{3-3}	5	1	2	4	2	3
N_{3-3}	4	3	1	2	1	3	N_{3-3}	4	4	1	8	1	3
W_{3-3}	4	3	1	5	4	4	W_{3-3}	4	2	1	4	5	3
	4	4	2	-	-	-		4	3	1	-	-	-
GA I							GA II						
S	4	4	1	6	6	5	S	4	4	1	7	6	5
E	4	3	1	4	3	2	E	4	2	1	4	2	4
N	4	3	1	3	2	4	N	4	3	1	3	2	4
W	4	2	1	2	3	5	W	4	2	1	2	3	5
	4	3	1	-	-	-		4	3	1	-	-	-

Table 4.24 represents the optimization results of the two AR and GA optimization runs. The average total energy demand for each room achieved by Step 2 for AR I is 456.2 kWh and 449.8 kWh for AR II. The average total energy demand for each room achieved by the GA I is 456.1 kWh and 456.9 kWh for GA II.

The results show that through the process of interpolation, the sub-problems achieve optimal solutions that are compromised with each other, thus some of the sub-problems in Step 3 and Step 4 don't achieve their global optimal. Therefore, the optimal results of ARs are larger than that achieved through the global optimal

Table 4.24: Comparison of Results for AR and GA – San Francisco

		S	E	N	W	Average	Runs
AR							
AR I	Step 1	375.4	637.3	462.9	585.3	515.2	1320
	Step 2	360.7	445.7	481.3	578.5	466.5	10580
	Step 3	413.8	601.6	556.9	595.9	542.1	
	Step 4	422.0	601.6	576.5	611.6	552.9	
	Total						11900
AR II	Step 1	382.1	635.3	445.0	598.4	515.2	1220
	Step 2	328.6	449.9	459.5	561.1	449.8	10340
	Step 3	318.1	557.1	545.6	570.9	497.9	
	Step 4	310.6	563.3	580.4	570.8	506.3	
	Total						11560
Average							11070
GA							
GA I		344.2	479.5	458.4	542.3	456.1	58420
GA II		348.5	483.8	449.6	545.8	456.9	53620
Average							56020

achieved by GAs. The main objective of the interpolation processes in Step 3 and Step 4 is to reduce the optimization time and improve the efficiency of optimization process, while the accuracy is undermined sometimes. However, GAs cannot find overall design solutions for the design variables v_1, v_2, v_3. The optimal solutions achieved by GAs for v_1, v_2 and v_3 are different for each room, thus still requires the designers to figure out a global optimization solution by experience.

Ideally, the solution achieved by the simple GA should be the same or better than the AR results for the same problem, since the optimal values for the design variables v_1, v_2 and v_3 are achieved for each room during the simple GA process. The optimization result shows that similar or better results have been derived by the AR processes until Step 2: The optimization process of Step 1 can help to find an overall optimal value for the design variables v_1, v_2 and v_3 at the system level of the AR allowed better convergence towards the true optimum. Additionally, partitioning of the problem results in Step 2 of optimization problem (3 variables per sub-problem as against 6 variables when the problem is solved in one step, and this increases the

performance of AR and also improves convergence. Even though the energy demand achieved by final steps (Step 4) of ARs have higher value than that of GAs, this is mainly because GA does not use an overall equivalent values for the design variables v_1, v_2 and v_3 for each sub-problem. This means the designers still need to select the appropriate overall equivalent values at this step, but cannot guarantee the overall minimum of energy demand for all the sub-problems.

It can also found in Table 4.24 that it needs 11900 simulations in total for AR I and 11600 simulations in total for AR II to find the global optimum. Compared with the AR runs, it requires 58420 simulations in total for the GA I and 53620 simulations in total for the GA II to find the global optimum. The total simulation time is reduced by 80.2%, which shows that the AR can achieve the optimal solutions with much less simulation effort than GA.

Chapter 4 has validated the applicability of AR in FPOs through a façade optimization problem of a typical square-floorplan mid-rise office. It is illustrated that the AR method can lead the façade design derives from the original generations and evolves into new generations. By selecting appropriate sub-problems and making interpolation of the achieved optimization results from the last step, this method can get optimal solutions for the remaining optimization groups without running unnecessary simulations, which may largely reduce simulation time. In this case study, AR took four steps to accomplish the optimization process. By using interpolation in Step 3 and Step 4, it can save up to 80.2% of the entire simulation time. Moreover, this method does not only considers the impacts from the climate, but also from the environmental situations in the site. Therefore, it validates the potential for more detailed solutions for complicated façade design.

To be adapted to contemporary architectural design, it is essential to use optimization techniques at the early design stage to solve FPO problems. AR can help architects to make design decisions efficiently. The obtained groups of appropriate

solutions are efficient and robustness to help architects to understand the trade-off relationship between different design solutions.

The above design guidance is valid only for this particular problem as defined by the ranges of input values and the constants used for these variables. This methodology can be used on an individual FPO problem in this design scenario, or further work could investigate this methodology using different design variables, objective and constraints, in order to observe the changes in results. For example, the problem used here could be run for different WWRs, or for a range of active design parameters to see how the design parameters generated differs. This in turn would enable more extensive design guidance to be formulated.

It's worth pointing out that since there are a limited number of sub-problems in Step 2, the optimization solutions achieved by Step 2 can only show a trend, but cannot guarantee the solutions are the global optimum for this FPO problem. AR has the potential to be more efficient and accurate when solving more complex façade optimization problems with more sub-problems, since there will be more gradients between different sub-problems.

CHAPTER V

Validation of AR in Different Climates

5.1 Chapter Outline

There have been various studies on the climate responsive building design strategies. The definition of these climatic zones is largely based on different criteria and the purpose of establishing such classification. In the early 1960s , Olgyay defined four main climate types for climatic building design strategies in his study, including cool, temperate, hot and arid, and hot and humid climate zones (*Olgyay*, 1992). In 1976, Givoni also defined four major climates for the building design climate, including hot, warm-temperate, cool-temperate and cold climate zones. The main purpose was to develop the impact of climatic characteristics on the human comfort and the buildings' thermal response (*Givoni*, 1976). However, there is still limited study for climate responsive building design strategies in the United States. Research has been done for climate impacts on building energy demand in different climate zones in the U.S. (*Wang and Chen*, 2014), Australia (*Karimpour et al.*, 2015), Turkey (*Mangan and Oral*, 2015) and India (*Singjh et al.*, 2007). These studies provided fundamental research of the impacts of climate on building performance and shown appropriate design solutions for climate responsive design strategies. However, these strategies are still mainly relied on the designer's experience. A simulation/optimization driven methodology is essential to be developed and more effective to provide solutions with

more accuracy at the early design stage.

The primary approaches of this chapter include:

(i) identify the major climates and select a major city in each climate zone, (ii) investigate the relationship between the design variables and objectives of FPOs in different climate zones in the United States, and (iii) provide climate responsive design strategies for high-performance façade for these climates.

AR are implemented in two other cities (Chicago, IL; Miami, FL) in the U.S. The purpose is to validate the applicability and stability of AR in solving FPOs in different climates. Section 5.2 describes the climatic characteristics of the selected cities. The optimization problem with the same design scenario in Chapter 4 is implemented in the two selected climates in Section 5.3 and Section 5.4, respectively. For each city, two AR optimization runs (AR I and AR II) are executed. The optimization results are compared and discussed. FPO design solutions for these two climates are then summarized.

5.2 Climate Discussion

The territory of United States is mainly located in in central North America between Canada and Mexico, which covers an area of approximately 9.84 million km^2. The United States includes most climate types with its large territory size and geographic variety. There are eight major climate zones in United States, which are based on temperature and humidity, including hot-humid, mixed-humid, hot-dry, mixed-dry, cold, very-cold, subarctic, marine regions (*PNNL*, 2015)(Figure 5.2).

ASHRAE 90.1-2010 gives definition of international climatic zones (Figure **??**), which can be found in ANSI/ASHRAE/IESNA Standard 90.1-2007 Normative Appendix B – Building Envelope Climate Criteria (*ASHRAE*, 2010). The information below is from Tables B-2, B-3, and B-4 in that appendix.

Three cities in different climate zones are discussed in this study, which represent

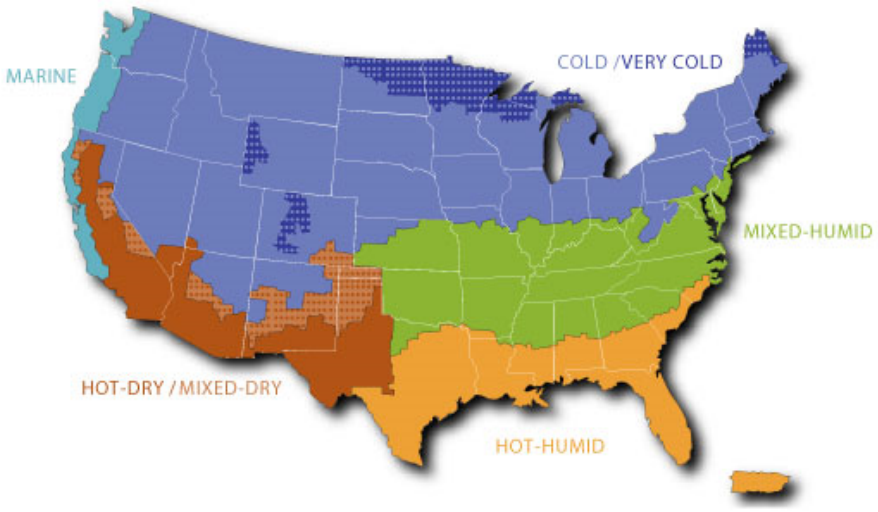

Figure 5.1: Seven of the eight US climate zones (Recognized by Building America occur in the continental United States. The sub-arctic U.S. climate zone, not shown on the map, appears only in Alaska (*PNNL*, 2015)

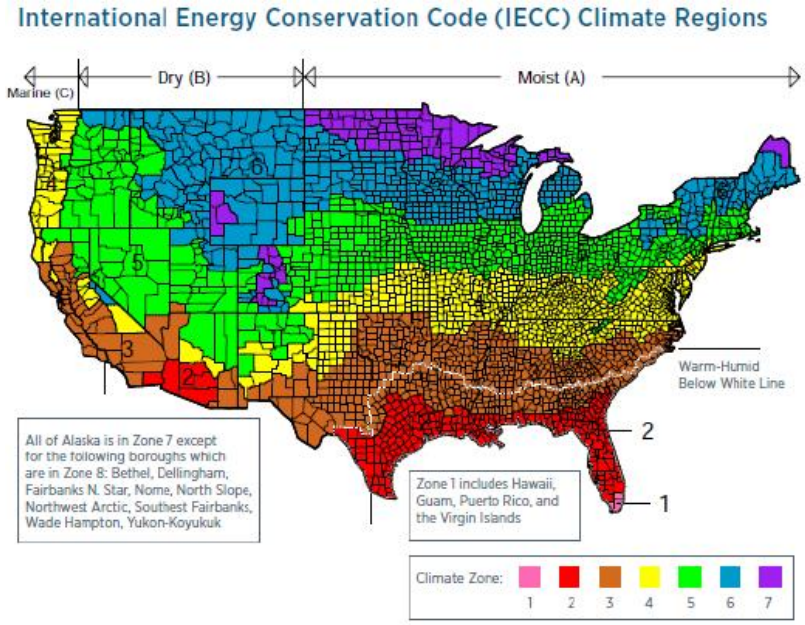

Figure 5.2: International Energy Conservation Code (IECC) climate regions (*PNNL*, 2015)

the climate zones defined in the ASHRAE Standard 90.1-2010 (*ASHRAE*, 2010). In addition to San Francisco (CA), which has been discussed in the case study in Chapter 4, the other two cities are Chicago (IL) and Miami (FL), representing the Cool-Humid and Very Hot-Humid climates. These cities are also representative for

Table 5.1: Definition of international climatic zones(*ASHRAE*, 2010)

Zone Number	Zone Name	Thermal Criteria (IP Units)	Thermal Criteria (SI Units)
1A and 1B	Very Hot - Humid (1A) Dry (1B)	9000 < CDD50°F	5000 < CDD10°C
2A and 2B	Hot-Humid (2A) Dry (2B)	6300 < CDD50°F ≤ 9000	3500 < CDD10°C ≤ 5000
3A and 3B	Warm - Humid (3A) Dry (3B)	4500 < CDD50°F ≤6300	2500 < CDD10°C < 3500
3C	Warm - Marine (3C)	CDD50°F ≤ 4500 and HDD 65°F ≤ 3600	CDD10°C ≤ 2500 ≤ HDD18°C ≤ 2000
4A and 4B	Mixed-Humid (4A) Dry (4B)	CDD50°F ≤ 4500 and 3600 < HDD 65°F ≤ 5400	CDD10°C ≤ 2500 and HDD18°C ≤ 3000
4C	Mixed - Marine (4C)	3600 < HDD 65°F ≤ 5400	2000 < HDD18°C ≤ 3000
5A, 5B, and 5C	Cool-Humid (5A) Dry (5B) Marine (5C)	5400 < HDD 65°F ≤ 7200	3000 < HDD18°C ≤ 4000
6A and 6B	Cold - Humid (6A) Dry (6B)	7200 < HDD 65°F ≤ 9000	4000 < HDD18°C ≤ 5000
7	Very Cold	9000 < HDD 65°F ≤ 12600	5000 < HDD18°C ≤ 7000
8	Subarctic	12600 < HDD 65°F	7000 < HDD18°C

the culture and commercial centers with more commercial office buildings case studies, in order to involve a broad range of climatic conditions in the United States. The details of typical meteorological year (TMY) weather data of these cities are readily available, which validates the feasibility of further study. All TMY weather data are derived from U.S. Department of Energy. The hourly TMY3 weather data for simulation are extracted from the EnergyPlus database.

Miami has a tropical climate with hot and mild summers and warm winters.

Table 5.2: Climate zones of the United States and reference cities.

Climate Zone	City			Latitude (°)
Longitude (°)				
1A	Miami	Very Hot-Humid	25°47'N	80°13'W
3C	San Francisco	Marine	37°47'N	122°25'W
5A	Chicago	Cool-Humid	41°53'N	87°38'W

The average monthly temperature of the coldest months (December and January) is around 20.1°C (68.2°F). The warmest months (July and August) have average monthly temperatures of 29-35°C (84-96°F), accompanied by high humidity. The lowest daily minimum temperature on record is 7°C (45°F) on February, 1990, and the highest is 29°C (84°F) on August 4, 1993.

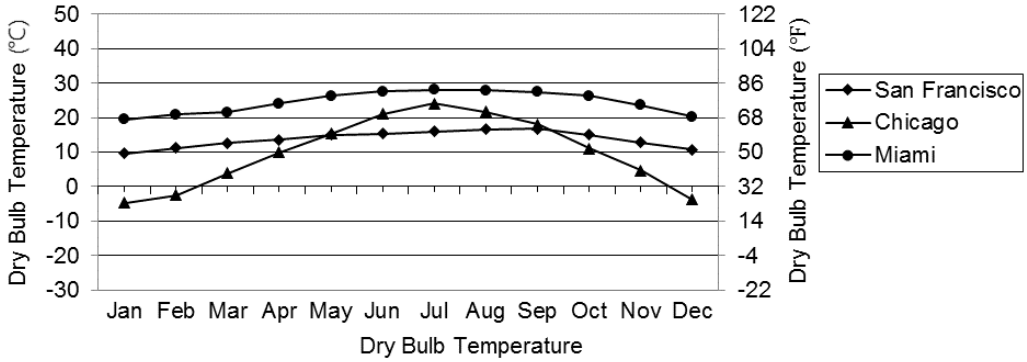

Figure 5.3: Monthly dry bulb temperatures for three cities in the United States (°C/°F)

Chicago has a climate characterized by four distinct seasons: wet, cool springs; somewhat hot, and often humid, summers; pleasantly mild autumns; and cold winters. The average monthly temperature of the coldest month (January) is around -4°C (25°F). The warmest month (July) has average monthly temperature of 24°C (76°F). The recorded lowest temperature is -32°C (-25°F) in January, and the highest is 43°C (109°F) in July.

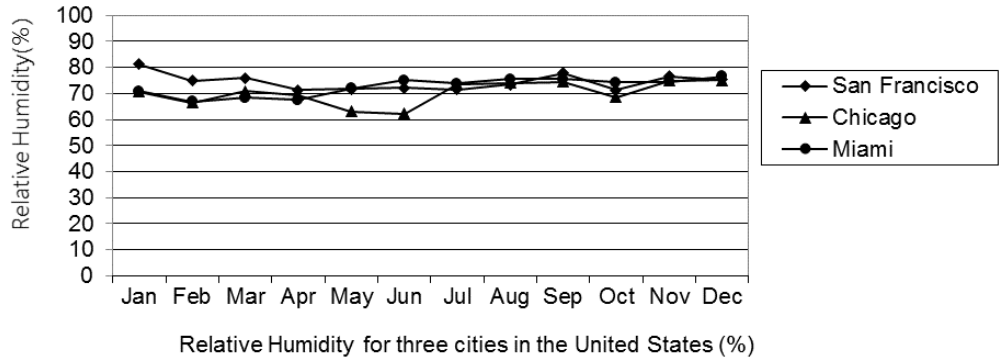

Figure 5.4: Monthly mean relative humidity for three cities in the United States (%)

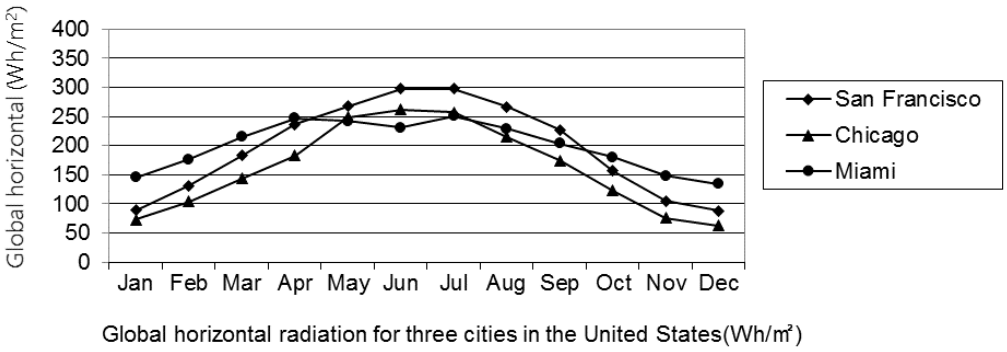

Figure 5.5: Monthly global horizontal radiation for three cities in the United States (Wh/m^2)

5.3 AR Results for Chicago

5.3.1 AR results I - Chicago

Step 1

Table 5.3 shows the optimization results achieved by Step 1 in AR optimization I for Chicago. Optimization runs for four sub-problems ($S_{3-3}, N_{3-3}, E_{3-3}, W_{3-3}$) are executed in this step. The first design three variables are achieved by averaging the optimization results, which are $v_1 = 6, v_2 = 5, v_3 = 4$. Therefore, the best glazing (glazing type 6), the third best insulation (0.26 W/m^2K) and the lowest infiltration rate (0.12) are shown for the climate of Chicago. The average total energy demand

for all sub-problems is 1370.1 kWh.

Table 5.3: AR Results I - Step 1 – San Francisco

Unit	v_1	v_2	v_3	v_4	v_5v	v_6	Q_{Total} [kWh]	Gene. [-]	Simu. [-]
S_{3-3}	6	5	3	2	9	7	1185.5	19	380
E_{3-3}	6	4	4	3	2	4	1465.2	17	340
N_{3-3}	6	5	3	8	4	7	1394.5	20	400
W_{3-3}	6	6	4	7	7	6	1435.1	18	360
Avg.	6	5	4	-	-	-			
Avg.							1370.1	19	370
Sum.								74	1480

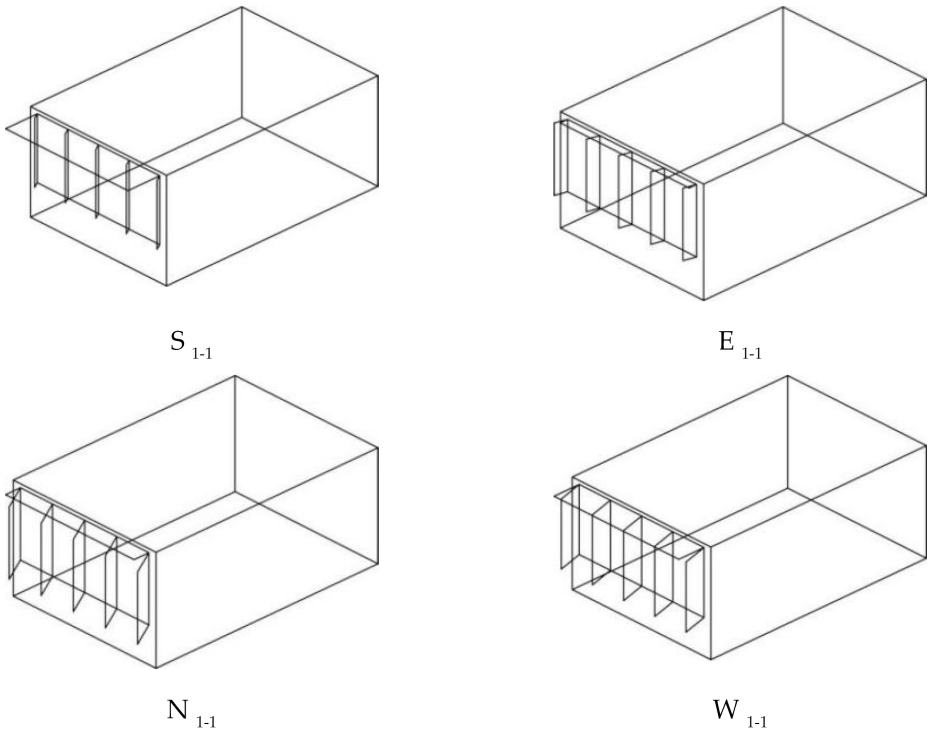

Figure 5.6: AR Results I – Step 1 – Chicago

Chicago has a distinct weather with cold winters and hot summers. High-quality wall insulation is imperative on all orientations in this climate to maintain the indoor temperature to reduce the heating energy demand. In addition, the southern façade

receives extensive solar radiation in the hot summer, therefore, well-insulated windows with high SHGC glazing are also essential to block the solar heat and reduce the cooling energy demand. Also, the western façade receives extensive solar radiation in the afternoons, thus requires high-value insulation. Additionally, the weather of Chicago is not severe cold climate, which also explains why the design solutions don't show the highest insulation values.

It also can be seen in Figure 5.6 that the overhang shading depths on the south and west façades are large, which are 900 mm and 700 mm, respectively. In contrast, the shading depths on the east and north façade are small, which are 200 mm and 400 mm.

Step 2

Table 5.4 shows the optimization results for south façade achieved by Step 2 of the AR optimization I. The first three design variables ($v_1 = 6, v_2 = 5, v_3 = 4$) stay unchanged. The optimization runs are executed for 9 selected sub-problems ($S_{1-1}, S_{1-3}, S_{1-5}, S_{3-1}, S_{3-3}, S_{3-5}, S_{5-1}, S_{5-3}, S_{5-5}$) on the south orientation. The façade design solutions for these sub-problems are shown in Figure 5.7.

Table 5.4: AR Results I - Step 2 – South façade – Chicago

Unit	v_1	v_2	v_3	v_4	v_5	v_6	Q_{Total} [kWh]	Gene. [-]	Simu. [-]
S_{1-1}	6	5	4	8	9	3	1062.8	16	320
S_{1-3}	6	5	4	6	3	6	1176.7	14	280
S_{1-5}	6	5	4	10	1	8	1151.6	11	220
S_{3-1}	6	5	4	1	10	3	1050.3	11	220
S_{3-3}	6	5	4	8	4	4	1147.7	16	320
S_{3-5}	6	5	4	6	5	7	1126.5	12	240
S_{5-1}	6	5	4	2	10	2	1043.6	13	260
S_{5-3}	6	5	4	4	7	4	1189.6	14	280
S_{5-5}	6	5	4	1	7	7	1123.6	16	320
Avg.							1119.1	13.7	273.3
Sum.								123	2460

It can be found in Table 5.4 and Figure 5.7 that the optimization solutions achieved

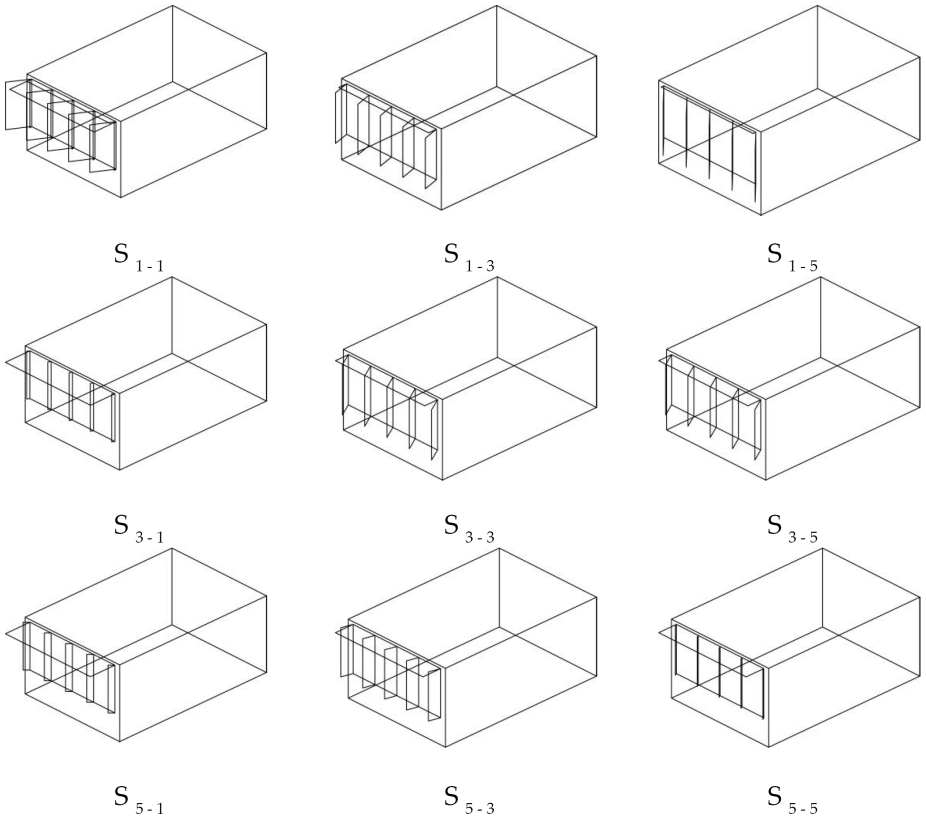

Figure 5.7: AR Results I – Step 2 – South façade - Chicago

by Step 2 show large fin and overhang shading depths on the south façade, which is consistent with the solutions achieved by Step 1. The average total energy demand for all the 9 sub-problems is 1191.1 kWh. This result is 5.6% smaller than the 1185.5 kWh achieved by Step 1.

Table 5.4 also shows the optimization results for south façade achieved by Step 2 of the AR optimization I. The first three design variables ($v_1 = 6, v_2 = 5, v_3 = 4$) stay unchanged. The optimization runs are executed for 9 selected sub-problems ($S_{1-1}, S_{1-3}, S_{1-5}, S_{3-1}, S_{3-3}, S_{3-5}, S_{5-1}, S_{5-3}, S_{5-5}$). The average total energy demand for all the 9 sub-problems is 1119.1 kWh. The façade design solutions for these sub-problems are shown in Figure 5.7.

The optimization solutions achieved by Step 2 show large overhang shading depths for the rooms located on the west side of the south façade ($S_{1-1}, S_{3-1}, S_{5-1}$), to prevent

extensive solar radiation in the afternoon. Also, the rooms located on the top floors $S_{5-1}, S_{5-3}, S_{5-5}$ have larger overhang depths, since they are less influenced by the high-rise building construction on the south.

Table 5.5 represents the optimization results for east façade achieved by Step 2 of the AR optimization I. The optimization runs are executed for 9 selected sub-problems ($E_{1-1}, E_{1-3}, E_{1-5}, E_{3-1}, E_{3-3}, E_{3-5}, E_{5-1}, E_{5-3}, E_{5-5}$) on the east orientation. The average total energy demand for all the 9 sub-problems is 1268.1 kWh. The façade design solutions for these sub-problems are shown in Figure 5.8.

Table 5.5: AR Results I - Step 2 – East façade – Chicago

Unit	v_1	v_2	v_3	v_4	v_5	v_6	Q_{Total} [kWh]	Gene. [-]	Simu. [-]
E_{1-1}	6	5	4	9	3	3	1228.8	19	380
E_{1-3}	6	5	4	9	2	3	1418.6	14	280
E_{1-5}	6	5	4	4	3	7	1208.9	15	300
E_{3-1}	6	5	4	1	5	1	1171.4	15	300
E_{3-3}	6	5	4	7	4	3	1456.4	11	220
E_{3-5}	6	5	4	1	7	9	1192.2	13	260
E_{5-1}	6	5	4	5	3	2	1148.6	14	280
E_{5-3}	6	5	4	7	5	2	1414.2	14	280
E_{5-5}	6	5	4	1	3	9	1174.0	15	300
Avg.							1268.1	14.4	288.9
Sum.								130	2600

The optimization solutions show relatively small overhang shading depths on the east façade than that on the south facade. The eastern façade mainly receives solar radiation in the morning, with a relatively lower temperature at that time in this climate. Also, most of the solar radiations is blocked by the high-rise construction on the east. Therefore, overhang large shading depths are not so imperative in this climate.

Figure 5.8 also shows that the fin angles are relatively small for the first two rooms on each floor ($E_{1-1}, E_{1-3}, E_{3-1}, E_{3-3}, E_{5-1}, E_{5-3}$), which shows a trend to face the south orientation as much to receive more solar radiation, as well as reflect more

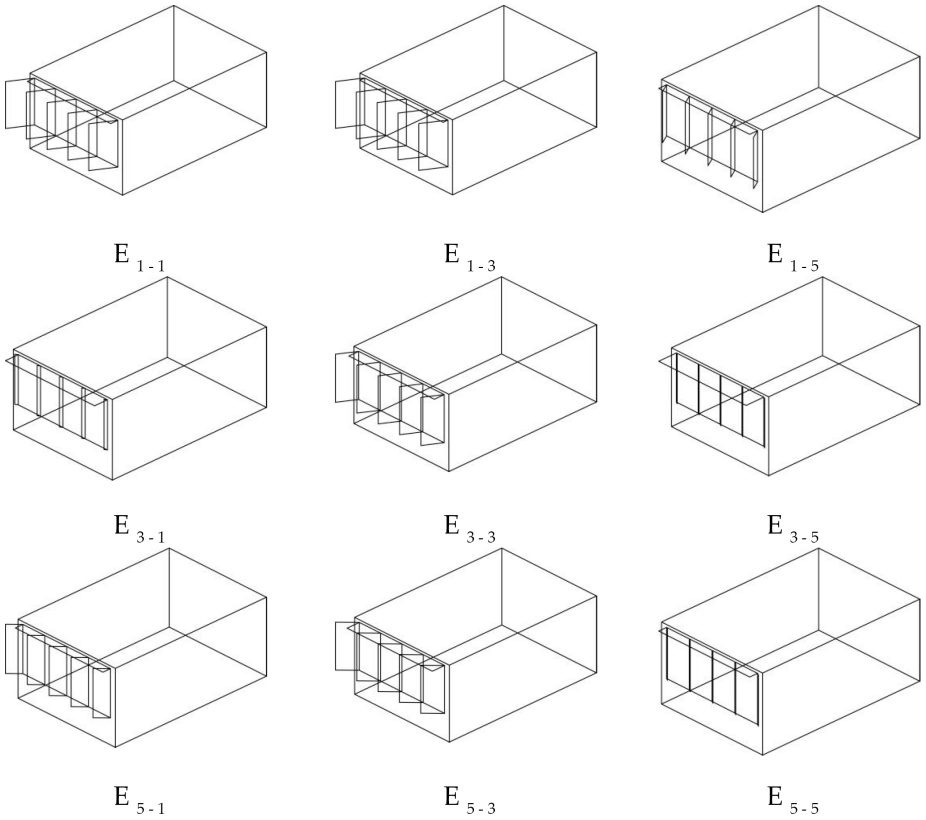

Figure 5.8: AR Results I – Step 2 – East façade – Chicago

daylight in to the room. In contrast, solutions for the third rooms on each floor ($E_{1-5}, E_{3-5}, E_{5-5}$) show a north-facing fin angle (120°). The reason is that the rooms on the northeast edge are blocked by the high-rise building on the east and north. The only available daylight and solar radiation is from the space between the east and north buildings. Therefore, the fin angles are facing this space to receive as much daylight and solar radiation as possible.

Table 5.6 represents the optimization results for north façade achieved by Step 2 of the AR optimization I. The optimization runs are executed for 9 selected sub-problems ($N_{1-1}, N_{1-3}, N_{1-5}, N_{3-1}, N_{3-3}, N_{3-5}, N_{5-1}, N_{5-3}, N_{5-5}$) on the north orientation. The average total energy demand for all the 9 sub-problems is 1301.4 kWh. The façade design solutions for these sub-problems are shown in Figure 5.9.

The optimization solutions show small depths for overhang shadings on the north

Table 5.6: AR Results I - Step 2 – North façade – Chicago

Unit	v_1	v_2	v_3	v_4	v_5	v_6	Q_{Total} [kWh]	Gene. [-]	Simu. [-]
N_{1-1}	6	5	4	2	2	6	1416.7	11	220
N_{1-3}	6	5	4	8	3	7	1422.1	12	240
N_{1-5}	6	5	4	9	4	7	1171.6	13	260
N_{3-1}	6	5	4	8	1	2	1342.1	14	280
N_{3-3}	6	5	4	6	1	7	1369.7	14	280
N_{3-5}	6	5	4	6	1	6	1163.4	11	220
N_{5-1}	6	5	4	1	3	6	1365.8	13	260
N_{5-3}	6	5	4	10	3	7	1317.0	13	260
N_{5-5}	6	5	4	1	1	3	1144.4	12	240
Avg.							1301.4	12.6	251.1
Sum.								113	2260

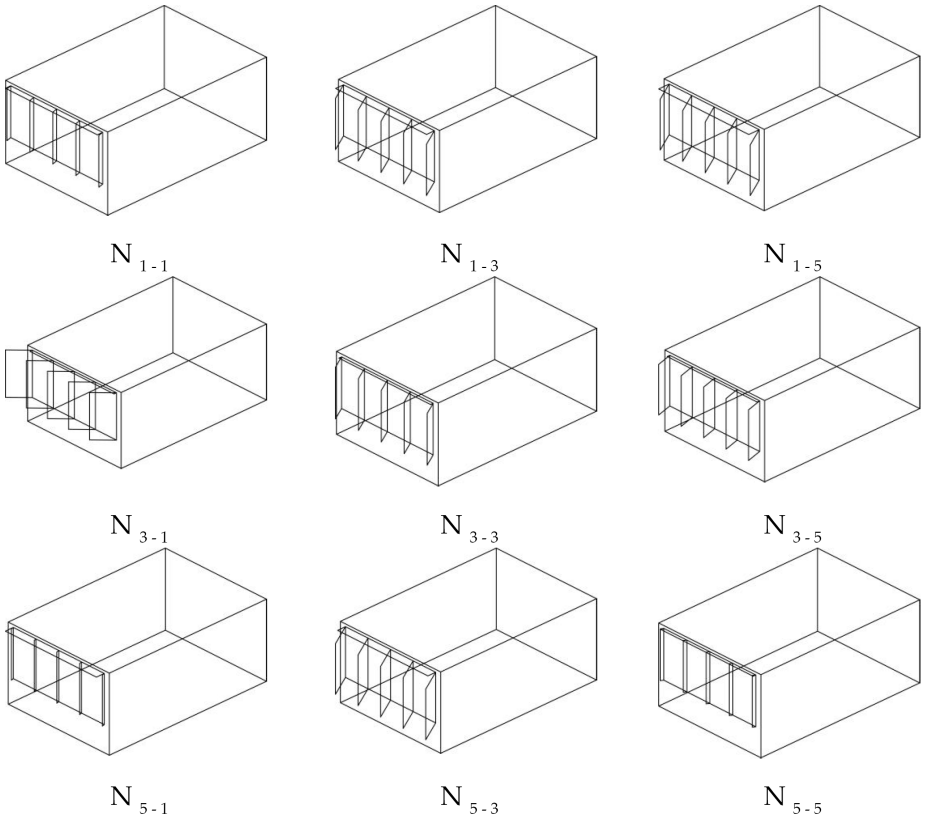

Figure 5.9: AR Results I – Step 2 – North façade – Chicago

façade. This is because the north façade does not achieve as much daylight and solar radiation during the entire year in the climate of Chicago. Thus overhang shading is not prerequisite. The fins are slightly facing west for most of the rooms, which can

help to receive as more as daylight and solar radiation through the reflections by the fin shadings.

Table 5.7: AR Results I - Step 2 – West façade – Chicago

Unit	v_1	v_2	v_3	v_4	v_5	v_6	Q_{Total} [kWh]	Gene. [-]	Simu. [-]
W_{1-1}	6	5	4	2	4	6	1456.7	15	300
W_{1-3}	6	5	4	1	4	7	1460.5	13	260
W_{1-5}	6	5	4	1	2	6	1370.3	14	280
W_{3-1}	6	5	4	1	4	6	1428.1	11	220
W_{3-3}	6	5	4	2	10	7	1390.2	12	240
W_{3-5}	6	5	4	1	1	3	1393.7	20	400
W_{5-1}	6	5	4	5	1	7	1393.6	11	220
W_{5-3}	6	5	4	9	3	4	1403.8	11	220
W_{5-5}	6	5	4	4	3	7	1372.7	12	240
Avg.							1407.7	13.2	264.4
Sum.								119	2380

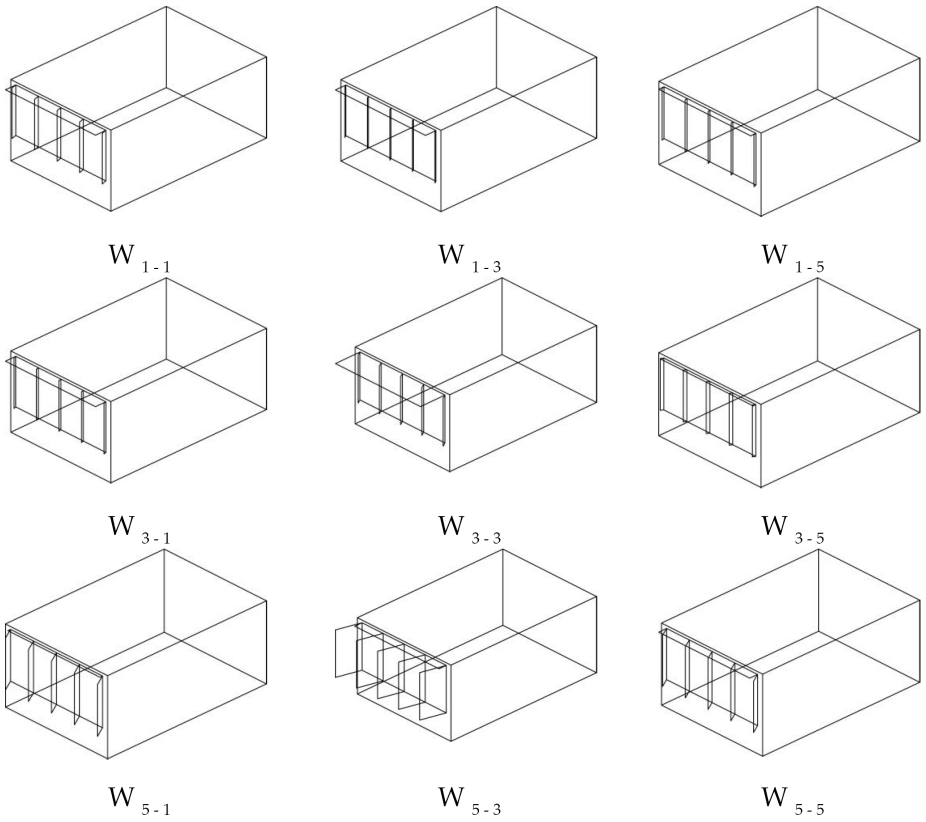

Figure 5.10: AR Results I – Step 2 – West façade – Chicago

Table 5.7 represents the optimization results for western façade achieved by Step

2 of the AR optimization I. The optimization runs are executed for 9 selected sub-problems ($W_{1-1}, W_{1-3}, W_{1-5}, W_{3-1}, W_{3-3}, W_{3-5}, W_{5-1}, W_{5-3}, W_{5-5}$) on the west orientation. The average total energy demand for all the 9 sub-problems is 1407.7 kWh. The façade design solutions for these sub-problems are shown in Figure 5.10.

The optimization solutions show small depths for fin and overhang shadings for most of the rooms. The rooms on the top floor ($W_{5-1}, W_{5-3}, W_{5-5}$) receive more solar radiation in the afternoons, thus fin shading depths are larger to reduce exposure to solar radiation on this orientation.

Step 3 and Step 4

Step 3 and Step 4 are shown in the Appendix D. The optimization solutions for the entire façade of AR II are shown in Figure 5.11 and Figure 5.12.

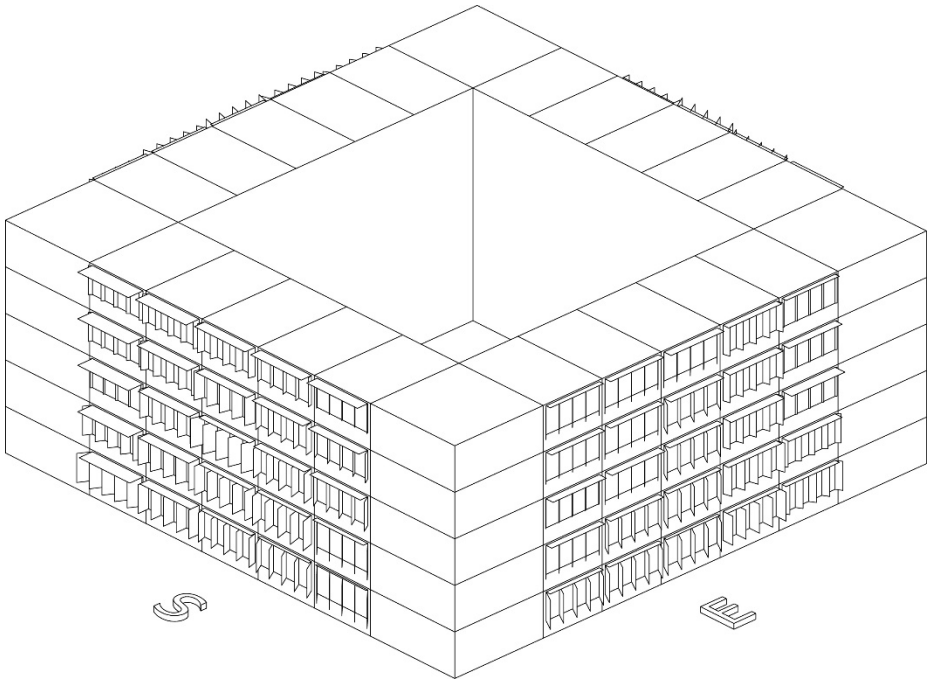

Figure 5.11: AR Results I – Step 4 – South and East façades – Chicago

Table 5.8 represents the optimization result on each step of AR optimization I. It can be seen that the average total energy demand for all the rooms is 1370.1 kWh in Step 1 and 1274.1 in Step 2. After interpolation processes in Step 3 and Step 4, the average total energy demand for each room is 1341.6 kWh. There are 11450

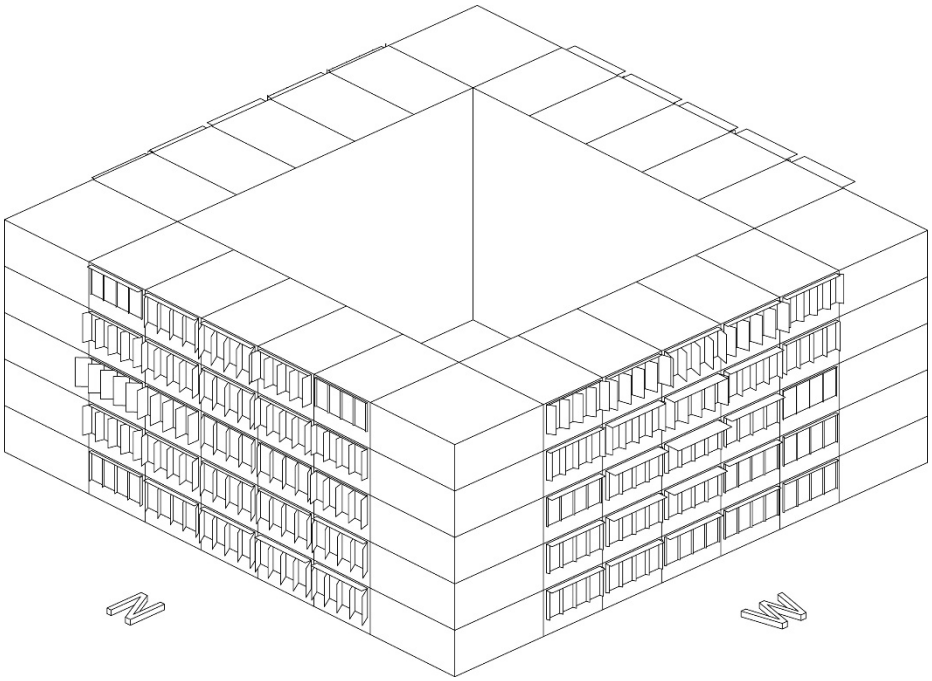

Figure 5.12: AR Results I – Step 4 – North and West façades – Chicago

simulations in total executed in AR optimization I for Chicago.

Table 5.8: AR Results I - Chicago

	S [kWh]	E [kWh]	N [kWh]	W [kWh]	Average [kWh]	Runs [-]
Step 1	1185.5	1465.2	1394.5	1435.1	1370.1	1480
Step 2	1119.1	1268.1	1301.4	1407.7	1274.1	9700
Step 3	1191.6	1348.0	1334.0	1419.2	1323.2	
Step 4	1223.0	1369.5	1345.4	1428.4	1341.6	
Total						11450

5.3.2 AR results II - Chicago

Step 1

Table 5.9 shows the optimization results achieved by Step 1 in AR optimization II for Chicago. Optimization runs for four sub-problems ($S_{3-3}, N_{3-3}, E_{3-3}, W_{3-3}$) are executed in this step. The values of the first design three variables are $v_1 = 6, v_2 = 6, v_3 = 4$. The best glazing (glazing type 6), the second best insulation ($0.19\ W/m^2K$) and the lowest infiltration rate (0.12) are shown. Compared with the optimal solutions

achieved in AR optimization I, AR optimization II shows the same glazing system and infiltration rate, while a lower value insulation is selected. The average total energy demand is 1339.8 kWh, which is 2.2% lower than the 1370.1 kWh achieved by AR optimization I.

Table 5.9: AR Results II - Step 1 – San Francisco

Unit	v_1	v_2	v_3	v_4	v_5v	v_6	Q_{Total} [kWh]	Gene. [-]	Simu. [-]
S_{3-3}	6	7	4	2	9	3	1109.3	14	280
E_{3-3}	6	6	3	9	9	3	1514.2	20	400
N_{3-3}	6	4	4	1	1	5	1365.7	15	300
W_{3-3}	6	7	3	4	1	3	1370.0	19	380
Avg.	6	6	4	-	-	-			
Avg.							1339.8	17	340
Sum.								68	1360

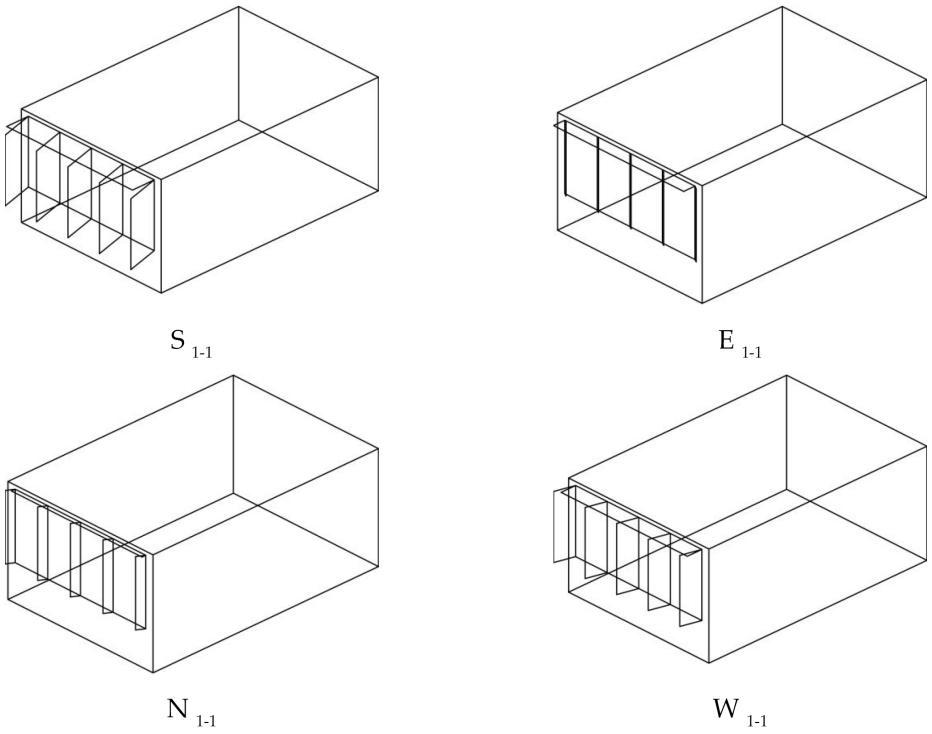

Figure 5.13: AR Results II – Step 1 – Chicago

Step 2

Table 5.10: AR Results II – Step 2 – South façade – Chicago

Unit	v_1	v_2	v_3	v_4	v_5v	v_6	Q_{Total} [kWh]	Gene. [-]	Simu. [-]
S_{1-1}	6	6	4	1	10	1	1146.4	21	420
S_{1-3}	6	6	4	2	10	1	1157.4	23	460
S_{1-5}	6	6	4	2	9	2	1172.3	17	340
S_{3-1}	6	6	4	2	7	2	1012.8	17	340
S_{3-3}	6	6	4	2	10	8	1175.7	18	360
S_{3-5}	6	6	4	1	10	1	1201.1	19	380
S_{5-1}	6	6	4	9	10	3	1204.0	23	460
S_{5-3}	6	6	4	9	10	3	1198.6	21	420
S_{5-5}	6	6	4	9	9	7	1213.7	25	500
Avg.							1164.7	20.4	408.9
Sum.								184	3680

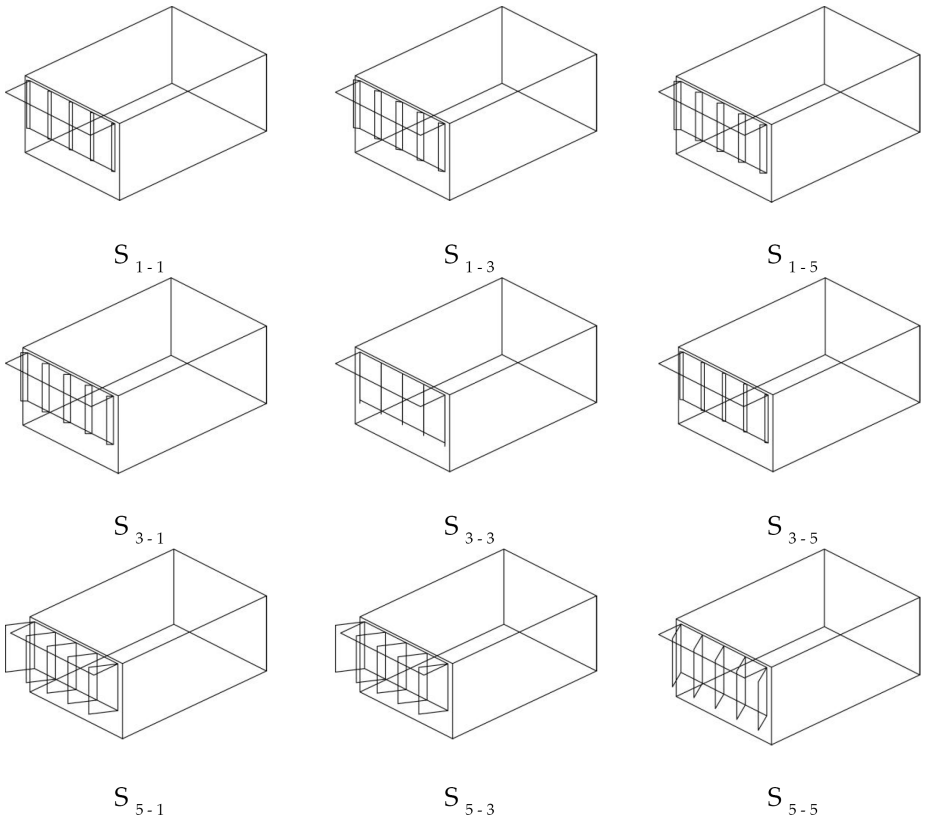

Figure 5.14: AR Results II – Step 2 – South façade – Chicago

Table 5.10 shows the optimization results for south façade achieved by Step 2 of the AR optimization I. The first three design variables ($v_1 = 6, v_2 = 6, v_3 = 4$) stay

unchanged. The façade design solutions for these sub-problems are shown in Figure 5.14. It can be found that the optimization solutions achieved by Step 2 show large overhang shading depths on the south façade. The average total energy demand for all the 9 sub-problems is 1164.7 kWh, which is lower than the 1339.8 kWh achieved by Step 1.

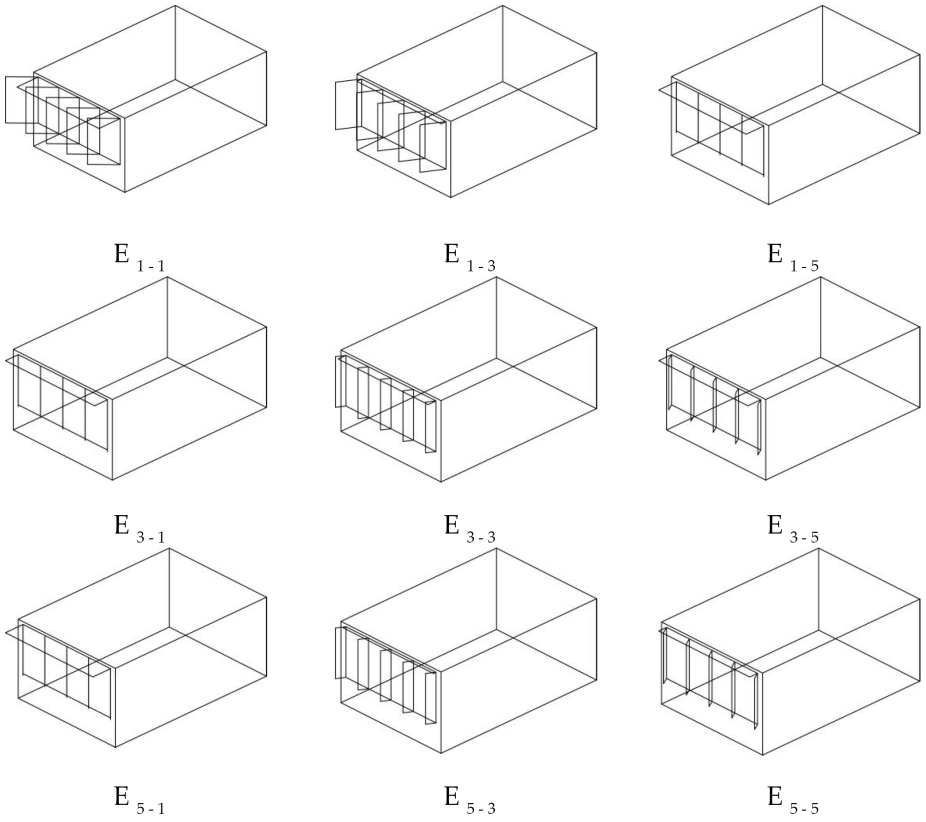

Figure 5.15: AR Results II – Step 2 – East façade – Chicago

Table 5.11 and Figure 5.15 show the optimization results for east façade achieved by Step 2. The optimization runs are executed for 9 selected sub-problems (E_{1-1}, E_{1-3}, $E_{1-5}, E_{3-1}, E_{3-3}, E_{3-5}, E_{5-1}, E_{5-3}, E_{5-5}$) on the east orientation. The average total energy demand for all the 9 sub-problems is 1290.1 kWh, which is 1.7% higher than 1268.1 kWh achieved by AR optimization I.

Table 5.12 represents the optimization results for north façade achieved. The optimization runs are executed for 9 selected sub-problems $N_{1-1}, N_{1-3}, N_{1-5}, N_{3-1}, N_{3-3}$,

Table 5.11: AR Results II – Step 2 – East façade – Chicago

Unit	v_1	v_2	v_3	v_4	v_5v	v_6	Q_{Total} [kWh]	Gene. [-]	Simu. [-]
E_{1-1}	6	6	4	5	1	2	1204.9	16	320
E_{1-3}	6	6	4	2	3	4	1475.7	11	220
E_{1-5}	6	6	4	1	7	8	1269.5	13	260
E_{3-1}	6	6	4	1	5	8	1233.8	23	460
E_{3-3}	6	6	4	3	3	3	1354.9	18	360
E_{3-5}	6	6	4	3	5	7	1282.0	19	380
E_{5-1}	6	6	4	7	6	3	1247.5	14	280
E_{5-3}	6	6	4	3	1	3	1394.7	17	340
E_{5-5}	6	6	4	3	3	7	1297.9	15	300
Avg.							1290.1	18.7	373.3
Sum.								168	3360

$N_{3-5}, N_{5-1}, N_{5-3}, N_{5-5}$) on the north orientation. The façade design solutions for these sub-problems are shown in Figure 5.16.

Table 5.12: AR Results II – Step 2 – North façade – Chicago

Unit	v_1	v_2	v_3	v_4	v_5v	v_6	Q_{Total} [kWh]	Gene. [-]	Simu. [-]
N_{1-1}	6	6	4	1	1	8	1355.6	18	360
N_{1-3}	6	6	4	6	1	3	1347.3	16	320
N_{1-5}	6	6	4	3	2	3	1272.7	22	440
N_{3-1}	6	6	4	3	2	3	1320.9	14	280
N_{3-3}	6	6	4	2	1	2	1309.4	14	280
N_{3-5}	6	6	4	6	5	8	1274.5	15	300
N_{5-1}	6	6	4	3	2	3	1304.4	22	440
N_{5-3}	6	6	4	2	1	2	1299.3	14	280
N_{5-5}	6	6	4	6	2	3	1265.2	12	240
Avg.							1305.5	17.4	348.9
Sum.								157	3140

The optimization solutions achieved by Step 2 show small depths for fin and overhang shadings on the north façade in this case study, which is constant with that in AR I. The solutions achieved by this step show a consistent trend compared with the solutions achieved by Step 1. The average total energy demand for all the 9 sub-problems is 1305.5 kWh, which is almost equal to the 1301.4 kWh achieved by AR optimization I.

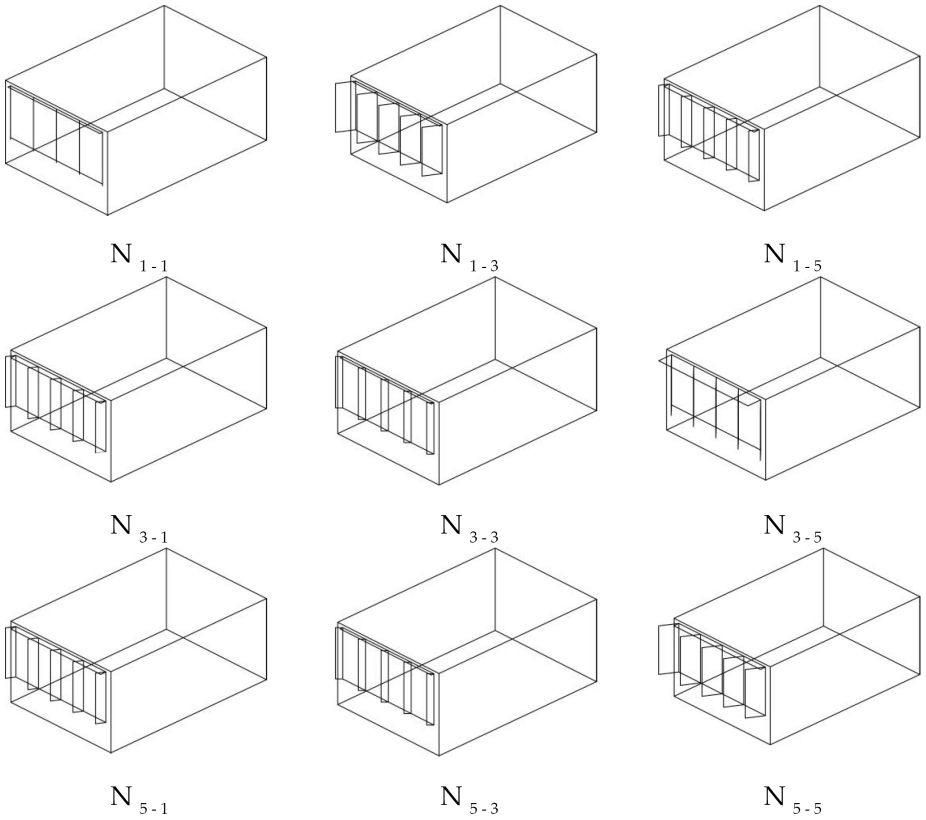

Figure 5.16: AR Results II – Step 2 – North façade – Chicago

Table 5.13 represents the optimization results for western façade achieved by Step 2 of the AR optimization I. The optimization runs are executed for 9 selected sub-problems ($W_{1-1}, W_{1-3}, W_{1-5}, W_{3-1}, W_{3-3}, W_{3-5}, W_{5-1}, W_{5-3}, W_{5-5}$) on the west orientation. The façade design solutions for these sub-problems are shown in Figure 5.17.

It can be seen that the optimization solutions achieved by Step 2 show relatively small depths for fin and overhang shadings on the lower and middle floors on the west façade in this case study. Comparatively, the shading depths for rooms on the top floor are larger. The solutions achieved by this step show a consistent trend compared with the solutions achieved by Step 1. The average total energy demand for all the 9 sub-problems is 1369.5 kWh, which is 2.7% lower than the 1407.7 kWh achieved by AR optimization I.

Table 5.13: AR Results II – Step 2 – West façade – Chicago

Unit	v_1	v_2	v_3	v_4	v_5v	v_6	Q_{Total} [kWh]	Gene. [-]	Simu. [-]
W_{1-1}	6	6	4	8	1	2	1425.2	10	200
W_{1-3}	6	6	4	2	1	2	1373.6	14	280
W_{1-5}	6	6	4	1	1	8	1367.9	20	400
W_{3-1}	6	6	4	9	1	8	1398.2	19	380
W_{3-3}	6	6	4	1	2	6	1372.1	21	420
W_{3-5}	6	6	4	1	3	7	1350.3	16	320
W_{5-1}	6	6	4	9	1	2	1313.8	15	300
W_{5-3}	6	6	4	9	2	2	1311.9	14	280
W_{5-5}	6	6	4	6	2	4	1412.2	15	300
Avg.							1369.5	16	320
Sum.								144	2880

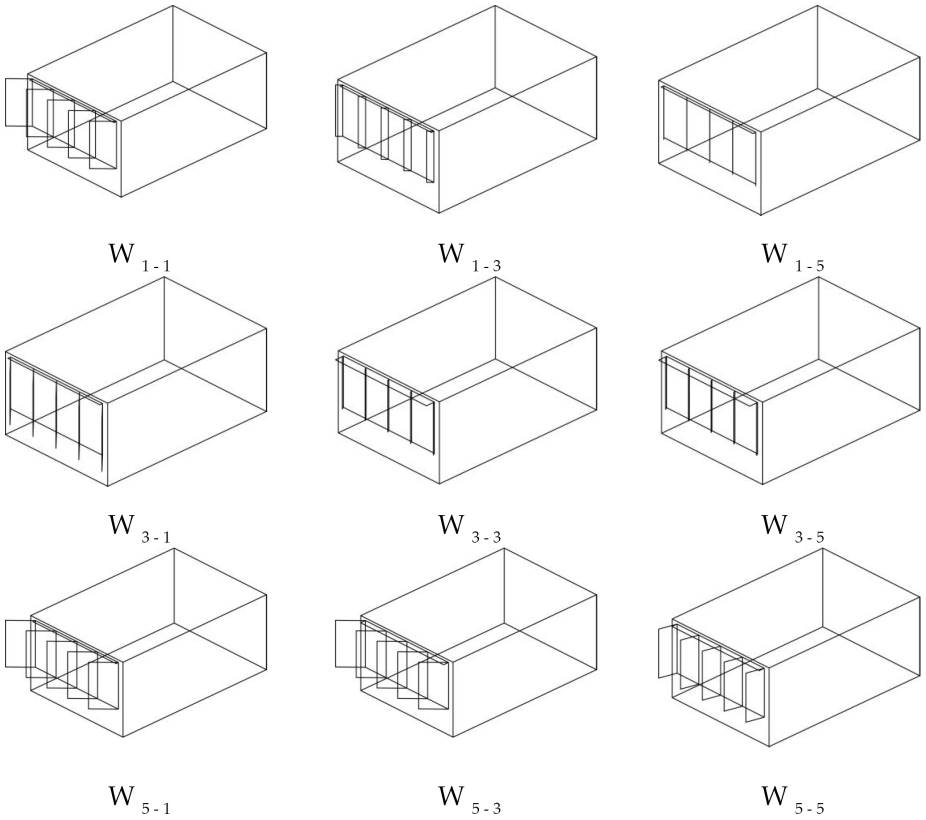

Figure 5.17: AR Results II – Step 2 – West façade – Chicago

Step 3 and Step 4

The average total energy demand for all the rooms achieved by AR II (1321.2 kWh$in the climate of Chicago is 1.5\% lower than that (1341.6 kWh$ achieved by AR I. The

optimization solutions for the entire façade of AR II are shown in Figure 5.18 and Figure 5.19. Details for Step 3 and Step 4 are shown in Appendix E.

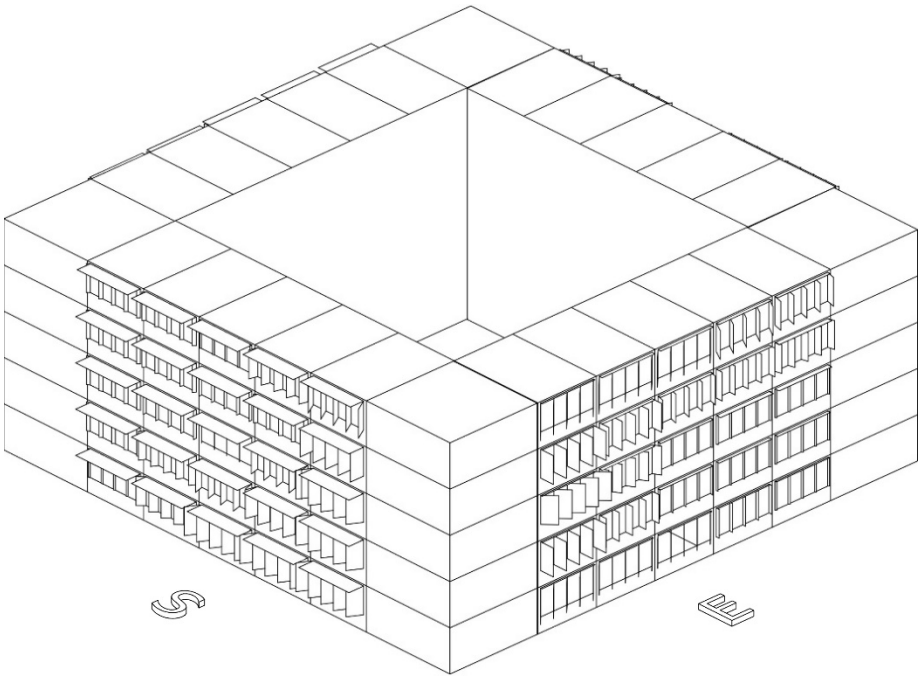

Figure 5.18: AR Results II – Step 4 – South and East façades – Chicago

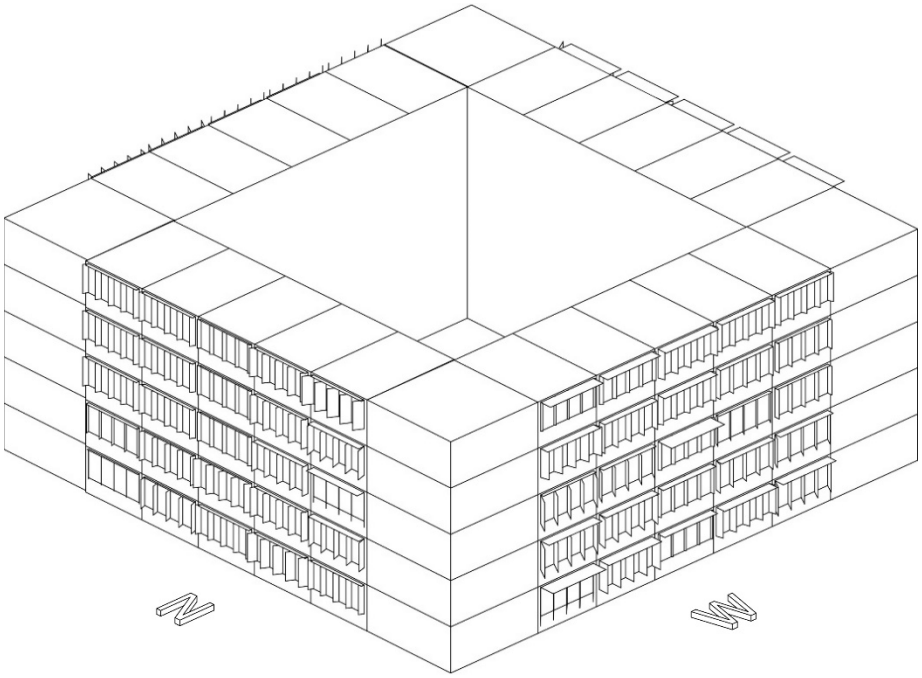

Figure 5.19: AR Results II – Step 4 – North and West façades – Chicago

Table 5.14 represents the optimization result of AR optimization II for Chicago. The average total energy demand for all the rooms is 1287.6 kWh in Step 2. After interpolation processes in step 3 and Step 4, the average total energy demand for each room is 1321.2 kWh.

Table 5.14: AR Results II - Chicago

	S	E	N	W	Average	Runs
Step 1	1109.3	1514.2	1365.7	1370.0	1339.8	1360
Step 2	1185.3	1290.1	1305.5	1369.5	1287.6	13060
Step 3	1203.8	1344.1	1320.3	1371.6	1310.0	
Step 4	1209.4	1361.9	1324.7	1389.1	1321.2	
Total						14420

5.3.3 Summary

Table 5.15 shows the optimal design variables achieved through the two AR optimization runs for Chicago. AR I achieves the optimal solutions for the glazing type, insulation and infiltration $v_1 = 6, v_2 = 5, v_3 = 4$. AR II achieves the optimal solutions for the glazing type, insulation and infiltration $v_1 = 6, v_2 = 6, v_3 = 4$. The solutions achieved by AR I and AR II are steady, as well as the solutions achieved for each orientation.

Table 5.15: Comparison of Design Variables for AR I and AR II – Chicago

AR I	v_1	v_2	v_3	v_4	v_5	v_6	AR II	v_1	v_2	v_3	v_4	v_5	v_6
S_{3-3}	6	5	3	2	9	7	S_{3-3}	6	7	4	2	9	3
E_{3-3}	6	4	4	3	2	4	E_{3-3}	6	6	3	9	9	3
N_{3-3}	6	5	0	8	4	7	N_{3-3}	6	4	4	1	1	5
W_{3-3}	6	6	4	7	7	6	W_{3-3}	6	7	3	4	1	3
	6	5	4	-	-	-		6	6	4	-	-	-

Table 5.16 represents the optimization results achieved through the two AR optimization runs for Chicago. The average total energy demand for each room achieved through AR I is 1341.6 kWh and 1321.2 kWh for AR II. There is only a 1.5% difference, which validates the stability of AR optimization method.

Table 5.16: Comparison of Results for AR I and AR II – Chicago

		S	E	N	W	Average	Runs
AR							
AR I	Step 1	1185.5	1465.2	1394.5	1435.1	1370.1	1480
	Step 2	1119.1	1268.1	1301.4	1407.7	1274.1	9700
	Step 3	1191.6	1348.0	1334.0	1419.2	1323.2	
	Step 4	1223.0	1369.5	1345.4	1428.4	1341.6	
	Total						11450
AR II	Step 1	1109.3	1514.2	1365.7	1370.0	1339.8	1360
	Step 2	1185.3	1290.1	1305.5	1369.5	1287.6	13060
	Step 3	1203.8	1344.1	1320.3	1371.6	1310.0	
	Step 4	1209.4	1361.9	1324.7	1389.1	1321.2	
	Total						14420
Avg.							12935

It can also found that it needs 11450 simulations in total for AR I and 14420 simulations in total for AR I and AR II, respectively. The number of average total simulation runs is 12935, which has the same magnitude with the 11070 for San Francisco. This also validates the robustness for the implementation of AR optimization methodology.

5.4 AR Results for Miami

5.4.1 AR results I - Miami

Table 5.17: AR Results I – Step 1 – Miami

Unit	v_1	v_2	v_3	v_4	v_5	v_6	Q_{Total} [kWh]	Gene. [-]	Simu. [-]
S_{3-3}	6	5	1	9	5	6	1714.4	20	400
E_{3-3}	6	3	2	9	4	3	2231.1	12	240
N_{3-3}	1	7	1	4	5	3	2021.3	11	220
W_{3-3}	4	2	1	5	8	4	1999.2	20	400
Avg.	4	5	1	-	-	-			
Avg.							1991.5	15.8	315
Sum.									1260

Table 5.18 represents the optimization result of AR optimization I on each Step.

Table 5.18: AR Results I - Miami

	S [kWh]	E [kWh]	N [kWh]	W [kWh]	Average [kWh]	Runs [-]
Step 1	1714.4	2231.1	2021.3	1999.2	1991.5	1260
Step 2	1712.8	1822.0	1883.2	1932.8	1837.7	10240
Step 3	1736.3	1934.5	1877.2	1898.1	1861.5	
Step 4	1755.8	1946.8	1880.9	1835.4	1854.7	
Total						11500

It could be seen that the average total energy demand for all the rooms is 1837.7 kWh in Step 2. After interpolation processes in Step 3 and Step 4, the average total energy demand for each room is 1991.5 kWh. In Step 2, the AR finds the optimal solutions for all the 36 sub-problems with the same design variables $v_1 = 4, v_2 = 5, v_3 = 1$.

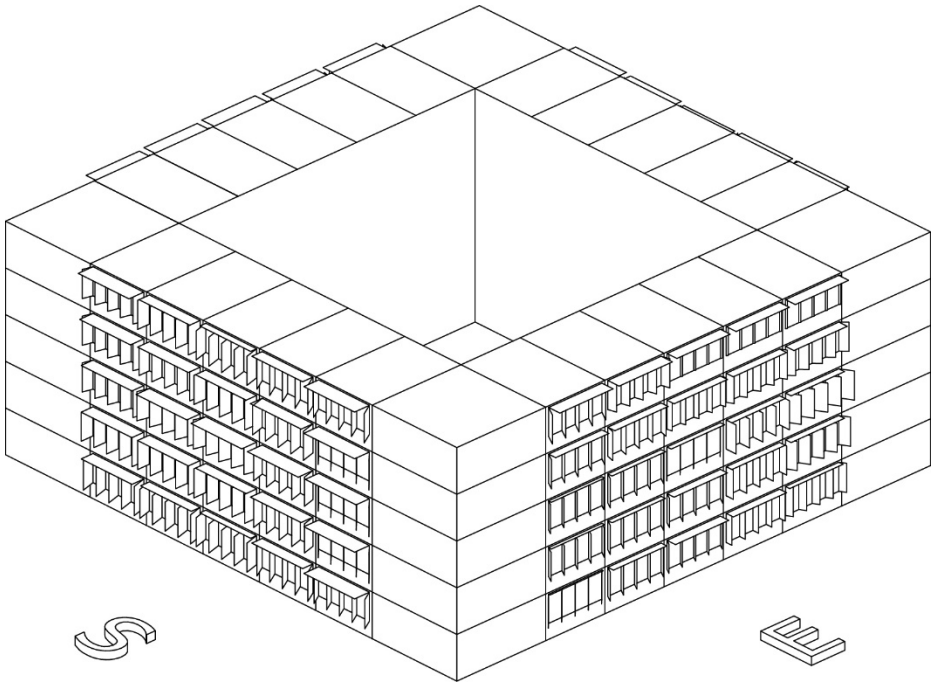

Figure 5.20: AR Results I – Step 4 – South and East façades - Miami

The optimization solutions for the entire façade of AR I are shown in Figure 5.20 and Figure 5.21. Details of the optimization procedures are shown in Appendix F.

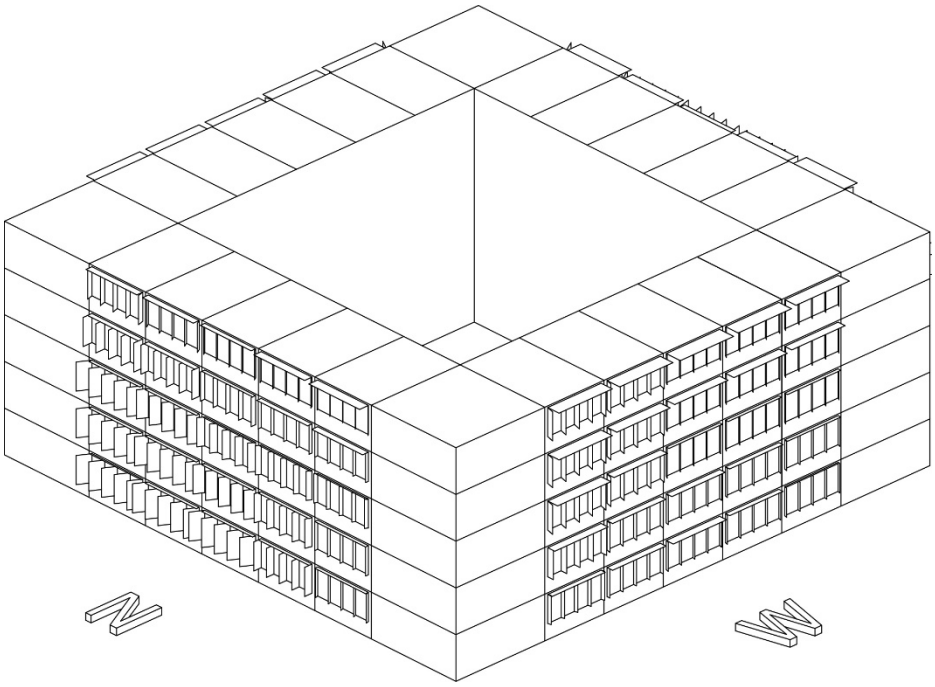

Figure 5.21: AR Results I – Step 4 – North and West façades - Miami

Table 5.19: AR Results II – Step 1 – Miami

Unit	v_1	v_2	v_3	v_4	v_5	v_6	Q_{Total} [kWh]	Gene. [-]	Simu. [-]
S_{3-3}	4	7	2	8	5	6	1750.1	20	400
E_{3-3}	4	1	2	9	1	3	2170.6	18	360
N_{3-3}	6	4	1	1	1	8	2121.8	14	280
W_{3-3}	6	3	1	3	2	4	1934.3	20	400
	5	4	1	-	-	-			
Avg							1994.2	18	360
Sum.									1440

Table 5.20: AR Results II - Miami

	S [kWh]	E [kWh]	N [kWh]	W [kWh]	Average [kWh]	Runs [-]
Step 1	1750.1	2170.6	2121.8	1934.3	1994.2	1440
Step 2	1643.4	1613.5	1562.0	1624.6	1610.9	13300
Step 3	1700.4	1774.3	1759.1	1730.5	1741.1	
Step 4	1699.0	1833.8	1792.8	1739.3	1766.2	
Total						14740

5.4.2 AR results II - Miami

Table 5.19 represents the optimization result of AR optimization II on each Step. It could be seen that the average total energy demand for all the rooms is 1610.9 kWh

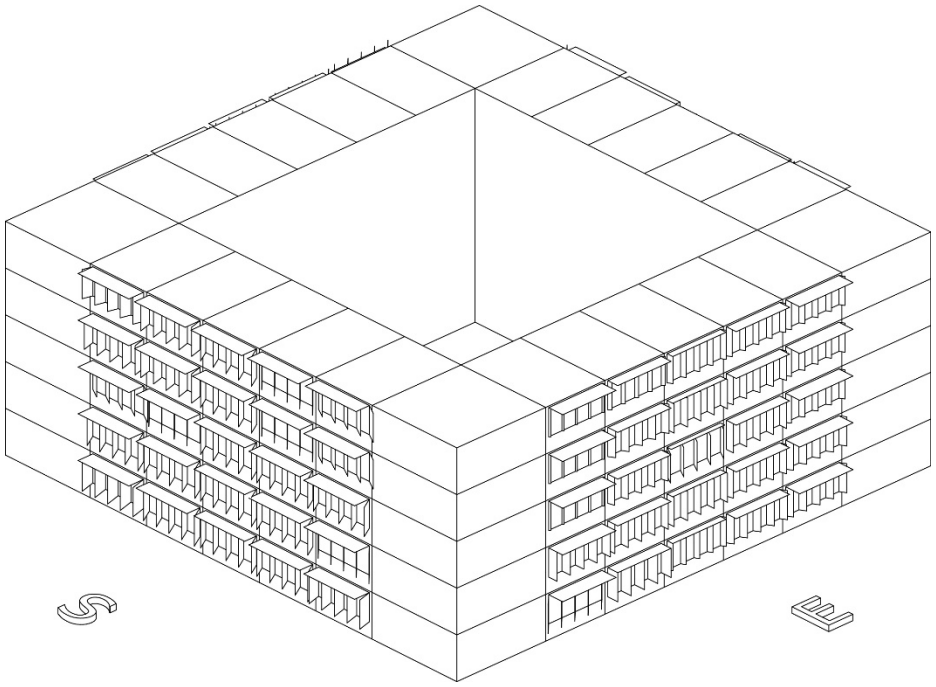

Figure 5.22: AR Results II – Step 4 – South and East façades - Miami

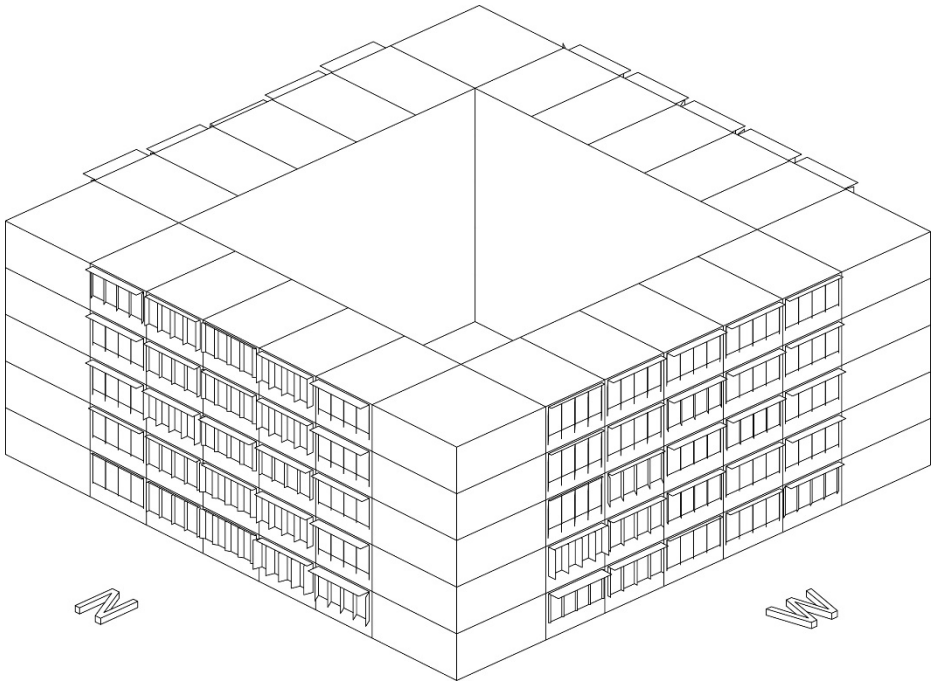

Figure 5.23: AR Results II – Step 4 – North and West façades - Miami

in Step 2. After interpolation processes in Step 3 and Step 4, the average total energy demand for each room is 1766.2 kWh. In Step 2 the AR achieves the optimal solutions for all the 36 sub-problems with the same design variables $v_1 = 5, v_2 = 4, v_3 = 1$.

The optimization solutions for the entire façade of AR II are shown in Figure 5.22 and Figure 5.23. Details of the optimization procedures are shown in Appendix G.

5.4.3 Summary

The optimization results show that AR is efficient and robust in solving façade optimization problems in different climates as well as providing façade design strategies at the early design stage.

Table 5.21: Comparison of Design Variables for AR I and AR II – Miami

AR I	v_1	v_2	v_3	v_4	v_5	v_6	AR II	v_1	v_2	v_3	v_4	v_5	v_6
S_{3-3}	6	5	1	9	5	6	S_{3-3}	4	7	2	8	5	6
E_{3-3}	6	3	2	9	4	3	E_{3-3}	4	1	2	9	1	3
N_{3-3}	1	7	1	4	5	3	N_{3-3}	6	4	1	1	1	8
W_{3-3}	4	2	1	5	8	4	W_{3-3}	6	3	1	3	2	4
	4	5	1	-	-	-		5	4	1	-	-	-

Table 5.22: Comparison of Results for AR I and AR II – Miami

		S	E	N	W	Average	Runs
AR							
AR I	Step 1	1714.4	2231.1	2021.3	1999.2	1991.5	1260
	Step 2	1712.8	1822.0	1883.2	1932.8	1837.7	10240
	Step 3	1736.3	1934.5	1877.2	1898.1	1861.5	
	Step 4	1755.8	1946.8	1880.9	1835.4	1854.7	
	Total						11500
AR II	Step 1	1750.1	2170.6	2121.8	1934.3	1994.2	1440
	Step 2	1643.4	1613.5	1562.0	1624.6	1610.9	13300
	Step 3	1700.4	1774.3	1759.1	1730.5	1741.1	
	Step 4	1699.0	1833.8	1792.8	1739.3	1766.2	
Total							14740
Avg.							13120

Table 5.21 shows the optimal design variables achieved through the two AR optimization runs for Miami. AR I achieves the optimal solutions for the glazing type, insulation and infiltration $v_1 = 4, v_2 = 5, v_3 = 1$. AR II achieves the optimal solutions for the glazing type, insulation and infiltration $v_1 = 5, v_2 = 4, v_3 = 1$. The solutions

achieved by AR I and AR II are steady, as well as the solutions achieved for each orientation.

Table 5.22 represents the optimization results achieved through the two AR optimization runs for Miami. The average total energy demand for each room achieved through AR I is 1854.7 kWh and 1766.2 kWh for AR II. There is only a 4.8 % difference, which validates the stability of AR optimization method.

It can also found that it needs 11500 simulations in total for AR I and 14740 simulations in total for AR I and AR II, respectively. The number of average total simulation runs is 13120, which has a similar magnitude to the 11070 for San Francisco, and the 12935 for Chicago. The consistent of these optimization results validates the robustness of the AR.

CHAPTER VI

Conclusions

6.1 Dissertation Summary

This dissertation is built upon the premise that hierarchical optimization methodology can improve the efficiency of simple genetic algorithm (GA) in solving façade optimization problems. The main goal of this dissertation is to improve the existing simple GA for reducing the simulation time while not undermining its robustness. As an outcome, a set of interrelated design-analysis tasks are posed in a multi-level hierarchical design optimization framework which is named Adaptive Radiation (AR). Three cities in different climates of the United States are analyzed and the optimal façade design solutions are achieved through this new methodology.

Genetic algorithm was proposed as an optimization methodology which can solve non-linear variables that are very common in building optimization problems. However, it's still very time-consuming for complicated problems with a large number of variables. Former studies have validated the efficiency and robustness of the genetic algorithm in solving FPO problems. Chapter 2 reviewed these studies and proposed a hierarchical GA which can solve FPO problems with much less simulation time. This chapter also provided an overview of simulation methods and techniques that can be implemented in solving FPO problems.

Chapter 3 presented the methodological framework of the algorithm of adaptive

radiation. The design optimization model was reviewed for recent developments in the field, with an emphasis on continuous or discrete, linear or non-linear formulations of optimization models. Adaptive Radiation (AR) was proposed as a hierarchical optimization framework for coordination decision-making tasks that require multiple and diverse simulations, and for extending the scope of optimization in facade design for deriving consistent and concurrent decisions. The main levels involved in implementing a façade design scenario in AR framework are also described in Chapter 3.

Chapter 4 presented a façade design scenario of typical mid-rise office building to demonstrate the AR process in simulation-based facade optimization. The optimization objective is the total annual energy demand of heating, cooling, and artificial lighting. Results of this case study presented that the method of adaptive radiation can improve the efficiency of simple genetic algorithm by largely reducing the computation time.

Chapter 5 further tested the robustness of adaptive radiation by implementing this methodology in two other climates of the U.S. The optimization results validated the efficiency and robustness of this process, and provided façade design strategies which are responsive to different local climates.

6.2 Contributions

The main accomplishment of this dissertation is proposing a hierarchical optimization algorithm – AR, based on the improvement of simple GA, and extending it towards solving façade optimization problems in different climates, thus providing a broadened context of design decision-making contributions at early design stage. The efficiency and robustness of AR are validated through design scenarios in different climates in the U.S.

This dissertation provides specific contributions in the building optimization field.

First, the optimization algorithms are organized in a hierarchical structure to solve complex façade optimization problems with a large number of design variables, based on the key interrelationships between the design variables and design objectives. Second, the organization of optimization is flexible and can be integrated with other optimization algorithms at different levels, and offers a new approach to coordinating multiple simulations in the decision-making process, thus can further improve the efficiency and accuracy of AR. Third, it is simple and easy for use by designers. The workflow represents a visualization platform between 3D/CAD modeling, building simulation and optimization process, and provides quick feedback of façade design variables, which helps architects to make design decisions at the early design stage and scrutinize the results clearly.

This dissertation has validated the potential of a hierarchical optimization methodology through façade design scenarios. The procedure can also be extended towards a broad field of complex simulation-based architectural optimization problems. The design variables of the design scenarios in this dissertations are only passive design strategies for façade optimization problem, and the design objective is solely total energy demand. Moreover, active design strategies together with more design objectives can also be involved. On each level of AR, the optimization will have the flexibility to subject the design to appropriate optimization algorithms and achieve values of design variables without undermining consistency with the values of design variables achieved at previous or future levels of the entire optimization process.

6.3 Directions for Future Research

The immediate steps following this study include:

1) Investigate the possibility to integrate different appropriate optimization algorithms on different levels of AR to further improve its efficiency and accuracy.

2) Extend the design variables to more complex façade optimization problems,

which are not only limited to passive design strategies, but also include active design strategies.

3) Extend the design scenarios to multi-objective optimization problems with different design objectives.

APPENDICES

APPENDIX A

AR I Result for San Francisco (partial)

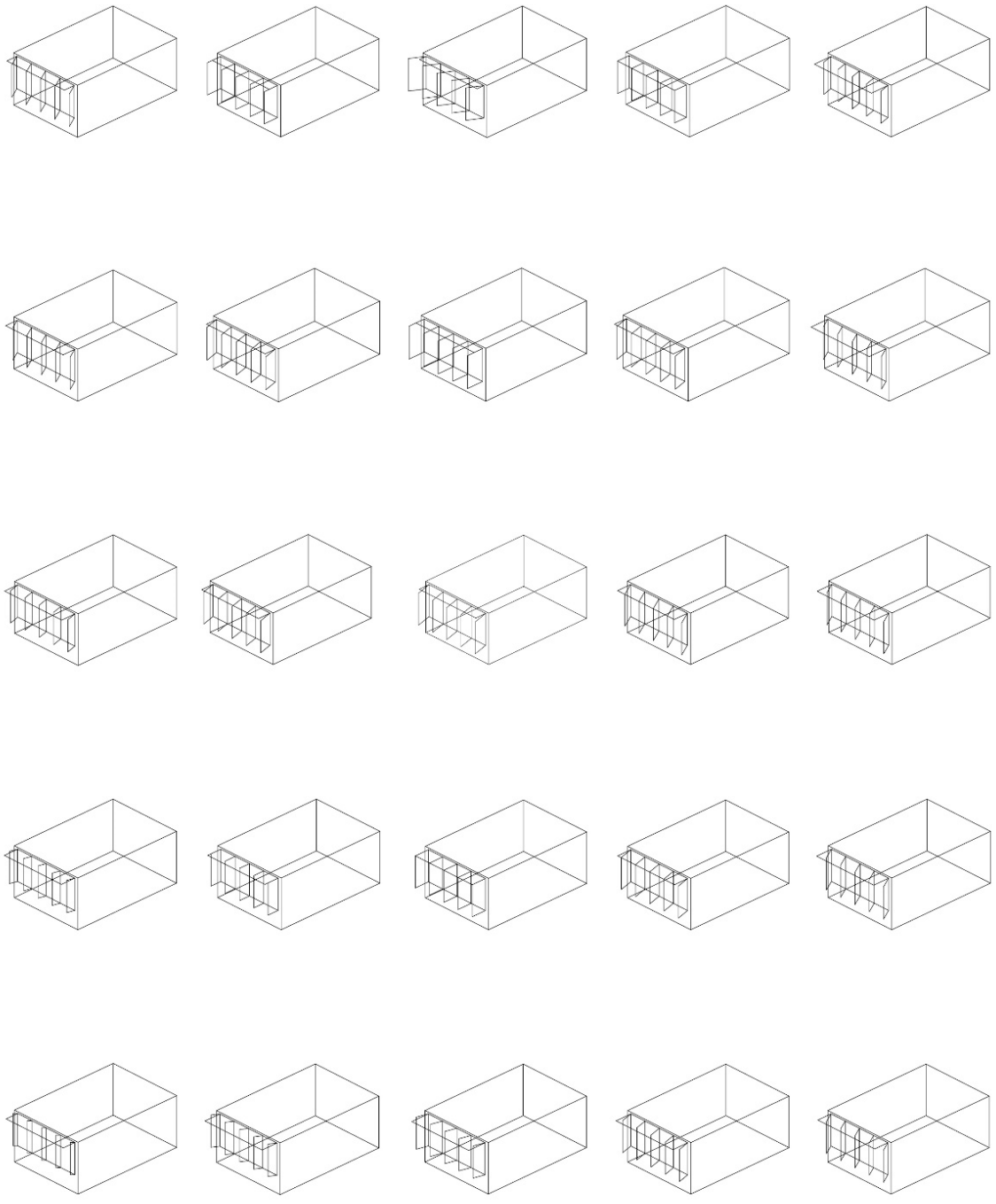

Figure A.1: AR Results I – South façade – San Francisco

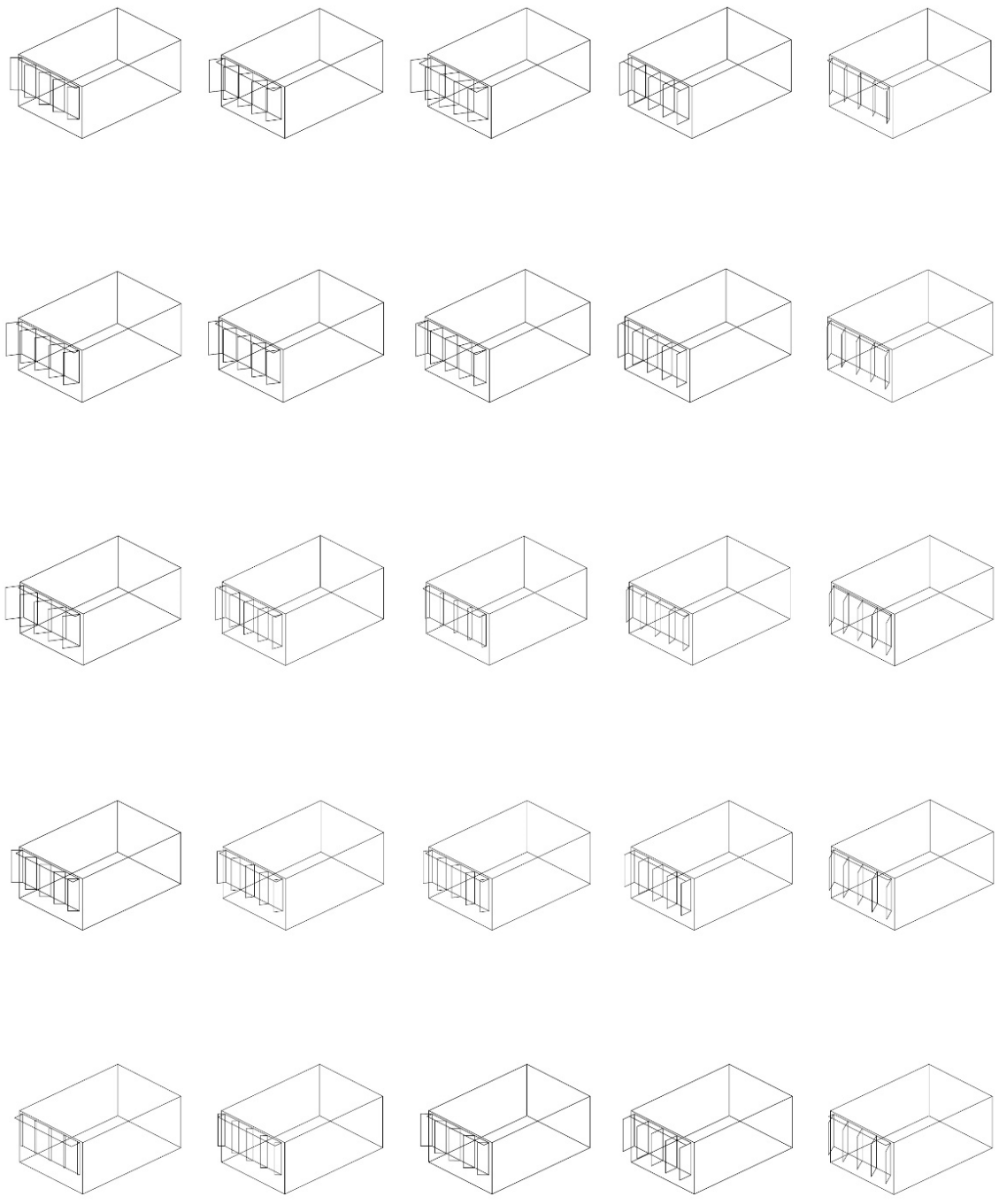

Figure A.2: AR Results I – East façade – San Francisco

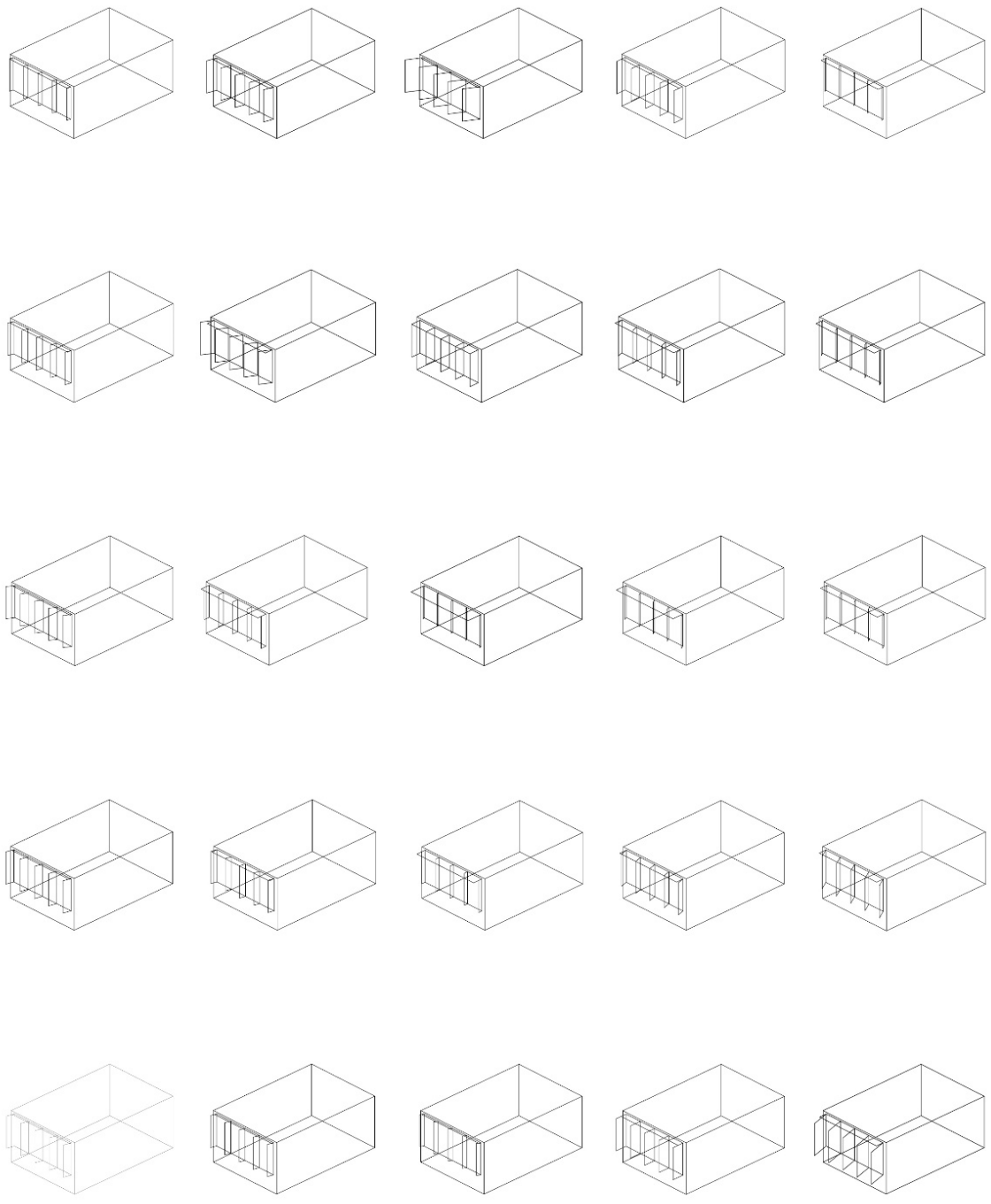

Figure A.3: AR Results I – North façade – San Francisco

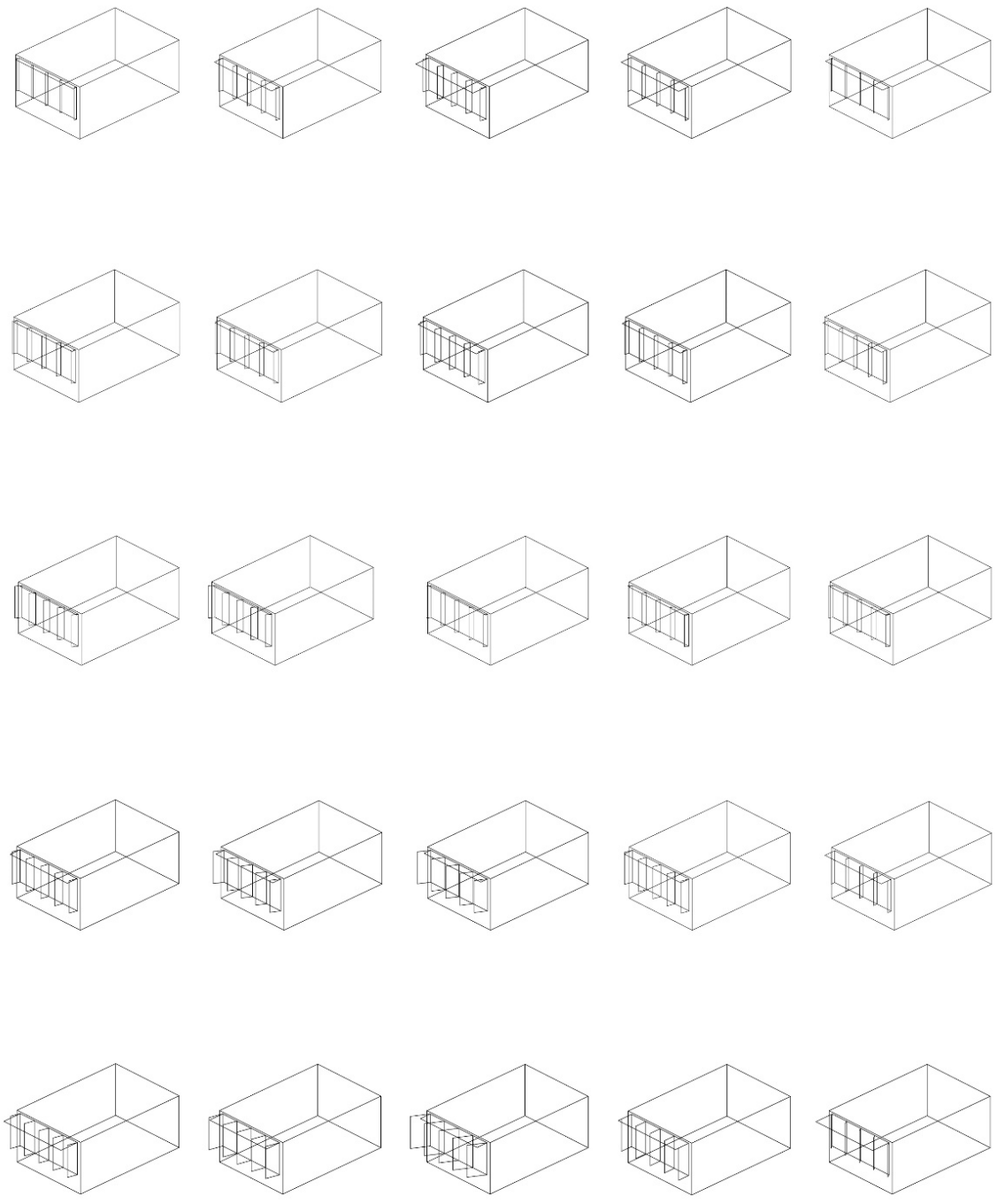

Figure A.4: AR Results I – West façade – San Francisco

APPENDIX B

AR II Result for San Francisco (partial)

Table B.1: AR Results II – Step 3 – San Francisco

	v_1	v_2	v_3	v_4	v_5	v_6	[kWh]		v_1	v_2	v_3	v_4	v_5	v_6	[kWh]
S_{1-1}	6	5	4	8	9	3	1062.8	E_{1-1}	6	5	4	9	3	3	1228.8
S_{1-2}	6	5	4	7	6	5	1246.8	E_{1-2}	6	5	4	9	3	3	1337.0
S_{1-3}	6	5	4	6	3	6	1176.7	E_{1-3}	6	5	4	9	2	3	1418.6
S_{1-4}	6	5	4	8	2	7	1298.4	E_{1-4}	6	5	4	7	3	5	1536.3
S_{1-5}	6	5	4	10	1	8	1151.6	E_{1-5}	6	5	4	4	3	7	1208.9
S_{3-1}	6	5	4	1	10	3	1050.3	E_{3-1}	6	5	4	1	5	1	1171.4
S_{3-2}	6	5	4	5	7	4	1280.0	E_{3-2}	6	5	4	4	5	2	1497.3
S_{3-3}	6	5	4	8	4	4	1147.7	E_{3-3}	6	5	4	7	4	3	1456.4
S_{3-4}	6	5	4	7	5	6	1365.1	E_{3-4}	6	5	4	4	6	6	1518.5
S_{3-5}	6	5	4	6	5	7	1126.5	E_{3-5}	6	5	4	1	7	9	1192.2
S_{5-1}	6	5	4	2	10	2	1043.6	E_{5-1}	6	5	4	5	3	2	1148.6
S_{5-2}	6	5	4	3	9	3	1275.2	E_{5-2}	6	5	4	6	4	2	1445.6
S_{5-3}	6	5	4	4	7	4	1189.6	E_{5-3}	6	5	4	7	5	2	1414.2
S_{5-4}	6	5	4	3	7	6	1336.6	E_{5-4}	6	5	4	4	4	6	1472.4
S_{5-5}	6	5	4	1	7	7	1123.6	E_{5-5}	6	5	4	1	3	9	1174.0
Avg.							1191.6	Avg.							1348.0
N_{1-1}	6	5	4	2	2	6	1416.7	W_{1-1}	6	5	4	2	4	6	1456.7
N_{1-2}	6	5	4	5	3	7	1445.1	W_{1-2}	6	5	4	2	4	7	1472.3
N_{1-3}	6	5	4	8	3	7	1422.1	W_{1-3}	6	5	4	1	4	7	1460.5
N_{1-4}	6	5	4	9	4	7	1360.9	W_{1-4}	6	5	4	1	3	7	1462.0
N_{1-5}	6	5	4	9	4	7	1171.6	W_{1-5}	6	5	4	1	2	6	1370.3
N_{3-1}	6	5	4	8	1	2	1342.1	W_{3-1}	6	5	4	1	4	6	1428.1
N_{3-2}	6	5	4	7	1	5	1398.5	W_{3-2}	6	5	4	2	7	7	1425.8
N_{3-3}	6	5	4	6	1	7	1369.7	W_{3-3}	6	5	4	2	10	7	1390.2
N_{3-4}	6	5	4	6	1	7	1358.4	W_{3-4}	6	5	4	2	6	5	1464.5
N_{3-5}	6	5	4	6	1	6	1163.4	W_{3-5}	6	5	4	1	1	3	1393.7
N_{5-1}	6	5	4	1	3	6	1365.8	W_{5-1}	6	5	4	5	1	7	1393.6
N_{5-2}	6	5	4	6	3	7	1382.8	W_{5-2}	6	5	4	7	2	6	1412.2
N_{5-3}	6	5	4	10	3	7	1317.0	W_{5-3}	6	5	4	9	3	4	1403.8
N_{5-4}	6	5	4	6	2	5	1351.4	W_{5-4}	6	5	4	7	3	6	1381.9
N_{5-5}	6	5	4	1	1	3	1144.4	W_{5-5}	6	5	4	4	3	7	1372.7
Avg.							1334.0	Avg.							1419.2

Table B.2: AR Results II – Step 4 – San Francisco

	v_1	v_2	v_3	v_4	v_5	v_6	[kWh]		v_1	v_2	v_3	v_4	v_5	v_6	[kWh]
S_{1-1}	4	3	1	8	8	3	321.2	E_{1-1}	4	3	1	5	2	2	349.0
S_{1-2}	4	3	1	8	8	3	276.8	E_{1-2}	4	3	1	4	5	3	681.8
S_{1-3}	4	3	1	8	7	3	345.3	E_{1-3}	4	3	1	2	8	4	735.9
S_{1-4}	4	3	1	8	8	5	327.1	E_{1-4}	4	3	1	3	5	7	878.1
S_{1-5}	4	3	1	8	8	7	290.4	E_{1-5}	4	3	1	3	2	9	394.2
S_{2-1}	4	3	1	7	9	4	289.1	E_{2-1}	4	3	1	7	4	3	440.9
S_{2-2}	4	3	1	8	8	4	292.7	E_{2-2}	4	3	1	6	4	3	562.9
S_{2-3}	4	3	1	8	6	5	304.2	E_{2-3}	4	3	1	6	5	4	818.2
S_{2-4}	4	3	1	8	6	6	307.0	E_{2-4}	4	3	1	4	3	6	820.5
S_{2-5}	4	3	1	9	5	8	386.6	E_{2-5}	4	3	1	2	2	9	316.4
S_{3-1}	4	3	1	6	10	4	286.6	E_{3-1}	4	3	1	8	6	3	312.9
S_{3-2}	4	3	1	7	8	6	254.9	E_{3-2}	4	3	1	9	4	3	602.9
S_{3-3}	4	3	1	8	5	7	330.7	E_{3-3}	4	3	1	9	1	3	541.1
S_{3-4}	4	3	1	9	4	8	352.6	E_{3-4}	4	3	1	5	1	6	782.9
S_{3-5}	4	3	1	9	2	8	319.0	E_{3-5}	4	3	1	1	1	9	334.3
S_{4-1}	4	3	1	4	10	3	313.8	E_{4-1}	4	3	1	9	7	3	435.6
S_{4-2}	4	3	1	6	8	4	252.3	E_{4-2}	4	3	1	7	4	3	623.7
S_{4-3}	4	3	1	8	6	6	260.6	E_{4-3}	4	3	1	5	1	2	541.7
S_{4-4}	4	3	1	9	5	7	295.5	E_{4-4}	4	3	1	5	2	5	842.4
S_{4-5}	4	3	1	9	4	8	293.1	E_{4-5}	4	3	1	5	3	8	324.5
S_{5-1}	4	3	1	2	9	2	318.5	E_{5-1}	4	3	1	9	7	3	407.3
S_{5-2}	4	3	1	5	8	3	356.2	E_{5-2}	4	3	1	5	4	2	613.1
S_{5-3}	4	3	1	8	7	4	415.1	E_{5-3}	4	3	1	1	1	1	635.7
S_{5-4}	4	3	1	9	7	6	245.6	E_{5-4}	4	3	1	5	3	4	748.5
S_{5-5}	4	3	1	9	6	7	330.8	E_{5-5}	4	3	1	8	4	7	338.6
Avg.							310.6	Avg.							563.3
N_{1-1}	4	3	1	2	1	4	592.3	W_{1-1}	4	3	1	2	3	6	603.0
N_{1-2}	4	3	1	5	4	6	848.1	W_{1-2}	4	3	1	2	2	5	640.2
N_{1-3}	4	3	1	8	7	7	592.3	W_{1-3}	4	3	1	2	1	4	576.8
N_{1-4}	4	3	1	6	8	7	734.2	W_{1-4}	4	3	1	4	1	5	655.8
N_{1-5}	4	3	1	3	8	6	378.8	W_{1-5}	4	3	1	6	1	5	612.2
N_{2-1}	4	3	1	2	2	4	772.5	W_{2-1}	4	3	1	2	2	6	598.2
N_{2-2}	4	3	1	3	3	4	826.9	W_{2-2}	4	3	1	2	4	5	603.4
N_{2-3}	4	3	1	5	5	5	851.2	W_{2-3}	4	3	1	2	5	4	650.8
N_{2-4}	4	3	1	4	5	6	665.9	W_{2-4}	4	3	1	3	4	5	599.9
N_{2-5}	4	3	1	2	6	7	393.4	W_{2-5}	4	3	1	4	2	6	544.7
N_{3-1}	4	3	1	1	2	3	572.0	W_{3-1}	4	3	1	1	1	6	567.7
N_{3-2}	4	3	1	2	2	3	590.2	W_{3-2}	4	3	1	2	5	5	556.2
N_{3-3}	4	3	1	2	2	3	467.4	W_{3-3}	4	3	1	2	9	3	586.0
N_{3-4}	4	3	1	2	3	5	713.6	W_{3-4}	4	3	1	2	6	5	579.2

	v_1	v_2	v_3	v_4	v_5	v_6	[kWh]		v_1	v_2	v_3	v_4	v_5	v_6	[kWh]
N_{3-5}	4	3	1	1	4	7	304.8	W_{3-5}	4	3	1	2	3	7	479.2
N_{4-1}	4	3	1	1	2	3	653.7	W_{4-1}	4	3	1	5	1	7	614.1
N_{4-2}	4	3	1	2	2	4	611.3	W_{4-2}	4	3	1	4	5	5	586.6
N_{4-3}	4	3	1	2	2	5	729.1	W_{4-3}	4	3	1	3	10	4	539.1
N_{4-4}	4	3	1	2	3	6	585.1	W_{4-4}	4	3	1	2	7	5	525.2
N_{4-5}	4	3	1	2	3	7	237.1	W_{4-5}	4	3	1	2	4	7	444.7
N_{5-1}	4	3	1	1	1	3	508.1	W_{5-1}	4	3	1	9	1	8	546.0
N_{5-2}	4	3	1	2	2	5	709.2	W_{5-2}	4	3	1	6	6	6	578.6
N_{5-3}	4	3	1	2	2	7	433.3	W_{5-3}	4	3	1	3	10	4	566.2
N_{5-4}	4	3	1	2	2	7	452.9	W_{5-4}	4	3	1	3	7	6	503.9
N_{5-5}	4	3	1	2	2	7	286.8	W_{5-5}	4	3	1	2	4	7	512.3
Avg.							580.4	Avg.							570.8

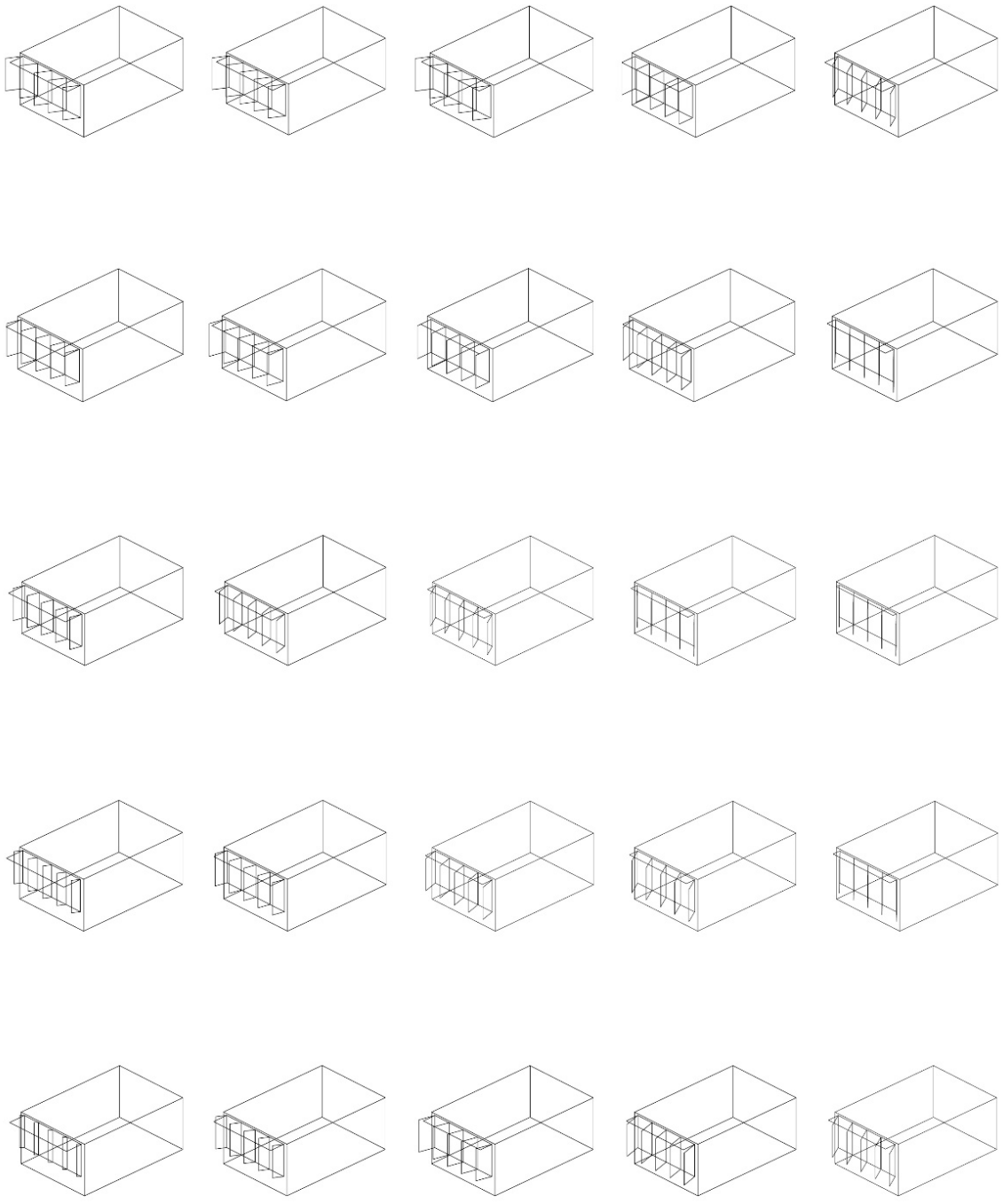

Figure B.1: AR Results II – South façade – San Francisco

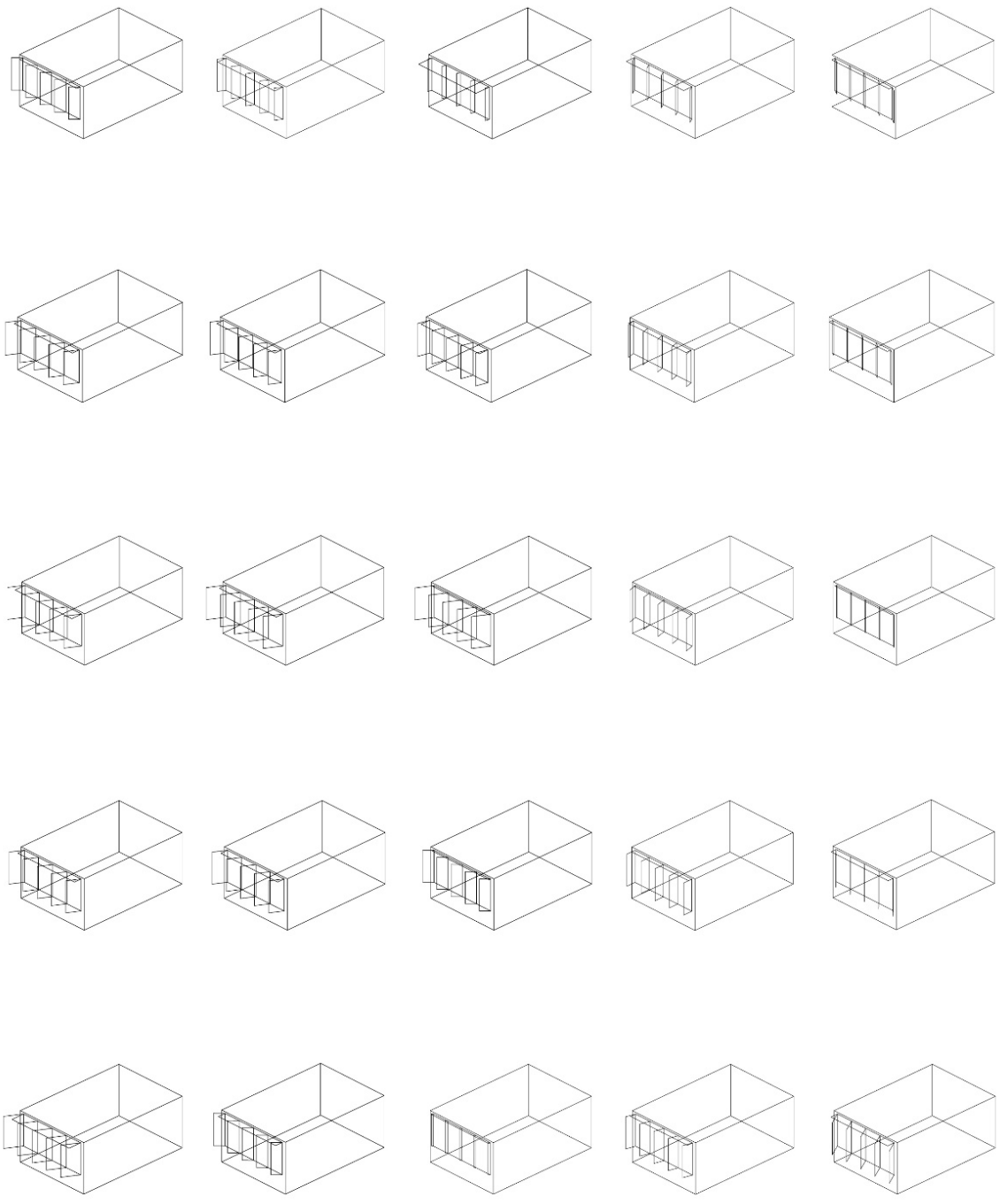

Figure B.2: AR Results II – East façade – San Francisco

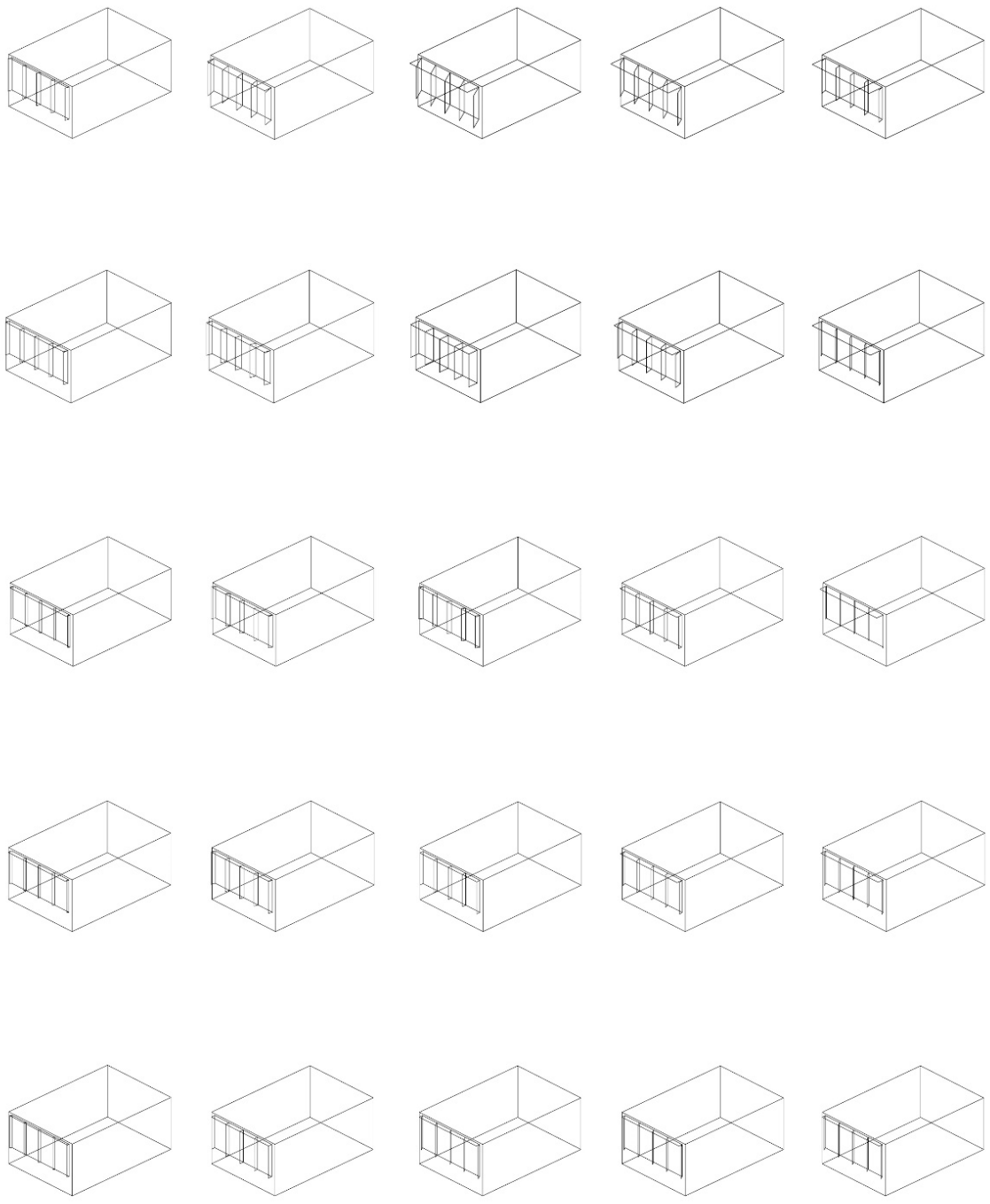

Figure B.3: AR Results II – North façade – San Francisco

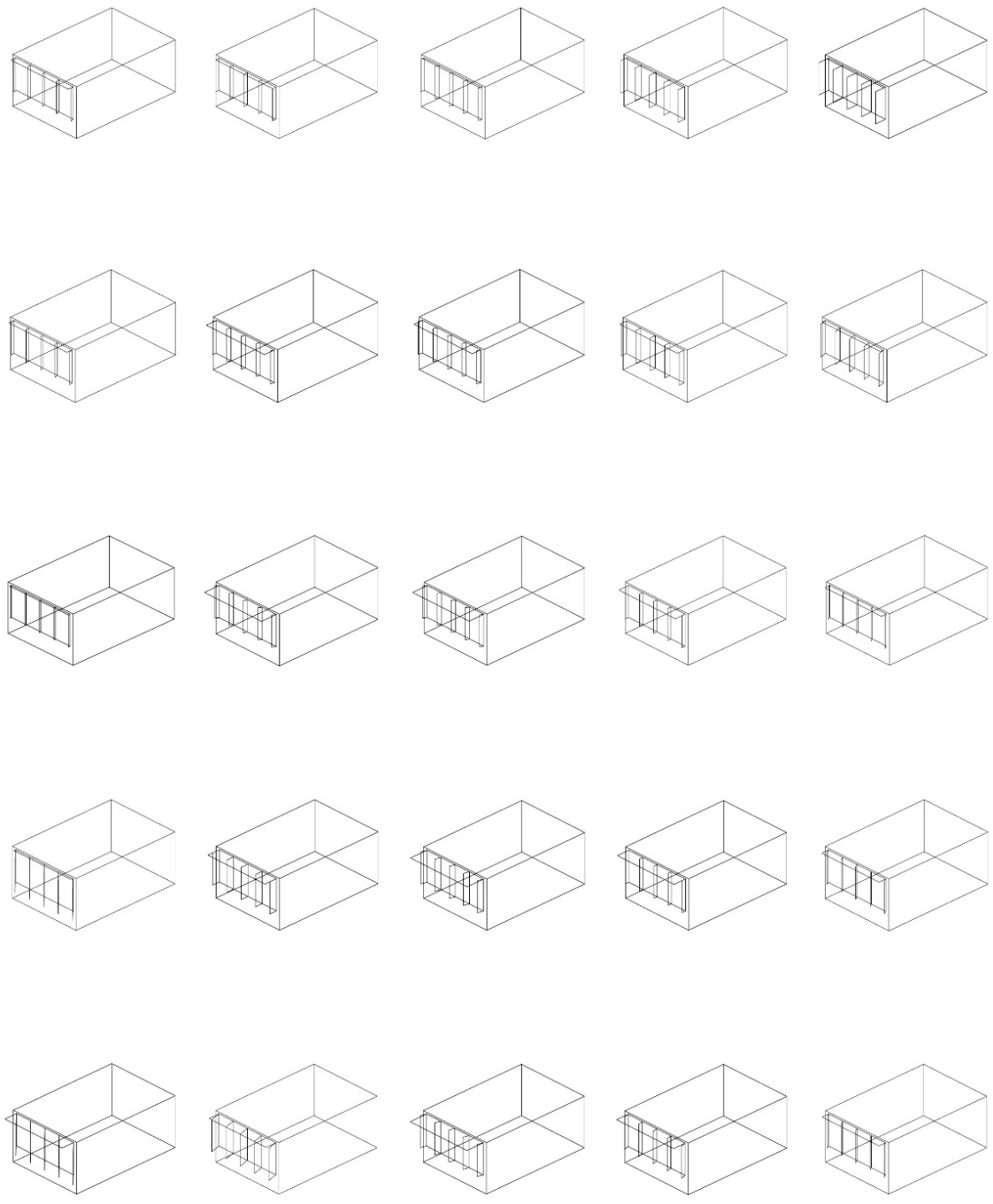

Figure B.4: AR Results II – West façade – San Francisco

APPENDIX C

GA II Result for San Francisco

Table C.1: GA Results II – South façade – San Francisco

Unit	v_1	v_2	v_3	v_4	v_5	v_6	Q_H [kWh]	Q_C [kWh]	Q_L [kWh]	Q_{Total} [kWh]	Gene. [-]	Simu. [-]
S_{1-1}	4	2	1	7	5	4	35.3	194.5	96.4	326.3	20	400
S_{1-2}	4	5	1	8	9	3	31.2	136.2	151.1	318.5	44	880
S_{1-3}	4	4	1	8	7	7	34.2	108.7	195.6	338.5	40	800
S_{1-4}	4	7	1	6	7	2	21.4	141.7	225.5	388.7	38	760
S_{1-5}	4	3	1	6	3	8	27.3	142.1	140.4	309.8	28	560
S_{2-1}	6	1	1	7	9	4	14.7	172.4	120.9	307.9	39	780
S_{2-2}	4	3	1	9	7	6	43.9	124.5	195.5	363.9	26	520
S_{2-3}	4	2	1	9	5	6	44.2	161.2	172.3	377.7	13	260
S_{2-4}	4	2	1	8	6	7	35.1	168.8	181.3	385.1	20	400
S_{2-5}	4	3	1	5	4	6	27.0	193.4	129.6	349.9	14	280
S_{3-1}	4	5	1	1	10	3	17.7	173.8	104.2	295.8	46	920
S_{3-2}	4	7	1	9	6	3	25.4	174.7	135.6	335.7	30	600
S_{3-3}	4	7	1	8	5	4	30.0	155.6	150.4	336.0	14	280
S_{3-4}	4	1	1	5	10	4	43.6	142.5	202.2	388.3	30	600
S_{3-5}	4	5	1	9	6	7	31.3	139.3	141.1	311.8	45	900
S_{4-1}	4	3	1	6	7	4	35.3	157.3	122.1	314.8	13	260
S_{4-2}	4	5	1	6	5	4	31.1	184.3	119.7	335.0	28	560
S_{4-3}	4	6	1	7	5	4	29.2	180.8	141.2	351.2	65	1300
S_{4-4}	4	4	1	7	8	4	40.0	129.3	229.1	398.5	16	320
S_{4-5}	4	6	1	9	2	8	27.0	146.2	132.3	305.5	31	620
S_{5-1}	4	4	1	7	9	6	38.5	153.1	148.5	340.0	12	240
S_{5-2}	4	2	1	9	5	3	37.8	195.6	111.9	345.2	25	500
S_{5-3}	4	4	1	4	7	6	22.0	247.3	150.9	420.2	18	360
S_{5-4}	4	4	1	7	7	4	36.6	167.6	212.0	416.3	20	400
S_{5-5}	4	3	1	7	5	7	31.5	185.4	135.4	352.3	15	300
Avg.	4	4	1	7	6	5	31.7	163.1	153.8	348.5	27.6	552
Sum.											690	13800

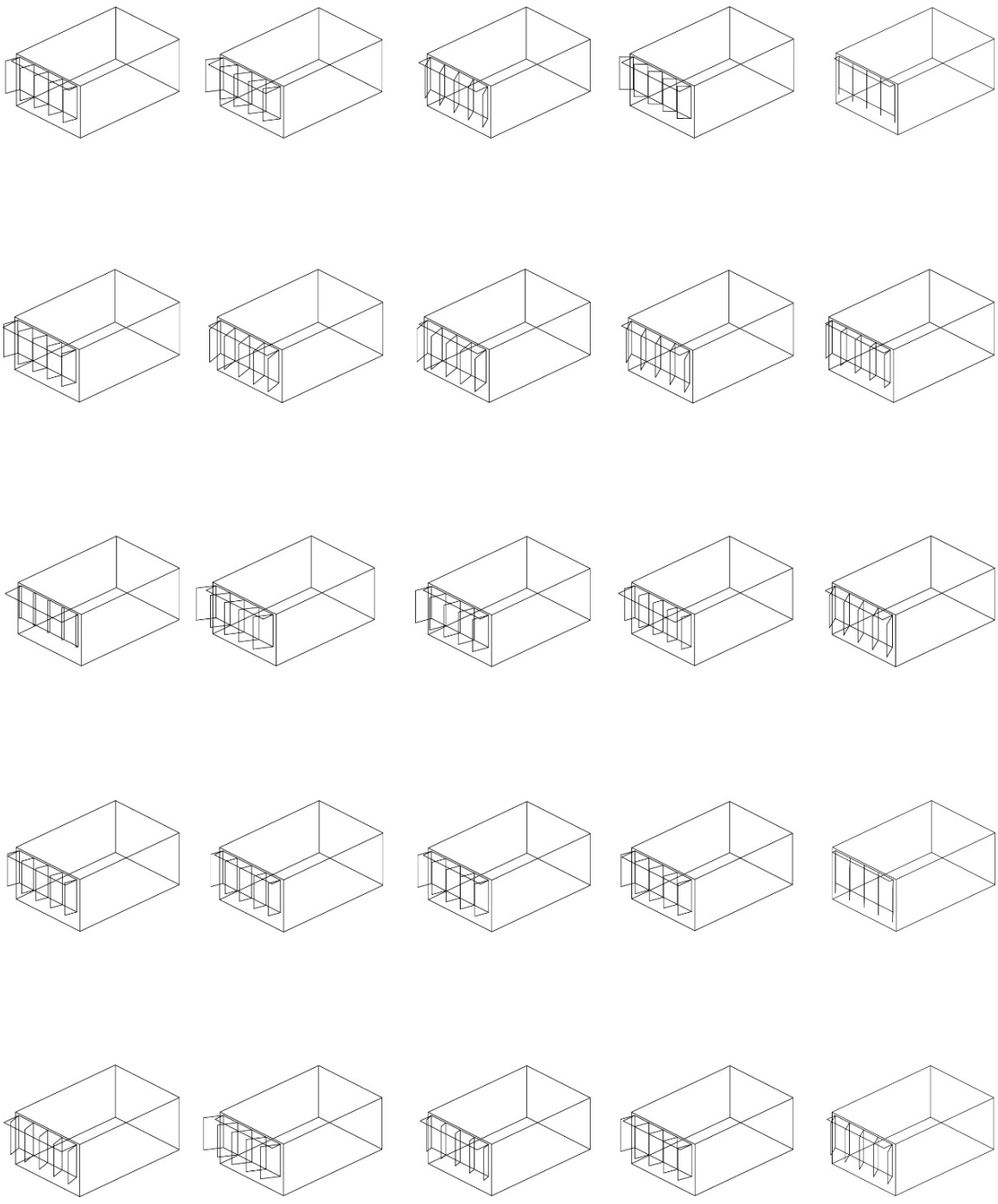

Figure C.1: AR Results II – South façade – San Francisco

Table C.2: GA Results II – East façade – San Francisco

Unit	v_1	v_2	v_3	v_4	v_5	v_6	Q_H [kWh]	Q_C [kWh]	Q_L [kWh]	Q_{Total} [kWh]	Gene. [-]	Simu. [-]
E_{1-1}	4	2	1	3	3	2	34.5	120.2	195.3	349.9	27	540
E_{1-2}	4	1	1	4	3	7	45.5	168.4	458.4	672.2	13	260
E_{1-3}	4	1	1	2	1	4	43.5	212.7	359.7	615.9	25	500
E_{1-4}	4	1	1	4	1	3	41.7	189.2	458.2	689.1	38	760
E_{1-5}	4	2	1	2	2	4	45.8	149.1	225.8	420.8	18	360
E_{2-1}	4	3	1	3	8	3	34.6	112.8	217.4	364.8	13	260
E_{2-2}	4	1	1	6	1	3	51.3	142.4	310.8	504.5	15	300
E_{2-3}	4	1	1	8	1	3	48.0	261.0	305.7	614.6	14	280
E_{2-4}	4	1	1	1	1	9	36.1	174.5	450.9	661.6	18	360
E_{2-5}	4	2	1	10	1	6	48.7	135.3	225.7	409.7	23	460
E_{3-1}	4	3	1	8	5	3	42.7	85.4	162.8	290.9	27	540
E_{3-2}	4	3	1	4	1	3	41.9	138.9	287.0	467.8	17	340
E_{3-3}	4	1	1	2	1	4	48.3	188.4	363.0	599.7	18	360
E_{3-4}	2	3	2	9	3	3	86.9	197.7	310.7	595.3	38	760
E_{3-5}	4	4	1	6	4	6	48.1	111.6	232.0	391.7	13	260
E_{4-1}	4	3	1	1	5	1	36.2	99.4	193.7	329.3	25	500
E_{4-2}	2	1	1	8	3	3	129.0	98.6	247.0	474.6	9	180
E_{4-3}	4	2	1	5	1	2	46.2	155.3	323.6	525.1	16	320
E_{4-4}	4	2	1	1	1	9	35.5	143.1	426.4	605.0	34	680
E_{4-5}	4	7	1	1	1	9	43.8	94.6	187.1	325.5	50	1000
E_{5-1}	4	6	1	1	4	1	26.2	129.4	185.6	341.2	45	900
E_{5-2}	4	2	1	8	1	3	50.7	152.1	224.4	427.1	27	540
E_{5-3}	4	1	1	5	1	2	53.7	162.3	307.3	523.3	14	280
E_{5-4}	4	1	1	1	2	9	48.2	129.5	397.9	575.6	28	560
E_{5-5}	4	7	1	1	4	9	46.9	84.6	187.4	318.8	41	820
Avg.	4	2	1	4	2	4	48.6	145.5	289.8	483.8	24.2	484.8
Sum.											606	12120

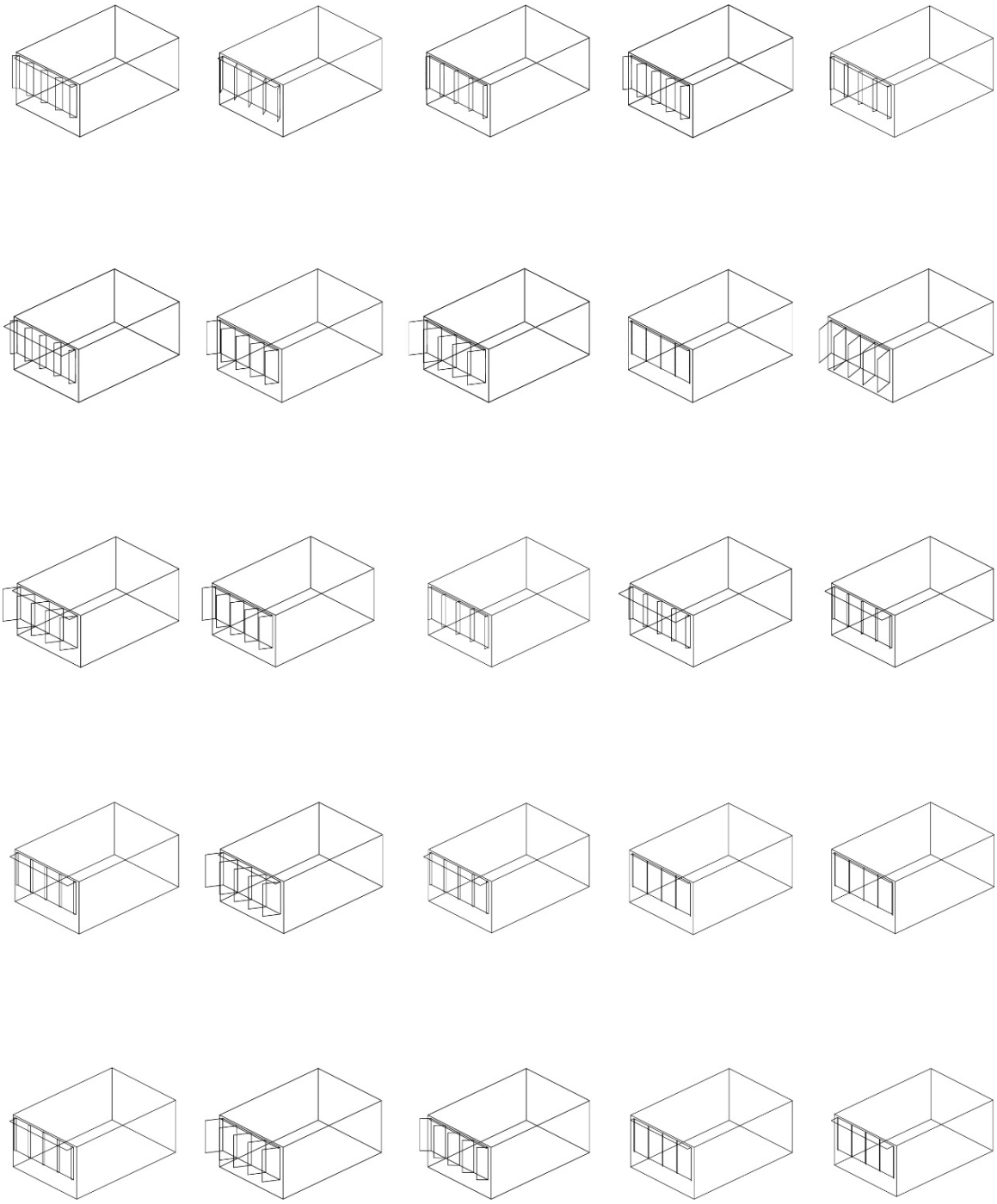

Figure C.2: AR Results II – East façade – San Francisco

Table C.3: GA Results II – North façade – San Francisco

Unit	v_1	v_2	v_3	v_4	v_5	v_6	Q_H [kWh]	Q_C [kWh]	Q_L [kWh]	Q_{Total} [kWh]	Gene. [-]	Simu. [-]
N_{1-1}	4	1	1	4	1	4	34.6	171.6	383.5	589.6	28	560
N_{1-2}	4	1	1	2	2	4	43.8	170.2	374.3	588.3	45	900
N_{1-3}	4	1	1	2	1	4	42.1	175.0	375.1	592.2	29	580
N_{1-4}	4	3	1	3	5	2	35.6	152.8	415.1	603.5	15	300
N_{1-5}	4	3	1	1	2	6	59.5	143.3	158.3	361.1	28	560
N_{2-1}	4	1	1	1	2	4	38.7	162.0	375.2	575.9	16	320
N_{2-2}	4	1	1	3	1	3	50.4	92.7	325.9	469.0	17	340
N_{2-3}	4	2	1	3	2	3	38.8	108.9	373.5	521.2	24	480
N_{2-4}	2	3	4	3	3	3	59.7	135.5	346.2	541.4	28	560
N_{2-5}	6	1	1	10	4	6	31.5	141.9	157.8	331.3	41	820
N_{3-1}	4	1	1	6	1	2	37.8	140.2	355.4	533.4	22	440
N_{3-2}	4	3	1	2	1	3	40.5	97.2	322.2	460.0	33	660
N_{3-3}	4	6	1	2	1	3	34.9	102.0	314.5	451.4	43	860
N_{3-4}	4	5	1	2	1	3	45.2	116.2	293.8	455.2	30	600
N_{3-5}	4	2	2	2	2	7	53.5	91.5	126.2	271.2	13	260
N_{4-1}	4	4	1	1	5	1	34.2	100.7	193.8	328.6	29	580
N_{4-2}	4	4	1	4	1	3	43.4	92.8	277.7	413.8	20	400
N_{4-3}	4	6	1	2	1	3	37.5	111.1	300.2	448.8	42	840
N_{4-4}	4	4	1	2	2	3	51.8	104.7	269.1	425.7	18	360
N_{4-5}	4	4	2	2	2	7	47.8	92.9	122.4	263.1	28	560
N_{5-1}	4	2	1	1	6	7	41.3	129.7	331.9	503.0	16	320
N_{5-2}	4	5	1	2	1	3	41.2	99.6	283.9	424.8	30	600
N_{5-3}	4	3	1	2	1	3	48.7	98.7	274.0	421.4	24	480
N_{5-4}	4	6	1	2	1	3	43.9	116.5	232.8	393.3	43	860
N_{5-5}	6	1	1	2	2	7	37.7	112.2	123.5	273.4	34	680
Avg.	4	3	1	3	2	4	43.0	122.4	284.3	449.6	27.8	556.8
Sum.											696	13920

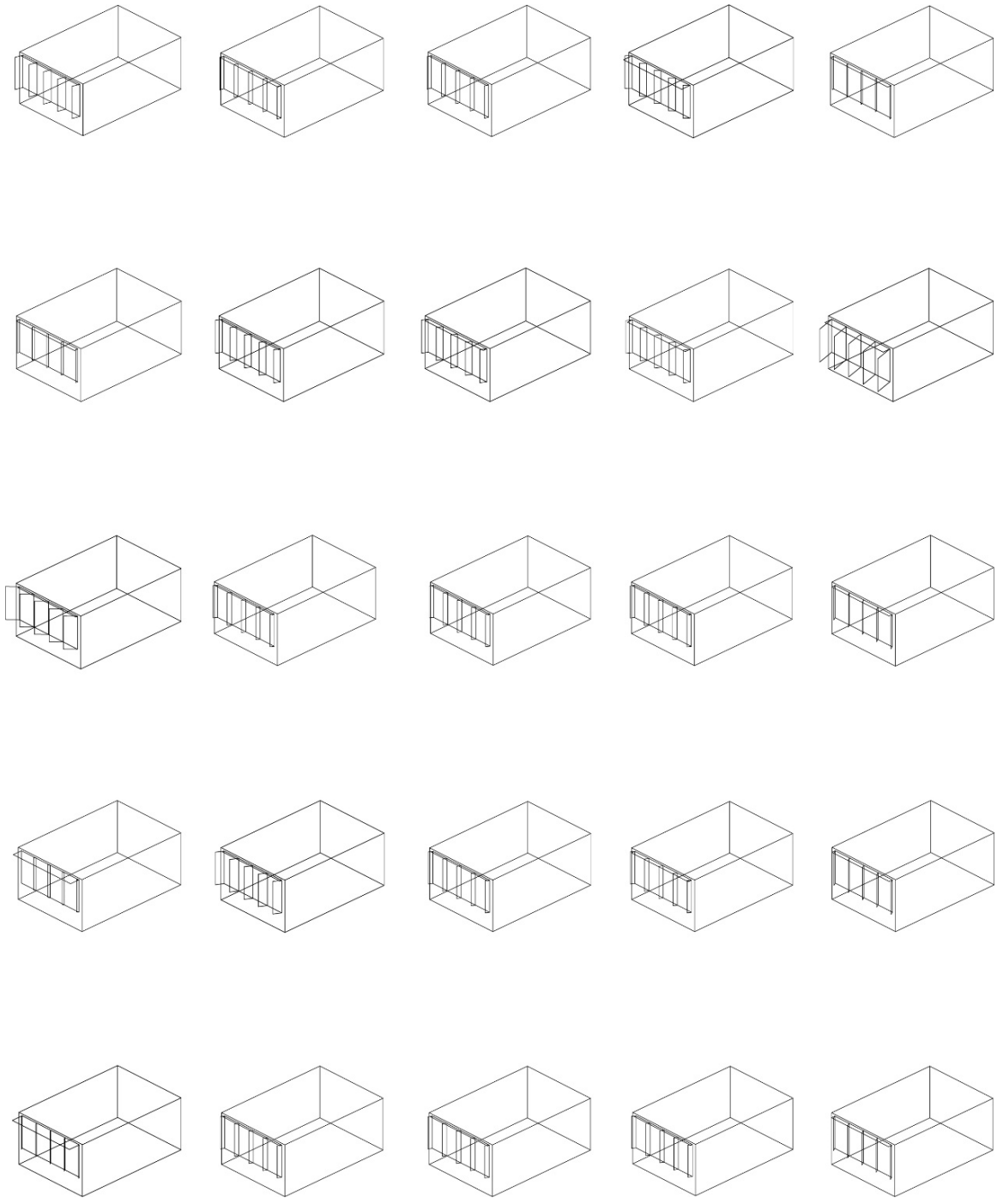

Figure C.3: AR Results II – North façade – San Francisco

Table C.4: GA Results II – West façade – San Francisco

Unit	v_1	v_2	v_3	v_4	v_5	v_6	Q_H [kWh]	Q_C [kWh]	Q_L [kWh]	Q_{Total} [kWh]	Gene. [-]	Simu. [-]
W_{1-1}	4	1	1	2	2	6	60.9	146.2	381.5	588.7	48	960
W_{1-2}	2	6	3	2	5	6	64.9	163.9	392.1	620.9	31	620
W_{1-3}	4	1	1	2	3	6	61.7	144.3	386.2	592.2	18	360
W_{1-4}	4	1	1	2	5	6	60.4	137.3	366.7	564.4	19	380
W_{1-5}	4	1	1	1	3	6	59.2	146.6	337.5	543.2	37	740
W_{2-1}	4	1	1	1	2	6	62.9	150.8	352.6	566.3	44	880
W_{2-2}	4	1	1	1	3	6	61.2	138.3	363.7	563.2	28	560
W_{2-3}	4	2	1	1	1	6	55.2	136.1	350.1	541.4	20	400
W_{2-4}	4	2	1	1	2	6	58.5	139.5	332.5	530.5	18	360
W_{2-5}	4	1	2	2	3	1	51.5	111.5	358.7	521.7	27	540
W_{3-1}	4	1	1	1	1	6	60.4	181.0	327.5	568.9	20	400
W_{3-2}	4	1	1	1	1	6	59.8	172.1	337.2	569.1	26	520
W_{3-3}	4	1	1	2	3	3	61.8	136.5	356.3	554.7	21	420
W_{3-4}	4	2	1	2	1	7	57.5	149.7	305.5	512.6	28	560
W_{3-5}	4	6	1	2	1	3	48.1	123.0	333.6	504.8	48	960
W_{4-1}	4	1	1	4	1	3	60.9	186.8	303.3	551.0	32	640
W_{4-2}	4	1	1	5	4	4	63.5	135.7	351.9	551.1	15	300
W_{4-3}	4	1	1	2	1	3	65.0	148.2	310.8	525.0	26	520
W_{4-4}	4	6	1	2	1	3	50.5	131.6	321.3	503.4	39	780
W_{4-5}	4	4	1	2	2	3	58.3	109.7	311.2	479.1	27	540
W_{5-1}	4	1	1	1	7	4	61.1	188.3	314.7	564.1	20	400
W_{5-2}	4	4	1	5	8	4	49.8	163.7	351.4	564.8	23	460
W_{5-3}	4	2	1	2	7	3	55.7	167.4	327.0	550.1	25	500
W_{5-4}	4	5	1	2	5	3	51.9	144.1	315.9	511.9	25	500
W_{5-5}	4	3	1	2	1	3	55.5	183.5	263.9	502.9	24	480
Avg.	4	2	1	2	3	5	58.2	149.4	338.1	545.8	27.6	551.2
Sum.											689	13780

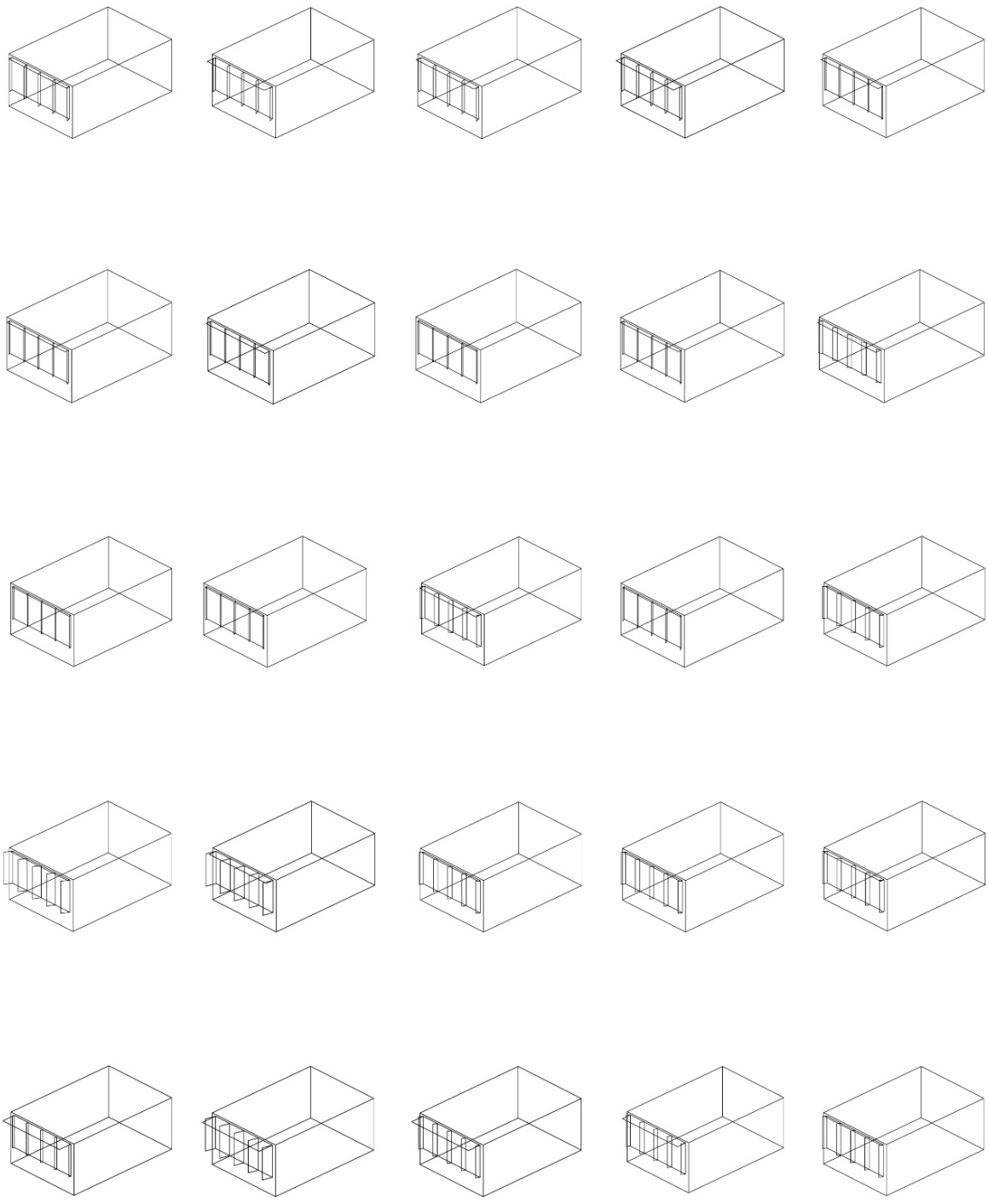

Figure C.4: AR Results II – West façade – San Francisco

APPENDIX D

AR I Result for Chicago

Table D.1: AR Results I – Step 3 - Chicago

	v_1	v_2	v_3	v_4	v_5	v_6	[kWh]		v_1	v_2	v_3	v_4	v_5	v_6	[kWh]
S_{1-1}	6	5	4	8	9	3	1062.8	E_{1-1}	6	5	4	9	3	3	1228.8
S_{1-2}	6	5	4	7	6	5	1246.8	E_{1-2}	6	5	4	9	3	3	1337.0
S_{1-3}	6	5	4	6	3	6	1176.7	E_{1-3}	6	5	4	9	2	3	1418.6
S_{1-4}	6	5	4	8	2	7	1298.4	E_{1-4}	6	5	4	7	3	5	1536.3
S_{1-5}	6	5	4	10	1	8	1151.6	E_{1-5}	6	5	4	4	3	7	1208.9
S_{3-1}	6	5	4	1	10	3	1050.3	E_{3-1}	6	5	4	1	5	1	1171.4
S_{3-2}	6	5	4	5	7	4	1280.0	E_{3-2}	6	5	4	4	5	2	1497.3
S_{3-3}	6	5	4	8	4	4	1147.7	E_{3-3}	6	5	4	7	4	3	1456.4
S_{3-4}	6	5	4	7	5	6	1365.1	E_{3-4}	6	5	4	4	6	6	1518.5
S_{3-5}	6	5	4	6	5	7	1126.5	E_{3-5}	6	5	4	1	7	9	1192.2
S_{5-1}	6	5	4	2	10	2	1043.6	E_{5-1}	6	5	4	5	3	2	1148.6
S_{5-2}	6	5	4	3	9	3	1275.2	E_{5-2}	6	5	4	6	4	2	1445.6
S_{5-3}	6	5	4	4	7	4	1189.6	E_{5-3}	6	5	4	7	5	2	1414.2
S_{5-4}	6	5	4	3	7	6	1336.6	E_{5-4}	6	5	4	4	4	6	1472.4
S_{5-5}	6	5	4	1	7	7	1123.6	E_{5-5}	6	5	4	1	3	9	1174.0
Avg.							1191.6	Avg.							1348.0
N_{1-1}	6	5	4	2	2	6	1416.7	W_{1-1}	6	5	4	2	4	6	1456.7
N_{1-2}	6	5	4	5	3	7	1445.1	W_{1-2}	6	5	4	2	4	7	1472.3
N_{1-3}	6	5	4	8	3	7	1422.1	W_{1-3}	6	5	4	1	4	7	1460.5
N_{1-4}	6	5	4	9	4	7	1360.9	W_{1-4}	6	5	4	1	3	7	1462.0
N_{1-5}	6	5	4	9	4	7	1171.6	W_{1-5}	6	5	4	1	2	6	1370.3
N_{3-1}	6	5	4	8	1	2	1342.1	W_{3-1}	6	5	4	1	4	6	1428.1
N_{3-2}	6	5	4	7	1	5	1398.5	W_{3-2}	6	5	4	2	7	7	1425.8
N_{3-3}	6	5	4	6	1	7	1369.7	W_{3-3}	6	5	4	2	10	7	1390.2
N_{3-4}	6	5	4	6	1	7	1358.4	W_{3-4}	6	5	4	2	6	5	1464.5
N_{3-5}	6	5	4	6	1	6	1163.4	W_{3-5}	6	5	4	1	1	3	1393.7
N_{5-1}	6	5	4	1	3	6	1365.8	W_{5-1}	6	5	4	5	1	7	1393.6
N_{5-2}	6	5	4	6	3	7	1382.8	W_{5-2}	6	5	4	7	2	6	1412.2
N_{5-3}	6	5	4	10	3	7	1317.0	W_{5-3}	6	5	4	9	3	4	1403.8
N_{5-4}	6	5	4	6	2	5	1351.4	W_{5-4}	6	5	4	7	3	6	1381.9
N_{5-5}	6	5	4	1	1	3	1144.4	W_{5-5}	6	5	4	4	3	7	1372.7
Avg.							1334.0	Avg.							1419.2

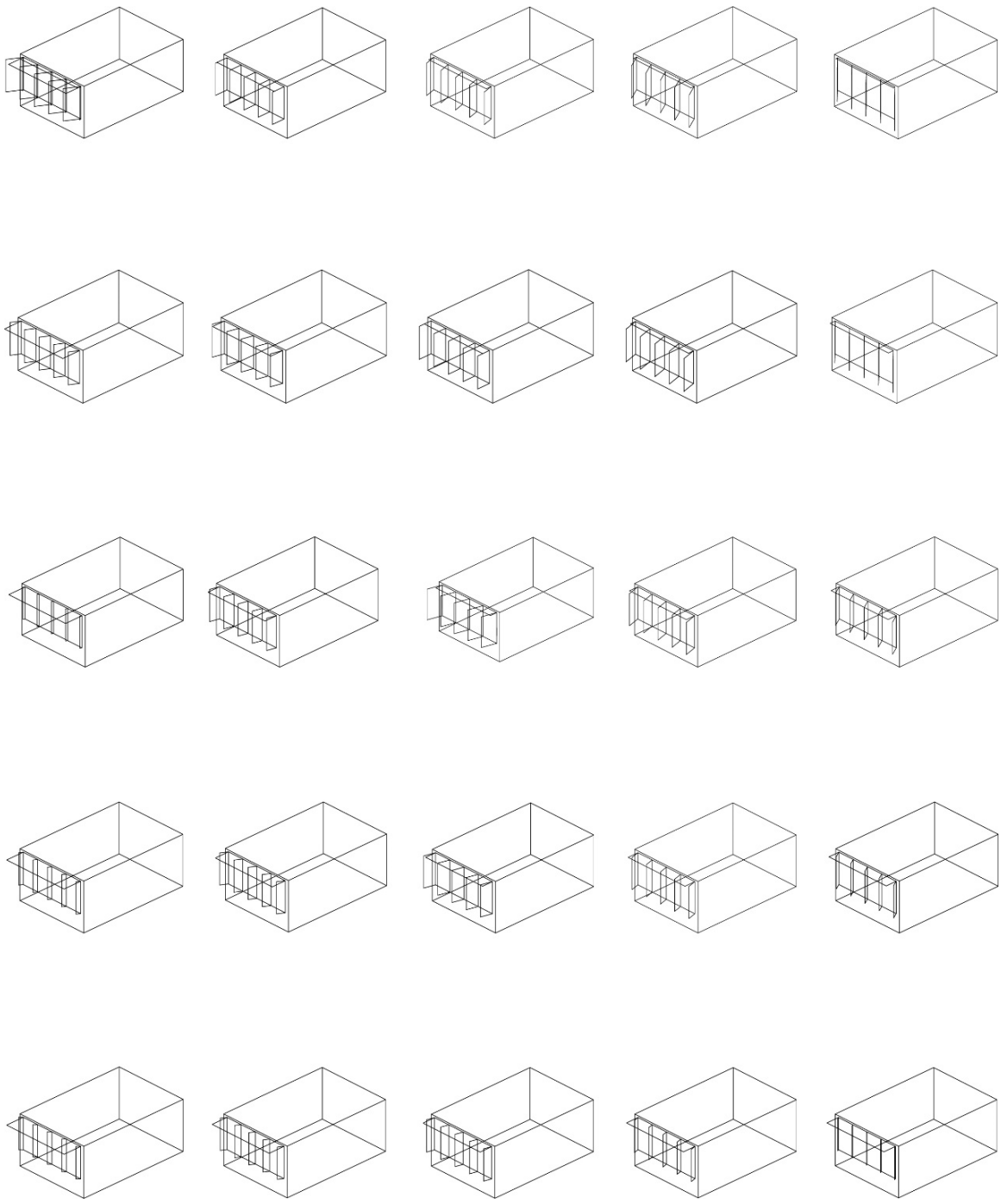

Figure D.1: AR Results I – South façade – Chicago

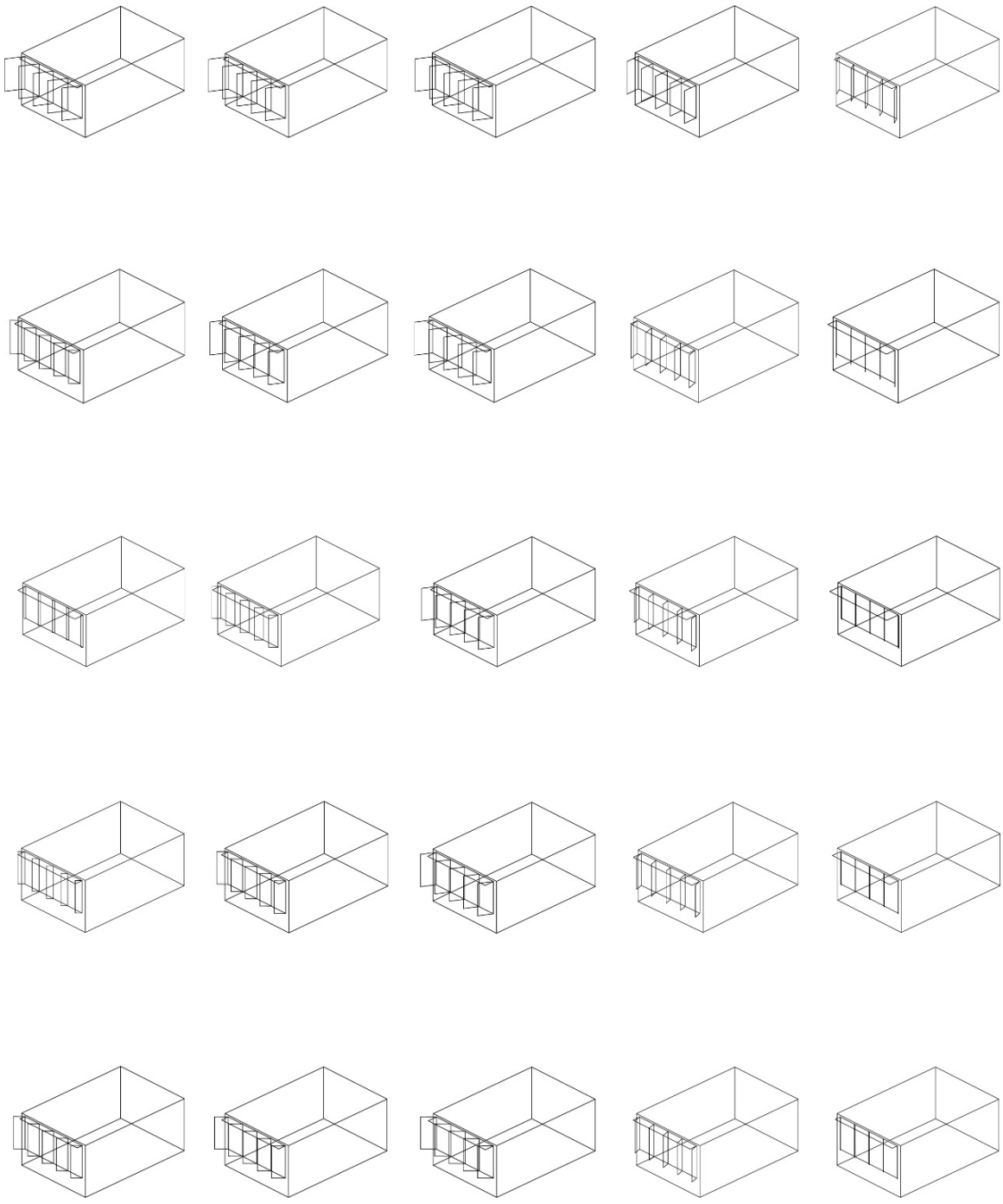

Figure D.2: AR Results I – East façade – Chicago

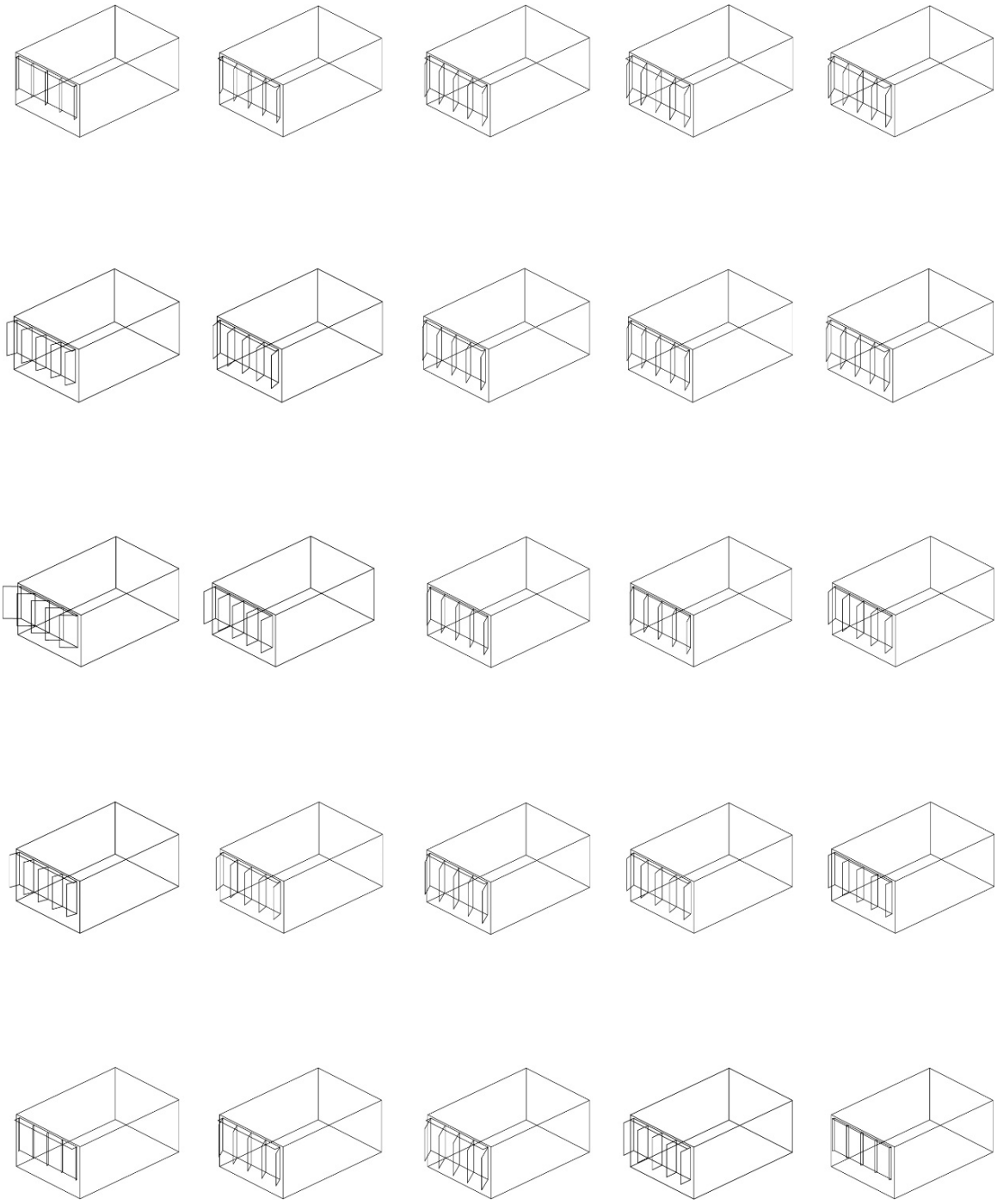

Figure D.3: AR Results I – North façade – Chicago

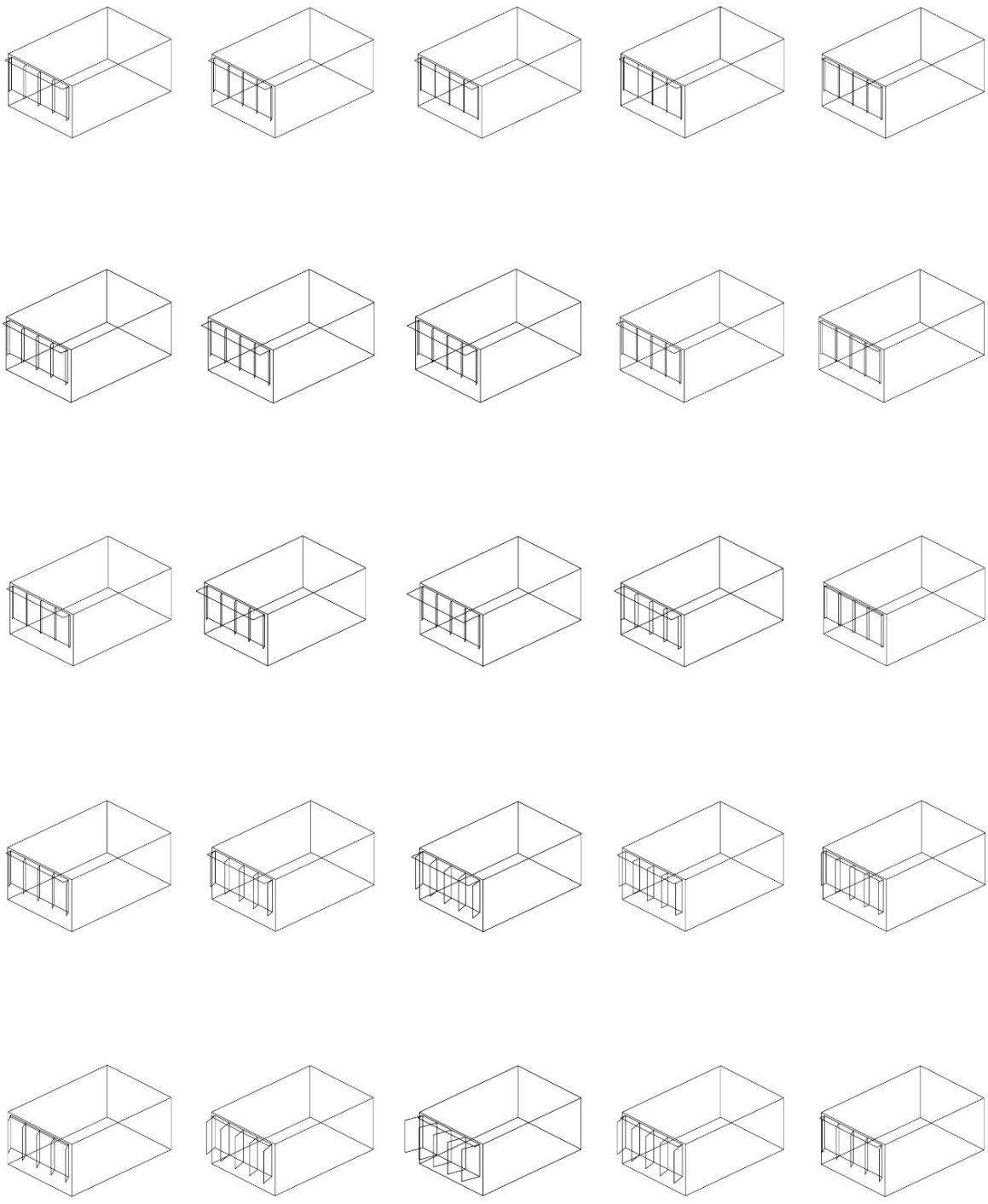

Figure D.4: AR Results I – West façade – Chicago

Table D.2: AR Results I – Step 4 - Chicago

	v_1	v_2	v_3	v_4	v_5	v_6	[kWh]		v_1	v_2	v_3	v_4	v_5	v_6	[kWh]
S_{1-1}	6	5	4	8	9	3	1062.8	E_{1-1}	6	5	4	9	3	3	1228.8
S_{1-2}	6	5	4	7	6	5	1246.8	E_{1-2}	6	5	4	9	3	3	1337.0
S_{1-3}	6	5	4	6	3	6	1176.7	E_{1-3}	6	5	4	9	2	3	1418.6
S_{1-4}	6	5	4	8	2	7	1298.4	E_{1-4}	6	5	4	7	3	5	1536.3
S_{1-5}	6	5	4	10	1	8	1151.6	E_{1-5}	6	5	4	4	3	7	1208.9
S_{2-1}	6	5	4	5	10	3	1183.3	E_{2-1}	6	5	4	5	4	2	1318.5
S_{2-2}	6	5	4	6	7	4	1211.9	E_{2-2}	6	5	4	7	4	3	1273.8
S_{2-3}	6	5	4	7	4	5	1282.6	E_{2-3}	6	5	4	8	3	3	1418.1
S_{2-4}	6	5	4	8	3	6	1310.0	E_{2-4}	6	5	4	5	4	6	1538.3
S_{2-5}	6	5	4	8	3	8	1251.2	E_{2-5}	6	5	4	3	5	8	1329.3
S_{3-1}	6	5	4	1	10	3	1050.3	E_{3-1}	6	5	4	1	5	1	1171.4
S_{3-2}	6	5	4	5	7	4	1280.0	E_{3-2}	6	5	4	4	5	2	1497.3
S_{3-3}	6	5	4	8	4	4	1147.7	E_{3-3}	6	5	4	7	4	3	1456.4
S_{3-4}	6	5	4	7	5	6	1365.1	E_{3-4}	6	5	4	4	6	6	1518.5
S_{3-5}	6	5	4	6	5	7	1126.5	E_{3-5}	6	5	4	1	7	9	1192.2
S_{4-1}	6	5	4	2	10	3	1294.3	E_{4-1}	6	5	4	3	4	2	1368.5
S_{4-2}	6	5	4	4	8	3	1273.7	E_{4-2}	6	5	4	5	4	2	1451.0
S_{4-3}	6	5	4	6	6	4	1262.5	E_{4-3}	6	5	4	7	5	3	1429.5
S_{4-4}	6	5	4	5	6	6	1362.4	E_{4-4}	6	5	4	4	5	6	1531.4
S_{4-5}	6	5	4	4	6	7	1269.4	E_{4-5}	6	5	4	1	5	9	1358.9
S_{5-1}	6	5	4	2	10	2	1043.6	E_{5-1}	6	5	4	5	3	2	1148.6
S_{5-2}	6	5	4	3	9	3	1275.2	E_{5-2}	6	5	4	6	4	2	1445.6
S_{5-3}	6	5	4	4	7	4	1189.6	E_{5-3}	6	5	4	7	5	2	1414.2
S_{5-4}	6	5	4	3	7	6	1336.6	E_{5-4}	6	5	4	4	4	6	1472.4
S_{5-5}	6	5	4	1	7	7	1123.6	E_{5-5}	6	5	4	1	3	9	1174.0
Avg.							1223.0	Avg.							1369.5
N_{1-1}	6	5	4	2	2	6	1416.7	W_{1-1}	6	5	4	2	4	6	1456.7
N_{1-2}	6	5	4	5	3	7	1445.1	W_{1-2}	6	5	4	2	4	7	1472.3
N_{1-3}	6	5	4	8	3	7	1422.1	W_{1-3}	6	5	4	1	4	7	1460.5
N_{1-4}	6	5	4	9	4	7	1360.9	W_{1-4}	6	5	4	1	3	7	1462.0
N_{1-5}	6	5	4	9	4	7	1171.6	W_{1-5}	6	5	4	1	2	6	1370.3
N_{2-1}	6	5	4	5	2	4	1406.6	W_{2-1}	6	5	4	2	4	6	1442.9
N_{2-2}	6	5	4	6	2	6	1424.5	W_{2-2}	6	5	4	2	6	7	1426.7
N_{2-3}	6	5	4	7	2	7	1428.3	W_{2-3}	6	5	4	2	7	7	1431.2
N_{2-4}	6	5	4	7	2	7	1361.6	W_{2-4}	6	5	4	1	4	6	1414.6
N_{2-5}	6	5	4	8	3	7	1302.3	W_{2-5}	6	5	4	1	2	5	1418.1
N_{3-1}	6	5	4	8	1	2	1342.1	W_{3-1}	6	5	4	1	4	6	1428.1
N_{3-2}	6	5	4	7	1	5	1398.5	W_{3-2}	6	5	4	2	7	7	1425.8
N_{3-3}	6	5	4	6	1	7	1369.7	W_{3-3}	6	5	4	2	10	7	1390.2
N_{3-4}	6	5	4	6	1	7	1358.4	W_{3-4}	6	5	4	2	6	5	1464.5

	v_1	v_2	v_3	v_4	v_5	v_6	[kWh]		v_1	v_2	v_3	v_4	v_5	v_6	[kWh]
N_{3-5}	6	5	4	6	1	6	1163.4	W_{3-5}	6	5	4	1	1	3	1393.7
N_{4-1}	6	5	4	5	2	4	1357.5	W_{4-1}	6	5	4	3	3	7	1437.0
N_{4-2}	6	5	4	6	2	6	1375.7	W_{4-2}	6	5	4	4	5	6	1459.6
N_{4-3}	6	5	4	8	2	7	1312.3	W_{4-3}	6	5	4	6	7	6	1484.6
N_{4-4}	6	5	4	6	2	6	1330.9	W_{4-4}	6	5	4	4	4	5	1472.6
N_{4-5}	6	5	4	4	1	5	1326.4	W_{4-5}	6	5	4	3	2	5	1433.8
N_{5-1}	6	5	4	1	3	6	1365.8	W_{5-1}	6	5	4	5	1	7	1393.6
N_{5-2}	6	5	4	6	3	7	1382.8	W_{5-2}	6	5	4	7	2	6	1412.2
N_{5-3}	6	5	4	10	3	7	1317.0	W_{5-3}	6	5	4	9	3	4	1403.8
N_{5-4}	6	5	4	6	2	5	1351.4	W_{5-4}	6	5	4	7	3	6	1381.9
N_{5-5}	6	5	4	1	1	3	1144.4	W_{5-5}	6	5	4	4	3	7	1372.7
Avg.							1345.4	Avg.							1428.4

APPENDIX E

AR II Result for Chicago

Table E.1: AR Results II – Step 3 - Chicago

	v_1	v_2	v_3	v_4	v_5	v_6	[kWh]		v_1	v_2	v_3	v_4	v_5	v_6	[kWh]
S_{1-1}	6	7	4	1	10	1	1146.4	E_{1-1}	6	7	4	10	9	2	1204.9
S_{1-2}	6	7	4	2	10	1	1165.3	E_{1-2}	6	7	4	9	6	3	1307.4
S_{1-3}	6	7	4	2	10	1	1157.4	E_{1-3}	6	7	4	8	2	3	1325.3
S_{1-4}	6	7	4	2	10	2	1212.6	E_{1-4}	6	7	4	5	5	6	1448.1
S_{1-5}	6	7	4	2	9	2	1172.3	E_{1-5}	6	7	4	1	7	8	1269.5
S_{3-1}	6	7	4	9	10	3	1198.8	E_{3-1}	6	7	4	1	5	8	1233.8
S_{3-2}	6	7	4	6	10	6	1235.1	E_{3-2}	6	7	4	2	4	6	1409.6
S_{3-3}	6	7	4	2	10	8	1175.7	E_{3-3}	6	7	4	3	3	3	1354.9
S_{3-4}	6	7	4	2	10	5	1278.8	E_{3-4}	6	7	4	3	4	5	1499.3
S_{3-5}	6	7	4	1	10	1	1201.1	E_{3-5}	6	7	4	3	5	7	1282.0
S_{5-1}	6	7	4	9	10	3	1204.0	E_{5-1}	6	7	4	7	6	3	1247.5
S_{5-2}	6	7	4	9	10	3	1165.2	E_{5-2}	6	7	4	5	4	3	1395.0
S_{5-3}	6	7	4	9	10	3	1198.6	E_{5-3}	6	7	4	3	1	3	1394.7
S_{5-4}	6	7	4	9	10	5	1332.4	E_{5-4}	6	7	4	3	2	5	1491.4
S_{5-5}	6	7	4	9	9	7	1213.7	E_{5-5}	6	7	4	3	3	7	1297.9
Avg.							1203.8	Avg.							1344.1
N_{1-1}	6	7	4	1	1	8	1355.6	W_{1-1}	6	7	4	8	1	2	1425.2
N_{1-2}	6	7	4	4	1	6	1414.0	W_{1-2}	6	7	4	5	1	2	1458.8
N_{1-3}	6	7	4	6	1	3	1347.3	W_{1-3}	6	7	4	2	1	2	1373.6
N_{1-4}	6	7	4	5	2	3	1389.3	W_{1-4}	6	7	4	2	1	5	1422.7
N_{1-5}	6	7	4	3	2	3	1272.7	W_{1-5}	6	7	4	1	1	8	1367.9
N_{3-1}	6	7	4	3	2	3	1320.9	W_{3-1}	6	7	4	9	1	8	1398.2
N_{3-2}	6	7	4	3	2	3	1289.4	W_{3-2}	6	7	4	5	2	7	1397.1
N_{3-3}	6	7	4	2	1	2	1309.4	W_{3-3}	6	7	4	1	2	6	1372.1
N_{3-4}	6	7	4	4	3	5	1365.1	W_{3-4}	6	7	4	1	3	7	1392.9
N_{3-5}	6	7	4	6	5	8	1274.5	W_{3-5}	6	7	4	1	3	7	1350.3
N_{5-1}	6	7	4	3	2	3	1304.4	W_{5-1}	6	7	4	9	1	2	1313.8
N_{5-2}	6	7	4	3	2	3	1284.5	W_{5-2}	6	7	4	9	2	2	1272.3
N_{5-3}	6	7	4	2	1	2	1299.3	W_{5-3}	6	7	4	9	2	2	1311.9
N_{5-4}	6	7	4	4	2	3	1313.1	W_{5-4}	6	7	4	8	2	3	1305.2
N_{5-5}	6	7	4	6	2	3	1265.2	W_{5-5}	6	7	4	6	2	4	1412.2
Avg.							1320.3	Avg.							1419.2
															1371.2

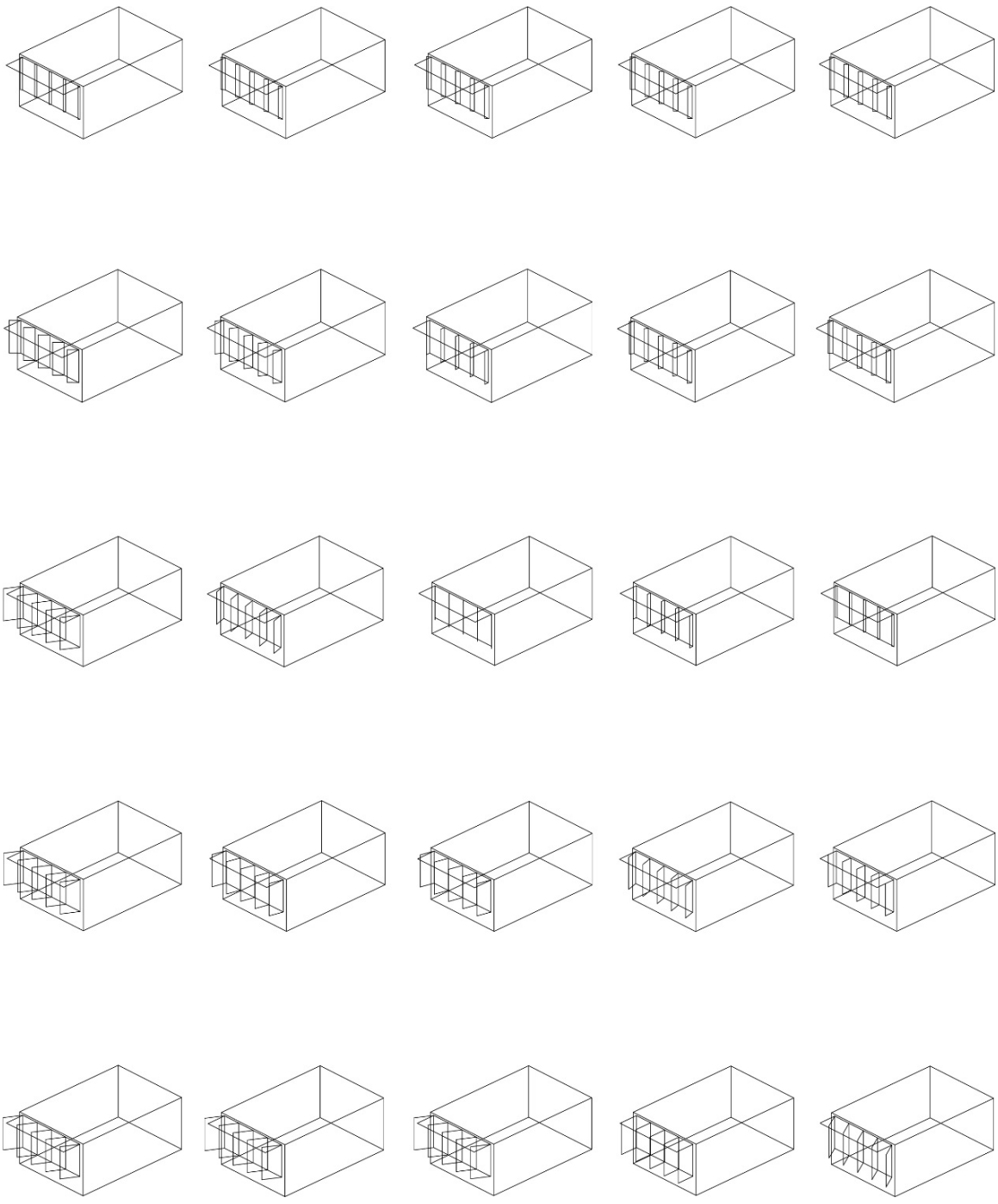

Figure E.1: AR Results II – South façade – Chicago

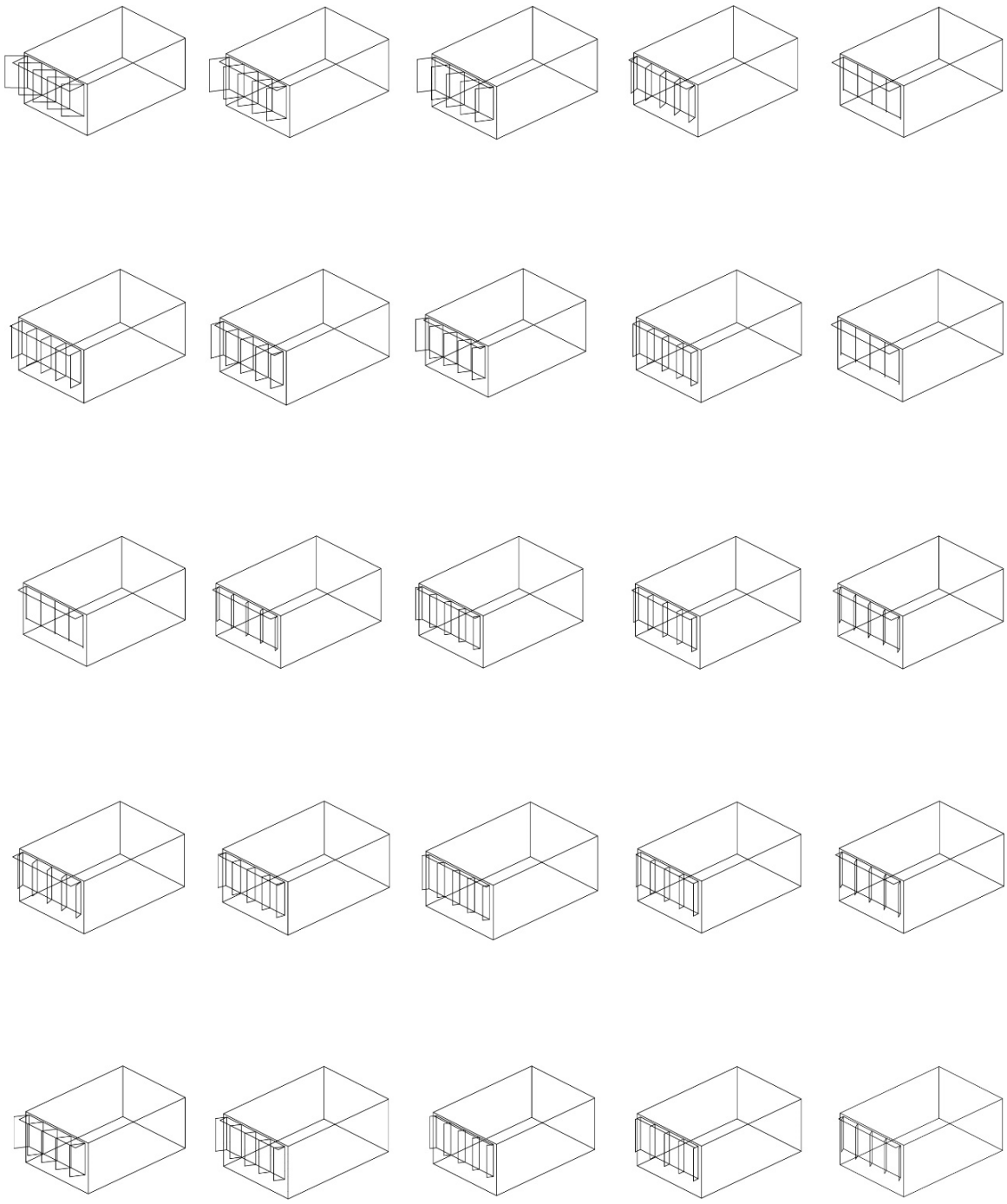

Figure E.2: AR Results II – East façade – Chicago

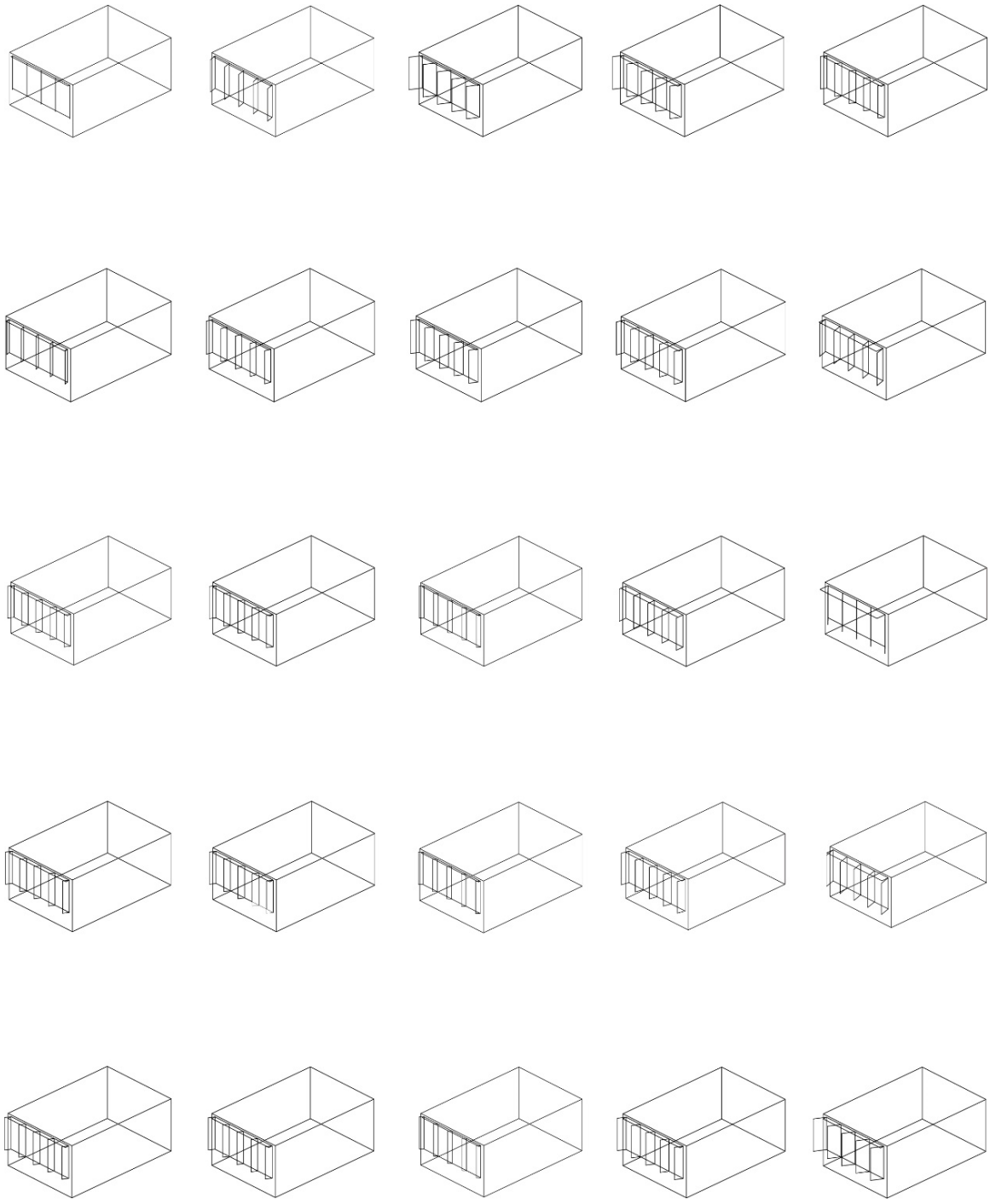

Figure E.3: AR Results II – North façade – Chicago

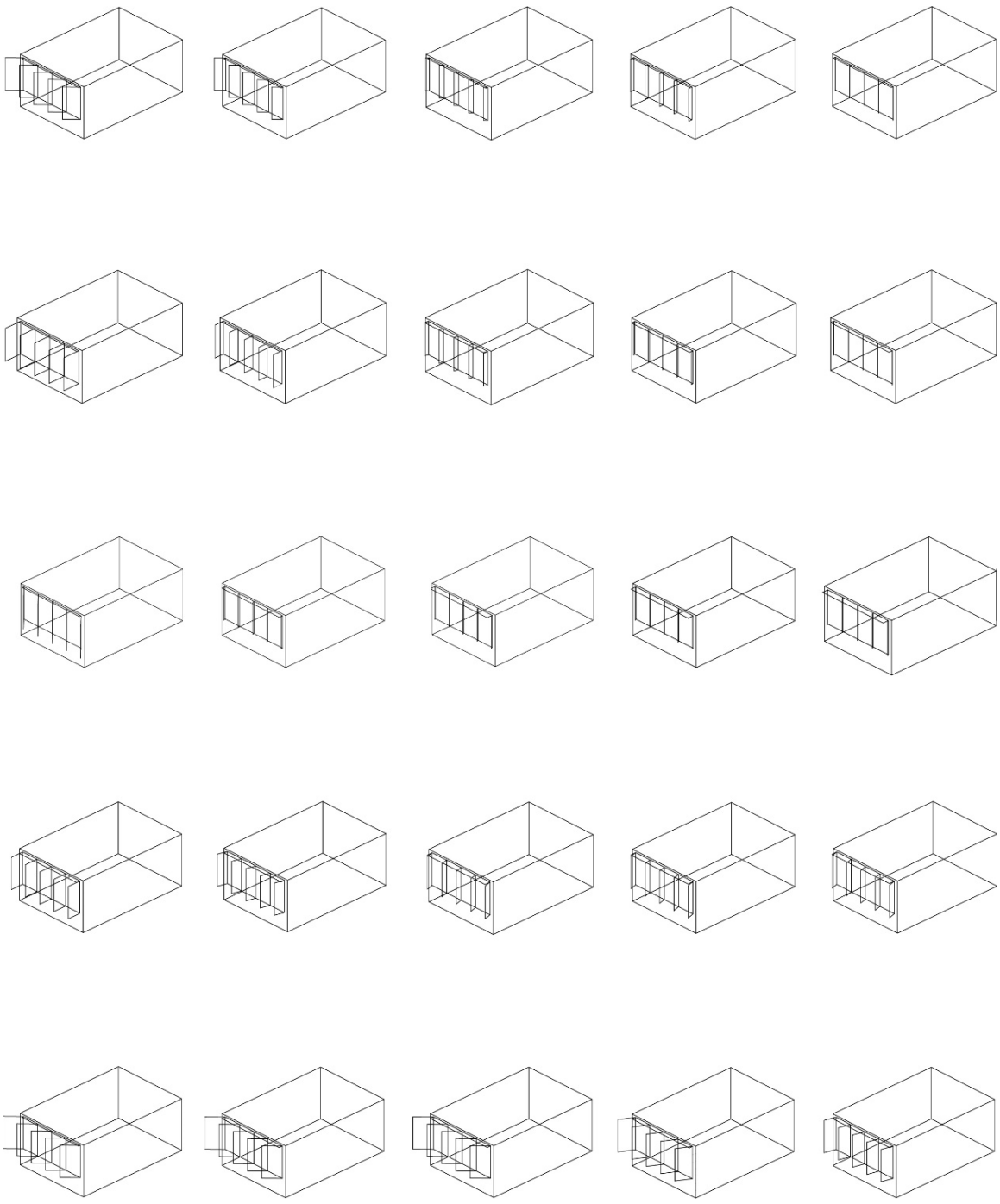

Figure E.4: AR Results II – West façade – Chicago

Table E.2: AR Results II – Step 4 - Chicago

	v_1	v_2	v_3	v_4	v_5	v_6	[kWh]		v_1	v_2	v_3	v_4	v_5	v_6	[kWh]
S_{1-1}	6	7	4	1	10	1	1146.4	E_{1-1}	6	7	4	10	9	2	1204.9
S_{1-2}	6	7	4	2	10	1	1165.3	E_{1-2}	6	7	4	9	6	3	1307.4
S_{1-3}	6	7	4	2	10	1	1157.4	E_{1-3}	6	7	4	8	2	3	1325.3
S_{1-4}	6	7	4	2	10	2	1212.6	E_{1-4}	6	7	4	5	5	6	1448.1
S_{1-5}	6	7	4	2	9	2	1172.3	E_{1-5}	6	7	4	1	7	8	1269.5
S_{2-1}	6	7	4	5	10	2	1194.1	E_{2-1}	6	7	4	6	7	5	1357.5
S_{2-2}	6	7	4	4	10	3	1174.2	E_{2-2}	6	7	4	6	5	4	1411.1
S_{2-3}	6	7	4	2	10	5	1189.7	E_{2-3}	6	7	4	6	3	3	1367.3
S_{2-4}	6	7	4	2	10	3	1224.7	E_{2-4}	6	7	4	4	4	5	1492.3
S_{2-5}	6	7	4	2	10	2	1198.8	E_{2-5}	6	7	4	2	6	8	1300.5
S_{3-1}	6	7	4	9	10	3	1198.8	E_{3-1}	6	7	4	1	5	8	1233.8
S_{3-2}	6	7	4	6	10	6	1235.1	E_{3-2}	6	7	4	2	4	6	1409.6
S_{3-3}	6	7	4	2	10	8	1175.7	E_{3-3}	6	7	4	3	3	3	1354.9
S_{3-4}	6	7	4	2	10	5	1278.8	E_{3-4}	6	7	4	3	4	5	1499.3
S_{3-5}	6	7	4	1	10	1	1201.1	E_{3-5}	6	7	4	3	5	7	1282.0
S_{4-1}	6	7	4	9	10	3	1164.7	E_{4-1}	6	7	4	4	6	6	1450.2
S_{4-2}	6	7	4	7	10	4	1228.1	E_{4-2}	6	7	4	4	4	4	1432.6
S_{4-3}	6	7	4	6	10	6	1235.9	E_{4-3}	6	7	4	3	2	3	1345.5
S_{4-4}	6	7	4	5	10	5	1314.4	E_{4-4}	6	7	4	3	3	5	1485.9
S_{4-5}	6	7	4	5	10	4	1253.3	E_{4-5}	6	7	4	3	4	7	1242.4
S_{5-1}	6	7	4	9	10	3	1204.0	E_{5-1}	6	7	4	7	6	3	1247.5
S_{5-2}	6	7	4	9	10	3	1165.2	E_{5-2}	6	7	4	5	4	3	1395.0
S_{5-3}	6	7	4	9	10	3	1198.6	E_{5-3}	6	7	4	3	1	3	1394.7
S_{5-4}	6	7	4	9	10	5	1332.4	E_{5-4}	6	7	4	3	2	5	1491.4
S_{5-5}	6	7	4	9	9	7	1213.7	E_{5-5}	6	7	4	3	3	7	1297.9
Avg.							1209.4	Avg.							1361.9
N_{1-1}	6	7	4	1	1	8	1355.6	W_{1-1}	6	7	4	8	1	2	1425.2
N_{1-2}	6	7	4	4	1	6	1414.0	W_{1-2}	6	7	4	5	1	2	1458.8
N_{1-3}	6	7	4	6	1	3	1347.3	W_{1-3}	6	7	4	2	1	2	1373.6
N_{1-4}	6	7	4	5	2	3	1389.3	W_{1-4}	6	7	4	2	1	5	1422.7
N_{1-5}	6	7	4	3	2	3	1272.7	W_{1-5}	6	7	4	1	1	8	1367.9
N_{2-1}	6	7	4	2	2	6	1406.3	W_{2-1}	6	7	4	9	1	5	1436.3
N_{2-2}	6	7	4	3	1	4	1419.9	W_{2-2}	6	7	4	5	1	5	1431.8
N_{2-3}	6	7	4	4	1	3	1390.2	W_{2-3}	6	7	4	2	2	4	1381.5
N_{2-4}	6	7	4	4	2	4	1362.0	W_{2-4}	6	7	4	1	2	6	1359.4
N_{2-5}	6	7	4	5	4	6	1271.9	W_{2-5}	6	7	4	1	2	8	1422.1
N_{3-1}	6	7	4	3	2	3	1320.9	W_{3-1}	6	7	4	9	1	8	1398.2
N_{3-2}	6	7	4	3	2	3	1289.4	W_{3-2}	6	7	4	5	2	7	1397.1
N_{3-3}	6	7	4	2	1	2	1309.4	W_{3-3}	6	7	4	1	2	6	1372.1
N_{3-4}	6	7	4	4	3	5	1365.1	W_{3-4}	6	7	4	1	3	7	1392.9

	v_1	v_2	v_3	v_4	v_5	v_6	[kWh]		v_1	v_2	v_3	v_4	v_5	v_6	[kWh]
N_{3-5}	6	7	4	6	5	8	1274.5	W_{3-5}	6	7	4	1	3	7	1350.3
N_{4-1}	6	7	4	3	2	3	1283.9	W_{4-1}	6	7	4	9	1	5	1433.0
N_{4-2}	6	7	4	3	2	3	1285.3	W_{4-2}	6	7	4	7	2	5	1420.0
N_{4-3}	6	7	4	2	1	2	1280.0	W_{4-3}	6	7	4	5	2	4	1424.8
N_{4-4}	6	7	4	4	2	4	1337.8	W_{4-4}	6	7	4	4	2	5	1439.8
N_{4-5}	6	7	4	6	4	6	1274.4	W_{4-5}	6	7	4	4	3	6	1403.6
N_{5-1}	6	7	4	3	2	3	1304.4	W_{5-1}	6	7	4	9	1	2	1313.8
N_{5-2}	6	7	4	3	2	3	1284.5	W_{5-2}	6	7	4	9	2	2	1272.3
N_{5-3}	6	7	4	2	1	2	1299.3	W_{5-3}	6	7	4	9	2	2	1311.9
N_{5-4}	6	7	4	4	2	3	1313.1	W_{5-4}	6	7	4	8	2	3	1305.2
N_{5-5}	6	7	4	6	2	3	1265.2	W_{5-5}	6	7	4	6	2	4	1412.2
Avg.							1324.7	Avg.							1389.1

APPENDIX F

AR I Result for Miami

Table F.1: AR Results I – Step 1 – Miami

Unit	v_1	v_2	v_3	v_4	v_5	v_6	[kWh]	Gene. [-]	Simu. [-]
S_{3-3}	6	5	1	9	5	6	1714.4	20	400
E_{3-3}	6	3	2	9	4	3	2231.1	12	240
N_{3-3}	1	7	1	4	5	3	2021.3	11	220
W_{3-3}	4	2	1	5	8	4	1999.2	20	400
	4	5	1	-	-	-			
Avg.							1991.5	15.8	315
Sum.								66	1260

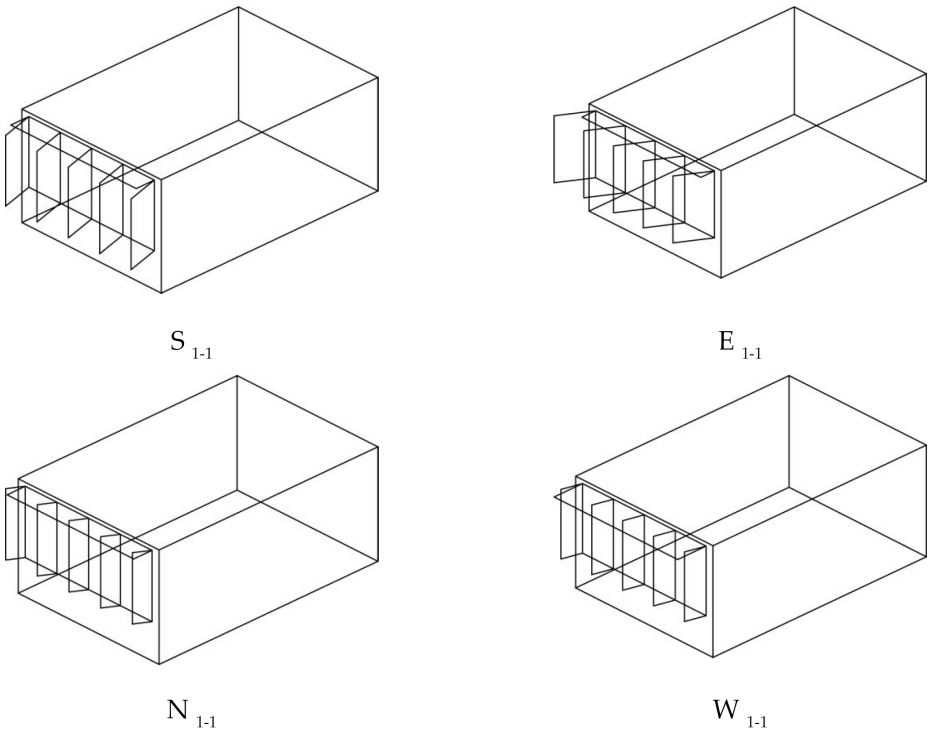

Figure F.1: AR Results I – Step 1 – Miami

Table F.2: AR Results I – Step 2 – South façade – Miami

Unit	v_1	v_2	v_3	v_4	v_5	v_6	Q_{total} [kWh]	Gene. [-]	Simu. [-]
S_{1-1}	4	5	1	9	8	6	1725.6	14	280
S_{1-3}	4	5	1	9	4	6	1722.9	11	220
S_{1-5}	4	5	1	8	10	7	1662.0	13	260
S_{3-1}	4	5	1	6	8	4	1663.7	12	240
S_{3-3}	4	5	1	7	10	4	1722.6	17	340
S_{3-5}	4	5	1	9	9	8	1675.3	11	220
S_{5-1}	4	5	1	6	10	4	1688.1	11	220
S_{5-3}	4	5	1	9	4	6	1808.5	14	280
S_{5-5}	4	5	1	9	10	7	1746.0	18	360
Avg.							1712.8	13.4	268.9
Sum.								121	2420

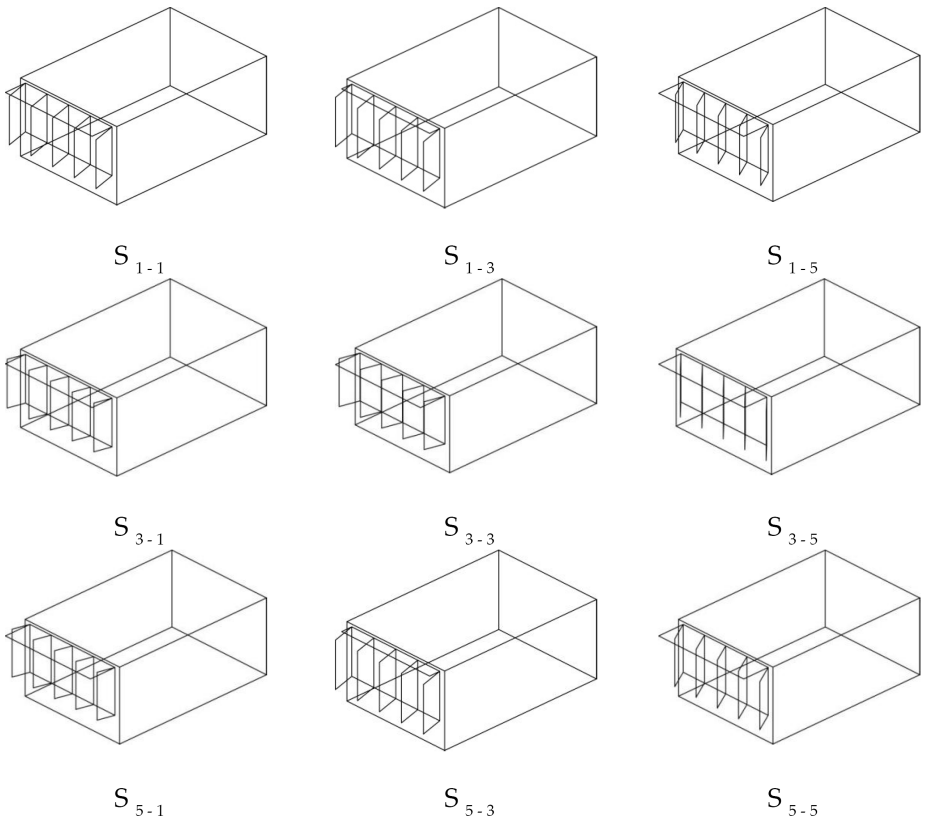

Figure F.2: AR Results I – Step 2 – South façade – Miami

Table F.3: AR Results I – Step 2 – East façade – Miami

Unit	v_1	v_2	v_3	v_4	v_5	v_6	Q_{total} [kWh]	Gene. [-]	Simu. [-]
E_{1-1}	4	5	1	5	1	2	1748.7	16	320
E_{1-3}	4	5	1	4	6	3	2209.3	12	240
E_{1-5}	4	5	1	4	3	7	1602.4	19	380
E_{3-1}	4	5	1	4	2	3	1752.9	18	360
E_{3-3}	4	5	1	5	3	2	2189.6	18	360
E_{3-5}	4	5	1	8	4	7	1571.5	12	240
E_{5-1}	4	5	1	8	8	3	1730.1	11	220
E_{5-3}	4	5	1	1	7	9	2079.8	16	320
E_{5-5}	4	5	1	1	7	9	1513.7	14	280
Avg.							1822.0	15.1	302.2
Sum.								136	2720

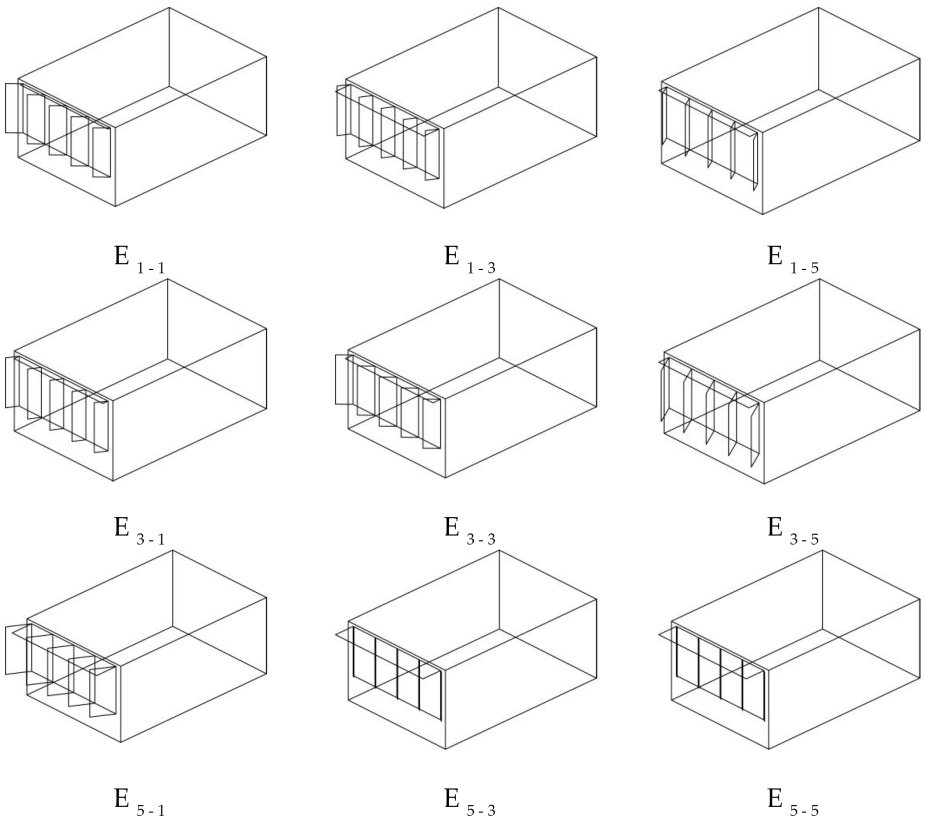

Figure F.3: AR Results I – Step 2 – East façade – Miami

Table F.4: AR Results I – Step 2 – North façade – Miami

Unit	v_1	v_2	v_3	v_4	v_5	v_6	Q_{total} [kWh]	Gene. [-]	Simu. [-]
N_{1-1}	4	5	1	8	1	3	2020.7	18	360
N_{1-3}	4	5	1	8	2	3	2090.3	15	300
N_{1-5}	4	5	1	2	2	6	1732.3	13	260
N_{3-1}	4	5	1	8	2	3	1985.0	17	340
N_{3-3}	4	5	1	4	1	3	1915.9	15	300
N_{3-5}	4	5	1	2	1	3	1626.4	15	300
N_{5-1}	4	5	1	4	4	6	2076.9	16	320
N_{5-3}	4	5	1	2	3	7	1917.6	12	240
N_{5-5}	4	5	1	1	6	7	1583.5	15	300
Avg.							1883.2	15.1	302.2
Sum.								136	2720

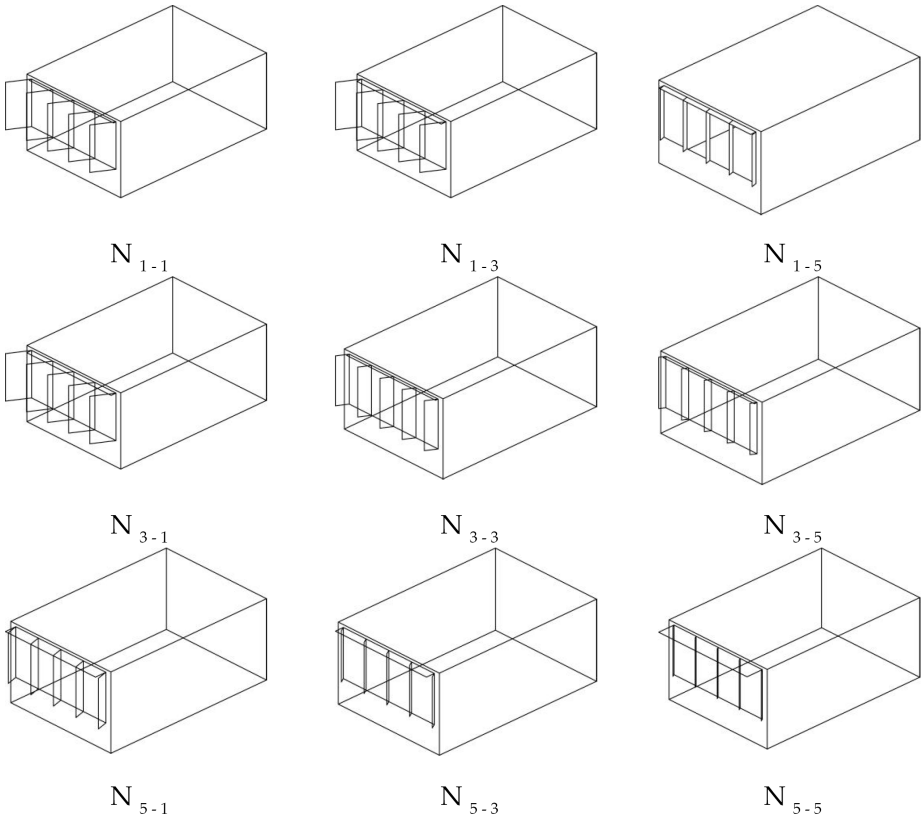

Figure F.4: AR Results I – Step 2 – North façade – Miami

Table F.5: AR Results I – Step 2 – West façade – Miami

Unit	v_1	v_2	v_3	v_4	v_5	v_6	Q_{total} [kWh]	Gene. [-]	Simu. [-]
W_{1-1}	5	4	1	1	7	8	1654.4	23	460
W_{1-3}	5	4	1	2	2	2	1578.2	13	260
W_{1-5}	5	4	1	3	4	1	1619.9	18	360
W_{3-1}	5	4	1	9	1	2	1709.3	20	400
W_{3-3}	5	4	1	1	5	3	1596.4	12	240
W_{3-5}	5	4	1	2	5	2	1627.0	27	540
W_{5-1}	5	4	1	9	2	2	1631.5	23	460
W_{5-3}	5	4	1	4	5	2	1545.1	14	280
W_{5-5}	5	4	1	2	3	2	1659.3	14	280
Avg.							1624.6	18.2	364.4
Sum.								164	3280

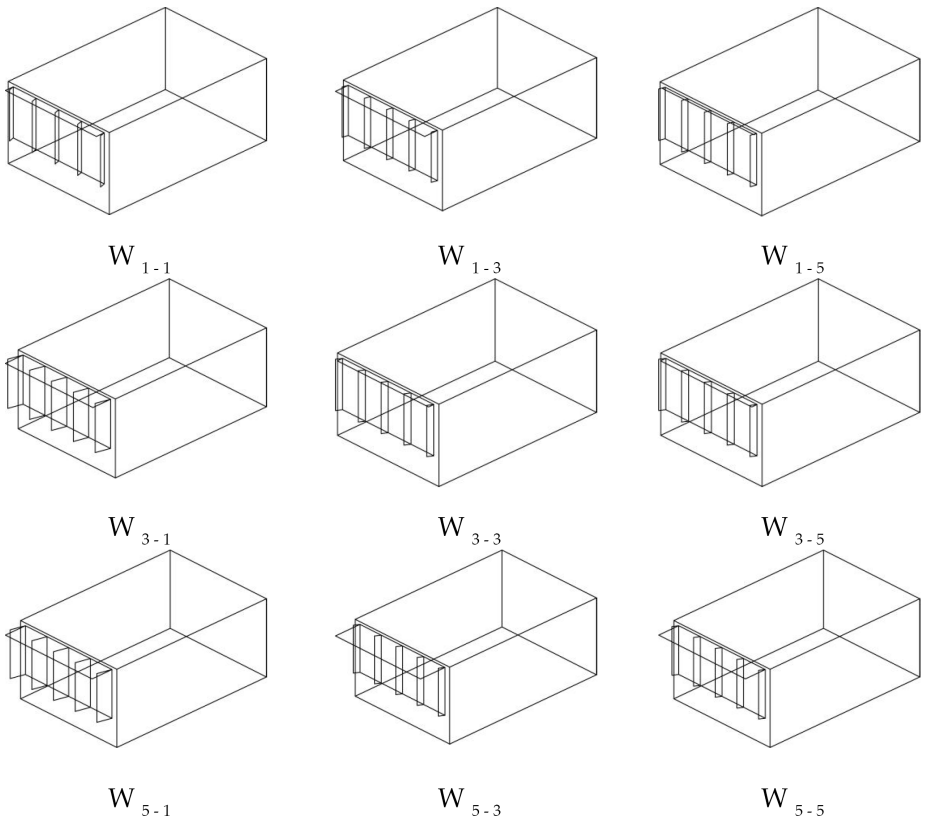

Figure F.5: AR Results I – Step 2 – West façade – Miami

Table F.6: AR Results I – Step 3 - Miami

	v_1	v_2	v_3	v_4	v_5	v_6	[kWh]		v_1	v_2	v_3	v_4	v_5	v_6	[kWh]
S_{1-1}	4	5	1	9	8	6	1725.6	E_{1-1}	4	5	1	5	1	2	1748.7
S_{1-2}	4	5	1	9	6	6	1682.9	E_{1-2}	4	5	1	5	4	3	2084.4
S_{1-3}	4	5	1	9	4	6	1722.9	E_{1-3}	4	5	1	4	6	3	2209.3
S_{1-4}	4	5	1	9	7	7	1655.5	E_{1-4}	4	5	1	4	5	5	2170.8
S_{1-5}	4	5	1	8	10	7	1662.0	E_{1-5}	4	5	1	4	3	7	1602.4
S_{3-1}	4	5	1	6	8	4	1663.7	E_{3-1}	4	5	1	4	2	3	1752.9
S_{3-2}	4	5	1	7	9	4	1944.8	E_{3-2}	4	5	1	5	3	3	2113.1
S_{3-3}	4	5	1	7	10	4	1722.6	E_{3-3}	4	5	1	5	3	2	2189.6
S_{3-4}	4	5	1	8	10	6	1796.8	E_{3-4}	4	5	1	7	4	5	2146.3
S_{3-5}	4	5	1	9	9	8	1675.3	E_{3-5}	4	5	1	8	4	7	1571.5
S_{5-1}	4	5	1	6	10	4	1688.1	E_{5-1}	4	5	1	8	8	3	1730.1
S_{5-2}	4	5	1	8	7	5	1908.0	E_{5-2}	4	5	1	5	8	6	1992.6
S_{5-3}	4	5	1	9	4	6	1808.5	E_{5-3}	4	5	1	1	7	9	2079.8
S_{5-4}	4	5	1	9	7	7	1642.2	E_{5-4}	4	5	1	1	7	9	2111.5
S_{5-5}	4	5	1	9	10	7	1746.0	E_{5-5}	4	5	1	1	7	9	1513.7
Avg.							1736.3	Avg.							1934.5
N_{1-1}	4	5	1	8	1	3	2020.7	W_{1-1}	4	5	1	2	3	6	2024.0
N_{1-2}	4	5	1	8	2	3	2028.5	W_{1-2}	4	5	1	2	4	5	1895.0
N_{1-3}	4	5	1	8	2	3	2090.3	W_{1-3}	4	5	1	2	5	4	2021.3
N_{1-4}	4	5	1	5	2	5	2025.6	W_{1-4}	4	5	1	2	3	4	1955.0
N_{1-5}	4	5	1	2	2	6	1732.3	W_{1-5}	4	5	1	2	1	4	2032.5
N_{3-1}	4	5	1	8	2	3	1985.0	W_{3-1}	4	5	1	5	7	4	1971.8
N_{3-2}	4	5	1	6	2	3	1765.8	W_{3-2}	4	5	1	4	5	4	1938.4
N_{3-3}	4	5	1	4	1	3	1915.9	W_{3-3}	4	5	1	2	2	3	1914.1
N_{3-4}	4	5	1	3	1	3	1622.4	W_{3-4}	4	5	1	2	2	3	1616.8
N_{3-5}	4	5	1	2	1	3	1626.4	W_{3-5}	4	5	1	2	2	3	1783.7
N_{5-1}	4	5	1	4	4	6	2076.9	W_{5-1}	4	5	1	5	8	4	1931.3
N_{5-2}	4	5	1	3	4	7	1566.6	W_{5-2}	4	5	1	4	9	4	1975.8
N_{5-3}	4	5	1	2	3	7	1917.6	W_{5-3}	4	5	1	2	10	3	1918.8
N_{5-4}	4	5	1	2	5	7	1888.5	W_{5-4}	4	5	1	2	9	3	1696.2
N_{5-5}	4	5	1	1	6	7	1895.0	W_{5-5}	4	5	1	2	8	3	1797.3
Avg.							1877.2	Avg.							1898.1

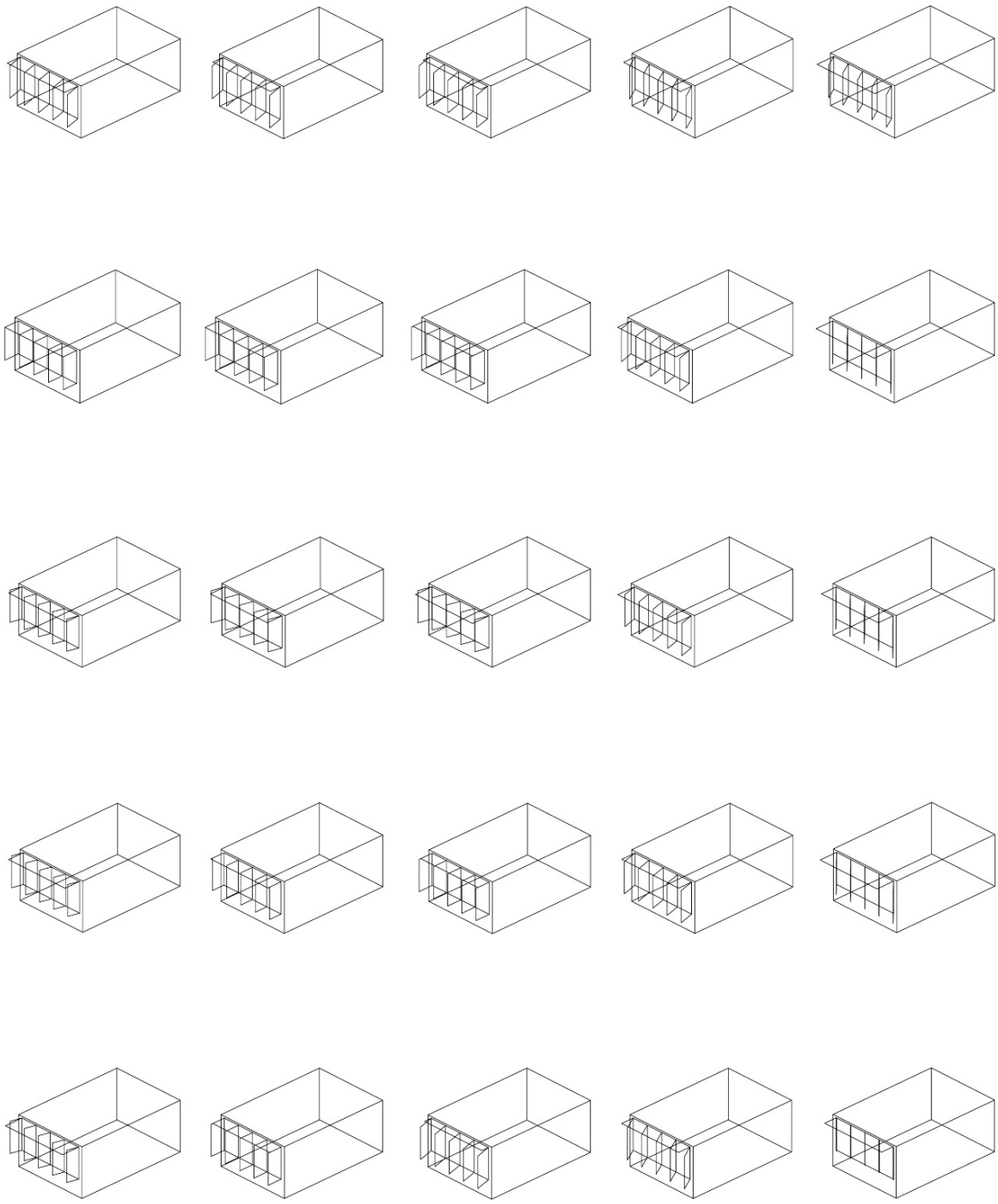

Figure F.6: AR Results I – South façade – Miami

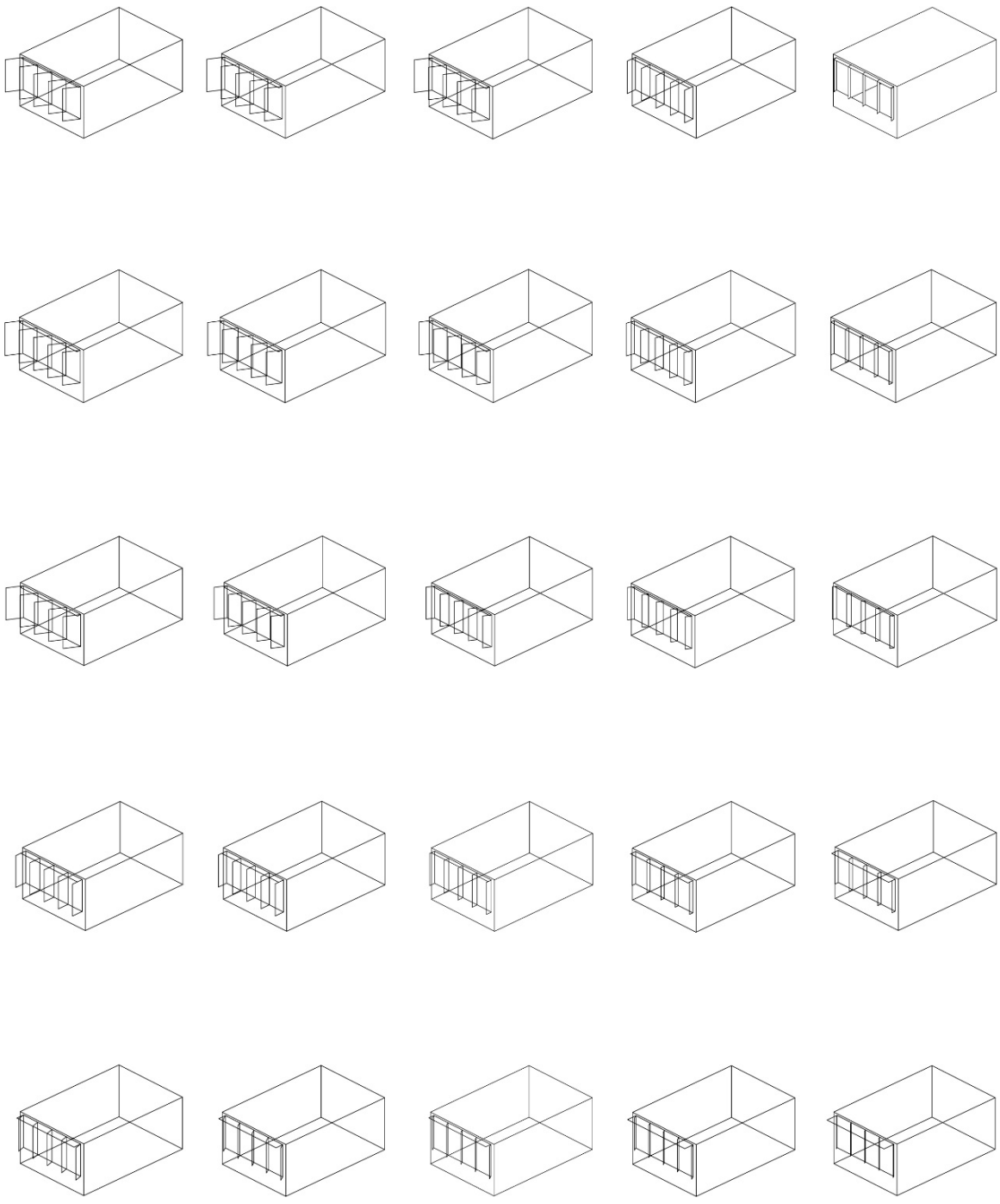

Figure F.7: AR Results I – East façade – Miami

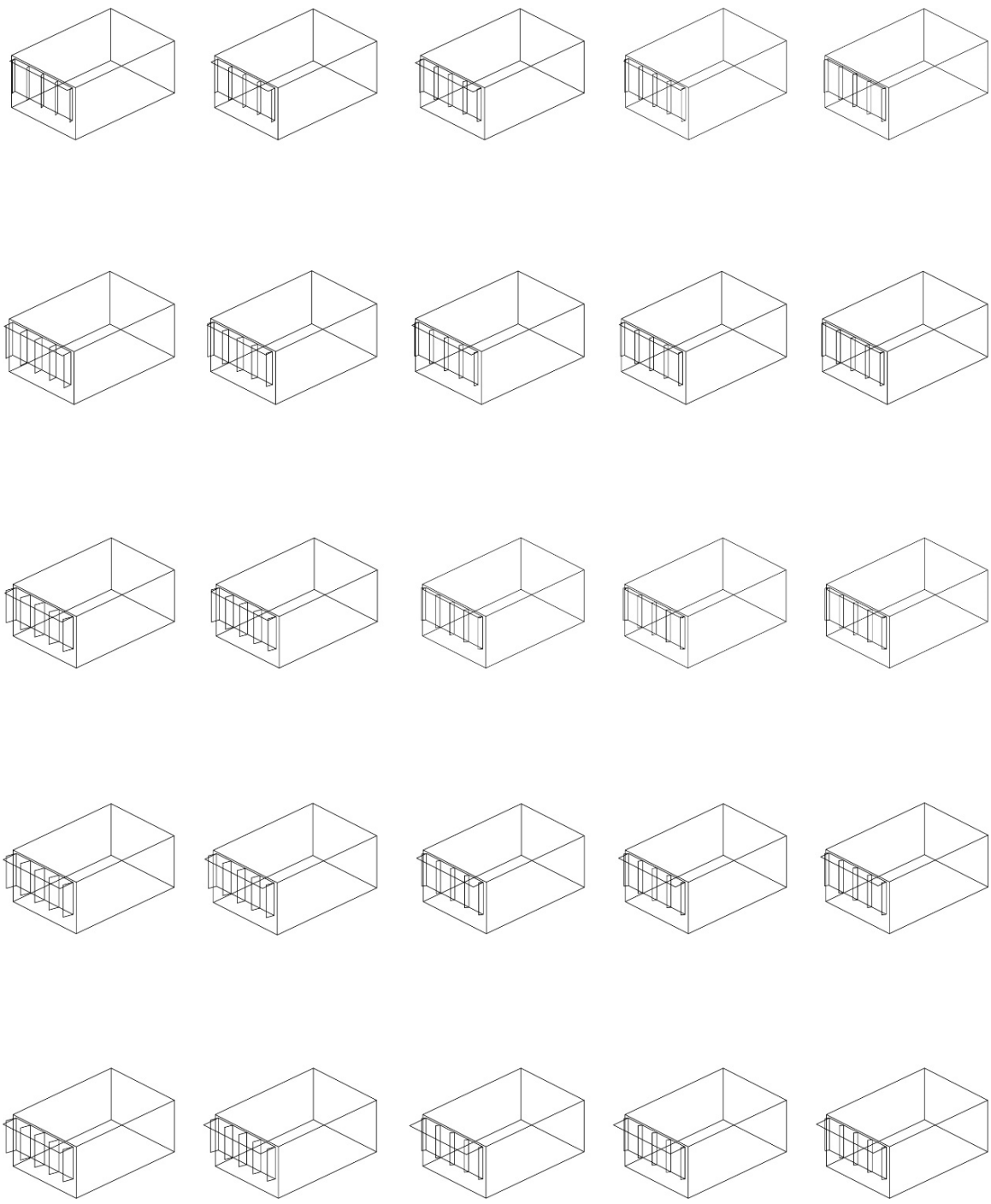

Figure F.8: AR Results I – North façade – Miami

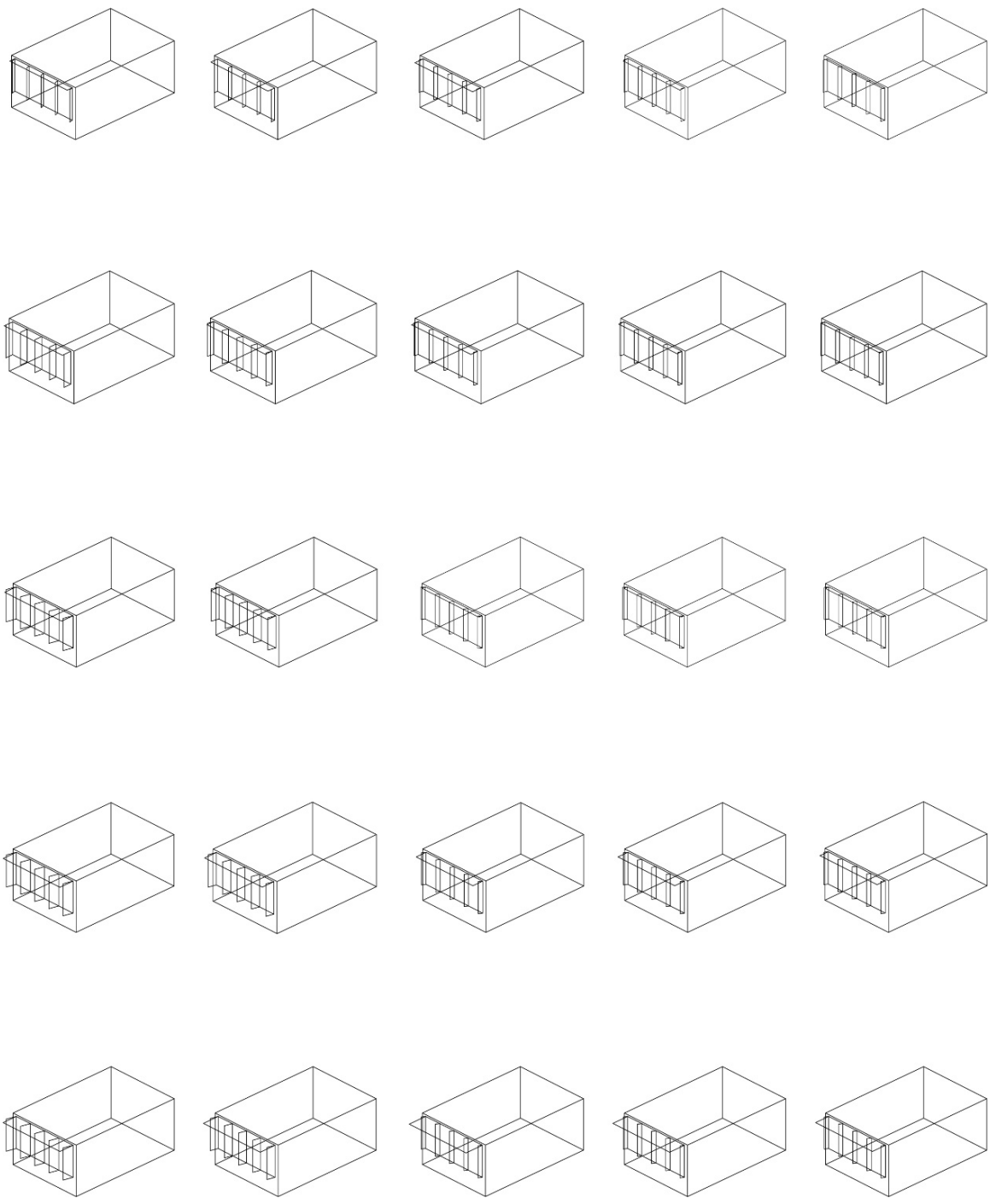

Figure F.9: AR Results I – West façade – Miami

Table F.7: AR Results I – Step 4 - Miami

	v_1	v_2	v_3	v_4	v_5	v_6	[kWh]		v_1	v_2	v_3	v_4	v_5	v_6	[kWh]
S_{1-1}	4	5	1	9	8	6	1725.6	E_{1-1}	4	5	1	5	1	2	1748.7
S_{1-2}	4	5	1	9	6	6	1682.9	E_{1-2}	4	5	1	5	4	3	2084.4
S_{1-3}	4	5	1	9	4	6	1722.9	E_{1-3}	4	5	1	4	6	3	2209.3
S_{1-4}	4	5	1	9	7	7	1655.5	E_{1-4}	4	5	1	4	5	5	2170.8
S_{1-5}	4	5	1	8	10	7	1662.0	E_{1-5}	4	5	1	4	3	7	1602.4
S_{2-1}	4	5	1	8	8	5	1779.0	E_{2-1}	4	5	1	5	2	3	2049.8
S_{2-2}	4	5	1	8	8	5	1733.5	E_{2-2}	4	5	1	5	3	3	2018.1
S_{2-3}	4	5	1	8	7	5	1698.5	E_{2-3}	4	5	1	5	5	3	2073.1
S_{2-4}	4	5	1	8	8	6	1696.5	E_{2-4}	4	5	1	5	4	5	2119.5
S_{2-5}	4	5	1	9	10	8	1742.3	E_{2-5}	4	5	1	6	4	7	1732.7
S_{3-1}	4	5	1	6	8	4	1663.7	E_{3-1}	4	5	1	4	2	3	1752.9
S_{3-2}	4	5	1	7	9	4	1944.8	E_{3-2}	4	5	1	5	3	3	2113.1
S_{3-3}	4	5	1	7	10	4	1722.6	E_{3-3}	4	5	1	5	3	2	2189.6
S_{3-4}	4	5	1	8	10	6	1796.8	E_{3-4}	4	5	1	7	4	5	2146.3
S_{3-5}	4	5	1	9	9	8	1675.3	E_{3-5}	4	5	1	8	4	7	1571.5
S_{4-1}	4	5	1	6	9	4	1859.7	E_{4-1}	4	5	1	6	5	3	2072.5
S_{4-2}	4	5	1	7	8	5	1912.0	E_{4-2}	4	5	1	5	5	4	1933.4
S_{4-3}	4	5	1	8	7	5	1869.6	E_{4-3}	4	5	1	3	5	6	2092.7
S_{4-4}	4	5	1	9	8	6	1709.1	E_{4-4}	4	5	1	4	5	7	2025.4
S_{4-5}	4	5	1	9	10	8	1849.0	E_{4-5}	4	5	1	5	6	8	1731.1
S_{5-1}	4	5	1	6	10	4	1688.1	E_{5-1}	4	5	1	8	8	3	1797.8
S_{5-2}	4	5	1	8	7	5	1908.0	E_{5-2}	4	5	1	5	8	6	1730.1
S_{5-3}	4	5	1	9	4	6	1808.5	E_{5-3}	4	5	1	1	7	9	2079.8
S_{5-4}	4	5	1	9	7	7	1642.2	E_{5-4}	4	5	1	1	7	9	2111.5
S_{5-5}	4	5	1	9	10	7	1746.0	E_{5-5}	4	5	1	1	7	9	1513.7
Avg.							1755.8	Avg.							1946.8
N_{1-1}	4	5	1	8	1	3	2020.7	W_{1-1}	4	5	1	2	3	6	2024.0
N_{1-2}	4	5	1	8	2	3	2028.5	W_{1-2}	4	5	1	2	4	5	1895.0
N_{1-3}	4	5	1	8	2	3	2090.3	W_{1-3}	4	5	1	2	5	4	2021.3
N_{1-4}	4	5	1	5	2	5	2025.6	W_{1-4}	4	5	1	2	3	4	1955.0
N_{1-5}	4	5	1	2	2	6	1732.3	W_{1-5}	4	5	1	2	1	4	2032.5
N_{2-1}	4	5	1	8	2	3	1851.0	W_{2-1}	4	5	1	4	5	5	1908.6
N_{2-2}	4	5	1	7	2	3	2006.9	W_{2-2}	4	5	1	3	4	4	1804.4
N_{2-3}	4	5	1	6	2	3	1797.0	W_{2-3}	4	5	1	2	4	4	1755.4
N_{2-4}	4	5	1	4	2	4	1901.1	W_{2-4}	4	5	1	2	3	4	1748.9
N_{2-5}	4	5	1	2	2	5	1864.2	W_{2-5}	4	5	1	2	2	4	1697.8
N_{3-1}	4	5	1	8	2	3	1985.0	W_{3-1}	4	5	1	5	7	4	1971.8
N_{3-2}	4	5	1	6	2	3	1765.8	W_{3-2}	4	5	1	4	5	4	1938.4
N_{3-3}	4	5	1	4	1	3	1915.9	W_{3-3}	4	5	1	2	2	3	1914.1
N_{3-4}	4	5	1	3	1	3	1622.4	W_{3-4}	4	5	1	2	2	3	1616.8

	v_1	v_2	v_3	v_4	v_5	v_6	[kWh]		v_1	v_2	v_3	v_4	v_5	v_6	[kWh]
N_{3-5}	4	5	1	2	1	3	1626.4	W_{3-5}	4	5	1	2	2	3	1783.7
N_{4-1}	4	5	1	6	3	5	1891.8	W_{4-1}	4	5	1	5	8	4	1740.0
N_{4-2}	4	5	1	5	3	5	2068.0	W_{4-2}	4	5	1	4	7	4	1896.2
N_{4-3}	4	5	1	3	2	5	2055.7	W_{4-3}	4	5	1	2	6	3	1603.3
N_{4-4}	4	5	1	2	3	5	1552.8	W_{4-4}	4	5	1	2	6	3	1579.7
N_{4-5}	4	5	1	2	4	5	1876.2	W_{4-5}	4	5	1	2	5	3	1677.6
N_{5-1}	4	5	1	4	4	6	2076.9	W_{5-1}	4	5	1	5	8	4	1931.3
N_{5-2}	4	5	1	3	4	7	1566.6	W_{5-2}	4	5	1	4	9	4	1975.8
N_{5-3}	4	5	1	2	3	7	1917.6	W_{5-3}	4	5	1	2	10	3	1918.8
N_{5-4}	4	5	1	2	5	7	1888.5	W_{5-4}	4	5	1	2	9	3	1696.2
N_{5-5}	4	5	1	1	6	7	1895.0	W_{5-5}	4	5	1	2	8	3	1797.3
Avg.							1880.9	Avg.							1835.4

APPENDIX G

AR II Result for Miami

Table G.1: AR Results II – Step 1 – Miami

Unit	v_1	v_2	v_3	v_4	v_5	v_6	[kWh]	Gene. [-]	Simu. [-]
S_{3-3}	4	7	2	8	5	6	1750.1	20	400
E_{3-3}	4	1	2	9	1	3	2170.6	18	360
N_{3-3}	6	4	1	1	1	8	2121.8	14	280
W_{3-3}	6	3	1	3	2	4	1934.3	20	400
	5	4	1	-	-	-			
Avg.							1994.2	18	360
Sum.								72	1440

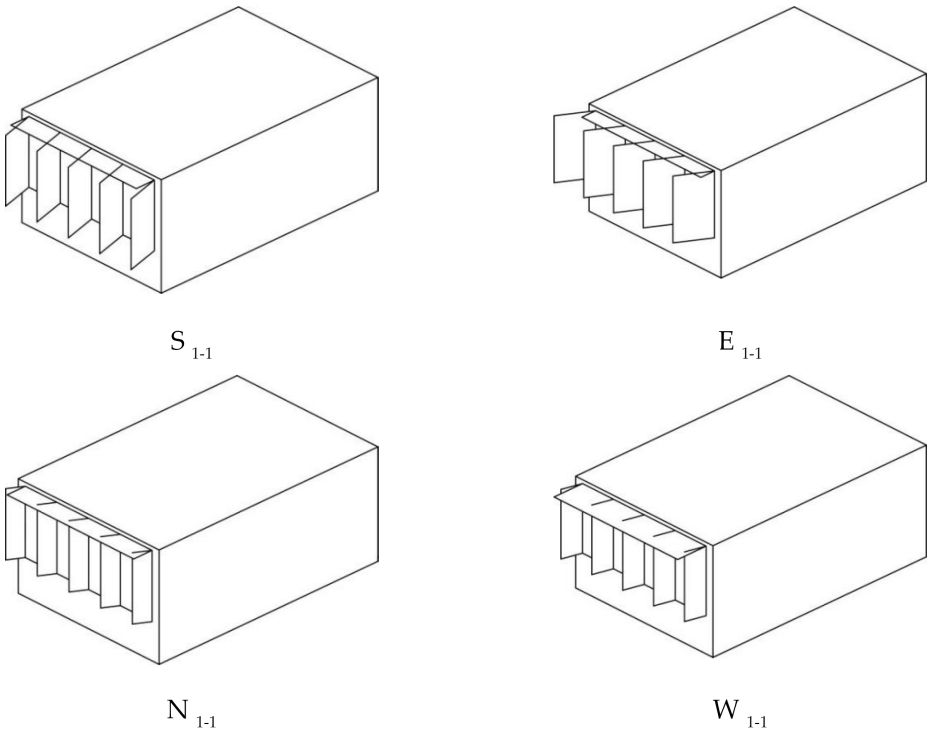

Figure G.1: AR Results II – Step 1 – Miami

Table G.2: AR Results II – Step 2 – South façade – Miami

Unit	v_1	v_2	v_3	v_4	v_5	v_6	Q_{total} [kWh]	Gene. [-]	Simu. [-]
S_{1-1}	5	4	1	10	10	6	1645.3	18	360
S_{1-3}	5	4	1	9	8	7	1594.4	15	300
S_{1-5}	5	4	1	9	10	6	1606.9	24	480
S_{3-1}	5	4	1	9	10	7	1706.1	11	220
S_{3-3}	5	4	1	9	8	7	1564.4	20	400
S_{3-5}	5	4	1	8	10	9	1629.8	19	380
S_{5-1}	5	4	1	6	10	4	1851.7	12	240
S_{5-3}	5	4	1	9	10	7	1564.2	23	460
S_{5-5}	5	4	1	8	9	9	1628.0	14	280
Avg.							1643.4	17.3	346.7
Sum.								156	3120

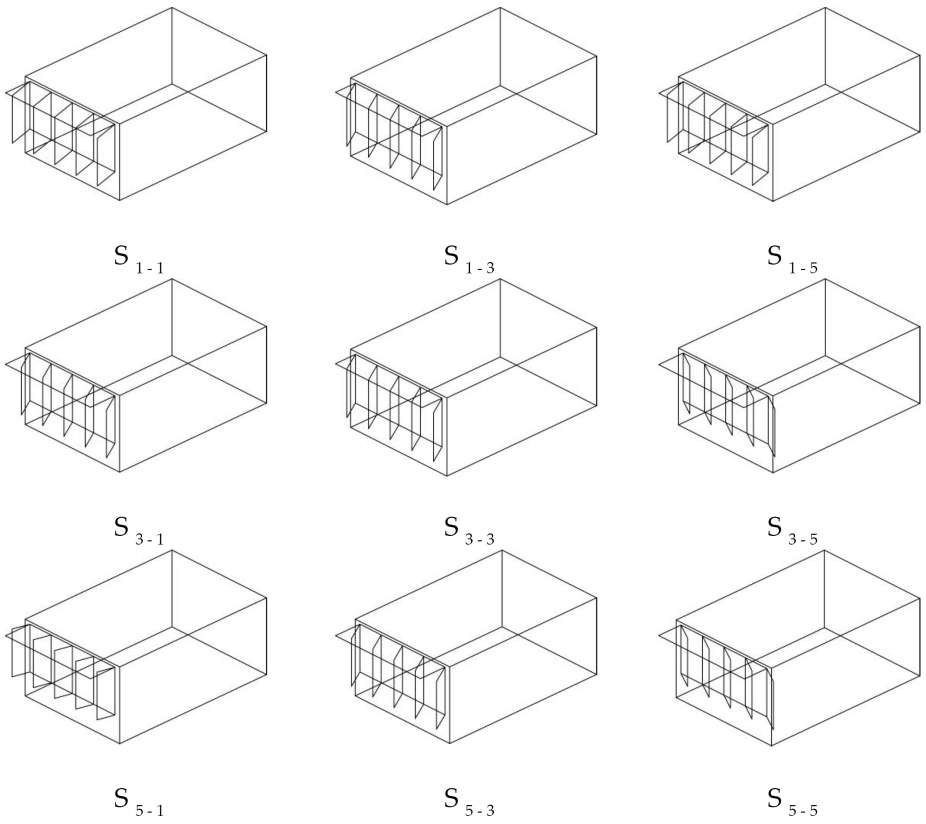

Figure G.2: AR Results II – Step 2 – South façade – Miami

Table G.3: AR Results II – Step 2 – East façade – Miami

Unit	v_1	v_2	v_3	v_4	v_5	v_6	Q_{total} [kWh]	Gene. [-]	Simu. [-]
E_{1-1}	5	4	1	10	10	2	1543	18	360
E_{1-3}	5	4	1	3	4	7	1782.1	27	540
E_{1-5}	5	4	1	4	10	7	1439.2	19	380
E_{3-1}	5	4	1	1	10	8	1618.1	21	420
E_{3-3}	5	4	1	7	3	3	1766.1	22	440
E_{3-5}	5	4	1	3	10	7	1458.5	22	440
E_{5-1}	5	4	1	1	10	8	1626.4	23	460
E_{5-3}	5	4	1	3	4	7	1808.6	19	380
E_{5-5}	5	4	1	3	10	7	1479.5	18	360
Avg.							1613.5	21	420
Sum.								189	3780

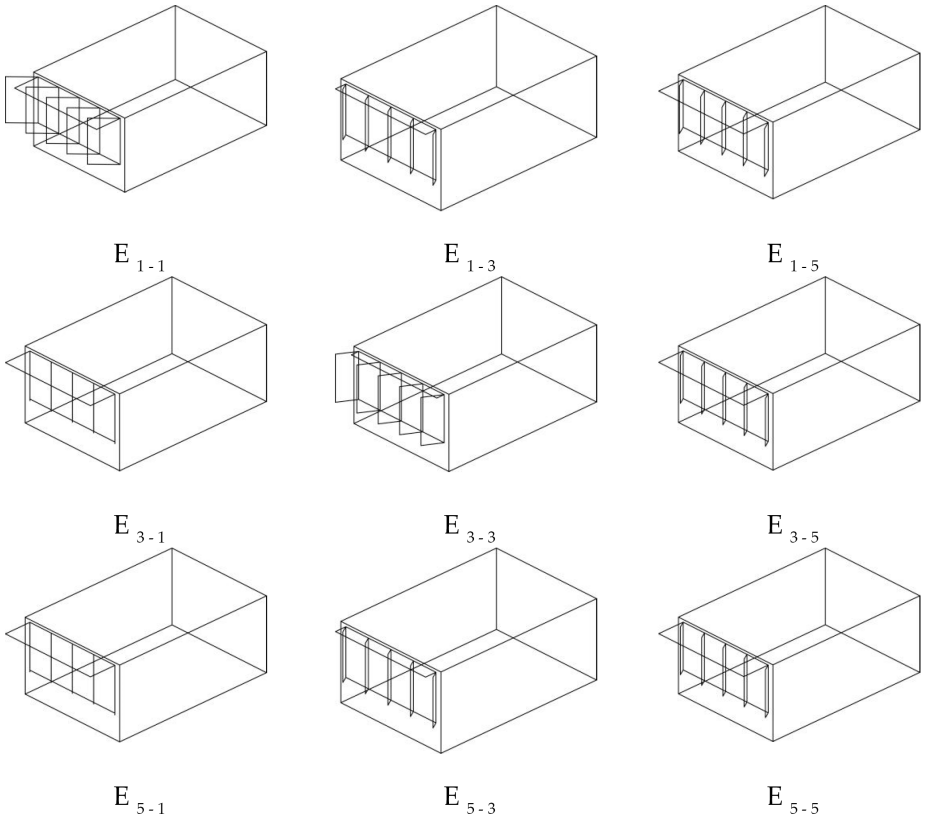

Figure G.3: AR Results II – Step 2 – East façade – Miami

Table G.4: AR Results II – Step 2 – North façade – Miami

Unit	v_1	v_2	v_3	v_4	v_5	v_6	Q_{total} [kWh]	Gene. [-]	Simu. [-]
N_{1-1}	5	4	1	1	1	8	1726.4	20	400
N_{1-3}	5	4	1	3	1	1	1595.3	20	400
N_{1-5}	5	4	1	6	7	7	1482.6	16	320
N_{3-1}	5	4	1	2	5	8	1692.6	10	200
N_{3-3}	5	4	1	2	5	2	1520.5	16	320
N_{3-5}	5	4	1	6	5	8	1482.4	18	360
N_{5-1}	5	4	1	3	5	7	1632.4	21	420
N_{5-3}	5	4	1	2	1	2	1449.4	22	440
N_{5-5}	5	4	1	6	6	8	1476.2	13	260
Avg.							1562.0	17.3	346.7
Sum.								156	3120

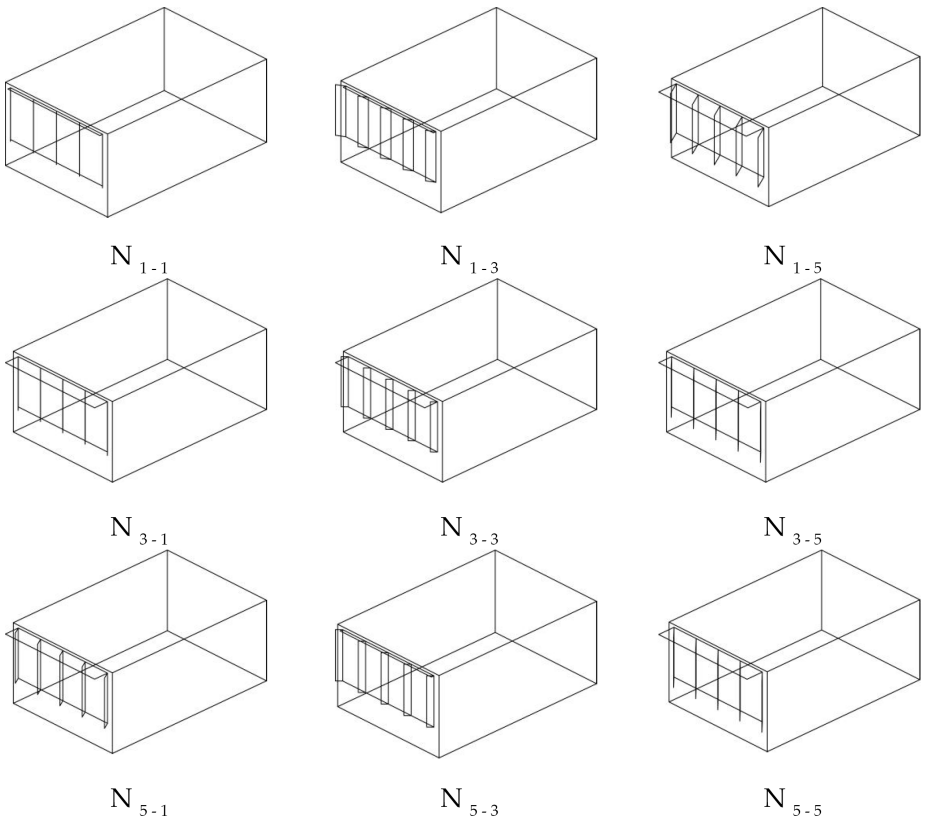

Figure G.4: AR Results II – Step 2 – North façade – Miami

Table G.5: AR Results II – Step 2 – West façade – Miami

Unit	v_1	v_2	v_3	v_4	v_5	v_6	Q_{total} [kWh]	Gene. [-]	Simu. [-]
W_{1-1}	5	4	1	1	7	8	1654.4	23	460
W_{1-3}	5	4	1	2	2	2	1578.2	13	260
W_{1-5}	5	4	1	3	4	1	1619.9	18	360
W_{3-1}	5	4	1	9	1	2	1709.3	20	400
W_{3-3}	5	4	1	1	5	3	1596.4	12	240
W_{3-5}	5	4	1	2	5	2	1627.0	27	540
W_{5-1}	5	4	1	9	2	2	1631.5	23	460
W_{5-3}	5	4	1	4	5	2	1545.1	14	280
W_{5-5}	5	4	1	2	3	2	1659.3	14	280
Avg.							1624.6	18.2	364.4
Sum.								164	3280

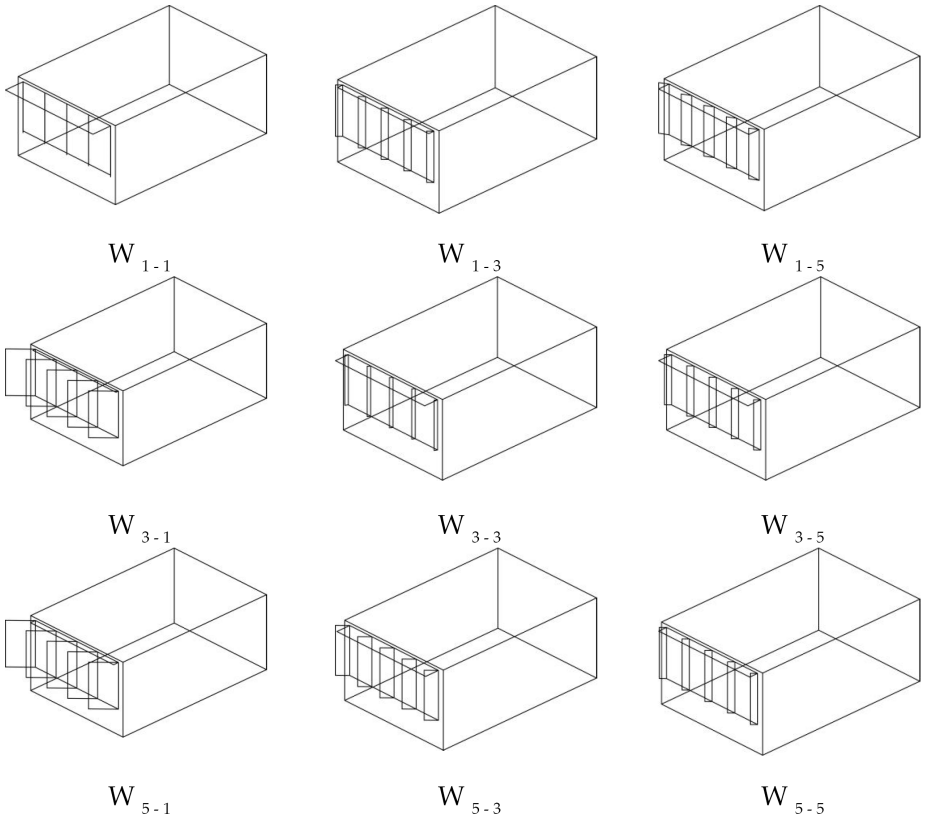

Figure G.5: AR Results II – Step 2 – West façade – Miami

Table G.6: AR Results II – Step 3 - Miami

	v_1	v_2	v_3	v_4	v_5	v_6	[kWh]		v_1	v_2	v_3	v_4	v_5	v_6	[kWh]
S_{1-1}	5	4	1	10	10	6	1645.3	E_{1-1}	5	4	1	10	10	2	1543.0
S_{1-2}	5	4	1	10	9	7	1670.9	E_{1-2}	5	4	1	7	7	5	2183.8
S_{1-3}	5	4	1	9	8	7	1594.4	E_{1-3}	5	4	1	3	4	7	1782.1
S_{1-4}	5	4	1	9	9	7	1660.8	E_{1-4}	5	4	1	4	7	7	1909.3
S_{1-5}	5	4	1	9	10	6	1606.9	E_{1-5}	5	4	1	4	10	7	1439.2
S_{3-1}	5	4	1	9	10	7	1706.1	E_{3-1}	5	4	1	1	10	8	1618.1
S_{3-2}	5	4	1	9	9	7	1604.7	E_{3-2}	5	4	1	4	7	6	2207.6
S_{3-3}	5	4	1	9	8	7	1564.4	E_{3-3}	5	4	1	7	3	3	1766.1
S_{3-4}	5	4	1	9	9	8	2006.0	E_{3-4}	5	4	1	5	7	5	2238.7
S_{3-5}	5	4	1	8	10	9	1629.8	E_{3-5}	5	4	1	3	10	7	1458.5
S_{5-1}	5	4	1	6	10	4	1851.7	E_{5-1}	5	4	1	1	10	8	1626.4
S_{5-2}	5	4	1	8	10	6	1838.3	E_{5-2}	5	4	1	2	7	8	1755.1
S_{5-3}	5	4	1	9	10	7	1564.2	E_{5-3}	5	4	1	3	4	7	1808.6
S_{5-4}	5	4	1	9	10	8	1934.0	E_{5-4}	5	4	1	3	7	7	1798.7
S_{5-5}	5	4	1	8	9	9	1628.0	E_{5-5}	5	4	1	3	10	7	1479.5
Avg.							1700.4	Avg.							1774.3
N_{1-1}	5	4	1	1	1	8	1726.4	W_{1-1}	5	4	1	1	7	8	1654.4
N_{1-2}	5	4	1	2	1	5	2123.0	W_{1-2}	5	4	1	2	5	5	1905.4
N_{1-3}	5	4	1	3	1	1	1595.3	W_{1-3}	5	4	1	2	2	2	1578.2
N_{1-4}	5	4	1	5	4	4	1998.3	W_{1-4}	5	4	1	3	3	2	2022.6
N_{1-5}	5	4	1	6	7	7	1482.6	W_{1-5}	5	4	1	3	4	1	1619.9
N_{3-1}	5	4	1	2	5	8	1692.6	W_{3-1}	5	4	1	9	1	2	1709.3
N_{3-2}	5	4	1	2	5	5	2114.9	W_{3-2}	5	4	1	5	3	3	1966.9
N_{3-3}	5	4	1	2	5	2	1520.5	W_{3-3}	5	4	1	1	5	3	1596.4
N_{3-4}	5	4	1	4	5	5	2052.5	W_{3-4}	5	4	1	2	5	3	1597.8
N_{3-5}	5	4	1	6	5	8	1482.4	W_{3-5}	5	4	1	2	5	2	1627.0
N_{5-1}	5	4	1	3	5	7	1632.4	W_{5-1}	5	4	1	9	2	2	1631.5
N_{5-2}	5	4	1	3	3	5	2054.7	W_{5-2}	5	4	1	7	4	2	1889.1
N_{5-3}	5	4	1	2	1	2	1449.4	W_{5-3}	5	4	1	4	5	2	1545.1
N_{5-4}	5	4	1	4	4	5	1985.3	W_{5-4}	5	4	1	3	4	2	1953.9
N_{5-5}	5	4	1	6	6	8	1476.2	W_{5-5}	5	4	1	2	3	2	1659.3
Avg.							1759.1	Avg.							1730.5

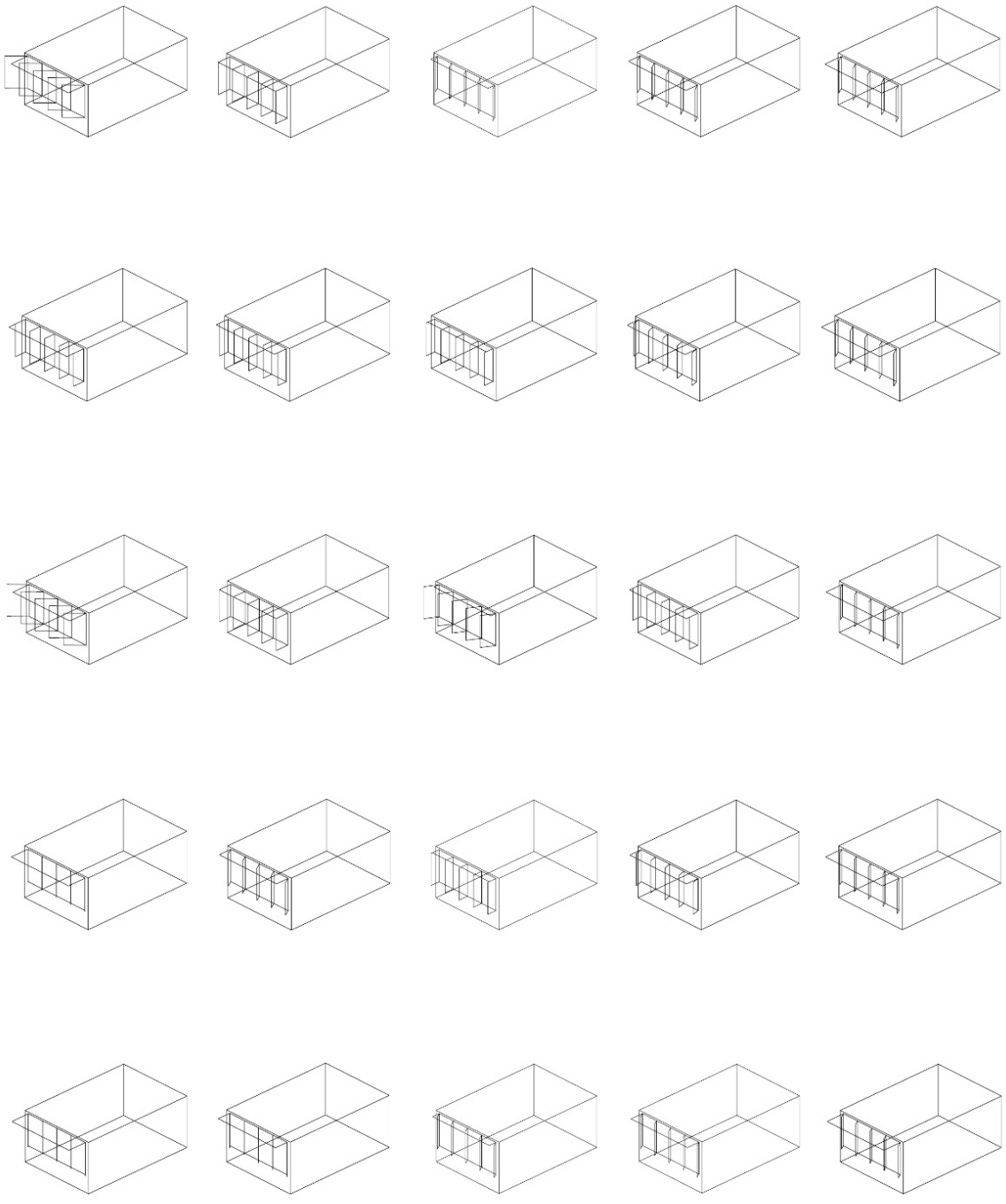

Figure G.6: AR Results II – South façade – Miami

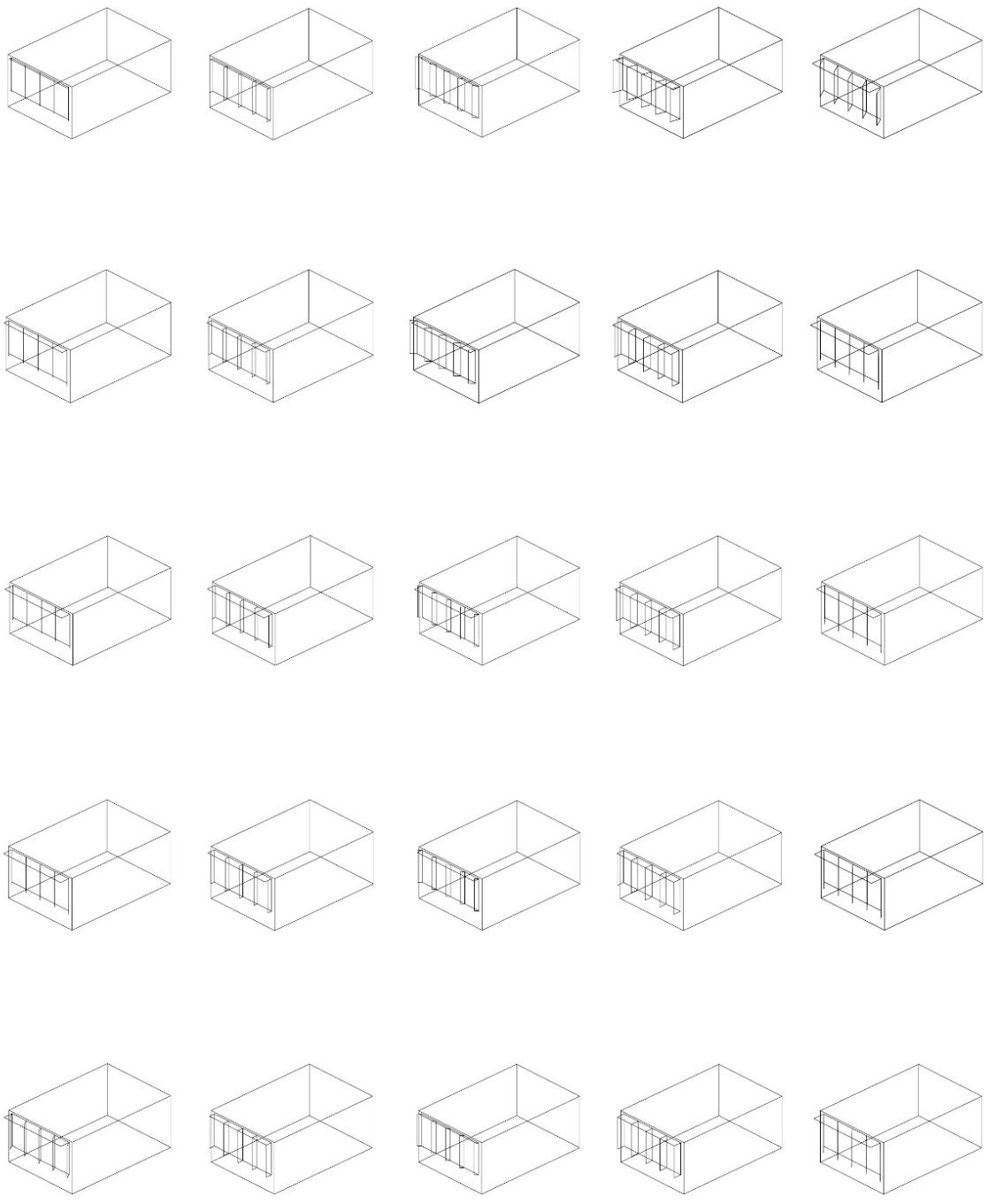

Figure G.7: AR Results II – East façade – Miami

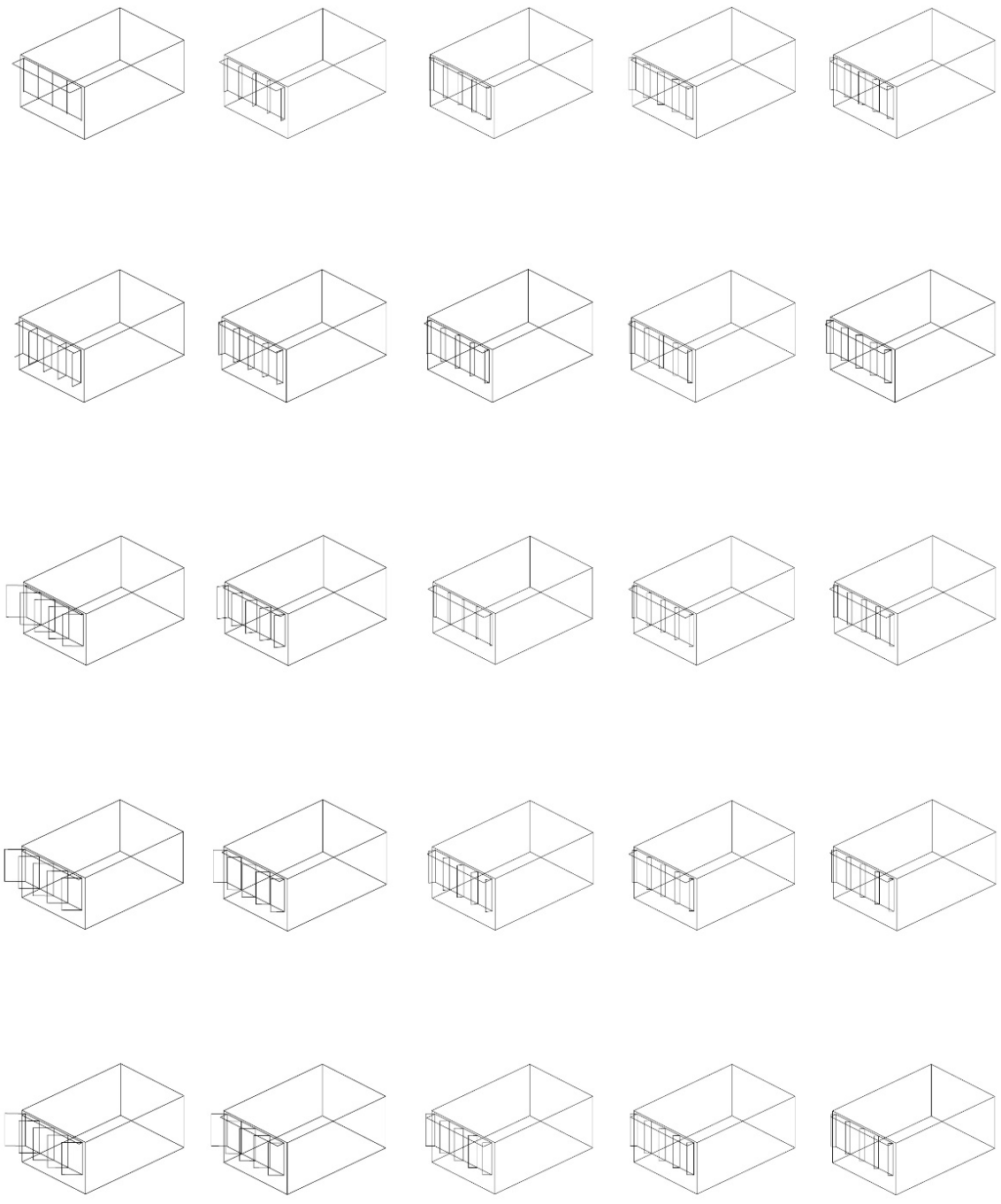

Figure G.8: AR Results II – North façade – Miami

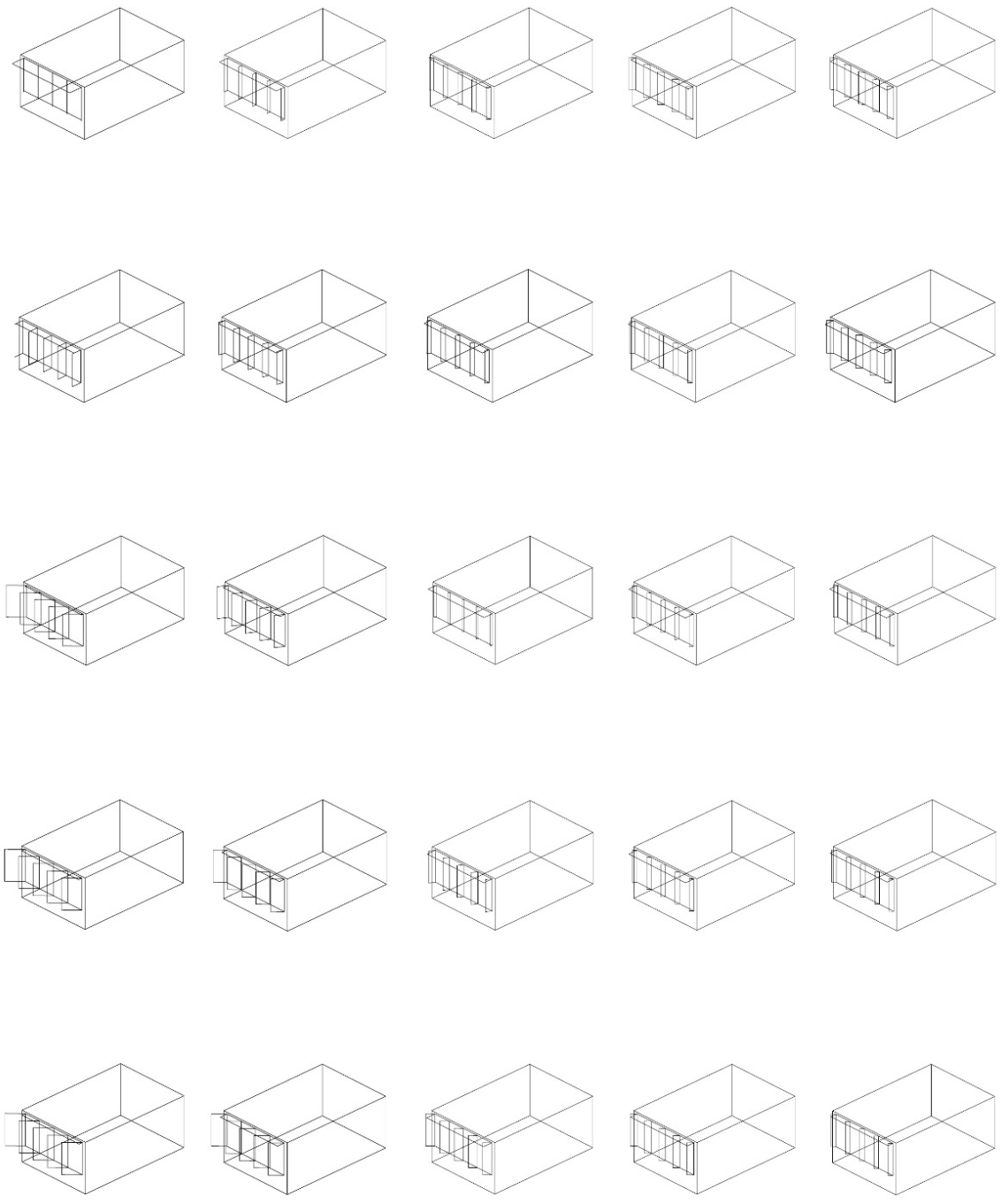

Figure G.9: AR Results II – West façade – Miami

Table G.7: AR Results II – Step 4 - Miami

	v_1	v_2	v_3	v_4	v_5	v_6	[kWh]		v_1	v_2	v_3	v_4	v_5	v_6	[kWh]
S_{1-1}	5	4	1	10	10	6	1645.3	E_{1-1}	5	4	1	10	10	2	1543.0
S_{1-2}	5	4	1	10	9	7	1670.9	E_{1-2}	5	4	1	7	7	5	2183.8
S_{1-3}	5	4	1	9	8	7	1594.4	E_{1-3}	5	4	1	3	4	7	1782.1
S_{1-4}	5	4	1	9	9	7	1660.8	E_{1-4}	5	4	1	4	7	7	1909.3
S_{1-5}	5	4	1	9	10	6	1606.9	E_{1-5}	5	4	1	4	10	7	1439.2
S_{2-1}	5	4	1	10	10	7	1689.1	E_{2-1}	5	4	1	6	10	5	1981.3
S_{2-2}	5	4	1	9	9	7	1563.5	E_{2-2}	5	4	1	5	7	5	2123.1
S_{2-3}	5	4	1	9	8	7	1533.1	E_{2-3}	5	4	1	5	4	5	2178.9
S_{2-4}	5	4	1	9	9	7	1586.7	E_{2-4}	5	4	1	4	7	6	2066.2
S_{2-5}	5	4	1	9	10	8	1755.2	E_{2-5}	5	4	1	4	10	7	1684.6
S_{3-1}	5	4	1	9	10	7	1706.1	E_{3-1}	5	4	1	1	10	8	1618.1
S_{3-2}	5	4	1	9	9	7	1604.7	E_{3-2}	5	4	1	4	7	6	2207.6
S_{3-3}	5	4	1	9	8	7	1564.4	E_{3-3}	5	4	1	7	3	3	1766.1
S_{3-4}	5	4	1	9	9	8	2006.0	E_{3-4}	5	4	1	5	7	5	2238.7
S_{3-5}	5	4	1	8	10	9	1629.8	E_{3-5}	5	4	1	3	10	7	1458.5
S_{4-1}	5	4	1	8	10	6	1839.8	E_{4-1}	5	4	1	1	10	8	1618.5
S_{4-2}	5	4	1	8	10	6	1821.4	E_{4-2}	5	4	1	3	7	7	1795.3
S_{4-3}	5	4	1	9	9	7	1569.1	E_{4-3}	5	4	1	5	4	5	2207.2
S_{4-4}	5	4	1	9	9	8	1972.9	E_{4-4}	5	4	1	4	7	6	2117.1
S_{4-5}	5	4	1	8	10	9	1638.8	E_{4-5}	5	4	1	3	10	7	1457.7
S_{5-1}	5	4	1	6	10	4	1851.7	E_{5-1}	5	4	1	1	10	8	1626.4
S_{5-2}	5	4	1	8	10	6	1838.3	E_{5-2}	5	4	1	2	7	8	1755.1
S_{5-3}	5	4	1	9	10	7	1564.2	E_{5-3}	5	4	1	3	4	7	1808.6
S_{5-4}	5	4	1	9	10	8	1934.0	E_{5-4}	5	4	1	3	7	7	1798.7
S_{5-5}	5	4	1	8	9	9	1628.0	E_{5-5}	5	4	1	3	10	7	1479.5
Avg.							1699.0	Avg.							1833.8
N_{1-1}	5	4	1	1	1	8	1726.4	W_{1-1}	5	4	1	1	7	8	1654.4
N_{1-2}	5	4	1	2	1	5	2123.0	W_{1-2}	5	4	1	2	5	5	1905.4
N_{1-3}	5	4	1	3	1	1	1595.3	W_{1-3}	5	4	1	2	2	2	1578.2
N_{1-4}	5	4	1	5	4	4	1998.3	W_{1-4}	5	4	1	3	3	2	2022.6
N_{1-5}	5	4	1	6	7	7	1482.6	W_{1-5}	5	4	1	3	4	1	1619.9
N_{2-1}	5	4	1	2	3	8	1703.2	W_{2-1}	5	4	1	5	4	5	1921.5
N_{2-2}	5	4	1	2	3	5	2136.9	W_{2-2}	5	4	1	3	4	4	1816.7
N_{2-3}	5	4	1	3	3	2	2061.0	W_{2-3}	5	4	1	2	4	3	1630.5
N_{2-4}	5	4	1	4	5	5	2068.8	W_{2-4}	5	4	1	2	4	2	1562.6
N_{2-5}	5	4	1	6	6	8	1470.4	W_{2-5}	5	4	1	3	5	2	1866.7
N_{3-1}	5	4	1	2	5	8	1692.6	W_{3-1}	5	4	1	9	1	2	1709.3
N_{3-2}	5	4	1	2	5	5	2114.9	W_{3-2}	5	4	1	5	3	3	1966.9
N_{3-3}	5	4	1	2	5	2	1520.5	W_{3-3}	5	4	1	1	5	3	1596.4
N_{3-4}	5	4	1	4	5	5	2052.5	W_{3-4}	5	4	1	2	5	3	1597.8

	v_1	v_2	v_3	v_4	v_5	v_6	[kWh]		v_1	v_2	v_3	v_4	v_5	v_6	[kWh]
N_{3-5}	5	4	1	6	5	8	1482.4	W_{3-5}	5	4	1	2	5	2	1627.0
N_{4-1}	5	4	1	3	5	8	1932.2	W_{4-1}	5	4	1	9	2	2	1729.7
N_{4-2}	5	4	1	2	4	5	2073.6	W_{4-2}	5	4	1	6	3	2	1792.3
N_{4-3}	5	4	1	2	3	2	1543.2	W_{4-3}	5	4	1	3	5	3	1988.7
N_{4-4}	5	4	1	4	4	5	1985.0	W_{4-4}	5	4	1	2	5	2	1554.4
N_{4-5}	5	4	1	6	6	8	1459.3	W_{4-5}	5	4	1	2	4	2	1662.9
N_{5-1}	5	4	1	3	5	7	1632.4	W_{5-1}	5	4	1	9	2	2	1631.5
N_{5-2}	5	4	1	3	3	5	2054.7	W_{5-2}	5	4	1	7	4	2	1889.1
N_{5-3}	5	4	1	2	1	2	1449.4	W_{5-3}	5	4	1	4	5	2	1545.1
N_{5-4}	5	4	1	4	4	5	1985.3	W_{5-4}	5	4	1	3	4	2	1953.9
N_{5-5}	5	4	1	6	6	8	1476.2	W_{5-5}	5	4	1	2	3	2	1659.3
Avg.							1792.8	Avg.							1739.3

BIBLIOGRAPHY

BIBLIOGRAPHY

Adamski, M. (2007), Optimization of the form of a building on an oval base, *Building and Environment*, *42*(4), 1632–1643, doi: http://dx.doi.org/10.1016/j.buildenv.2006.02.004.

Asadi, E., M. G. da Silva, C. H. Antunes, and L. Dias (2012a), A multi-objective optimization model for building retrofit strategies using TRNSYS simulations, GenOpt and MATLAB, *Building and Environment*, *56*, 370–378, doi: http://dx.doi.org/10.1016/j.buildenv.2012.04.005.

Asadi, E., M. G. da Silva, C. H. Antunes, and L. Dias (2012b), Multi-objective optimization for building retrofit strategies: A model and an application, *Energy and Buildings*, *44*, 81–87, doi:http://dx.doi.org/10.1016/j.enbuild.2011.10.016.

Ascione, F., N. Bianco, C. De Stasio, G. M. Mauro, and G. P. Vanoli (2015), A new methodology for cost-optimal analysis by means of the multi-objective optimization of building energy performance, *Energy and Buildings*, *88*, 78–90, doi: http://dx.doi.org/10.1016/j.enbuild.2014.11.058.

ASHRAE (2010), ASHRAE 90.1- 2010 Energy Standard for Buildings Except Low-Rise Residential Buildings.

Attia, S., M. Hamdy, W. O'Brien, and S. Carlucci (2013), Assessing gaps and needs for integrating building performance optimization tools in net zero energy buildings design, *Energy and Buildings*, *60*, 110–124, doi: http://dx.doi.org/10.1016/j.enbuild.2013.01.016.

Baglivo, C., and P. M. Congedo (2015), Design method of high performance precast external walls for warm climate by multi-objective optimization analysis, *Energy*, *90, Part 2*, 1645–1661, doi:http://dx.doi.org/10.1016/j.energy.2015.06.132.

Baglivo, C., P. M. Congedo, and A. Fazio (2014), Multi-criteria optimization analysis of external walls according to ITACA protocol for zero energy buildings in the mediterranean climate, *Building and Environment*, *82*, 467–480, doi: http://dx.doi.org/10.1016/j.buildenv.2014.09.019.

Baños, R., F. Manzano-Agugliaro, F. G. Montoya, C. Gil, A. Alcayde, and J. Gómez (2011), Optimization methods applied to renewable and sustainable energy: A review, *Renewable and Sustainable Energy Reviews*, *15*(4), 1753–1766, doi:http://dx.doi.org/10.1016/j.rser.2010.12.008.

Bichiou, Y., and M. Krarti (2011), Optimization of envelope and HVAC systems selection for residential buildings, *Energy and Buildings*, *43*(12), 3373–3382, doi: http://dx.doi.org/10.1016/j.enbuild.2011.08.031.

Bigot, D., F. Miranville, H. Boyer, M. Bojic, S. Guichard, and A. Jean (2013), Model optimization and validation with experimental data using the case study of a building equipped with photovoltaic panel on roof: Coupling of the building thermal simulation code ISOLAB with the generic optimization program GenOpt, *Energy and Buildings*, *58*, 333–347, doi:http://dx.doi.org/10.1016/j.enbuild.2012.10.017.

Brownlee, A. E. I., and J. A. Wright (2015), Constrained, mixed-integer and multi-objective optimisation of building designs by NSGA-II with fitness approximation, *Applied Soft Computing*, *33*, 114–126, doi: http://dx.doi.org/10.1016/j.asoc.2015.04.010.

Caldas, L. (2008), Generation of energy-efficient architecture solutions applying GENE_ARCH: An evolution-based generative design system, *Advanced Engineering Informatics*, *22*(1), 59–70.

Caldas, L. G. (2001), An Evolution-Based Generative Design System: Using Adaptation to Shape Architectural Form, Ph.D. thesis.

Caldas, L. G., and L. K. Norford (2002), A design optimization tool based on a genetic algorithm, *Automation in Construction*, *11*(2), 173–184, doi: http://dx.doi.org/10.1016/S0926-5805(00)00096-0.

Carlucci, S., G. Cattarin, F. Causone, and L. Pagliano (2015), Multi-objective optimization of a nearly zero-energy building based on thermal and visual discomfort minimization using a non-dominated sorting genetic algorithm (NSGA-II), *Energy and Buildings*, *104*, 378–394, doi:http://dx.doi.org/10.1016/j.enbuild.2015.06.064.

Černỳ, V. (1985), Thermodynamical approach to the traveling salesman problem: An efficient simulation algorithm, *Journal of optimization theory and applications*, *45*(1), 41–51.

Chen, S., M. D. Levine, H. Li, P. Yowargana, and L. Xie (2012), Measured air tightness performance of residential buildings in North China and its influence on district space heating energy use, *Energy and Buildings*, *51*, 157–164, doi: http://dx.doi.org/10.1016/j.enbuild.2012.05.004.

Coello, C. (2006), Evolutionary multiobjective optimisation: a historical view of the field, *IEEE Computational Intelligence Magazine*, (1), 28–36.

Coffey, B., F. Haghighat, E. Morofsky, and E. Kutrowski (2010), A software framework for model predictive control with GenOpt, *Energy and Buildings*, *42*(7), 1084–1092, doi:http://dx.doi.org/10.1016/j.enbuild.2010.01.022.

Collette Y, S. P. (2013), Multi-objective optimization: principles and case studies, *Springer Science & Business Media*.

Cook, S. A. (1983), An overview of computational complexity, *Communications of the ACM*, *26*(6), 400–408.

Darwin, C. (1859), On the origin ofspecies by means of natural selection, or the preservation of favoured races in the struggle for life, *New York, NY: D. Appleton and Company*.

DOE (2011), 2011 Buildings Energy Data Book, Prepared for the DOE Office of Energy Efficiency and Renewable Energy by D&R International.

Dorigo, M., V. Maniezzo, and A. Colorni (1996), The ant system: optimization by a colony of cooperating agents., *IEEE Transactions on Systems ,Man,and Cybernetics—Part B*, *26*(1), 29–41.

Dounis, A. I., and C. Caraiscos (2009), Advanced control systems engineering for energy and comfort management in a building environment—A review, *Renewable and Sustainable Energy Reviews*, *13*(6–7), 1246–1261, doi: http://dx.doi.org/10.1016/j.rser.2008.09.015.

Emmerich, M., J. Zhou, and M. Özdemir (2003), TOP – a toolbox for the optimisation of parameters.

Emmerich, M., C. Hopfe, and L. Stoelinga (2008), Evaluating optimisation methodologies for future integration in building performance tools, in *Proceedings of the 8th Int. Conf. on Adaptive Computing in Design and Manufacture (ACDM)*, pp. 1–7, Bristol.

Evins, R., P. Pointer, R. Vaidyanathan, and S. Burgess (2012), A case study exploring regulated energy use in domestic buildings using design-of-experiments and multi-objective optimisation, *Building and Environment*, *54*, 126–136.

Fazli, T., R. Y. Yeap, and B. Stephens (2015), Modeling the energy and cost impacts of excess static pressure in central forced-air heating and air-conditioning systems in single-family residences in the U.S, *Energy and Buildings*, *107*, 243–253, doi: http://dx.doi.org/10.1016/j.enbuild.2015.08.026.

Fernandes, L. L., E. S. Lee, and G. Ward (2013), Lighting energy savings potential of split-pane electrochromic windows controlled for daylighting with visual comfort, *Energy and Buildings*, *61*, 8–20, doi: http://dx.doi.org/10.1016/j.enbuild.2012.10.057.

Fogel, L. J. (1966), *Intelligence through simulated evolution: forty years of evolutionary programming.*, Wiley-Blackwell.

Franzetti, C., G. Fraisse, and G. Achard (2004), Influence of the coupling between daylight and artificial lighting on thermal loads in office buildings, *Energy and Buildings*, *36*, 117–126.

Futrell, B. J., E. C. Ozelkan, and D. Brentrup (2015), Bi-objective optimization of building enclosure design for thermal and lighting performance, *Building and Environment*, *92*, 591–602, doi:http://dx.doi.org/10.1016/j.buildenv.2015.03.039.

Geem, Z. W., and J. H. Kim (2001), A new heuristic optimization algorithm: harmony search., *Simulation*, *76*(2), 60–68.

Givoni, B. (1976), *Man, Climate and Architecture*, Applied Science Publishers Limited, London.

Goldberg, D. E. (1989), *Genetic algorithms in search, optimization, and machine learning* , Addison-Wesley.

Gossard, D., B. Lartigue, and F. Thellier (2013), Multi-objective optimization of a building envelope for thermal performance using genetic algorithms and artificial neural network, *Energy and Buildings*, *67*, 253–260, doi: http://dx.doi.org/10.1016/j.enbuild.2013.08.026.

Hamdy, M., A. Hasan, and K. Siren (2011), Impact of adaptive thermal comfort criteria on building energy use and cooling equipment size using a multi-objective optimization scheme, *Energy and Buildings*, *43*(9), 2055–2067, doi: http://dx.doi.org/10.1016/j.enbuild.2011.04.006.

Hansen, N., S. D. Müller, and P. Koumoutsakos (2003), Reducing the time complexity of the derandomized evolution strategy with covariance matrix adaptation (cma-es), *Evolutionary computation*, *11*(1), 1–18.

Hasan, A., M. Vuolle, and K. Sirén (2008), Minimisation of life cycle cost of a detached house using combined simulation and optimisation, *Building and Environment*, *43*(12), 2022–2034, doi:http://dx.doi.org/10.1016/j.buildenv.2007.12.003.

Heiselberg, P., H. Brohus, A. Hesselholt, H. Rasmussen, E. Seinre, and S. Thomas (2009), Application of sensitivity analysis in design of sustainable buildings, *Renewable Energy*, *34*(9), 2030–2036, doi:http://dx.doi.org/10.1016/j.renene.2009.02.016.

Holland, J. H. (1975), *Adaptation in Natural and Artificial Systems: An Introductory Analysis with Applications to Biology*, Control & Artificial Intelligence University of Michigan Press.

Hu, J., and P. Karava (2014), Model predictive control strategies for buildings with mixed-mode cooling, *Building and Environment*, *71*, 233–244, doi: http://dx.doi.org/10.1016/j.buildenv.2013.09.005.

Janak, M. (1997), Coupling building energy and lighting simulation, in *Building Simulation*, vol. 2, pp. 313–319.

Junghans, L., and N. Darde (2015), Hybrid single objective genetic algorithm coupled with the simulated annealing optimization method for building optimization, *Energy and Buildings*, *86*, 651–662, doi: http://dx.doi.org/10.1016/j.enbuild.2014.10.039.

Karimpour, M., M. Belusko, K. Xing, J. Boland, and F. Bruno (2015), Impact of climate change on the design of energy efficient residential building envelopes, *Energy and Buildings*, *87*, 142–154, doi:http://dx.doi.org/10.1016/j.enbuild.2014.10.064.

Kennedy, J. (1995), Particle swarm optimization, *IEEE International Conference on Neural Networks*, pp. 129–132.

Keoleian, G. A., S. Blanchard, and P. Reppe (2000), Lifecycle energy, costs, and strategies for improving a singlefamily house, *Journal of Industrial Ecology*, *4*(2), 135–156.

Kirkpatrick, Scott, and M. P. Vecchi. (1983), Optimization by simmulated annealing, *science*, *220*(4598), 671–680.

Kolda, T. G., R. M. Lewis, and V. Torczon (2003), Optimization by Direct Search: New Perspectives on Some Classical and Modern Methods, *SIAM Rev.*, *45(3), 385*.

Lee, J. H. (2007), Optimization of indoor climate conditioning with passive and active methods using GA and CFD, *Building and Environment*, *42*(9), 3333–3340, doi: http://dx.doi.org/10.1016/j.buildenv.2006.08.029.

Lu, Y., S. Wang, Y. Zhao, and C. Yan (2015), Renewable energy system optimization of low/zero energy buildings using single-objective and multi-objective optimization methods, *Energy and Buildings*, *89*, 61–75, doi: http://dx.doi.org/10.1016/j.enbuild.2014.12.032.

Machairas, V., A. Tsangrassoulis, and K. Axarli (2014), Algorithms for optimization of building design: A review, *Renewable and Sustainable Energy Reviews*, *31*, 101–112, doi:http://dx.doi.org/10.1016/j.rser.2013.11.036.

Magnier, L., and F. Haghighat (2010), Multiobjective optimization of building design using TRNSYS simulations, genetic algorithm, and Artificial Neural Network, *Building and Environment*, *45*(3), 739–746, doi: http://dx.doi.org/10.1016/j.buildenv.2009.08.016.

Mangan, S. D., and G. K. Oral (2015), Assessment of residential building performances for the different climate zones of Turkey in terms of life cycle energy and cost efficiency, *Energy and Buildings*, p. Table 11 Climate zones of China included in this s, doi:http://dx.doi.org/10.1016/j.enbuild.2015.11.002.

Michalek, J., R. Choudhary, and P. Papalambros (2002), Architectural layout design optimization, *Engineering optimization*, *34*(5), 461–484.

Negendahl, K., and T. R. Nielsen (2015), Building energy optimization in the early design stages: A simplified method, *Energy and Buildings*, *105*, 88–99, doi: http://dx.doi.org/10.1016/j.enbuild.2015.06.087.

Nguyen, A.-T., S. Reiter, and P. Rigo (2014), A review on simulation-based optimization methods applied to building performance analysis, *Applied Energy*, *113*, 1043–1058, doi:http://dx.doi.org/10.1016/j.apenergy.2013.08.061.

Olgyay, V. (1992), *Design with Climate—A bioclimatic Approach to Architectural Regionalism*, Van Nostrand Reinhold, New York.

Oliveira Panão, M. J. N., H. J. P. Gonçalves, and P. M. C. Ferrão (2008), Optimization of the urban building efficiency potential for mid-latitude climates using a genetic algorithm approach, *Renewable Energy*, *33*(5), 887–896, doi: http://dx.doi.org/10.1016/j.renene.2007.04.014.

Padovan, R., and M. Manzan (2014), Genetic optimization of a PCM enhanced storage tank for Solar Domestic Hot Water Systems, *Solar Energy*, *103*, 563–573, doi: http://dx.doi.org/10.1016/j.solener.2013.12.034.

Palonen, M., A. Hasan, and K. Siren (2009), A genetic algorithm for optimization of building envelope and HVAC system parameters, in *Building simulation, Glasgow, Scotland*.

Parker, D. S. (2009), Very low energy homes in the United States: Perspectives on performance from measured data, *Energy and Buildings*, *41*(5), 512–520, doi: http://dx.doi.org/10.1016/j.enbuild.2008.11.017.

PNNL (2015), Guide to Determining Climate Regions by County, *Tech. rep.*

Price, K., and R. Storn (1997), Differential Evolution-A simple evolution strategy for fast optimization, *Dr Dobb's Journal*.

Rapone, G., and O. Saro (2012), Optimisation of curtain wall façades for office buildings by means of PSO algorithm, *Energy and Buildings*, *45*, 189–196, doi: http://dx.doi.org/10.1016/j.enbuild.2011.11.003.

Rechenberg, I. (1965), Cybernetic solution path of an experimental problem.

Rhodes, J. D., W. H. Gorman, C. R. Upshaw, and M. E. Webber (2015), Using BEopt (EnergyPlus) with energy audits and surveys to predict actual residential energy usage, *Energy and Buildings*, *86*, 808–816, doi: http://dx.doi.org/10.1016/j.enbuild.2014.10.076.

Robertson, J. J., B. J. Polly, and J. M. Collis (2015), Reduced-order modeling and simulated annealing optimization for efficient residential building utility bill calibration, *Applied Energy*, *148*, 169–177, doi: http://dx.doi.org/10.1016/j.apenergy.2015.03.049.

Schluter, D. (2000), *The Ecology of Adaptive Radiation*, Oxford University Press.

Seo, D., P. Ihm, and M. Krarti (2011), Development of an optimal daylighting controller, *Building and Environment*, *46*(5), 1011–1022, doi: http://dx.doi.org/10.1016/j.buildenv.2010.10.026.

Sette, S., and L. Boullart (2001), Genetic programming: principles and applications, *Engineering Applications of Artificial Intelligence*, *14*(6), 727–736, doi: http://dx.doi.org/10.1016/S0952-1976(02)00013-1.

Shi, X. (2011), Design optimization of insulation usage and space conditioning load using energy simulation and genetic algorithm, *Energy*, *36*(3), 1659–1667, doi: http://dx.doi.org/10.1016/j.energy.2010.12.064.

Singjh, M. K., S. Mahapatra, and S. K. Atreya (2007), Development of bio-climatic zones in north-east India, *Energy Building*, *39*, 1250–1257.

Stazi, F., A. Mastrucci, and P. Munafò (2012), Life cycle assessment approach for the optimization of sustainable building envelopes: An application on solar wall systems, *Building and Environment*, *58*, 278–288, doi: http://dx.doi.org/10.1016/j.buildenv.2012.08.003.

Sung, K. J. (2014), Optimal Control Methods for PV-integrated Shading Devices, Ph.D. thesis, Ann Arbor.

Tregenza, P. R. (1980), The daylight factor and actual illuminance ratios, *Lighting Research & Technology*, *12*(6), 64–68.

Tregenza, P. R. (1983), Daylight coefficients, *Lighting Research and Technology*, *15*(2), 65–71.

Tuhus-Dubrow, D., and M. Krarti (2010), Genetic-algorithm based approach to optimize building envelope design for residential buildings, *Building and Environment*, *45*(7), 1574–1581, doi:http://dx.doi.org/10.1016/j.buildenv.2010.01.005.

Wang, H., and Q. Chen (2014), Impact of climate change heating and cooling energy use in buildings in the United States, *Energy and Buildings*, *82*, 428–436, doi: http://dx.doi.org/10.1016/j.enbuild.2014.07.034.

Wang, L., H. Wong Nyuk, and S. Li (2007), Facade design optimization for naturally ventilated residential buildings in Singapore, *Energy and Buildings*, *39*(8), 954–961, doi:http://dx.doi.org/10.1016/j.enbuild.2006.10.011.

Wang, L., N. H. Wong, and S. Li (2010), Corrigendum to "Facade design optimization for naturally ventilated residential buildings in Singapore" [Energy Buildings 39 (2007) 954–961], *Energy and Buildings*, *42*(10), 1968, doi: http://dx.doi.org/10.1016/j.enbuild.2010.05.001.

Wang, W., R. Zmeureanu, and H. Rivard (2005), Applying multi-objective genetic algorithms in green building design optimization, *Building and Environment*, *40*(11), 1512–1525, doi:http://dx.doi.org/10.1016/j.buildenv.2004.11.017.

Weber, C., F. Maréchal, D. Favrat, and S. Kraines (2006), Optimization of an SOFC-based decentralized polygeneration system for providing energy services in an office-building in Tky, *Applied Thermal Engineering*, *26*(13), 1409–1419, doi: http://dx.doi.org/10.1016/j.applthermaleng.2005.05.031.

Wetter, M. (2001), GenOpt® – A Generic Optimization Program.

Wetter, M. (2004), Simulation-based building energy optimization, *University of California, Berkeley*.

Wetter, M., and E. Polak (2004), A convergent optimization method using pattern search algorithms with adaptive precision simulation, *Build Serv Eng Res Technol*, *25(4):327–*.

Wetter, M., and J. Wright (2003), Comparison of a generalized pattern search and a genetic algorithm optimization method, in *Eighth International IBPSA Conference*, Eindhoven, Netherlands.

Wetter, M., and J. Wright (2004), A comparison of deterministic and probabilistic optimization algorithms for nonsmooth simulation-based optimization, *Building and Environment*, *39*(8), 989–999, doi: http://dx.doi.org/10.1016/j.buildenv.2004.01.022.

Wright, J. (2005), The robustness of genetic algorithms in solving unconstrained building optimization problems.

Wright, J. A. (1986), The optimized design of HVAC systems, *Loughborough University of Technology*.

Wright, J. A., H. A. Loosemore, and R. Farmani (2002), Optimization of building thermal design and control by multi-criterion genetic algorithm, *Energy and Buildings*, *34*(9), 959–972, doi:http://dx.doi.org/10.1016/S0378-7788(02)00071-3.

Yang, Z., Y. Zhao, X. Xu, and B. Zhai (2012), Analysis and comparison of building energy saving reconstruction in hot summer and warm winter regions of South China and cold regions of North China, *Energy and Buildings*, *54*, 192–195, doi: http://dx.doi.org/10.1016/j.enbuild.2012.07.006.

Yi, Y. K., and A. M. Malkawi (2009), Optimizing building form for energy performance based on hierarchical geometry relation, *Automation in Construction*, *18*(6), 825–833, doi:10.1016/j.autcon.2009.03.006.

Yu, J., L. Tian, C. Yang, X. Xu, and J. Wang (2013), Sensitivity analysis of energy performance for high-rise residential envelope in hot summer and cold winter zone of China, *Energy and Buildings*, *64*, 264–274, doi: http://dx.doi.org/10.1016/j.enbuild.2013.05.018.